Investigation of Hepatitis B Virus entry mechanism

Chidinma Raymond

MSc, BSc

Thesis submitted to the Univeristy of Nottingham

for the degree of Doctor of Philosophy

School of Life Sciences

August, 2021.

Student Declaration:

I declare that the data presented is entirely my work, except where otherwise stated.

Abstract

Hepatitis B infection is a global public health challenge that attacks the liver, resulting in severe hepatic and non-hepatic complications, particularly liver cirrhosis and hepatocellular carcinoma. This infection caused by the Hepatitis B virus (HBV) is the cause of the world's most common liver infection and the second leading cause of cancer worldwide. HBV is known to have a complicated replication cycle in which it utilises a reverse transcriptase with proofreading inability. The overlapping nature of the HBV genome, in addition to the proofreading inability of the HBV polymerase, culminates in high mutation rates with pleiotropic effects on both the polymerase and the surface genes. Mutations in the surface gene (HBsAg) have been linked to several clinical implications, such as vaccine escape and failure of HBV diagnostic assays. We hypothesised that the HBsAg variability would go beyond immune escape mutants, potentially extending to its interaction with cell receptors and entry. Therefore, in this study, we have studied the effect of HBsAg mutations on HBsAg interactions with cell receptors and on HBV entry using the pseudotyping system.

The entry of HBV pseudotyped particles into the Huh7 hepatoma cell line transduced to express the NTCP receptor was studied. This study has generated several unusual data particularly focused on the unusual entry phenotype of the clinical isolate BT10D4 and its ability to infect Huh7 cells independent of the NTCP receptor. Sequence analysis of this isolate identified 2 rare amino acid substitutions at positions s69 and s96 that possibly interact with each other and with one or more other amino acid positions to achieve the unusual entry phenotype. Data from this study showed that BT10D4 utilised the HBsAg PreS2-48 amino acids, the epidermal growth factor receptor (EGFR), the clathrin-dependent endocytosis for entry and internalisation. Interestingly, this study showed that unlike the entry into Huh7 cells, BT10D4 could not infect HepG2 hepatoma cells in the absence of NTCP.

In light of the above findings, we propose that the presence of the mutations in BT10D4, which interact with each other, alter the conformation of the HBsAg in such a way that favours its interaction with one or more unknown Huh7 cell receptors. Consequently, future work will explore this hypothesis to provide the much-needed answers about the BT10D4 isolate, the rare amino acid substitutions and its unusual entry phenotype.

Acknowledgements

I am eternally grateful to the almighty God, for in Him I live and move and have my being. I am grateful to Him for life, the abilities, the physical, mental and psychological strength to start and successfully finish this PhD. I appreciate my amazing supervisors, Dr Alexander Tarr and Prof William Irving, for their immeasurable support and guidance. I couldn't wish for a better supervision team.

I am incredibly grateful to my bespoke husband, Dr Misueneivi Limejuice, for your unconditional love. Thank you for the small and big sacrifices, thank you for the constant push and for always being there. I would love to thank my parents and siblings for their prayers and love. Thank you for making the family an invaluable support system. Thank you to my brother, Dr Onyekachi Raymond, for going ahead of me in this PhD journey and for being an amazing role model.

I appreciate my friend Fernando Ruiz for being an absolute God-sent throughout this PhD period; you define true friendship. A big thank you to my covenant friends, Nelly and Nneoma. Thank you for spiritually and physically standing with me throughout this PhD. I would also like to say thank you to Dr Barnabas King, Dr Patrick McClure, Dr Richard Urbanowicz, and Dr Jonathan Ball for your support and help. Thank you to my colleagues Yemisi, Jayseree, Arwa, Terry, Timothy, and Chun for your encouragement along the way.

Finally, this study would not have been possible without the sponsorship of the University of Nottingham and Schlumberger Faculty for the Future Foundation. Thank you for believing in me enough to sponsor me.

Table of Contents

Contents

List of Figures

List of Tables

List of Abbreviations

Abbreviation Definition

μL	Microlitre
μg	Microgram
%	Percentage
h	Hour (s)
^0C	Degree Celsius
CO_2	Carbondioxide
B	Beta
sec	Second (s)
min	Minute (s)
mL	Millilitre
mg	Milligram
ng	Nanogram
ALT	Alanine transaminase
AA	Amino acid (s)
AGL	Antigenic loop
ANXA2	Annexin 2
BCA	Bicinchoninic acid assay
Baf	Bafilomycin
Bref	Brefeldin A
BCP	Basal core promoter
BSL	Biosafety level
cccDNA	Covalently closed circular DNA
CMV	Cytomegalovirus
CSNC	Clinical sample from Nottingham cohort
CPZ	Chlorpromazine
ΔE	Delta E
DMEM	Dulbecco's Modified Eagle's Media

DMSO	Dimethyl sulfoxide
DNA	Deoxyribonucleic Acid
EDTA	Ethylenediaminetetraacetic acid
EBV	Ebola virus
EGF	Epidermal growth factor
EGFR	Epidermal growth factor receptor
ER	Endoplasmic Reticulum
ERGIC	Endoplasmic reticulum-Golgi intermediate compartment
e-PreS	External PreS
ESCRT	Endosomal sorting complex required for transport
GFP	Green fluorescent protein
Gt	Genotype
HBIg	Hepatitis B immune globulin
HBV	Hepatitis B virus
HCC	Hepatocellular carcinoma
HCV	Hepatitis C virus
HDV	Hepatitis D virus
HEK293	Human embryonic kidney 293 cells
HIV	Human immunodeficiency virus
HRP	Horseradish peroxidase
HSPG	Heparan Sulfate Proteoglycan
HSV	Herpes Simplex virus
IAV	Influenza A virus
IFN	Interferon
i-PreS	Internal PreS
LB	Lysogeny broth
Log	Logarithm
LTR	Long terminal repeat
luc	Luciferase
LV	Lentiviral vector
Ma	Monoclonal antibody

MCD	Methyl-β-cyclodextrin
MEGA	Molecular Evolutionary Genetics Analysis
MERS	Middle East respiratory syndrome–related coronavirus
MHR	Major hydrophilic region
MLV	Murine leukemia virus
mRNA	Messenger Ribonucleic acid
MVB	Multivesicular bodies
MyrB	Myrcludex B
NAATs	Nucleic Acid Amplification Tests
NAs	Nucleoside/Nucleotide analogues
NTCP	Sodium Taurocholate Cotransporting Polypeptide
ORF	Open reading frame
PBS	Phospate buffered saline
PCR	Polymerase chain reaction
PEG	Polyethylene glycol
PEI	Polyethylenimine
pgRNA	Pregenomic RNA
pp(s)	Pseudotypes
PVDF	Polyvinylidene fluoride
rcDNA	Relaxed circular RNA
RLU	Relative light units
RNA	Ribonucleic acid
RRE	Rev response elements
rt	Reverse transcriptase
TGF	Transforming growth factor
TM	Transmembrane
SD	Standard deviation
SDM	Site-directed mutagenesis
SDS	Sodium dodecyl sulfate
SV40	Simian vacuolating virus 40
SVPs	Subviral particles

| VSV-G | Vesicular stomatitis virus glycoprotein |
| WHO | World Health Organisation |

Chapter 1

Introduction and Literature Review

1.1 Hepatitis B Infection

Viral hepatitis is a worldwide health threat caused by five known hepatitis viruses (hepatitis A-E) having different pathogenesis and epidemiology. Hepatitis A virus (HAV) and hepatitis E virus (HEV), endemic in low-income countries, are transmitted through the faecal-oral route. Despite being self-limiting (as with HEV), they can also result in fulminant hepatitis and chronic infection (as with HBV/HCV). Hepatitis B and C viruses are bloodborne viruses implicated in acute and chronic hepatitis and progressively result in debilitating liver diseases such as cirrhosis, liver fibrosis and a high risk of hepatocellular carcinoma (HCC) [1-3]. Hepatitis B infection is a global public health challenge that attacks the liver, resulting in severe hepatic and non-hepatic complications, particularly liver cirrhosis and hepatocellular carcinoma. About 2 billion people have been infected, with 30 million new infections yearly, 300 million chronic infections globally and 884,000 yearly deaths. HBV is the cause of the world's most common liver infection and the second leading cause of cancer worldwide [4, 5].

1.2 History of Viral Hepatitis and Hepatitis B Infection

The earliest record of viral hepatitis, which may or may not have been caused by HBV, was between 300 to 400 BC as recorded by Hippocrates in his writings, revealing that the jaundice being reported was probably infectious and was affecting the liver. In 1885, a German doctor, Lürmann, published a record of the 'icterus epidemic', an epidemiological study of a serum hepatitis outbreak affecting 191 out of 1289 shipyard workers in Bremen, Germany, after receiving the smallpox vaccine made from human lymph. Several other large epidemics were recorded during the American Civil War (1861-1865), the Franco-Prussian War (1870), World War I (1914-1918) and World War II (1939-1945). However, the causative agent of the serum hepatitis remained unknown [6, 7]. In 1942, after a batch of yellow fever vaccine stabilised with human serum had been given to American soldiers, an epidemic occurred, affecting 28,585 soldiers and causing 62 deaths [8, 9]. A breakthrough was made in 1963 when geneticist, haematologist and Nobel prize winner Baruch S. Blumberg discovered the

Australian antigen (AuAg) as a specific marker for viral hepatitis, and in 1965 when he discovered hepatitis B virus surface antigen (HBsAg) [10, 11]. Additionally, in 1967, Saul Krugman identified the two types of hepatitis agents and their transmission mode. He showed that one group had a faecal-oral transmission route while the other had a parenteral mode of transmission. This led to increased hygienic measures, screening assays and a consequent decrease in post-transfusion cases of hepatitis [12, 13]. In 1970, while using electron microscopy to examine donor plasma, David Dane discovered that the Australian antigen was part of a large 42 nm-sized virus particle now known as the Dane particle [14]. Recent studies have shown the presence of HBV DNA in an Italian child mummy from the mid-16th century. Phylogenetic analysis of the ancient strain showed a relationship with some HBV genotype D strains indicating that HBV had undergone diversity before the 16th century [15].

1.3   Taxonomy of Hepatitis B Virus

In 1980, the International Committee on Taxonomy of Viruses (ICTV) recognised and classified human HBV alongside other related animal viruses as members of a new family named Hepadnaviridae [16]. This family was further divided into two genera which are avihepadnaviruses and orthohepadnaviruses. Avihepadnaviruses, some of which are: Duck HBV, Grey Teal HBV, Snow Goose HBV and Stork HBV, are known to infect birds and have a 40 % nucleic acid homology with human HBV [17-19]. Orthohepadnaviruses of which human HBV is a member infect mammals; other members include Woodchuck HBV, Chimpanzee HBV, Orangutan HBV, Woolly Monkey HBV, Roundleaf Bat HBV, Gorilla HBV and Ground Squirrel HBV. Members of the orthohepadnaviruses are more closely related to the human HBV, with an 83% nucleic acid homology with human HBV. HBV in bats has been shown to be highly genetically diverse and geographically distributed. A study by Nie, F.-Y., *et al.,* reported that hepadnaviruses sampled in 11 bat species across 5 locations had an overall prevalence of 13.3 % [20]. However, hepadnaviruses are known to have a narrow host range and a high liver tropism [21-29].
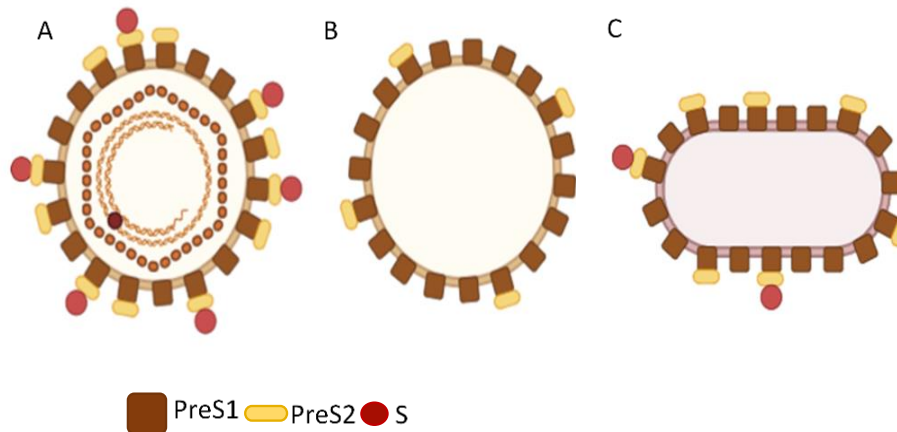
Figure 1.1 HBV Morphology. A. 42 nm spherical HBV Dane Particle carrying the viral genome, B. 20 nm spherical HBV subviral particle, C. 22 nm filamentous HBV subviral particle. The figure was created at http://biorender.com/.

1.4 Morphology of Hepatitis B Virus

Electron microscopy of infectious serum samples has shown that HBV viral particles exist in three types with different sizes. HBV is the smallest DNA virus, with its infectious Dane particle being a 42 nm spherical viral particle and carrying the viral genome, which is surrounded by an icosahedral capsid and a lipid envelope. The non-infectious subviral particles (SVPs) are the 20 nm spherical and the 22 nm filamentous particles having only the viral lipid envelope and lacking the viral genome (Figure 1.1) [30-32].

1.5 HBV Genome and Viral Proteins

HBV, known as the smallest DNA virus, consists of a 3.2 kb partially double-stranded relaxed-circular DNA (rcDNA) with gaps in the positive strand of the DNA, encoding four overlapping open reading frames (ORFs P, S, C and X). ORF P is the largest ORF and encodes the viral polymerase; ORF S encodes the HBV

envelope proteins known as large (L-), middle (M-), and small (S-) surface antigen (HBsAg). ORF C encodes the HBV core (HBcAg) and precore (HBeAg) proteins, while ORF X encodes the HBV X protein (HBxAg). These ORFs encode genomic and subgenomic RNA transcripts that are capped and polyadenylated. ORFs S and X encode the 2.4, 2.1 and 0.7 kb subgenomic transcripts, and ORFs P and C encode the 3.5 kb genomic transcript. Also, at the 5' end of the positive strand of the HBV genome are two direct repeats (DR1 and DR2), essential for the specificity of DNA synthesis. The HBV genome also contains two enhancer elements (Enh1 and Enh2) that are known to regulate the expression of HBV gene products in hepatocytes (Figure 1.2) [5, 30, 33-35].
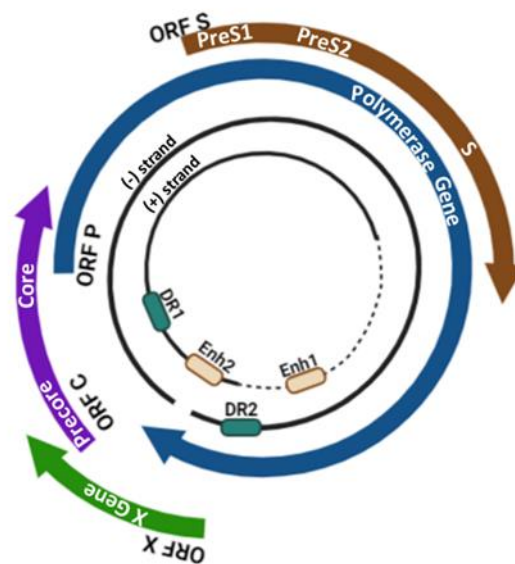
Figure 1.2 HBV genome. HBV is a partially double-stranded relaxed-circular DNA with gaps in the positive strand of the DNA. It encodes four overlapping open reading frames (ORFs P, S, C and X). The figure was created at http://biorender.com/.

1.5.1 HBV Polymerase

HBV polymerase protein is an 800-845 amino acid multifunctional protein with four domains and has three discrete enzymatic functions. The HBV polymerase comprises a unique terminal protein (TP) domain at the N-terminal, which is

necessary for the polymerase binding and packaging with the pregenomic RNA (pgRNA) and priming for initiation of negative-strand synthesis. A highly variable spacer domain with an unknown function is between the TP and reverse transcriptase (RT) domains. The RT consists of catalytic domains (A-F) and is responsible for the reverse transcriptase ability of HBV polymerase that is similar to retroviruses; it reverse-transcribes the pgRNA into a negative strand of the DNA, which it then uses as a template to synthesise the positive strand of the DNA. The fourth domain is the RNase H domain which degrades the pgRNA as the negative strand of the DNA is being synthesised, leaving 15 to 18 oligoribonucleotides at the 5' end to serve as a primer for the positive strand synthesis (Figure 1.3) [36-42].
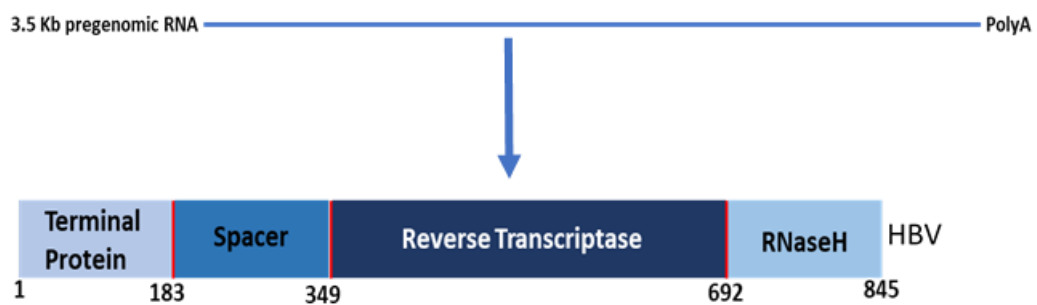
Figure 1.3 3.5 kb pregenomic RNA transcript generates the HBV polymerase.

1.5.2 HBV Core and Precore Proteins

At the start of the ORF C, the basal core promoter drives the transcription of the 3.5 kb genomic precore mRNA and the pgRNA transcripts. The presence of multiple in-frame translation initiation sites in the precore mRNA results in the generation of two functionally distinct proteins, HBcAg (nucleocapsid), when translation starts at the core initiation site or HBeAg when translation starts at the precore initiation site (Figure 1.4). HBeAg is a 15 kD protein secreted from the endoplasmic reticulum (ER) and is an important diagnostic marker in the management of HBV infection. HBcAg is the assembling framework for the HBV

virion but is simply not an inert packaging for the genome; this 21 kD core protein carries other regulatory roles. The first 149 amino acids of the core make up the assembly domain, while the arginine-rich C-terminal domain (CTD) comprises the remaining 34-36 amino acids. The CTD plays critical roles in pgRNA encapsidation, its reverse transcription and regulation of the chromatin structure of the covalently closed circular DNA (cccDNA) [34, 43-47].
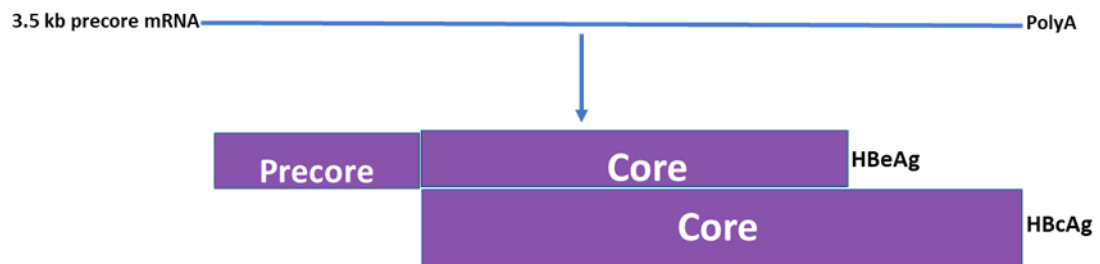
Figure 1.4 3.5 kb precore mRNA transcript generates HBeAg and HBcAg.

1.5.3 HBV Surface Proteins

The ORF S contains three in-frame start codons that encode the envelope regions; pre-S1, pre-S2 and S, depending on the start codon at which translation is initiated. As a result, there are three different HBsAg proteins called L-HBsAg (pre-S1+pre-S2+S), M-HBsAg (pre-S2+S), and S-HBsAg (S) surface antigen (HBsAg). The pre-S1 promoter drives L-HBsAg expression, while the pre-S2/S promoter drives the expression of M and S-HBsAg. 24 kD S-HBsAg, the smallest of the envelope proteins, has 226 amino acids and a shared C-terminal with L and M-HBsAg. 31 kD M-HBsAg has 281 amino acids made up of 55 amino acids pre-S2 in addition to S amino acids. 39 kD L-HBsAg contains 389, 399 or 400 amino acids made up of 108, 118 or 119 amino acids (depending on the genotype) in the pre-S1 region in addition to the pre-S2 and S amino acids (Figure 1.5) [48-51]. Hepatitis D virus, the satellite virus for HBV, has a viral envelope that contains the three HBV envelope proteins – large, medium, and small hepatitis B surface antigens. The HBV Dane particle contains the S, M and L proteins in approximately a 4:1:1 ratio; the spherical SVPs are made up largely of

S, a few M and very little L proteins and the filamentous SVPs contain few more L than the spherical SVPs (Figure 1.1). Within the S-HBsAg is the antigenic loop (AGL) or the major hydrophilic region (MHR), from amino acids 99 to 169, within which is the "a" determinant from amino acids 124 to 147. HBsAg contains two cytosolic domains and four transmembrane domains (TMs): TM1 (amino acids 7-29), TM2 (amino acids 80-98), TM3 (amino acids 170-192), TM4 (amino acids 202-224) (Figure 1.6) [52-57]. S-HBsAg is glycosylated at amino acid 146 (asparagine) of the S domain, M-HBsAg has glycosylation at amino acid 4 (asparagine) of the preS2 domain in addition to the glycosylation in the S domain. In contrast, L-HBsAg has one glycosylation in the S domain and myristoylation at amino acid 2(glycine) of the preS1 domain (Figure 1.6). The S domain contains 14 cysteine residues that form disulphide bridges which are common to L, M and S-HBsAg proteins, out of which 8 are in the MHR [58-61]. HBV envelope proteins contain two infectivity/entry determinants found within the L and S-HBsAg; M-HBsAg has been shown not to be involved in the entry. The best-characterised determinant is a myristoylated motif 2–75 within the N-terminal pre-S1 subdomain, the receptor-binding site. Inhibition of entry by the insertion and/or deletion within the pre-S1 domain of L-protein highlights an essential role for amino acids 2–75 in particle infectivity [62]. Importantly, an N-terminal myristoylated synthetic peptide encoding 2–78 inhibits HBV infection [63]. The second determinant of unknown function is a conformation-dependent determinant within the antigenic loop in the S domain [62-68].
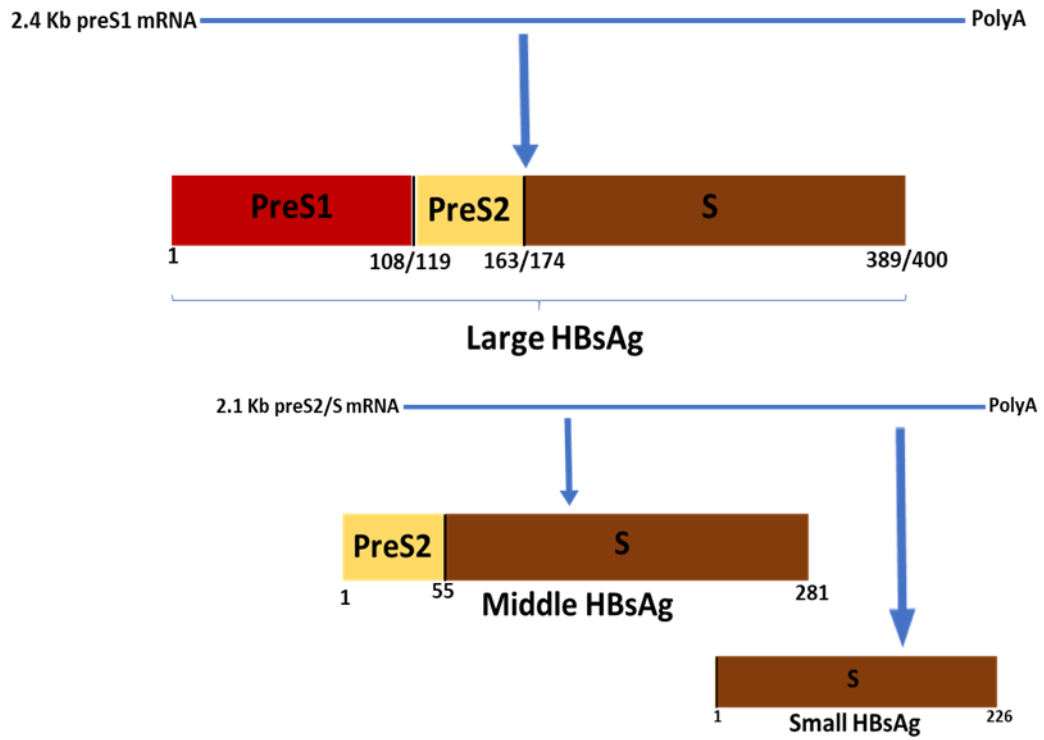
Figure 1.5 2.4 kb preS1 mRNA transcript generates the large HBsAg protein, 2.1Kb preS2/S mRNA generates the middle and small HBsAg proteins.

A
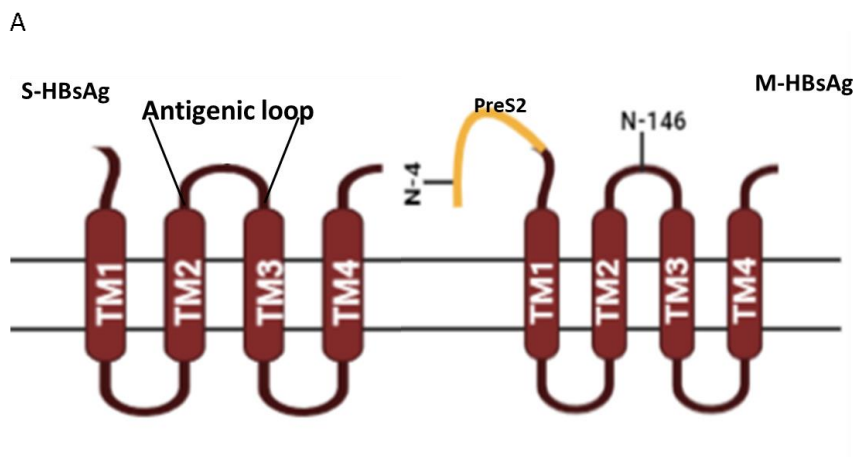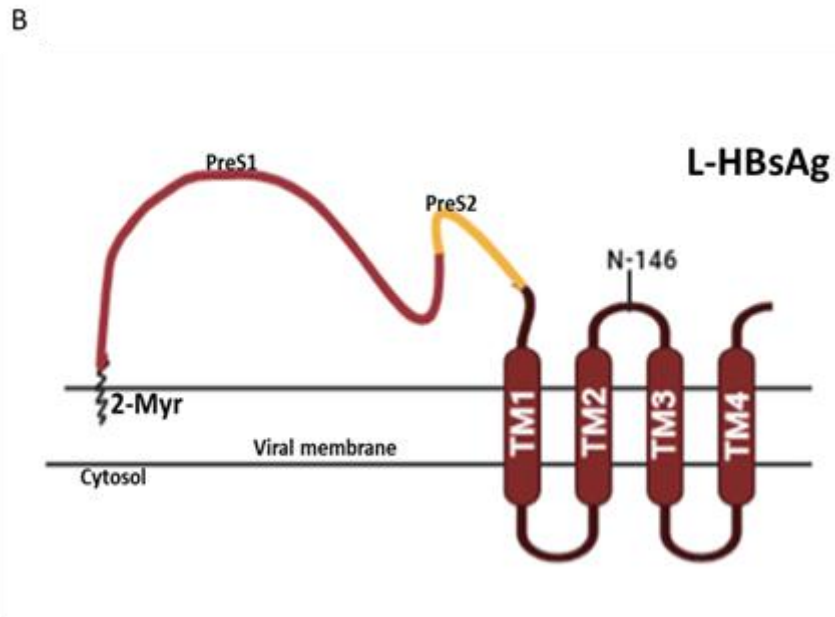
Figure 1.6 Structure of (A) small and middle (B) large HBV surface proteins showing the transmembrane domains (TM 1, 2, 3, 4), glycosylation and myristoylation domains, the antigenic loop within which is the major hydrophilic region. The figure was created at http://biorender.com/.

1.5.4 HBV X Protein

The 17 kD regulatory HBxAg protein containing 154 amino acids is encoded by HBV ORF X, the smallest ORF (Figure 1.7). In addition to being a crucial part of HBV replication, where it binds to cccDNA and is also involved in regulating transcription from cccDNA, HBxAg has been shown to possess oncogenic potential. It is unclear if its oncogenicity is directly involved in HCC development or a co-factor that induces subtle hepatocyte changes and stimulates the cells to respond to other direct oncogenes that result in HCC development or maintenance. Studies have described HBxAg as a multifunctional protein that is linked to cell transformation mechanisms such as calcium modulation, apoptosis, and activation of transcription factors (such as activator proteins 1 and 2 (AP-1 and AP-2), and nuclear factor of activated T cells (NFAT)), as well as regulation of cellular signalling factors including p53, Wnt/β-catenin and Akt known to be involved in HCC [69-77].

Figure 1.7 0.7 Kb X mRNA transcript generates HBxAg.

1.6   HBV Life Cycle

Viral specificity to host cells is primarily determined by attachment interactions between the virus and host cells. Although HBV has a strict tropism for hepatocytes, evidence has shown that other extrahepatic cells such as lymphocytes, mononuclear cells, the spleen can support its replication at a much lesser degree [78-80]. The HBV replication pathway is initiated by a reversible, low-affinity interaction between heparan sulfate proteoglycans (HSPGs) on the cell membrane and HBV envelope proteins, bringing the virus in close proximity to make specific interaction. This is followed by high-affinity binding of viral surface antigen to a specific receptor identified in 2012 as a human sodium-taurocholate co-transporting polypeptide (hNTCP/SLC10A1), an integral membrane protein exclusively expressed on the basolateral membrane of hepatocytes, hence the HBV tropism for the liver [81-85]. Mouse NTCP does not confer susceptibility to HBV infection, supporting findings that HBV cannot infect mouse hepatocytes [86]. Its interaction with its receptor triggers HBV internalisation, and it is believed to be internalised by clathrin-dependent endocytosis [87]. Recent studies have shown that epidermal growth factor receptor (EGFR), a tyrosine kinase receptor, directly interacts with NTCP and contributes to HBV internalisation [88, 89]. It has also been shown that the ability of NTCP to oligomerise modulates its mediation of viral internalisation [90]. HBV nucleocapsid is taken into the cytoplasm, and the DNA is trafficked to the nucleus by mechanisms that remain unclear, although active transportation of the nucleocapsid through the nuclear pore has been postulated as a potential mechanism [91].

Host-specific factors modify the HBV rcDNA in the nucleus by removing the RNA oligonucleotide at the 5' end of the positive strand and the redundant pol-linked sequence at the 5' end of the negative strand. These modifications also involve repairing the gaps in the rcDNA and ligation of the DNA to form the cccDNA [30, 92-94]. Studies have suggested that the Flap structure-specific endonuclease 1 (FEN1) could be involved in the removal of the redundant Pol and RNA primers while DNA polymerase κ and α (Pol κ and Pol α), DNA ligase 1 and 3 (LIG1 and LIG3), and topoisomerase I and II (TOP1 and TOP2) have been implicated in the repair and ligation of the rcDNA [95-99]. HBV cccDNA, a long-term template for replication, is maintained episomally as a minichromosome in the nucleus. Although it is unclear how this happens, apolipoprotein B editing complex 3 (APOBEC3), a cytidine deaminase, has been shown to modulate cccDNA stability by APOBEC3A and APOBEC3B degradation [100, 101]. Studies have shown the association of HBx with cccDNA and its role in the epigenetic regulation of the cccDNA. HBx has been shown to be involved in controlling the phosphorylation, methylation, and acetylation of cccDNA-associated histones necessary for the cccDNA transcription [102-104]. Also, it is now known that there is an integration of part of the HBV DNA into the host cell genome, and this occurs through double-stranded DNA breaks. In as much as this integrated DNA occurs with several deletions and is said to be replication-incompetent, these deletions affect the expression of all other ORFs save the S ORF which is maintained and expresses S protein driven by its promoter [105-107].

Host DNA-dependent RNA polymerase II transcribes the cccDNA template to all viral RNAs for protein production and replication. Transcription is initiated at various positions by 4 promoters: core, preS1, preS2 and X, generating 4 major polyadenylated RNA transcripts of various sizes. These RNAs are transported out of the nucleus to the cytoplasm to be translated by host factors. Aside from being a bicistronic mRNA translated to core (HBcAg) and polymerase (P) proteins, the pregenomic (pg) RNA is also the RNA transcript for replication and is selectively packaged for conversion to the progeny DNA by an HBV RNA encapsidation signal (Ɛ) situated near the 5' end of the HBV pregenomic RNA [43,

108, 109]. Upon encapsidation of the pgRNA by the core protein, the polymerase recognises the stem-loop and bulge region of the pgRNA. A deoxyguanosine molecule covalently binds to the polymerase, and base pairs with a cytosine within the stem-loop and two deoxyadenosine triphosphates are then added to form a 3-base DNA priming sequence [110]. This primer is then translocated and base pairs with the direct repeat 1 (DR1), serving as the initiation point for the synthesis of the negative-strand DNA by reverse transcription of the pgRNA. RNase H degrades the pgRNA leaving 15 to 18 oligoribonucleotides at the 5' end to serve as a primer for positive-strand synthesis. Shortly after, the short primer sequence is translocated to the direct repeat 2 (DR2) at the start of the negative-strand DNA and serves as a primer for the synthesis of the positive strand DNA, generating a circular partially double-stranded DNA [111, 112]. This results in the maturation of RNA-containing nucleocapsids to DNA-containing nucleocapsids within the cytoplasm. Mature nucleocapsids can be trafficked back to the nucleus and converted to cccDNA to sustain persistent infection or enveloped for secretion from the host cell. The amount of L-HBsAg is known to influence which pathway the nucleocapsid goes through; early on in establishing the cccDNA pool, low levels of L-HBsAg contribute to the trafficking of the nucleocapsid to the nucleus (Figure 1.7) [113-115].

As a membrane protein, HBV envelope proteins are generated in the endoplasmic reticulum (ER). Amino acids 8-22, the N-terminal signal sequence, initiate the S protein insertion into the ER membrane. The second signal (amino acids 80 to 98) is a transmembrane domain within the lipid bilayer; the peptide chain downstream of this domain is translocated into the ER lumen while the upstream chain stays in the cytosol. As a result of this, amino acids 23 to 79 in the C-terminal region form a cytosolic loop both in the ER and in the viral particles, while amino acids 99 to 169, which is the MHR, form a luminal loop which is then on the outside of viral particles [49, 116]. Similar to the topology of the S protein, the translocation of the preS2 domain to the ER lumen is by the first signal sequence located in the S domain [48]. The topology of the L protein

13

is slightly more complex than the M and S proteins as it possesses two conformations during and after translation (Figure 1.8). In the e-preS isoform, the preS region is positioned on the outside of the virus, and this is important in receptor binding and cell entry, whereas in the i-preS isoform, the preS region is positioned on the inside of the virion and is crucial for nucleocapsid interaction for envelopment. During translation, the preS (preS1 and preS2) domain of L is in the cytosol of the ER membrane, which is the internal-preS (i-preS) conformation. After translation, translocation occurs in about 50 % of the L proteins, causing a change in their conformation to the external-preS (e-preS) conformation in which the preS domain is in the ER lumen (Figure 1.8) [117-122]. How this posttranslational move occurs remains unclear. It is now known that the HBV S envelope proteins can bud efficiently through the post-ER/post-Golgi compartment (otherwise known as ER-Golgi intermediate compartment, ERGIC) as spherical subviral particles without enveloping the nucleocapsid and are secreted from cells in large amounts [123, 124]. On the other hand, the L protein is not excreted alone, and its presence inhibits the secretion of subviral particles in a dose-dependent manner due to retention motifs in the preS1 N-terminal 19 amino acids. As a result, secretion of the infectious virus particle, which contains high amounts of L protein, is dependent on the L and S ratio during morphogenesis.

Mature capsids move to the post-ER, pre-Golgi compartment, where they interact with the L envelope protein for envelopment and subsequent secretion. Interestingly, mechanisms that prevent the envelopment of capsids with the immature genome (single-stranded DNA or RNA) have been shown, albeit not completely understood [125, 126]. Studies have recently shown that proteins in the endosomal sorting complex required for transport (ESCRT) pathway are involved in the secretion of the infectious HBV Dane particle by forming multivesicular bodies [127-131]. It has been demonstrated that the HBV virions and filamentous subviral particles are released via the endosomal sorting complex required for transport (ESCRT)- multivesicular bodies (MVBs) pathway. It has been shown that alpha-taxilin (interleukin-14) mediates the interaction

between HBV and the ESCRT-MVB complex by binding to the preS1 of the L-HBsAg domain and the ESCRT-I component [132-135].
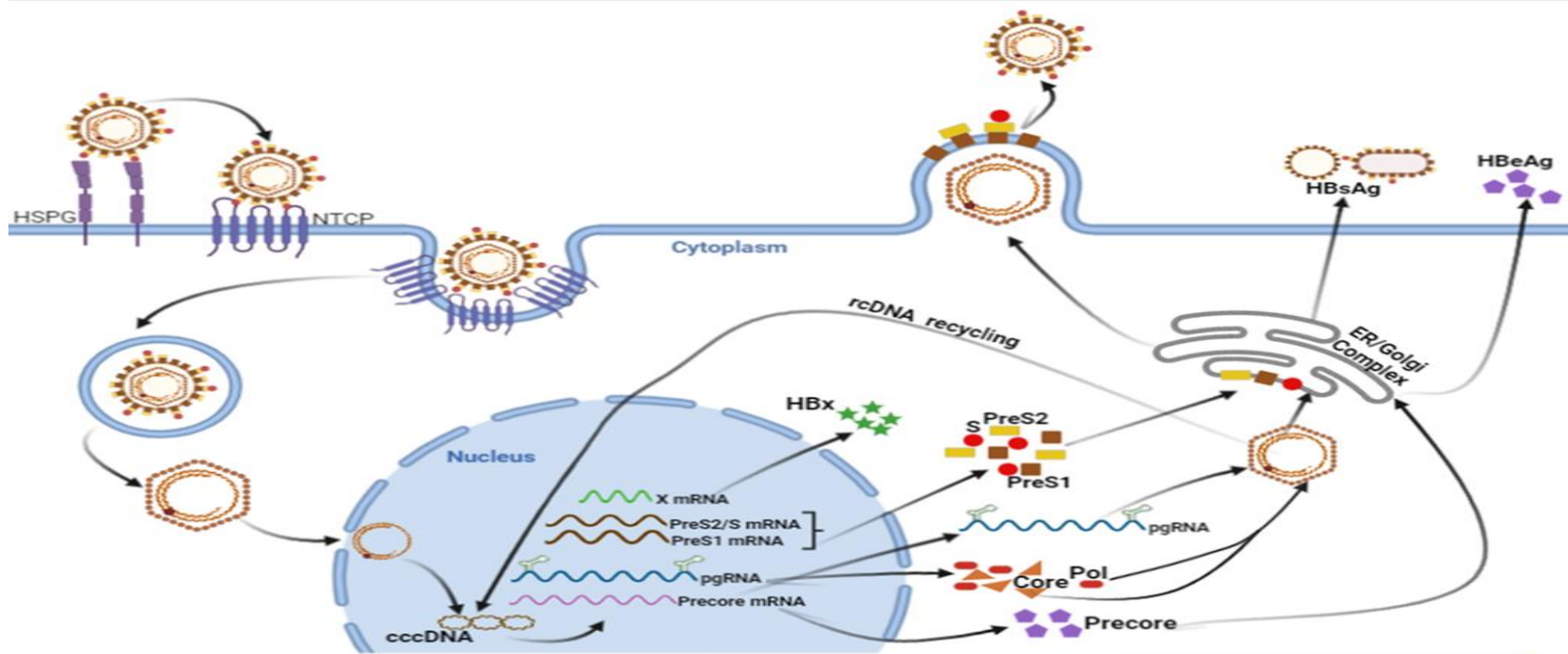
Figure 1.8 HBV lifecycle. HBV binds reversibly to HSPG, then specifically to NTCP, and subsequent endocytosis. HBV relaxed circular DNA (rcDNA) is trafficked to the nucleus and repaired to form the covalently closed circular DNA (cccDNA). HBV cccDNA is the template for the transcription of the pregenomic RNA (pgRNA), precore mRNA, preS1 mRNA, preS2/S mRNA, and X mRNA. These are translated to the polymerase (pol), precore (HBeAg), core (HBcAg), HBsAg (preS1, PreS2 and S), and HBxAg proteins. The pgRNA is encapsidated by HBcAg and is either enveloped by HBsAg for secretion or trafficked back to the cccDNA pool in the nucleus. The figure was created at http://biorender.com/.
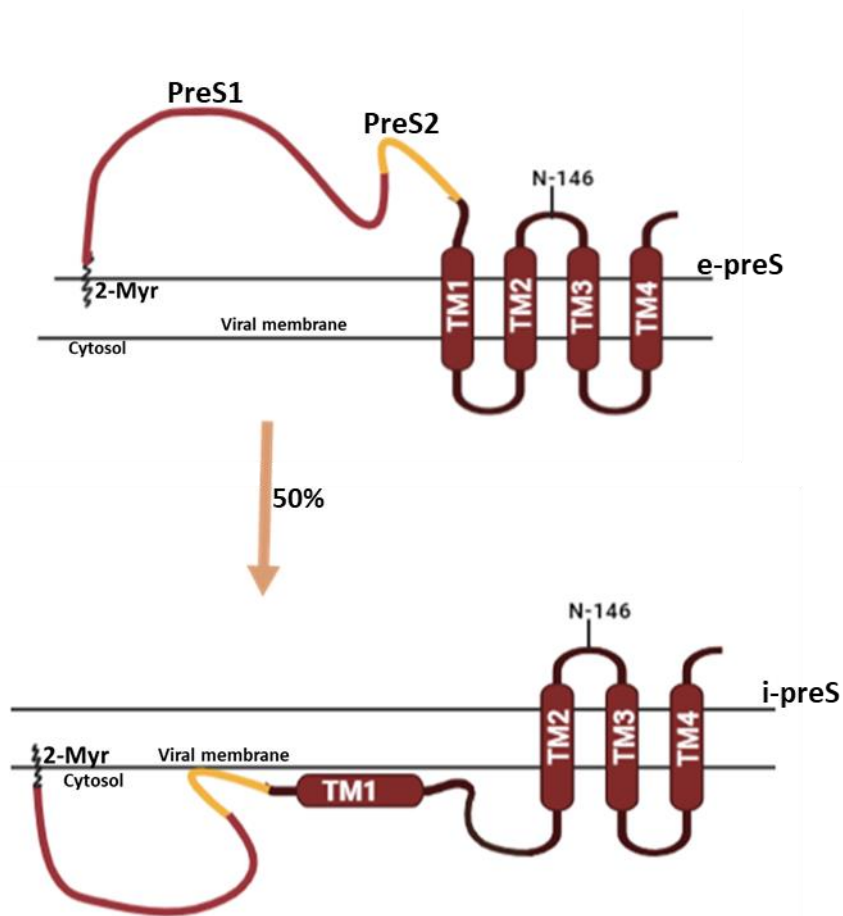
Figure 1.9 External-preS (i-preS) and internal-preS (e-preS) conformations. During translation, the preS (preS1 and preS2) domain of large HBsAg is in the cytosol of the ER membrane, which is the internal-preS (i-preS) conformation. After translation, a translocation occurs in about 50 % of the large HBsAg, causing a change in their conformation to the external-preS (e-preS) conformation in which the preS domain is in the ER lumen. The figure was created at http://biorender.com/.

1.7 HBV Epidemiology

Approximately 300 million people are chronically infected with HBV globally, resulting in 884,000 deaths, mostly from complications [136, 137]. HBV prevalence in different parts of the world has been defined in 3 different levels of endemicity based on the prevalence of HBsAg - low, moderate and high, being <2 %, 2-7 % and >8 %, respectively [138]. Developing regions such as Southeast

Asia, China, sub-Saharan Africa and the Amazon Basin with a large population have a high endemicity, with 70–95 % of the population showing past or present serological evidence of HBV infection, and at least 8% are chronic HBV carriers. In these regions, HBV infections occur majorly during infancy or childhood, leading to high rates of chronic liver disease and liver cancer rates in adults. Regions such as Eastern and Southern Europe, the Middle East, Japan, and South America are moderately endemic, with 10–60 % of the population having evidence of infection, and 2-7 % are chronic carriers. Infections in these regions are commonly acute HBV infection in adolescents and adults; however, chronic infection occurs mainly through infections in infants and children. Most developed areas, such as North America, Northern and Western Europe and Australia, have low endemicity, with only 5–7 % of the population infected in these regions, and only 0.5–2 % of the population are chronic carriers. Most of the infections in these regions are in adolescents and young adults and well-defined high-risk groups such as patients who require regular blood transfusion or haemodialysis, health care workers, injection drug users, and men who have sex with men (Figure 1.9) [139-143].
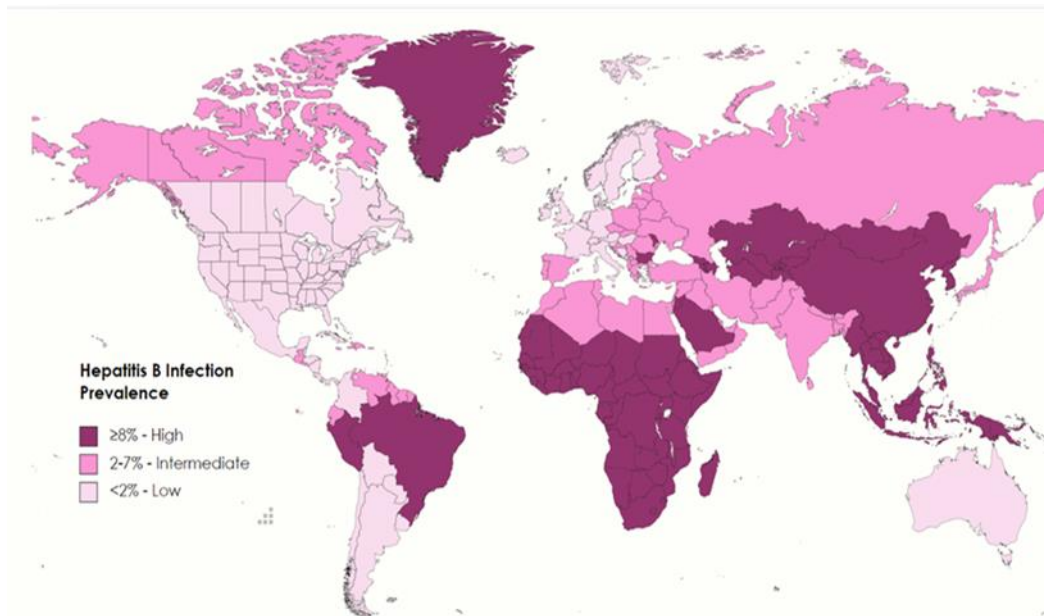
Figure 1.10 Global prevalence of HBV infection showing regions of high, intermediate, and low endemicity. The figure was created at https://mapchart.net/.

1.8 HBV Genotypes and Sub-genotypes

At least 9 HBV genotypes (A-I), a putative genotype J and over 30 sub-genotypes have been identified from isolates worldwide and are characterised by nucleotide divergence of >8 % among genotypes and 4 %-8 % among sub-genotypes. Several studies have reported the differences between these genotypes and sub-genotypes based on geographical distribution, mode of transmission, disease progression, clinical prognosis, and antiviral therapy response. For instance, Genotypes B, C, F, and H possess a genome size of 3215 nucleotides, while the others have varying nucleotide numbers due to in-frame deletions and insertions, notably, genotype D with an 11 amino acid deletion in preS1 of L-HBsAg (Table1.1). In 1971, HBV isolates were classified according to their serological reactivities and based on the amino acid sequences at codons 122 and 160 of the S region, specifying them into the d/y and w/r with a common 'a' determinant, giving four serotypes, namely; adw, adr, ayw, or ayr [26, 144, 145].

Table 1.1 Comparison of Virological, Geographical, and Clinical Features of HBV genotypes [146-148].

Genotype	Genome size (nucleotides)	Sub-genotypes	Geographical distribution	Virological features and Clinical Importance
A	3221	A1-4	Africa, South Asia, Europe, North America	Secretes multiple sizes of HBeAg; earlier HBeAg seroconversion; cause of chronic infection in adults.
B	3215	B1-5	Japan, East Asia, Indonesia, Philippines	Perinatal transmission route; a major cause of chronic infection; better response to interferon therapy than C.
C	3215	C1-16	Australia, Asia	Oldest HBV genotype; higher prevalence of basal core promoter mutations resulting in delayed HBeAg seroconversion; perinatal transmission route; a major cause of chronic infection with a higher risk of HCC and cirrhosis.
D	3182	D1-7	India, Middle East, Mediterranean	Secretes less HBsAg than A-C; perinatal transmission route; major cause acute infection in adults. 11 amino acid deletion in pre S1 of L-HBsAg.
E	3212	----	Sub-Saharan Africa	Closest to genotype D
F	3215	F1-4	Central and southern America	Associated with early HCC development in Alaskan natives than other genotypes.
G	3248	----	France, Germany, and the United States; common among men that have sex with men	36-nucleotide insertion in the core results in high core protein expression; unable to express HBeAg; co-infection with genotypes A or H and HIV.
H	3215	----	Central and South America	Closest to genotype F.
I	----	----	Vietnam and Laos	Complex recombination between genotypes A, C, G.
J	----	----	Japan	Close relationship with gibbon/orangutan genotypes and human genotype C.

1.9 Pathogenesis of HBV Infection

Hepatitis B is a viral infection that targets the liver, causing a wide range of hepatic diseases such as acute and chronic hepatitis, fulminant hepatitis, liver cirrhosis and hepatocellular carcinoma. Initial infection presents no symptoms in many people, but symptoms like vomiting, tiredness, yellowish skin (jaundice), abdominal pain and dark urine can also be seen in others. The infection can be diagnosed 30 to 60 days after exposure, but symptoms may take up to 30 to 180 days to begin and can last a few weeks but rarely results in death [149].

HBV is transmitted by contact with blood or body fluids, making HBV an occupational hazard, particularly in healthcare occupations. In areas where HBV infection is common, vertical transmission from mother to child is the most frequent mode of transmission, while in areas where the disease endemicity is low, the common mode of transmission is horizontal transmission includes: sexual intercourse, intravenous drug use, blood transfusion, tattoo needles, acupuncture needles, body and ear-piecing needles, as well as accidental needlestick injuries [150].

Hepatitis B virus infects and replicates in the liver using the hepatocyte-expressed receptor (s) and co-receptor (s). Hepatocellular damage and viral clearance in HBV infection are caused by an immune response, contributed primarily by virus-specific cytotoxic T lymphocytes (CTLs). Although CTLs kill HBV infected cells and release cytokines, the outcome can be worsened by inflammatory cells and platelets activated at the site of infection [151].

Fulminant hepatitis (massive liver cell death) is a life-threatening complication of acute hepatitis. Death due to fulminant hepatitis has been reported to result from complications of severe liver damage such as sepsis, gastrointestinal bleeding, cerebral oedema, respiratory failure, or kidney failure [152].

1 to 10 % of HBV infected patients may present with extrahepatic manifestations such as papular acrodermatitis, membranous glomerulonephritis, serum-sickness-like syndrome, and acute necrotising vasculitis. Though the pathogenesis of these disorders is unknown, a high level of antigenemia resulting in immune complex-mediated injury is hypothesised to be the cause [153, 154].

1.10 Manifestations of HBV Infection

1.10.1 Acute Hepatitis B

Otherwise called short-term HBV infection, this is defined as HBV infection lasting for less than 6 months. 90 % of healthy adults infected with HBV have acute hepatitis and clear the infection within 6 months. Two-thirds of acutely infected patients have undetected subclinical, asymptomatic illness, while the other one-third present with symptoms and signs of hepatitis ranging from mild fatigue and nausea to jaundice and severe acute liver failure [155]. The prodromal or preicteric period occurring after the incubation period constitutes symptoms such as fever, fatigue, nausea, body aches and anorexia. This phase lasting a few days to 1 week is characterised by detectable DNA, high HBsAg levels and a rise in serum alanine transaminase (ALT). A decrease in viral level marks the icteric phase lasting for 1 to 2 weeks. The convalescence period lasts for weeks or months, during which jaundice resolves, HBsAg is cleared, and HBV DNA disappears from serum. However, acute liver failure occurs in 1 % of acutely infected patients [156-158].

1.10.2 Occult or Latent Hepatitis B (OBI)

OBI is defined as the presence of HBV DNA in the liver tissue or peripheral blood of the patient with undetectable HBsAg in the serum outside the acute phase window period. Based on the antibodies detected, OBI may be seropositive if anti-HBcAg and/or anti-HBsAg are positive or seronegative if anti-HBcAg and/or anti-HBsAg are negative. The cause of occult HBV infection remains unknown, though it is thought to be a long-term consequence of acute hepatitis B resolution [159]. It has been hypothesised that occult HBV infection could involve HBV-DNA integration into host cell chromosomes, mutations of HBV-DNA sequence or altered host immune response; however, OBI, which is due to infection with HBsAg escape mutants, is referred to as false OBI. Clinically OBI is a potential risk factor for HBV transmission through blood transfusion, organ transplantation and haemodialysis, a possible cause of cryptogenic liver disease,

an exacerbating factor of chronic hepatitis B resulting in the development of hepatocellular carcinoma and treatment difficulty. There is no report of the treatment of occult hepatitis B infection. The main characteristic of OBI is detectable HBV DNA and undetectable HBsAg; this implies that OBI diagnosis is done through an HBV-DNA PCR test [160].

1.10.3 Chronic Hepatitis B (CHB)

When hepatitis continues for more than six months, as indicated by the persistence of HBsAg, it is categorised as chronic hepatitis. For unknown reasons, an effective immune response does not begin in chronic infection for years; hence it is asymptomatic early in its course and can be detected only by laboratory tests or evaluating non-specific symptoms. Although 5 %-10 % of adults infected with the virus become chronically infected, 90 % of infected infants infected below the age of 5 become chronically infected. This chronic infection shows no symptoms until after several years when cirrhosis and liver cancer may develop, resulting in 15 %-25 % deaths. As the disease progresses, inflammation progresses, and patients develop symptoms such as fatigue, nausea, vomiting, joint pain, and low appetite. Jaundice occurs later in the disease process and is usually an indication of advanced disease. Severe liver damage and scarring over a long period could result in cirrhosis, a pathological term indicating replacement of the normal liver architecture by nodules of fibrous tissue. Complications of cirrhosis include variceal bleeding due to raised portal pressure, encephalopathy, ascites (fluid in the abdomen) and jaundice due to liver failure. Cirrhosis predisposes to the development of HCC. Chronic hepatitis B is a variable and dynamic disease having four natural stages. However, the overall prognosis is directly related to the severity of the disease, and not all patients go through all four stages [161-164].

1.11 Stages of Chronic HBV Infection

1.11.1 HBeAg positive chronic infection

This stage is characterised by high serum DNA levels, presence of HBeAg, normal serum levels of the liver enzyme alanine aminotransferase (ALT) and minimal or no liver inflammation. In late childhood or adult-acquired HBV, this stage is the incubation period before an immune response to HBV, whereas, in perinatal or early childhood-acquired HBV, this stage may last several years to decades. There is also very low spontaneous HBeAg loss at this stage. The patients at this stage are highly contagious as a result of high viral replication. Since antiviral therapy is not given at this stage, patients are monitored closely for progression [165, 166].

1.11.2 HBeAg positive chronic hepatitis

In this stage, the maturation of the host immune system results in the onset of the inflammatory process that leads to the destruction of HBV-infected cells and their replacement of normal liver tissue by fibrous tissue. Characteristics of this active phase include lower virus level than the HBeAg positive chronic infection phase when viral replication is unopposed, presence of HBeAg, elevated aminotransferase levels and inflammation and fibrosis in the liver. This stage is correlated with the highest risk of progression to cirrhosis and hepatocellular carcinoma. The spontaneous flares of liver necroinflammation indicating intensification of the immune response to HBV is a typical feature of this phase. The flare-ups of hepatitis in this stage precede the disappearance of HBeAg and the development of HBeAg antibody, resulting in the remission of hepatitis. Treatment is given according to the level of viral replication (HBV DNA levels), liver damage, as shown by ALT levels and liver biopsy [166, 167].

1.11.3 HBeAg negative chronic infection

The inflammatory phase leads to HBeAg seroconversion, signifying clinical remission and entry to the HBeAg negative chronic infection phase, though there

could be mild liver inflammation and minimal cirrhosis. This stage is characterised by negative HBeAg, positive HBeAg antibody, normal ALT and low or undetectable DNA levels. The progress of this phase is usually benign, and patients in this phase form the largest group of chronic HBV patients. Although most adults enter this stage rapidly, chronically infected neonates and children can take up to 20 years to achieve HBeAg seroconversion. The prognosis for patients in this phase is good; hence antiviral treatment is not generally recommended. When a patient is confirmed to be in this phase, regular lifelong monitoring of ALT levels and DNA measurements every 6-12 months is usually advised [168, 169].

1.11.4 HBeAg negative chronic hepatitis

This stage is characterised by negative serum HBeAg, detectable anti-HBe, moderate to high HBV DNA levels, and elevated ALT values. There is usually moderate to severe necroinflammation and fibrosis in the liver. Despite the good prognosis of the HBeAg negative chronic infection phase, reactivation of active hepatitis, though rare, is possible and could result in complications such as cirrhosis and hepatocellular carcinoma. Patients with detectable HBV DNA in the serum are particularly vulnerable to HBV reactivation, and this has been observed to occur during or after cytotoxic treatments for malignancies and in cases of co-infection [166, 170].

1.11.5 HBsAg negative

This stage, also called occult HBV is characterised by HBsAg negative, anti-HBc, with or without anti-HBsAg. In this phase, patients have normal ALT and could have low-level HBV replication that may persist with HBV DNA detectable in the liver, although usually not in the serum [166].

Table 1.2 Stages of HBV Infection.

Stage of HBV Infection	HBsAg	HBeAg	HBV DNA	ALT	Liver disease
HBeAg positive Chronic infection	High HBsAg	Positive	High; >10^7	Normal	Low
HBeAg positive Chronic hepatitis	High HBsAg	Positive	High; 10^4-10^7	Elevated	Moderate to severe
HBeAg negative Chronic infection	Low HBsAg	Negative	Low; <2000 IU/mL	Normal	Low
HBeAg negative Chronic hepatitis	Intermediate	Negative	Low; >2000 IU/mL	Elevated	Moderate to severe
HBsAg negative*	Negative HBsAg, with or without anti-HBs	Negative	Low/undetectable	Normal	Low

*HBsAg-negative with undetectable HBV DNA would represent a 'functional cure'.

1.12 Hepatitis D Virus and other HBV Co-infections

The human hepatitis D virus (HDV) is known as the satellite virus of HBV as it requires the hepatitis B virus for infection and replication. HDV is a small virus of about 36 nm and has a small single-stranded circular RNA genome of approximately 1.7 kb. HDV entry into host cells is via the interaction of the N-terminal domain of L-HBsAg with NTCP, and it replicates using the host RNA polymerase II because its genome does not code for a polymerase [171]. HDV can either co-infect simultaneously with HBV or can subsequently super-infect an HBV-infected patient [172]. At least 5 % of chronic HBV patients are affected by HDV infection, accounting for about 12 million HBV and HDV co-infected individuals. Simultaneous co-infection of HBV and HDV usually results in the clearing of both viruses, whereas the subsequent super-infection of HDV typically results in chronic HBV/HDV co-infection that exacerbates liver damage compared to HBV mono-infection and increases the risk of HCC, with 50-70 % developing cirrhosis within 5-10 years [173, 174].

Furthermore, HBV co-infection with HCV is not uncommon, and although the exact number of patients co-infected with HBV and HCV is unknown resulting from the unavailability of large-scale population-based studies [175, 176]. As a result of their similar mode of transmission, HBV/HCV simultaneous co-infection is more common than a super-infection, although, in the occurrence of super-infection, HCV super-infection is reported to be more common than HBV super-infection. In HBV/HCV co-infection, HCV more commonly becomes the dominant virus, reducing HBV DNA levels and resulting in a chronic HCV and occult HBV infection [177, 178].

HBV also co-infects with HIV and has been reported to have a prevalence of 5-20 % of HBV infection in HIV patients. Regions of high HBV endemicity are reported to have a 10-20 % prevalence, while regions of low HBV endemicity have about 5-7 % prevalence [179]. Previously, HBV co-infection with HIV adversely impacted the course of HBV infection and consequently sped up HBV disease progression. However, this picture has been completely modified by adequate treatment and it has now been shown that HBV/HIV coinfected

patients do better because they are in sustained clinical care and on therapy [180].

1.13 Diagnosis of HBV Infection

HBV diagnosis involves the assessment of samples from patients, particularly blood samples for virological and serological markers. Virological tests such as the HBV DNA test is a viral load quantification test that is also used to track the effectiveness of therapeutic agents. In contrast, serological tests are typically used for diagnostic screening and identify acute, self-limited infections, chronic HBV infections and vaccine-induced immunity. HBV DNA – the viral load - is an important diagnostic parameter in HBV clinical management; however, HBsAg, which is the initial serological marker, is the primary diagnostic marker for HBV infection. HBsAg is used to identify chronic HBV infection, whereas HBV DNA could predict infection and treatment prognosis, such as the risk of hepatocellular carcinoma [181]. The major hydrophilic region (MHR) within the S-domain of HBsAg contains highly conformational epitopes recognised by neutralising antibodies in routine diagnostic tests. Table 2 describes the laboratory markers of HBV infection [182-184].

Table 1.3 Laboratory markers of HBV infection.

HBV Marker	Clinical Significance
HBsAg	present in acute or chronic infection.
Anti-HBsAg	A marker of immunity; can be acquired through natural HBV infection, vaccination, or passive antibody (immunoglobulin).
Anti-HBcAg	IgM—indicates HBV infection in the past six months.
	IgG—indicates a more distant HBV infection that could have been cleared by the immune system or that could still be present.
	A positive HBsAg and anti-HBc IgG—indicates persistent chronic HBV infection.
HBeAg	It is associated with a high level of viral replication, often known as the marker of infectivity.
Anti-HBeAg	Indicates a low level of viral replication
HBV DNA	A marker of viral replication; could predict infection and treatment prognosis, such as the risk of hepatocellular carcinoma

1.14 Treatment and Prevention

A combination of serum ALT, serum HBV DNA levels, and other HBV markers are used as indications for HBV treatment. Ultimately, antiviral therapy seeks to eradicate HBV infection from the host, although the stable cccDNA in the hepatocyte nucleus makes this goal difficult to achieve. Alternatively, available therapies are focused on achievable goals such as reducing the risk of hepatocellular carcinoma by suppressing HBV replication, reducing liver inflammation, and preventing liver failure and cirrhosis. Treatment success is measured by a decrease in HBV DNA level, a loss of HBeAg (an indication of seroconversion), normalised ALT levels, and improved liver histology [185]. There are currently two groups of approved antiviral agents for managing chronic HBV infection: immunomodulatory agents (including conventional and pegylated interferon-α) and oral nucleotide/nucleoside analogues (NAs). Interferons are known to exert a weak direct antiviral effect on HBV by acting on different parts of the lifecycle and supporting cell-mediated immunity. Although the mechanism(s) by which interferon affects HBV is(are) not clear, it has been shown to decrease the transcription of pregenomic RNA (pgRNA) and subgenomic RNA from the HBV cccDNA minichromosome, both in cultured cells and in mice. Treatment with interferon has also been reported to result in cccDNA transcriptional co-repressor active recruitment and cccDNA-bound histone hypoacetylation. Also, studies have shown its ability to upregulate class I major histocompatibility complex (MHC) antigen expression in infected hepatocytes and activate various immune pathways and cytokines that inhibit viral replication [101, 186-191]. The finite duration of therapy and the lack of drug resistance are the pros of the use of interferon-based therapy, although a proportion of patients will not respond to treatment or will still require long-term treatment with NAs upon completion of interferon therapy [192]. On the other hand, interferon treatment may result in significant adverse effects, including flu-like symptoms, abnormal blood counts, psychological side effects such as depression, suicidal feelings, aggression, and psychosis. Also, high interferon levels can lead to damage to vital parts of the body, such as the heart,

liver, bone marrow, kidney, and heart. Patients on interferon therapy need to be closely monitored for any side effects [193].

Nucleoside/nucleotide analogues are a polymerase-targeting group of antiviral drugs used in chronic HBV management. Nucleoside analogues contain a nucleic acid analogue and a sugar, whereas nucleotide analogues contain a nucleic acid analogue, a sugar, and 1 to 3 phosphate groups. Five of these analogues, including three nucleoside analogues (lamivudine, telbivudine and entecavir) and two nucleotide analogues (adefovir and tenofovir), have been approved for use as a chronic HBV therapy. Upon phosphorylation and being similar to nucleotides, these analogues are incorporated into growing DNA strands where they act as chain terminators and inhibit the reverse transcriptase activity of viral DNA polymerase [169, 194, 195]. The potential for the development of drug resistance mutations as HBV therapy continues is a major demerit of the use of nucleos(t)ide analogues. HBV has a high replication rate with approximately 1×10^{11} virus particles being released every day, which in addition to the lack of an effective proofreading mechanism in the HBV polymerase enzyme, contributes to the development of mutations. It has been estimated that an error rate of $1.4–3.2 \times 10^{-5}$ nucleotide substitutions per site per cycle is made by the HBV polymerase, resulting in many natural mutations, out of which some would confer drug resistance. Selective pressure resulting from nucleos(t)ide analogue therapy drives drug-resistance mutations that can alter the interaction between the HBV polymerase binding sites and antiviral agents. Consequently, due to the overlapping nature of the HBV genome, mutations in polymerase gene driven by antiviral drugs can also lead to mutations in the S gene, which may evade neutralising antibodies [196-199].

Recent HBV studies have led to more knowledge of the HBV lifecycle and provided a better understanding of the virus. This has resulted in a drive for the identification of novel antiviral compounds and an improved HBV therapy. The discovery of the NTCP receptor has expedited research into the identification of possible entry inhibitors. Several compounds have been identified with the ability to interfere with HBV entry into hepatocytes, and the most popular is

Myrcludex [200]. Myrcludex or Bulevirtide is a synthetic myristoylated peptide made up of amino acids 2-48 from the PreS1 region. It functions by binding to and inactivating the NTCP receptor, thus preventing HBV and HDV from infecting hepatocytes. This drug has recently been conditionally approved (as hepcludex) by European Union in July 2020 for use as an HDV drug in HBV/HDV co-infected patients [201, 202]. Several other compounds being developed include cyclosporin, irbesartan, rapamycin, and ezetimibe. Some of the other therapeutic targets which are currently being researched include drugs that directly target the HBV cccDNA to inactivate or degrade the cccDNA, drugs that target the innate immune system, targeting pathogen recognition receptors and triggering the immune cells to produce pro-inflammatory factors and drugs that target the adaptive immune system to increase the HBV-specific T-cell immune response [203, 204].

Prevention strategies for HBV infection are focused mainly on active immunisation, passive immunoprophylaxis and behavioural modifications. Hepatitis B vaccine is a recombinant vaccine consisting of a sterile suspension of non-infectious HBV subunit derived from HBsAg produced in yeast cells. This vaccine given in 3 or 4 shots at different times has been widely used worldwide since its approval in 1981. The HBV vaccine has been shown to have an efficacy of up to 95 % and provides protection for at least 20 years. It functions by stimulating the production of anti-HBsAg antibody by the immune system into the bloodstream, which provides protection against future infections. Passive immunoprophylaxis against HBV infection is conferred using the Hepatitis B Immune Globulin (HBIG), a sterile solution of ready-made antibodies against hepatitis B infection. HBIG is an antibody preparation made from pooled human blood from selected donors with high hepatitis B antibody. Passive immunoprophylaxis is administered following sexual exposure, needle or sharp object exposure, organ transplantation, and babies born to HBV positive mothers. In 2017, WHO recommended that all infants be given the hepatitis B vaccine within 24 h after birth followed by 2 or 3 doses at least 4 weeks apart. This recommendation has been adopted by several member countries of the

WHO, including the UK [205]. Although behavioural modifications such as safe sexual practices, safe handling of sharps and improved screening of blood products are beneficial, active immunisation and passive immunoprophylaxis are the most effective prevention strategies [138].

1.15 Laboratory Study of HBV

HBV, similar to other hepadnaviruses, is strictly hepatotropic and possesses a narrow host range, causing infection by interaction with specific receptors in the host hepatocytes. Usually, hepadnaviruses only infect differentiated primary hepatocytes or cultured hepatocytes from their respective hosts. As a result, available cell and animal systems for the study of HBV infection and life cycle have been limited, impeding HBV research. The discovery of NTCP as a receptor for HBV infection has expanded the cell and animal culture study models, thus facilitating the study of HBV entry and pathogenesis.

1.15.1 Cell culture systems for HBV study

The primary cell culture systems used to study HBV infection include primary human hepatocytes (PHH) and primary Tupaia hepatocytes (PTH). Primary human hepatocytes directly isolated from liver tissue are the closest representation of *in vivo* human liver hepatocytes. Hence, they support the complete lifecycle of HBV and are crucial in studying cellular immune and metabolic responses to HBV infection. In addition to being limited in supply and expensive, PHHs are highly variable among batches, have low proliferation ability in culture, and dedifferentiate rapidly in culture, thus losing their susceptibility to infection and supporting a limited spread infection [206-209]. The high variability in PHH batches has been said to be due to the quality of the isolated cells and host genetic differences. As a result of their importance in HBV research, primary human hepatocytes have constantly been improved to enhance differentiation and proliferation via various methods such as Dimethyl sulfoxide (DMSO) incubation, PHHs co-culture with non-parenchymal liver cells, and 3-dimensional

32

(3D) culture organisation [210]. Studies have shown that 3D cultured PHHs express hepatocyte genes and maintain function stably for 4 weeks or more and are susceptible to HBV infection in the absence of Polyethylene glycol (PEG) or DMSO [211]. PTHs have also been an alternative system for HBV study, and interestingly, the NTCP receptor was discovered using PTHs [81, 212].

HepaRG cells were derived in 2002 as a bipotent progenitor cell line from a chronic hepatitis C infected patient. It was found that culturing HepaRG with DMSO, PEG and hydrocortisone increased their differentiation into hepatocyte-like epithelium-like cells, enabling them to support HBV infection and replication, producing infectious particles for over 100 days [64, 213]. HepaRG cells have been used to show the reversible binding of HBV to its low-affinity co-receptor, HSPG and other entry inhibition studies such as Myrcludex B studies. Studies investigating cellular immune responses to HBV infection have shown that a transitory type I interferon response is mounted by cells after HBV infection, which could suppress HBV replication [50, 214-216].

Hepatoma cell lines include but are not limited to HepG2, derived in 1975 from a 15-year-old HCC patient, Huh7, derived in 1982 from a 57-year-old liver tumour patient and Hep 3B, derived in 1976 from an 8-year-old HCC patient [217]. For a long time, these hepatoma cell lines have been used to study HBV replication and virion production by transfecting them with cloned HBV DNA constructs carrying overlength HBV genomes. Transient and stable transfection of these cells with the HBV constructs has enabled researchers to study HBV cccDNA, transcription, gene expression, assembly and secretion of infectious and subviral particles. This knowledge has enhanced the study of antiviral compounds and the characterisation of HBV variants and drug-resistant mutants [218, 219]. Several stable cell lines producing HBV have been generated and used to produce HBV inocula and to investigate HBV host interaction and drug screenings. They include HepAD38 and HepDE19, which use a tetracycline-repressible promoter to drive pgRNA expression and HepG2.2.15 cell line, previously used to study HBV integration into the host genome [92, 220-222]. As much as HepG2 and Huh7 support HBV replication, they are known to poorly express the NTCP receptor

and are not susceptible to HBV infection, just like several other human hepatoma cell lines. They also provide a less than optimum environment for transcription and do not fully mimic *in vivo* infection of hepatocytes and the host immune response [81, 223].

Following the discovery of NTCP as a functional receptor of HBV infection, hepatoma cell lines that stably express the human NTCP gene have been generated. The establishment of these new cell culture systems (HepG2.NTCP and Huh7.NTCP) have expanded the *in vitro* assays and accelerated our knowledge of steps involved in HBV early infection [223-226]. As a result, other host factors such as glypican 5 and epidermal growth factor receptor (EGFR) have been shown to be additional factors in HBV entry [89, 227]. In addition to supporting HBV entry and cccDNA establishment, HepG2.NTCP, in the presence of PEG, has been shown to support the spread of HBV infection among cultured cells [228]. However, the use of NTCP-expressing hepatoma cells is typically impeded by low infection levels, the need for large viral inocula and low virus release from infected cells [86, 229]. In spite of these drawbacks, NTCP-expressing hepatoma cells are relevant *in vitro* systems for studying the HBV life cycle, particularly the early steps of infection that are potential therapeutic targets.

1.15.2 Virus Pseudotyping

Pseudotyping is a process that involves the generation of a virus with envelope glycoproteins not encoded by the genome within the virus. Hence, a pseudotyped virus, also called pseudotype, is known as a virus comprising of a genome and capsid enveloped by foreign surface glycoproteins (Figure 1.10) [230, 231]. This implies that a pseudotyped virus can only carry out a single round of infection as it enters a susceptible cell and drives nucleic acid replication but is unable to generate infectious particles. The foundation of pseudotyping was first laid by Peyton Rous in 1911 when he identified the Rous sarcoma virus (RSV) from chicken sarcoma cells [230]. Years after, Harry Rubin

and colleagues reported from their observations that RSV is a defective virus that is unable to produce mature virus except in the presence of a helper virus which they called Rous-associated virus (RAV).
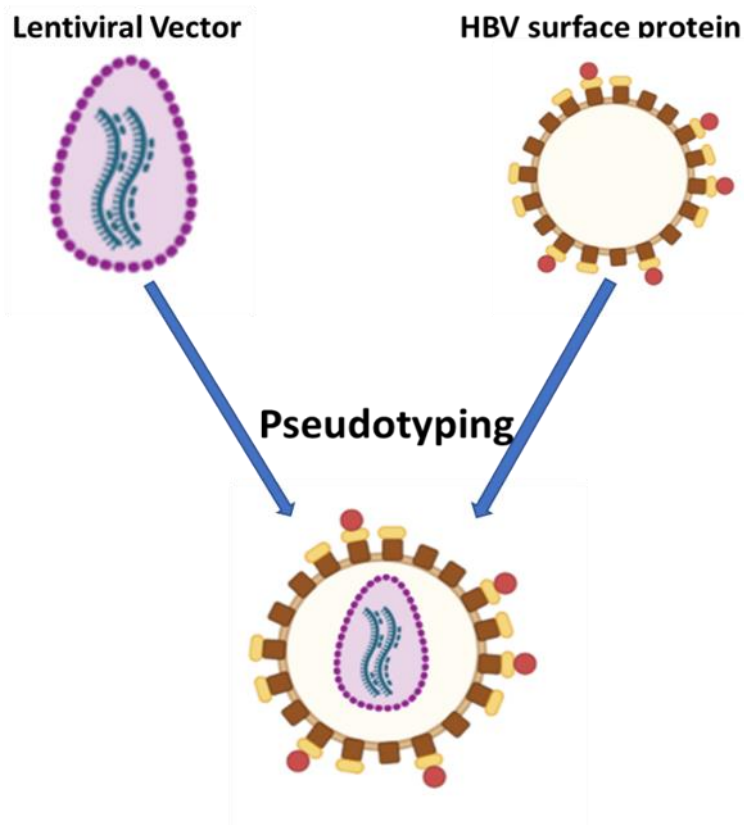
Figure 1.11 Schematic representation of Pseudotyping technique. The figure was created at http://biorender.com/.

Consequently, although RSV and RAV were antigenically unrelated, the mature virus generated by a co-infection of both viruses resulted in pseudotypes carrying the RSV nucleic acid and the RAV outer coat [232-234]. The pseudotyping system has been applied severally in various experimental and clinical setups. Pseudotyping enables studying viral envelope proteins, their tropism, and their interaction with host cell receptors, thus enabling the identification of new entry receptors and attachment factors. Pseudotyped viruses enable studies that examine the envelope gene, thus isolating steps in the virus life cycle that the envelope gene is responsible for. Also, pseudotyping provides ease for experimental genetic manipulation of the virus gene, allowing

the introduction and study of mutations in the envelope gene to understand how these mutations affect the virus entry steps. In addition to the safety benefits of pseudotyping, which enables the study of higher biosafety level (BSL) viruses in lower biosafety level (BSL) laboratories, chemical entry inhibitors and antibodies can also be specifically screened.

Essentially, pseudotypes are produced when a viral vector plasmid, otherwise called the backbone carrying the nucleic acid and core protein, is transfected in a producer cell together with the envelope protein plasmid and the reporter plasmid. Due to their advantageous ability to incorporate other viruses' envelope proteins and stably integrate their genome into the host genome, retroviral vectors have been the preferred vector for a long time. There are two retroviral vector systems: gammaretroviral vectors exemplified by the murine leukaemia virus (MLV) and the lentiviral vectors exemplified by HIV-1. Although MLV vectors have been commonly used in the past for several clinical trials, there has been a shift of preference to lentiviral vectors because of their ability to translocate through nuclear membranes and transduce dividing and non-dividing cells as well as their ability to be produced at high titres. Lentiviral vectors are made up of the lentiviral vector genome bordered by 5' and 3' long terminal repeats (LTRs) that are essential for regulating viral genome expression, the HIV rev response element (RRE), that is involved in the export of RNAs from the nucleus to the cytoplasm for translation and packaging via an encapsidation signal sequence (ψ). There are three generations of lentiviral vectors, each designed to improve on safety from the previous one. First-generation lentiviral vectors, which still contain all viral genes except the envelope gene, have a high risk of generating replication-competent lentiviruses, particularly if working with HIV positive samples. Second-generation lentiviral vectors contain all HIV genes except the envelope gene and other accessory genes such as nef, vpu, vpr that are not crucial for lentiviral production. In as much as this is safe, care has to be taken in handling as there might still be a chance of generating replication-competent lentiviruses, especially when working with HIV positive cells and samples of unknown viral composition. Third-generation lentiviral vectors have

been significantly improved with the elimination and inactivation of all lentiviral genes except gag, pol, rev and RRE to ensure it is safe for research and clinical use. In the third-generation vectors, a CMV promoter is inserted to drive the transcription of genes, eliminating the need for the Tat gene that drives gene expression from the LTRs in the previous generations. Also, the 5' LTR promoter is removed while the rev gene is separated and is expressed from a different plasmid. Other ways to improve safety are still being investigated as there is also a chance of mutation or recombination, leading to the generation of replication-competent lentiviruses.

The human Embryonic Kidney cell line, HEK293T, is the preferred cell line for producing pseudotypes using lentiviral vectors primarily because it carries the simian virus SV40 T-antigen that enhances its efficiency for vector production. Lentiviral vectors mostly contain the SV40 origin of replication; thus, binding the SV40 T-antigen from the SV40 origin of replication stimulates replication of the lentiviral genome. The presence of SV40 T-antigen also suppresses tumour suppressor proteins that increase cell growth and transfection efficiency. In pseudotype generation, HEK293T cells are co-transfected with the lentiviral vector and an envelope plasmid of choice; internal promoters drive the expression of both plasmids. The pseudotyped virus buds out of the cell with the expressed envelope proteins on the outside and the lentiviral nucleocapsid within. The pseudotyped virus can be harvested from the cell culture supernatant for use in subsequent studies. A reporter gene such as luciferase (Luc) or green fluorescent protein (GFP) is usually cloned into the lentiviral vector plasmid and is essential for monitoring replication and gene expression of the pseudotyped virus. Pseudotyped viruses have been and continue to be an essential part of molecular and clinical research by offering flexibility and safety and enabling the study of highly pathogenic biosafety level BSL 3 or 4 organisms in BSL 1 or 2 labs. It also enables *ex vivo* genes to be studied without the possibility of tissue culture adaptation of the virus [235, 236]. Following the Middle Eastern respiratory syndrome (MERS) outbreak in 2012, pseudotyping was an effective rapid tool to track the viral prevalence, study the viral proteins

and test the efficacy of neutralising antibodies [237-240]. During and after the Ebola virus outbreak, pseudotyping has been actively used in research to study genetic variations, show a human adaptation in the outbreak, and study the viral proteins to identify potential entry inhibitors and antiviral therapy [241-244]. Pseudotyping has also been widely used to study Hepatitis C virus (HCV) glycoproteins and their entry characteristics *in vitro*. With the use of pseudotyping, host and cell entry properties have been characterised, leading to the identification of entry co-receptors such as claudin-1, claudin-6, claudin-9, CD81 tetraspanin, and SR-B1 scavenger receptor [245-250].

1.16 Previously reported mutations in HBV genome

During HBV infection and due to different selection pressures, random point mutations may arise during replication, cleavage or ligation of the viral genome or editing and splicing of the pgRNA. Mutations that occur at specific infection stages have been found in different genetic regions such as in the precore, core region, the basal core promoter region, pre-S1, or pre-S2 regions, the 'a' determinant of HBsAg, and the polymerase. These mutations are essential in the persistence and escape of the virus from immune detection. Interestingly, it is known that HBV wild type strains have remained unreplaced for centuries, which strongly suggest that they are advantageous, particularly early on in the infection, after which quasispecies begin to develop in later stages of infection [251, 252].

Mutations in the basal core promoter (BCP) that controls HBeAg transcription and the precore (PC) region that controls HBeAg translation have been thoroughly studied. Mutations such as the 1762T/1764A double mutation in the BCP and 1896A in the PC regions are the most commonly studied and have been shown to impact the stability of the pgRNA secondary structure and replication. Adenine to Thymine at position 1762 and Guanine to Adenine at position 1764 are within the CCAAT/Enhancer binding protein binding region. Studies have shown that their presence is implicated with a significant decrease in the precore

and core mRNA transcription that could lower HBeAg production. These mutations are less common in asymptomatic HBV carriers and are detected more frequently in chronic, fulminant and HCC HBV patients. Also, at position 1896, a Guanine to Adenine substitution that occurs in the epsilon (ε) of the precore gene results in a stop codon (TAG) at codon 28 of HBeAg [253-257].

In recent years, antiviral drug-resistance mutations in the pol gene have increased due to the increased use of nucleoside and nucleotide analogues as HBV antiviral agents. The most commonly studied drug-resistance mutation is the rtM204V/I in domain C, a known lamivudine resistance mutation. This mutation changes the conserved YMDD motif to YVDD or YIDD and is compensated by an upstream secondary mutation at rtL180M or rtV173L in the HBV polymerase domain B said to improve the replicative efficiency of the resistant mutant. Additionally, rtN236T in domain D and rtA181T/V in domain B are reported to be adefovir dipivoxil resistance mutations. rtT184S/A/I/G/C/M, rtS202I/C/G, and rtM250I/V have also been mapped to domains B, C, and D and are entecavir resistance mutations [258-263]. Furthermore, deletions or insertions in the BCP result in a shift of the X gene frame, leading to the production of truncated X proteins that lack the C terminus domain (amino acids 130–140) necessary for the transactivation activity of HBx antigen [264].

Several point mutations, recombinations and deletions have been found in the HBsAg, particularly the "a" determinant of the major hydrophilic region (MHR). The S ORF is highly heterogeneous, having mutations that can change the protein conformation, affecting HBsAg antigenicity. In the "a" determinant that is crucial for the generation of protective antibody, mutations could result in escape from vaccine-induced immunity, immunoglobulin therapy, and serological diagnostic tests [251, 265-267]. The G145R (glycine to arginine at residue 145 of HBsAg) identified in 1988 from vaccinated Italian children who have HBsAg positive mothers has now been described as an immune escape mutation [268-270]. Interestingly, in as much as the HBV vaccine is highly efficient in preventing HBV infection, vaccine escape mutations such as D144A/E, T116N, P120S/E, I/T126A/N/I/S, Q129H/R, M133L that have been identified in vaccinated

individuals have been associated with breakthrough infections. Furthermore, in their report, Salpini *et al.,* showed that 75.9 % of that had undergone reactivated HBV infection in the study carried more than one of the mutations: M103I-L109I-T118K-P120A-Y134H-S143L-D144E-S171F located in the MHR [271]. Several recent studies, such as Cassini *et al.,* have suggested that mutations such as C695T that leads to a stop codon in amino acid 181 in HBsAg could be responsible for substantially reducing HBsAg production seen in occult HBV infection [272]. Also, mutations in the pre-S region have been shown to contribute to hepatocarcinogenesis. Lee *et al.,* have discovered and associated the mutation W4P/R in pre-S1 to increased disease severity and liver disease [273-278].

1.17 Research Aims

The proofreading inability of the HBV polymerase and the overlapping nature of the HBV genome culminates in high mutation rates with pleiotropic effects on both the polymerase and the surface genes. Hence, the emergence of mutations in the surface gene, particularly in the MHR, results in mutant selection by antiviral therapy or the host immune system. Previous studies have shown that mutations in the surface gene of HBV potentially influence HBsAg expression and secretion, which could be the underlying mechanism for HBsAg level fluctuations of clinical relevance, such as in occult HBV infection [271, 279]. However, amino acid mutations in HBsAg have also been linked to several clinical implications such as vaccine escape or failure of HBV diagnostic assays that could potentially result in the spread of HBV from blood and organ donation and delayed clinical management [251, 268, 280-283]. Hence, it is essential to further characterise HBsAg and the effects of the mutations on the protein phenotype, particularly its antigenicity and immunogenicity. Studies exist that have sought to characterise different HBV entry stages and the effect of mutations on HBV entry using infectious HBV inoculum or vectors carrying the HBV full-length genome [87, 284-287]. However, in this study, we aim to isolate the potential effect of HBsAg mutations on HBV entry using the pseudotyping system to study only the S gene and mutations present in it. Therefore, the objectives of this study were to:

• Identify areas of variability within HBsAg.

• Design and optimise a pseudotyping system for the *in vitro* study of HBsAg.

• Determine the phenotypic characteristics of HBsAg mutants.

• Examine the entry and immunogenic properties of HBsAg mutants.

• Determine the clinical diagnostic properties of HBsAg mutants.

Chapter 2

Phylogenetic Analysis of Hepatitis B Surface Protein (HBsAg)

2.1 Introduction

Hepatitis B virus (HBV) infection is a global health challenge that has infected about 2 billion people, with 30 million new infections yearly, and chronically infects 300 million people globally with 884,000 yearly deaths [136, 137]. HBV infection can present as an acute or chronic infection; an acute infection presents with symptoms and signs of hepatitis ranging from mild fatigue and nausea to jaundice and severe acute liver failure, particularly in adults [288]. On the other hand, chronic infection is more long-term, showing no symptoms until after several years when cirrhosis and liver cancer may develop, accounting for deaths of 15 %-25 % of chronically infected patients [161]. HBV has been classed into 9 genotypes (A-I) based on genetic similarity and a putative genotype J. These genotypes possess nucleotide divergence of >8 % between them, and there are over 30 sub-genotypes with nucleotide divergence of 4 %-8 %. These genotypes and sub-genotypes differ in their geographical distribution, mode of transmission, disease progression, clinical prognosis, and response to antiviral therapy [289]. Genotype A is predominant in Europe, North America and some parts of Africa, B and C are predominant in east and southeast Asia, D is predominant in India, Middle East, Mediterranean, while genotype E is restricted to Central and West Africa. Genotype F is predominant in Central and Southern America; genotype G has been reported in France, Germany, and the United States; genotype H has been identified in Central and South America, genotype I has been reported in Vietnam and Laos, while the newest HBV genotype, genotype J, has been reported in Japan [144]. Regions such as the Asia Pacific and sub-Saharan African are known as high-HBV prevalence regions, having 45 % of the world's HBV population. In contrast, regions such as Australia, Asia, Northern and Western Europe, Japan, North America have low prevalence with approximately 12 % of the world's HBV population [144, 145].

HBV ORF P encodes the HBV polymerase, which carries the reverse transcriptase enzyme responsible for the reverse transcription of the pgRNA and synthesis of the DNA, while the ORF S encodes the HBV envelope proteins [5, 30]. The HBV reverse transcriptase, similar to HIV-1, carries 7 catalytic domains A-G; the conserved motif of tyrosine-methionine-aspartate-aspartate (YMDD), the reverse

transcriptase enzyme active site, is contained in domain C. The reverse transcriptase enzyme lacks proofreading due to the absence of an exonuclease activity responsible for eliminating mispaired nucleotides [290, 291]. Consequently, the reverse transcriptase has a higher error rate than other DNA polymerases resulting in the accumulation of mutations faster during replication. Generally, the HBV mutation rate has been estimated to be between 1.4 and 3.2×10^{-5} base substitutions per site per year, about 100 times more than other DNA viruses but 100-1000 times less than RNA viruses [292, 293]. The error-prone characteristic of the reverse transcriptase enables HBV quasispecies, an HBV viral population consisting of a mix of variants [294].

HBV quasispecies continually undergo positive/Darwinian selection and negative/purifying selection brought about by antiviral therapy and host immune surveillance. Positive/Darwinian selection enables the spread of advantageous variants, whereas negative/purifying selection results in the selective elimination of harmful variants. As a result, *in vivo* HBV infection exists as a flexible, constantly evolving, highly variable population [295, 296]. The overlapping nature of the HBV genome presumably limits the number of viable variants because an amino substitution would have to be beneficial or neutral in the overlapping genes for the variant to be stable and infectious. On the other hand, an increased fitness in one gene may mitigate any deleterious effect of the second substitution. Notwithstanding, several characteristic mutations present in the polymerase and surface genes have been described and associated with antiviral resistance and immunological escape [297-300].

Prediction of the clinical outcomes of HBV infection is variable and dependent on viral factors, host factors, HBV genotype and the presence of specific viral mutations. Having a better understanding of the genetic variability of HBV in infected patients is crucial for monitoring clinical progression and enhancing clinical management. Ultimately, an investigation of the phenotypic effect of the HBsAg mutations is needed to gain insight into the effects on protein expression and function. However, evaluating the HBsAg variability and identifying common and rare mutations in the sequences is foundational, and this chapter aims to achieve that.

2.2 Methods

2.2.1 Demographics of the Nottingham cohort

73 samples of Nottingham outpatients were recruited within the Nottingham cohort and taken for this study. Their clinical characteristics and demographics which were previously characterised in the clinics are listed in table 2.1.

Table 2.1 Demographics and Clinical data of the Nottingham cohort.

Patient's sample number	Genotype	Gender	Ethnicity	Age (years)	Therapy	HBeAg	Anti-HBe	Viral load	HBsAg Index (IU/ML)
CSNC1	B	Male	Chinese	52	None	Negative	Positive	2.80×10^4	8.83×10^2
CSNC2	A	Male	British	63	Tenofovir and Lamivudine	Positive	Negative	3.10×10^3	2.29×10^3
CSNC3	B	F	Chinese	39	None	Positive	Negative	5.00×10^7	1.24×10^4
CSNC4	B	F	Chinese	39	Interferon	Positive	Negative	2.50×10^5	8.89×10^3
CSNC5	B	F	Chinese	39	Interferon	Positive	Negative	6.30×10^3	9.76×10^2
CSNC6	E	F	African	58	None	Negative	Positive	2.20×10^4	8.61×10^2
CSNC7	B	F	Chinese	39	Interferon	Positive	Negative	Unknown	5.04×10^2
CSNC8	B	F	Chinese	39	Interferon	Positive	Negative	Unknown	3.46×10^2
CSNC9	B	F	Chinese	39	Interferon	Positive	Negative	9.80×10^2	1.65×10^2
CSNC10	A	F	White British	70	None	Negative	Positive	6.80×10^3	5.38×10^3
CSNC11	B	F	Asian	54	None	Positive	Negative	2.00×10^7	1.85×10^4
CSNC12	B	F	Chinese	38	None	Positive	Negative	2.20×10^8	1.57×10^4
CSNC13	B	F	Asian	33	None	Positive	Negative	2.10×10^8	3.68×10^4

CSNC14	A	Male	British	42	None	Positive	Negative	3.70×10^2	3.53×10^4
CSNC15	C	F	Chinese	35	None	Positive	Negative	5.60×10^8	5.38×10^4
CSNC16	C	F	Chinese	44	None	Positive	Negative	4.30×10^8	7.17×10^4
CSNC17	D	Male	Pakistani	43	None	Negative	Positive	1.60×10^5	5.61×10^2
CSNC18	C	Male	Asian	53	None	Positive	Negative	1.50×10^7	3.53×10^3
CSNC19	D	Male	Unknown	45	Tenofovir and Lamivudine	Negative	Positive	3.90×10^3	1.40×10^3
CSNC20	B	F	Asian	40	None	Negative	Positive	3.20×10^3	3.35×10^3
CSNC21	A	F	White British	38	None	Negative	Positive	6.60×10^3	5.96×10^4
CSNC22	D	F	Unknown	59	None	Negative	Positive	2.20×10^4	2.86×10^3
CSNC23	E	F	African	33	None	Positive	Negative	1.80×10^1	5.47×10^3
CSNC24	B	F	Chinese	65	None	Negative	Positive	1.50×10^2	1.76×10^1
CSNC25	D	F	Unknown	38	None	Negative	Positive	2.30×10^2	9.37×10^2
CSNC26	D	F	Unknown	36	None	Negative	Positive	4.20×10^1	3.21×10^4
CSNC27	B	F	Asian	54	None	Positive	Negative	2.70×10^7	4.00×10^3
CSNC28	E	F	African	43	None	Negative	Positive	2.70×10^2	6.57×10^3
CSNC29	A	Male	African	43	None	Negative	Positive	2.10×10^2	6.31×10^3
CSNC30	B	Male	Asian	34	None	Negative	Positive	2.10×10^2	7.09×10^3

CSNC31	B	F	Chinese	62	None	Negative	Positive	1.30×10^7	1.41×10^3
CSNC32	D	F	Indian	42	None	Negative	Positive	2.10×10^3	2.10×10^4
CSNC33	D	F	Unknown	38	None	Negative	Positive	7.70×10^1	1.80×10^4
CSNC34	A	F	Caribbean	61	None	Negative	Positive	7.70×10^2	3.31×10^2
CSNC35	B	F	Chinese	39	Interferon	Positive	Negative	5.40×10^2	1.37×10^2
CSNC36	A	F	Unknown	57	None	Negative	Positive	2.10×10^3	4.46×10^1
CSNC37	B	Male	Asian	46	Interferon	Positive	Negative	7.00×10^1	2.09×10^1
CSNC38	C	F	Chinese	36	None	Positive	Negative	6.50×10^8	1.06×10^5
CSNC39	B	Male	Asian	49	Tenofovir	Positive	Negative	8.10×10^2	9.98×10^4
CSNC40	B	F	Chinese	41	None	Positive	Negative	1.60×10^8	6.03×10^4
CSNC41	D	Male	Pakistani	44	None	Negative	Positive	2.50×10^3	5.75×10^2
CSNC42	B	F	Asian	39	None	Negative	Positive	8.50×10^2	6.61×10^3
CSNC43	D	Male	Unknown	32	None	Negative	Positive	8.70×10^2	2.48×10^3
CSNC44	C	F	Asian	64	None	Positive	Negative	9.90×10^7	1.45×10^4
CSNC45	A	Male	Unknown	76	None	Positive	Negative	1.80×10^8	6.67×10^3
CSNC46	D	Male	Pakistani	39	None	Positive	Negative	5.50×10^8	2.12×10^4
CSNC47	D	F	Unknown	33	Interferon	Negative	Positive	1.90×10^3	6.45×10^2
CSNC48	B	F	Chinese	46	None	Negative	Positive	5.40×10^2	1.66×10^1

CSNC49	B	F	Chinese	39	Interferon	Positive	Negative	1.40×10^2	8.39×10^1
CSNC50	A	Male	White British	41	None	Negative	Positive	6.60×10^4	1.92×10^3
CSNC51	C	F	Asian	59	None	Negative	Positive	1.60×10^4	9.30×10^3
CSNC52	A	F	European	52	Interferon	Negative	Positive	1.60×10^2	1.65×10^2
CSNC53	C	F	Asian	35	None	Positive	Negative	2.60×10^4	3.17×10^2
CSNC54	C	Male	Chinese	34	None	Positive	Negative	2.80×10^8	6.39×10^4
CSNC55	E	Male	African	42	None	Negative	Positive	2.70×10^3	1.18×10^4
CSNC56	E	Male	African	45	Tenofovir	Positive	Negative	Unknown	8.63×10^3
CSNC57	D	Male	Pakistani	47	None	Negative	Positive	5.30×10^6	4.89×10^3
CSNC58	D	Male	Pakistani	39	None	Positive	Negative	4.20×10^8	1.73×10^4
CSNC59	D	Male	Unknown	53	None	Negative	Positive	1.40×10^3	1.42×10^2
CSNC60	B	F	Chinese	41	None	Positive	Negative	8.80×10^7	5.90×10^4
CSNC61	B	F	Asian	43	Interferon	Negative	Positive	1.00×10^3	2.54×10^2
CSNC62	A	F	African	43	None	Negative	Positive	5.30×10^2	1.28×10^4
CSNC63	D	Male	Indian	75	Tenofovir and Lamivudine	Positive	Negative	5.80×10^7	1.68×10^5
CSNC64	A	F	Caribbean	56	None	Negative	Positive	1.70×10^3	1.66×10^3
CSNC65	D	F	Bangladeshi	41	None	Positive	Negative	4.60×10^7	1.97×10^4

CSNC66	C	M	Asian	52	None	Negative	Positive	8.00×10^2	9.10×10^2
CSNC67	A	F	White British	41	None	Negative	Positive	6.20×10^2	1.17×10^4
CSNC68	C	F	Chinese	41	None	Positive	Negative	2.00×10^8	5.15×10^4
CSNC69	C	F	Chinese	44	None	Positive	Negative	7.80×10^7	3.34×10^4
CSNC70	B	M	Chinese	42	Tenofovir and Lamivudine	Positive	Negative	1.10×10^1	1.73×10^4
CSNC71	A	F	African	30	Interferon	Positive	Negative	3.20×10^3	3.29×10^3
CSNC72	B	F	Chinese	69	None	Positive	Negative	2.30×10^3	1.62×10^2
CSNC73	C	F	Chinese	39	Interferon	Negative	Positive	9.40×10^4	1.07×10^2

2.2.2 Phylogenetic analysis

250 L-HBsAg sequences (genotypes A-E) consisting of 50 sequences per genotype were downloaded from GenBank. Selection number criteria was based on the genotype with the least number of available sequences on GenBank. Sequences were screened and duplications were deleted. The sequences were then aligned using the MUSCLE alignment in MEGA7 software using standard parameters [301]. HBV DNA from clinical samples from the Nottingham clinical cohort (2010-2012) was extracted and the S-HBsAg was amplified and Sanger-sequenced by a previous colleague, Gemma Clark. Sequences from the clinical samples were aligned alongside 20 L-HBsAg sequences (4 of each genotypes A-E) downloaded from GenBank, and HBV genotypes A-E HBsAg reference sequences from the study by McNaughton, A.L., *et al.,* using the MUSCLE alignment in MEGA7 software [302]. Sequence variability patterns among alignments were assessed by calculating the Shannon entropy using Bio Edit software and plotting the entropy plots on GraphPad Prism 9.0 (GraphPad Software, Inc., San Diego, CA) [303]. Pairwise Distance Estimation and maximum likelihood trees were calculated and generated in MEGA 7 software with confidence values of 1000 bootstrap replicates. Nucleotides and amino acid p-distances were generated using aligned nucleotide and amino acid sequences of S-HBsAg and strong bootstrap support of ≥70. Evolutionary analyses were conducted in MEGA7. The evolutionary history was inferred by using the Maximum Likelihood method based on the JTT matrix-based model. The tree with the highest log likelihood was generated. Initial tree(s) for the heuristic search were obtained automatically by applying Neighbor-Join and BioNJ algorithms to a matrix of pairwise distances estimated using a JTT model, and then selecting the topology with superior log likelihood value. A discrete Gamma distribution was used to model evolutionary rate differences among sites (5 categories (+G, parameter = 0.2703)). The rate variation model allowed for some sites to be evolutionarily invariable ([+I], 35.62% sites). The analysis involved 98 amino acid sequences. All positions containing gaps and missing data were eliminated. There were a total of 226 positions in the final dataset.

2.3 Results

2.3.1 Genetic Variability in HBsAg sequences from GenBank

To investigate the sequence variability of the L-HBsAg of the different HBV genotypes, entropy plots of aligned L-HBsAg protein sequences downloaded from GenBank were compared. Our data showed that all genotypes had regions of high and low variability; however, there were differences in the HBsAg variability pattern of the different genotypes. Genotype A showed variability spikes between amino acids 40 and 170 in the PreS1 region, amino acids 210 and 230, and amino acids 360 and 400, both in the S region (Figure 2.1A). Genotypes B and C showed similar variability patterns with spikes between amino acids 0 and 10, at amino acid 40 in the PreS1 region and 180 in the S region, between amino acids 220 and 240, amino acids 290 and 310, and amino acids 380 and 400 in the S region (Figure 2.1B, C). Genotype D showed spikes in variability between amino acids 70 and 150 in the PreS1/2 regions, at amino acid 210, between amino acids 290 and 310, and amino acids 360 and 380 in the S region (Figure 2.1D). Genotype E showed variability spikes between amino acids 50 and 60, amino acids 80 and 90, amino acids 120, 140 and 170 in the PreS1/2 regions, at amino acid 180 in the S region, between amino acids 270 and 290, and amino acids 370 and 380 in the S region (Figure 2.1E). Only genotype A showed conservation in the antigenic loop (AGL), which is amino acids 273 to 343 in genotypes A, B and C, amino acids 262 to 332 in genotype D and amino acids 272 to 342 in genotype E (Figure 2.1A).
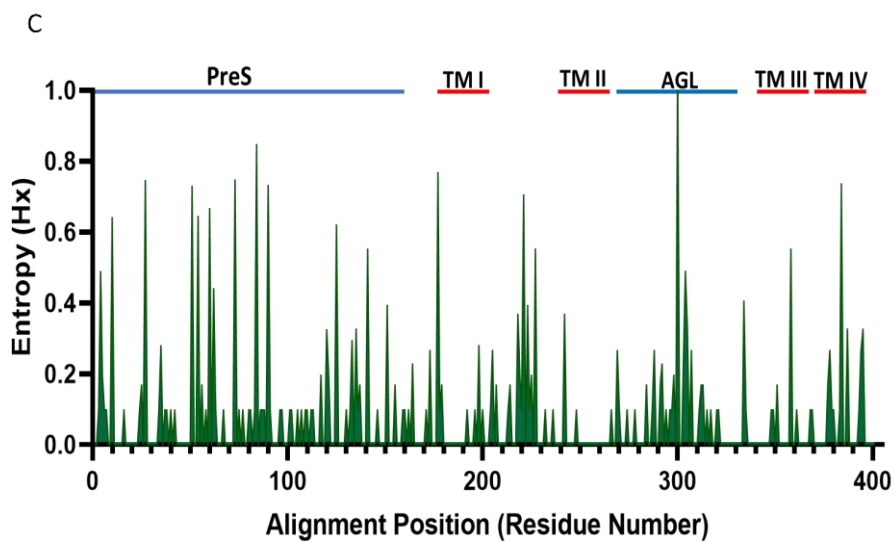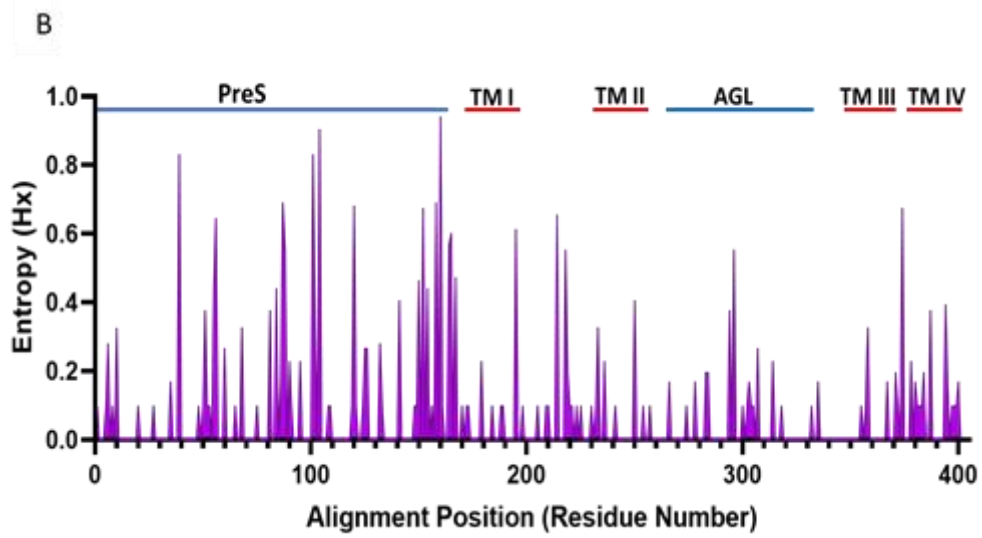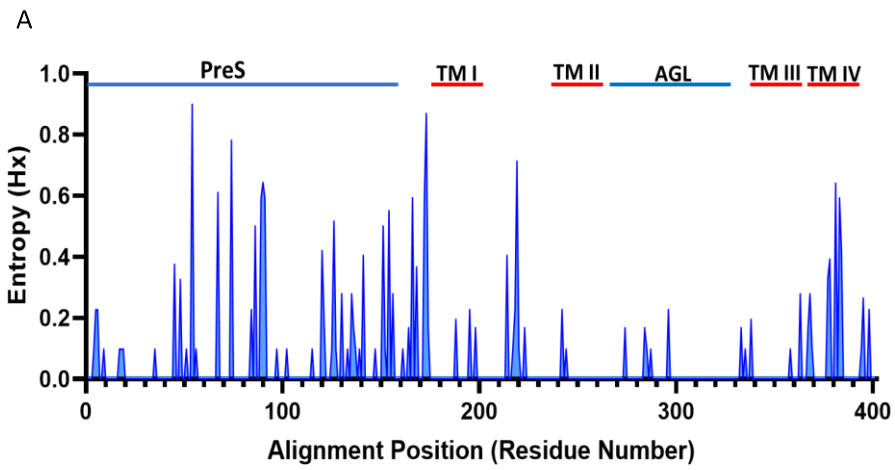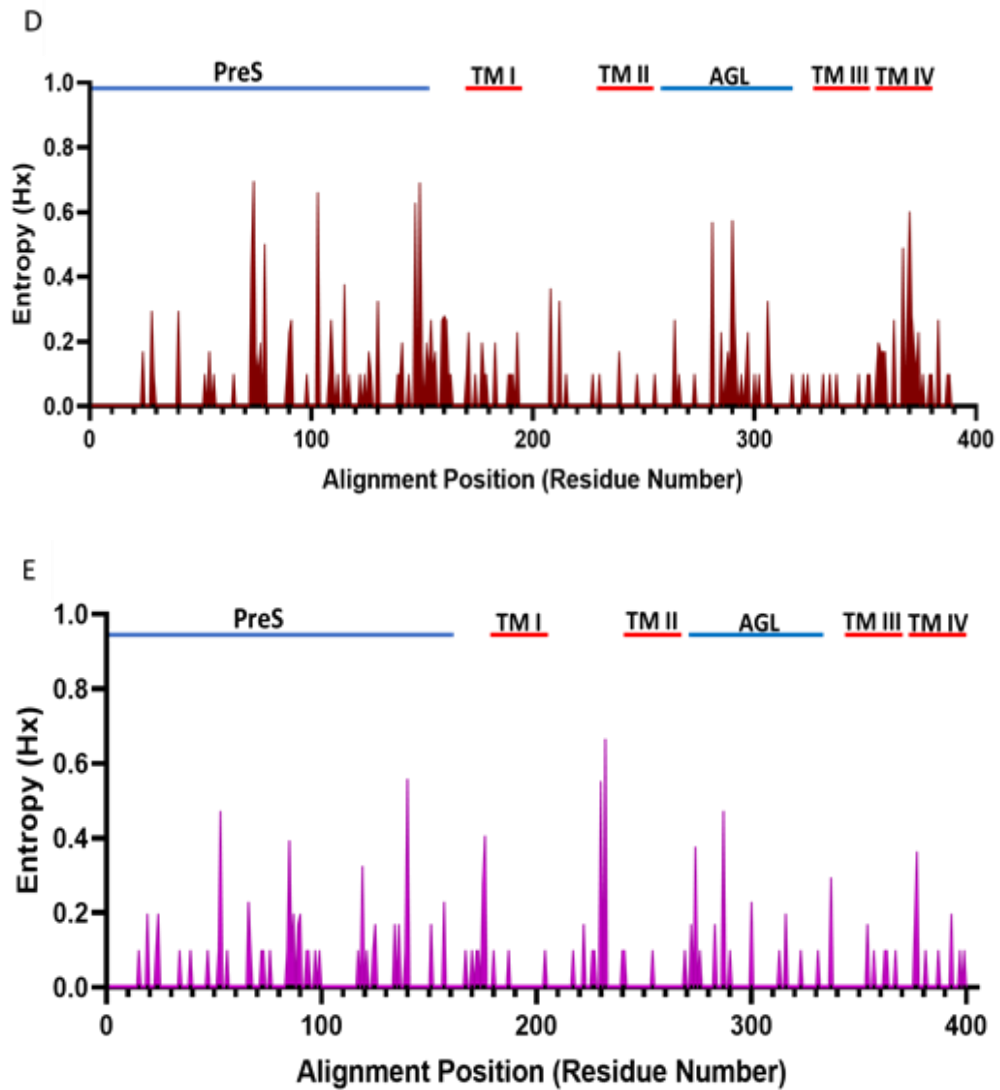
Figure 2.1 Variability pattern of L-HBsAg sequences downloaded from GenBank. Shannon entropy (Hx) was calculated for HBV genotypes (A) A, (B) B (C) C (D) D (E) E from sequence alignment of 50 sequences per genotype, previously aligned on MEGA7. Entropy data was calculated using Bio Edit software, and the entropy plots were generated using GraphPad prism. Marked regions are PreS (PreS1 and 2), TM I, II, III, IV (Transmembrane regions), and AGL (antigenic loop) regions of the S.

2.3.2 Phylogenetic analysis of the Nottingham Cohort

Sequences generated by amplifying the HBsAg S region from the clinical samples of the Nottingham cohort were aligned and reviewed for any errors which were corrected appropriately.

Maximum likelihood phylogenetic trees were constructed for the nucleotide sequence, the surface amino acids and the polymerase amino acids. The phylogenetic tree of the nucleotide, surface amino acids and polymerase amino acids showed a distinct genotype clustering (Figure 2.2A, B, C). Also, samples within each genotype cluster were from patients of similar ethnic origin. Patients with genotype A were Europeans, those with genotype B and C samples were Asians, patients with genotype D samples were Indian subcontinent, while those with genotype E samples were Africans by origin. Interestingly, samples CSNC3, CSNC4, CSNC5, CSNC7, CSNC8, CSNC9, CSNC35, CSNC49 and CSNC73 were identified to be taken at different times from the same patient. Sequences from this patient are marked; dark red star highlights the sequence from the patient's first sample prior to treatment while the pink stars highlight the sequences from the patient's samples during treatment. (Figure 2.2A, B, C). However, although they are of the same clade, the CSNC3 clustered differently. Our trees also show that the nucleotides' divergence resulted in much less divergence in the polymerase amino acids than the surface gene amino acids (Figure 2.2A, B, C).

A

56
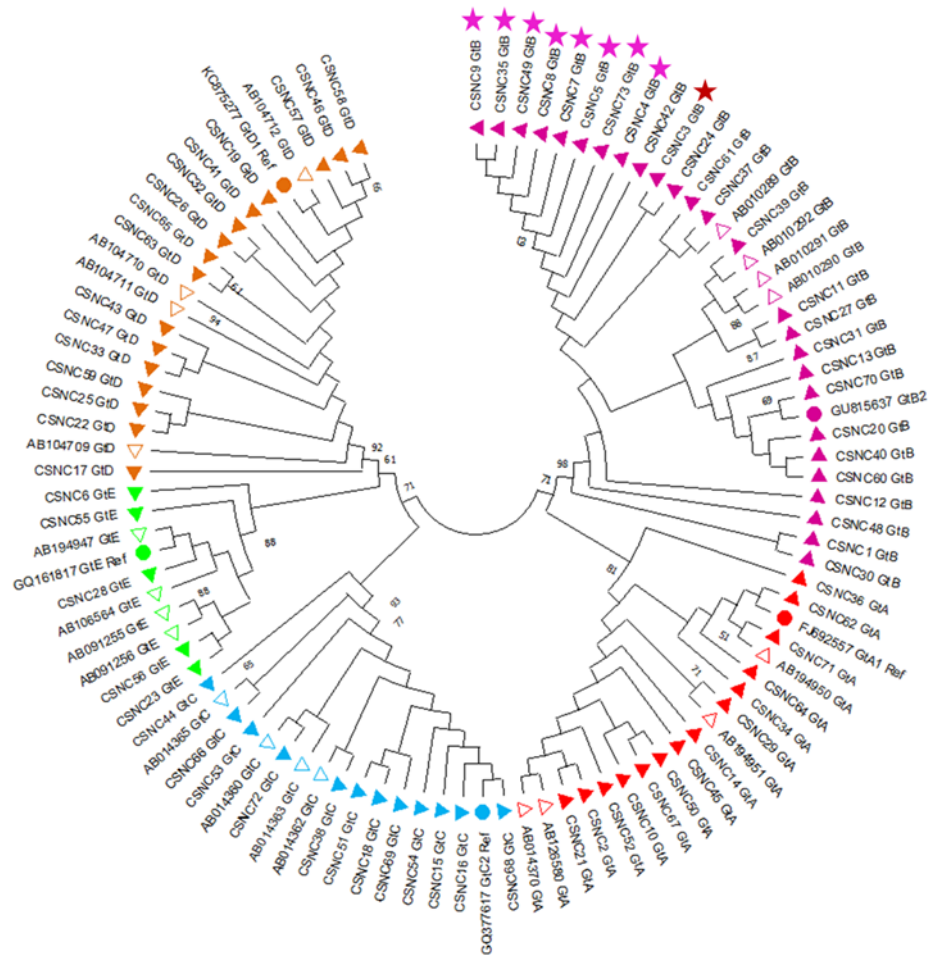
Figure 2.2 Phylogenetic analysis of (A) S-HBsAg nucleotides (B) Amino acids of the overlapping polymerase region (C) S-HBsAg amino acids. Sequences from 73 clinical samples from the Nottingham cohort were aligned with 20 GenBank sequences and 5 reference sequences. Clinical samples from the Nottingham cohort (CSNC) and GenBank sequences (beginning with AB) in this study are noted as filled triangles. Reference sequences are noted as filled circles.The accession numbers for GenBank sequences and reference sequences are noted. The tree was assembled using the Maximum Likelihood method and Tamura-Nei model in MEGA 7 with confidence values of 1000 bootstraps and strong bootstrap support of ≥70. The tree is drawn to scale with branch lengths measured in the number of substitutions per site. Bootstrap values are shown. Sequences from the same patient are shown; dark red star highlights the sequence from the patient's first sample prior to treatment while the pink stars highlight the sequences from the patient's samples during treatment. GtA, GtB, GtC, GtD, GtE stand for Genotypes A (red), B (pink), C (blue), D (brown), E (green).

2.3.3 Genetic Variability in HBsAg sequences from the Nottingham Clinical Cohort

The sequence data of the HBsAg S region, generated from clinical samples in the Nottingham cohort were aligned, and variability within the S-HBsAg and the overlapping reverse transcriptase (RT) of the polymerase was assessed. Our data showed that variability within the S-HBsAg was at amino acids 0 to 10, 20 to 30, 40 to 90, 110 to 140, 160 to 170 and amino acids 180 to 215 (numbering starts from the first amino acid with the S region of HBsAg) (Figure 2.3). Comparing the variability of the S-HBsAg with RT of the polymerase showed an overlap in the regions of variability at amino acids 0 to 10, 40 to 50, 90 to 140 and amino acids 190 to 215 (Figure 2.3). However, amino acids at regions 20 to 30 and 160 to 170 in which there was variability in the S-HBsAg showed conservation in the RT-polymerase (Figure 2.3). Interestingly, variability in the antigenic loop of the HBsAg showed a corresponding variability in the catalytic domains (B, C, D) of the polymerase. Also, assessing the variability of the S-HBsAg, we identified several amino acid variants in the S-HBsAg, including sQ101K/H, sL109P, sP120S, sT123A sT126I/S/A, sP127L/T/A/I/S, sA128V, sQ129R, sT140S/I, sT189I, sS193L, sS204R/N/C, and sS207N/R/K, most of which have been previously reported (Figure 2.4) [304-310]. Interestingly, the previously reported L216 stop codon mutation was identified in our cohort (Figure 2.4) [300, 311]. Also, assessing the cysteines in HBsAg, our results showed conservation in the cysteines except at position sC76 and sC221, where we identified cysteine to tyrosine amino acid changes (Figure 2.4). There were other amino acid substitutions involving cysteines, such as the sS64C and sF85C. Another interesting amino acid substitution was the methionine to valine substitution at position 1 of the S-HBsAg (sM1V).

Additionally, the overlapping polymerase reverse transcriptase was assessed for amino acid changes corresponding to changes in the S-HBsAg. Mutations such as rtA194T/V, rtQ215S/P/R/H, rtV214A, rtL91I, rtS135Y, rtM129L, rtH126R/Y, and rtY141F were identified in the overlapping polymerase reverse transcriptase, and these have been previously reported to be associated with drug resistance (Figure 2.4) [312-317]. Some of the mutations in the reverse transcriptase of the

polymerase have corresponding mutations in the surface gene, as shown in table 1.1.
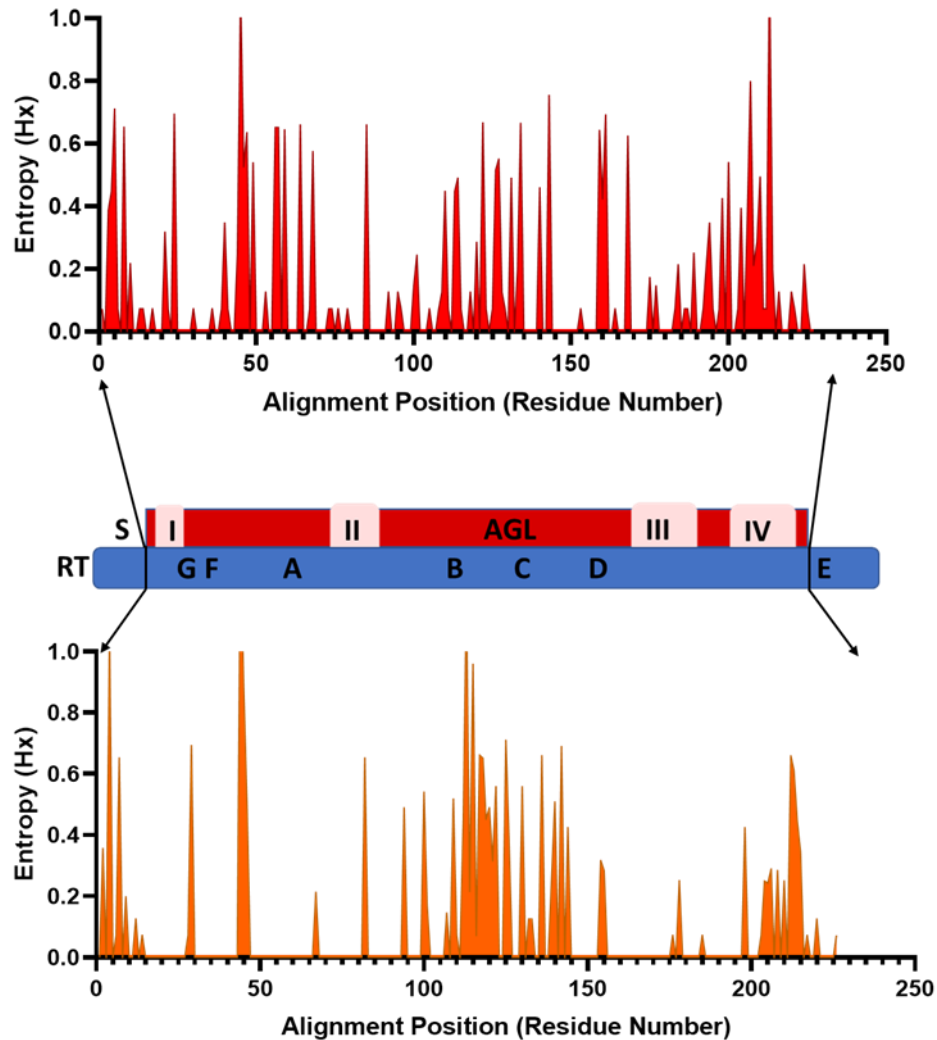
Figure 2.3 Variability pattern of S-HBsAg and overlapping polymerase sequences from 73 clinical samples from the Nottingham cohort. Shannon entropy was calculated for S-HBsAg and overlapping polymerase sequences from the alignment of 73 clinical samples from the Nottingham cohort, previously aligned on MEGA7. Entropy data was calculated using Bio Edit software, and the entropy plots were generated using GraphPad prism. S-HBsAg transmembrane domains I, II, III and IV are marked; the antigenic loop (AGL) is marked; the reverse transcriptase catalytic domains (A-F) are marked.

Table 2.2 Polymerase gene mutations and corresponding surface gene mutations.

Polymerase gene mutation	Surface gene mutation
rtQ215S/P/R/H	sY206N/R/C/L
rtS135Y	sT126A/I/S/V
rtM129L	sP120S
rtH126R/Y	sS117I

1 E$_{73}$ N$_{65}$ I$_{61}$ T$_{47}$ S$_{72}$ G$_{73}$ F$_{47}$ L$_{73}$ G$_{70}$ P$_{73}$ L$_{73}$ L$_{72}$ V$_{72}$ L$_{73}$ Q$_{73}$ A$_{72}$ G$_{73}$ F$_{73}$ F$_{73}$ L$_{66}$ L$_{72}$ T$_{73}$ R$_{37}$ I$_{73}$ L$_{73}$ T$_{73}$ I$_{73}$ P$_{73}$ Q$_{72}$ S$_{73}$ L$_{73}$ D$_{73}$ S$_{73}$ W$_{73}$ W$_{72}$ T$_{73}$ S$_{73}$ L$_{72}$ N$_{65}$ F$_{72}$ L$_{73}$ G$_{73}$ G$_{68}$ T$_{42}$ **45**

Transmembrane domain (TM) I

M$_{72}$
V$_1$
    S$_7$ T$_{12}$ A$_{25}$ L$_1$ L$_{26}$ K$_1$ P$_1$ A$_1$ E$_1$ S$_7$ W$_1$ K$_{36}$ R$_1$ L$_1$ P$_1$ S$_8$ S$_1$ E$_5$ A$_{22}$
    T$_1$ S$_1$ R$_1$ S$_7$
    A$_1$ P$_2$

46 P$_{56}$ V$_{59}$ C$_{73}$ L$_{59}$ G$_{73}$ Q$_{73}$ N$_{73}$ S$_{71}$ Q$_{73}$ S$_{73}$ P$_{47}$ T$_{47}$ S$_{73}$ N$_{48}$ H$_{73}$ S$_{73}$ P$_{73}$ T$_{73}$ S$_{46}$ C$_{73}$ P$_{73}$ P$_{72}$ I$_{57}$ C$_{73}$ P$_{73}$ G$_{73}$ Y$_{73}$ R$_{72}$ W$_{72}$ M$_{73}$ C$_{72}$ L$_{73}$ R$_{73}$ R$_{72}$ F$_{73}$ I$_{73}$ I$_{73}$ F$_{73}$ L$_{73}$ F$_{46}$ I$_{73}$ L$_{73}$ L$_{73}$ L$_{73}$ C$_{73}$ L$_{73}$ Transmembrane domain (TM) II **91**

T$_{16}$ T$_{11}$ P$_{13}$ L$_2$ Q$_{26}$ I$_{26}$ S$_{25}$ C$_{27}$ Q$_1$ T$_{19}$ P$_1$ L$_1$ Y$_1$ H$_1$ C$_{27}$
A$_1$ R$_1$
K$_1$

92 E$_1$ TM II I$_{71}$ F$_{73}$ L$_{73}$ L$_{71}$ V$_{72}$ L$_{73}$ L$_{73}$ D$_{73}$ Y$_{71}$ Q$_{69}$ G$_{73}$ M$_{73}$ L$_{73}$ P$_{72}$ V$_{73}$ C$_{73}$ P$_{72}$ L$_{71}$ I$_{61}$ P$_{72}$ G$_{73}$ S$_{61}$ S$_{59}$ S$_{72}$ T$_{73}$ S$_{71}$ T$_{71}$ G$_{73}$ P$_{67}$ C$_{73}$ K$_{45}$/R$_{28}$ T$_{72}$ C$_{73}$ T$_{72}$ T$_{62}$ P$_{64}$ A$_{71}$ Q$_{72}$ G$_{73}$ T$_{59}$ S$_{73}$ M$_{70}$ F$_{55}$ P$_{73}$ **135**

T$_2$ W$_2$ G$_1$ C$_1$ K$_3$ R$_1$ S$_1$ P$_2$ L$_{12}$ S$_1$ T$_{12}$ T$_{14}$ N$_1$ I$_2$ V$_2$ S$_6$ A$_1$ M$_1$ I$_9$ L$_4$ V$_2$ R$_1$ N$_{14}$ L$_2$ Y$_{16}$
S$_1$ H$_1$ S$_1$ T$_2$ T$_1$ T$_1$
A$_1$ A$_1$ I$_1$
I$_1$
S$_1$

136 S$_{73}$ C$_{73}$ C$_{73}$ C$_{73}$ T$_{64}$ K$_{73}$ P$_{73}$ T$_{38}$ D$_{73}$ G$_{73}$ N$_{73}$ C$_{73}$ T$_{73}$ C$_{73}$ I$_{73}$ P$_{73}$ I$_{73}$ P$_{72}$ S$_{73}$ S$_{73}$ W$_{73}$ A$_{73}$ F$_{73}$ A$_{53}$ K$_{11}$/R$_{62}$ Y$_{39}$ L$_{73}$ W$_{73}$ E$_{72}$ W$_{73}$ A$_{73}$ S$_{73}$ V$_{51}$ R$_{73}$ F$_{73}$ S$_{73}$ W$_{73}$ L$_{73}$ S$_{73}$ L$_{70}$ V$_{71}$ P$_{73}$ F$_{73}$ V$_{73}$ **180**

S$_5$ S$_{34}$ L$_1$ G$_{19}$ F$_{34}$ V$_1$ A$_{22}$ S$_3$ L1 TM III
I$_4$ M$_1$ V$_1$ A$_1$

181 Transmembrane domain (TM) III Q$_{73}$ W$_{73}$ F$_{72}$ V$_{69}$ G$_{73}$ L$_{72}$ S$_{72}$ P$_{73}$ T$_{68}$ V$_{73}$ W$_{73}$ L$_{72}$ S$_{70}$ V$_{65}$ I$_{72}$ W$_{73}$ M$_{72}$ M$_{62}$ W$_{73}$ Y$_{62}$ W$_{73}$ G$_{73}$ P$_{72}$ S$_{66}$ Y$_{68}$ N$_{52}$ I$_{69}$ L$_{67}$ S$_{64}$ P$_{72}$ F$_{72}$ L$_{25}$ P$_{70}$ L$_{73}$ L$_{71}$ P$_{73}$ I$_{73}$ F$_{73}$ F$_{71}$ C$_{72}$ L$_{73}$ W$_{73}$ V$_{69}$ Y$_{72}$ I$_{73}$ **226**

S$_1$ A$_4$ F$_1$ F$_1$ I$_5$ P$_1$ L$_3$ A$_8$ T$_1$ T$_1$ I$_{11}$ F$_8$ R$_1$ R$_5$ C$_1$ S$_{17}$ T$_4$ V$_6$ N$_4$ H$_1$ S$_1$ I$_{24}$ Q$_2$ *   L$_2$ Y$_1$ A$_4$ F$_1$
S$_2$ N$_1$ N$_1$ R$_2$ R$_4$ M$_{21}$ L$_1$ *
C$_1$ C$_1$ R$_1$ A$_1$ K$_1$ T$_1$
L$_1$ I$_1$
H$_1$

Figure 2.4 Identification of amino acid substitutions in S-HBsAg. Sequences from the 73 clinical samples from the Nottingham cohort were aligned and analysed to identify amino acid substitutions. Previously reported clinically relevant amino acid substitutions have been highlighted (yellow highlight), Stop codons have been highlighted (blue highlight), cysteine substitutions have been highlighted (red highlight), substitutions corresponding to known drug-resistant mutations in the polymerase gene have been highlighted (green highlight), and other unusual amino acid substitutions have been highlighted (pink highlight).

2.4 Discussion

Hepatitis B virus is a DNA virus with a complex replication cycle that involves a reverse transcriptase with poor proofreading ability that drives high genetic variability [292, 318]. This variability provides the basis for genotype and subgenotype classification as well as viral variants that exist as quasispecies [299, 319]. Studies have shown striking differences between HBV genotypes and subgenotypes that cut across their virological features, geographical distribution, and transmission routes. A good example is HBV subgenotypes A1 and A2, which are genetically close enough to be classified into the same genotype yet have very different characteristics. Subgenotype A1, found in Africa and Southern Asia, is majorly transmitted perinatally and is associated with rapid disease progression. On the other hand, subgenotype A2 is found in Europe and North America; it is primarily transmitted parenterally or sexually, resulting in a less rapid disease progression [320-322].

In this study, we have analysed the genetic variability of HBsAg genotypes A-E sequences downloaded from GenBank. Our data showed that the different HBV genotypes had different variability patterns, and genotype E showed the least variability. Several papers have studied the different HBV genotypes and compared them based on the frequency of specific viral mutations, disease progression, and clinical outcomes. Studies have reported a high viral load, a higher frequency of basal core promoter (BCP) A1762T/G1764A mutations and preS deletion in genotype C than genotype B. A higher prevalence of BCP A1762T/G1764A mutations has also been shown in genotype D than in genotype A [323-325]. HBV genotypes C and D have been reported to have a delay in the onset of spontaneous HBeAg seroconversion, more severe outcomes, and an increased chance of cirrhosis and HCC [326-330]. Our data showed that the HBV genotypes showed different variability patterns except for genotypes B and C, which showed some similarity between them, which could be related to their sharing similar geographical distribution [145]. Although the relationship between HBV genotypes and the clinical prognosis of HBV infection has been shown, it remains unclear the phenotypic effects of genetic variability across the

genotypes. The existence of HBV quasispecies faced with therapeutic pressure, competition and selection, resulting in evolutionary changes within them, has been shown previously [331-335]. It is important to note that variability observed in the genotypes stem from viral quasispecies within an infected host; small changes eventually add up to make highly diverse populations. In their study on the early changes in quasispecies variant after antiviral therapy for chronic hepatitis B, Liang, Y., *et al.,* examined the presence of HBV quasispecies during the early period of nucleos(t)ide analogue treatment using ultra-deep sequencing and showed initial changes of HBV quasispecies which might affect the long-term drug sensitivity to treatment [336]. A pool of quasispecies generated in an infected patient undergoes positive and purifying selection facilitated by immune and antiviral selection pressures, resulting in the domination of the fittest phenotype favouring viral replication, secretion, antigenicity and infectivity. Hence, several host, viral and environmental factors influencing the natural selection of the best fit would mean that the presence of amino acid substitutions and genetic variability across HBV genotypes in our data could have varying and somewhat challenging to predict the impact on the phenotype and clinical characteristics.

HBV genotypes and their geographical distribution has been followed closely and studied in different parts of the world. The clustering of the Nottingham samples according to genotypes show the distinct genetic variations between genotypes. However, each genotype A-E was represented within the Nottingham cohort, and each patient's ethnic origin seemed to tally with the recognised predominant region for that genotype. We cannot say from our data whether the individual HBV infection was contracted locally or from abroad; however, the ethnic origin of each patient and the HBV genotype they are infected with strongly suggests that their infection was contracted abroad. This is unsurprising as the studies of Sloan, R., *et al.,* [337] and Tedder, R.S., *et al.,* [338] both showed ethnic and genotypic diversity among the HBV infected population in the UK. Tedder, R.S., *et al.,* highlighted that the ethnicity and the infecting genotype were significantly a reflection of the predominant genotype in the birth country, with 80 % of their study population being non-UK born [337, 338]. Similar to

these studies, our data showed that population migration and travel is changing the genotype distribution and diversity of HBV in the UK.

Furthermore, the CSNC3 sample clustered separately from CSNC4, CSNC5, CSNC7, CSNC8, CSNC9, CSNC8, CSNC35, CSNC49 and CSNC73 though they were from the same patient. The CSNC3 sample was taken from the patient prior to the commencement of 48-week interferon therapy, suggesting that mutation build-up resulting from the therapy could be the reason for their different clustering. This is supported by Liang, Y., *et al.,* which showed mutation patterns, particularly in the reverse transcriptase and small S regions present during the early period of treatment which were predicted to alter the viral secondary structure and antigenicity [336]. Additionally, despite the overlapping nature of the HBV genome, the polymerase gene showed less divergence than the overlapping S gene. This suggests that the HBV polymerase is more strictly limited than the S gene in its accumulation of mutations such that nucleotide changes that result in amino acid changes of the S gene do not affect the polymerase.

Furthermore, due to the overlapping nature of the HBV genome, mutations arising from the polymerase gene could result in mutations in the S gene, which completely overlaps the reverse transcriptase [5, 32]. This is important because the reverse transcriptase, which is crucial for the generation of HBV nucleocapsids carrying the HBV DNA, is the target of HBV antiviral drugs. In contrast, the S gene, essential for the generation of the envelope proteins, is the target of the anti-HBsAg vaccine, immunoglobulin and diagnostic assays. Variability analysis of the sequences from the Nottingham cohort as well as GenBank showed variability spikes at the active site of the reverse transcriptase enzyme and the antigenic loop of the HBsAg. The emergence of mutations in any of these genes and their potential to lead to drug-resistant and immunological variants is one of the urgent problems associated with hepatitis B infection. Analysis of the clinical samples from the Nottingham cohort revealed several mutations, most of which have been previously identified and reported. Hosseini, S.Y. *et al.,* in their comparative study of the HBsAg variations present in HBV asymptomatic carriers and HCC/cirrhosis patients, reported the sL109P,

sP120S, sT126I, sT140I, sS193L, sS207R, and the sL216 stop HBsAg mutations. Their study also showed that the HBsAg sP120S mutation was significantly increased in the HCC/cirrhotic group compared to the asymptomatic group [300]. The sP120S mutation found in the AGL has been described as an immune escape mutant; it has been previously identified in immunised infants by Chong-Jin, O., *et al.,* [339] and among blood donors by Harris, B.J., *et al.,* [340]. Colagrossi, L., et al., [308]and Ko, K., *et al.,* [341] in their studies also reported the HBsAg sP120S, sT126S, and sP127S/T/A mutations from chronic HBV infected patients in Europe undergoing therapy and among infected mothers and children's pairs in Cambodia, respectively.

Interestingly, in our cohort, there was conservation in the HBsAg cysteines except for the sC76Y and sC221Y mutations, which by Hu, A.-q., *et al.,* [342] have previously reported in HBV infected mother-infant pairs and by Kim, J.H., *et al.,* [343] among chronic HBV patients with adefovir resistance. The absence of amino acid substitutions in the other HBsAg cysteines except for sC76 and sC221 is in line with Mangold, C.M., *et al.,* who in their study have shown that sC76 and sC221 possess free sulfhydryl group(s) and are dispensable for secretion of 20 nm particles. However, it would be expected that amino acid substitutions at sC48, sC65, and sC69 would impact on the viral phenotype as their study showed that these cysteines are essential for 20 nm particles secretion [344]. There were other unusual amino acid substitutions that could likely have an impact on the viral phenotype, such as the sM1V substitution which could result in low expression of sHBsAg as the start codon has been substituted by a valine. Also, the sL216* substitution would likely result in a truncated HBsAg protein that could equally impact the protein expression. Additionally, analysis of the polymerase gene in the Nottingham cohort revealed important reverse transcriptase mutations previously associated with drug resistance. The rtA194T mutation has been described as a primary resistance mutation and has been shown by Sheldon, J., *et al.,* to be associated with tenofovir resistance and to confer reduced susceptibility to tenofovir *in vitro* [297, 298]. The rtQ215P/S, rtL91I, rtV214A have also been reported and described in several studies as secondary mutations associated with lamivudine and adefovir dipivoxil

66

resistance [297, 298, 316, 345]. Interestingly, the patients from which the samples having these mutations were derived had not been on treatment prior to when the samples were taken. This could imply that the patients were infected with HBV strains carrying these mutations, or these mutations were acquired due to pressure from the host immune system. The presence of mutations in the polymerase gene resulted in mutations such as the previously described immune escape mutant sP120S in the surface gene. This exemplifies how mutations go hand-in-hand in the HBV genome.

This foundational chapter exposes the variability present in the HBsAg both in GenBank sequences and in clinical samples from the Nottingham cohort. The data has not shown if there is a possibility for mutations in the viral polymerase to induce mutations in the HBsAg and vice versa; however, the consequences are far-reaching. On the other hand, the HBsAg is responsible for viral tropism, entry into cells, and infectivity [287]. These vital roles involve having a specific protein conformation that interacts with cellular receptors, resulting in viral entry. It is expected that amino acid substitutions in the HBsAg would have some effect, which has been shown to be the case [346, 347]. However, these studies have investigated the effect of HBsAg mutations on HBV entry using a full-length genome or HBV inoculum. Although this is a good representation of an *in vivo* infection, it does not provide information on the specific effect of these mutations on HBsAg protein only and the consequences on its interaction with cell receptors. Hence, there is the need for an efficient system that enables the investigation of the phenotypic consequences of amino acid substitutions present in the HBsAg on the protein's interaction, tropism, and cell entry. Future work will be focused on developing and optimising this system.

Chapter 3

Optimisation of the Pseudotyping System

3.1 Introduction

Pseudotyped viral particles or pseudotypes (pps) are chimeric constructs with an envelope protein different from the viral core and replication-defective genetic material within it. It has been an essential tool in virology research, enabling the study of envelope proteins, entry mechanisms, cell receptors, antibody responses, and antiviral compounds. This system allows for the sequence-directed study of virus glycoproteins and mutations within them [230, 348-351]. Pseudotyped viral particles are generated by co-transfecting a producer cell with a viral vector and the viral glycoprotein cloned into an expression vector. The HEK 293T cell line, a variant of the HEK 293 cell line, is commonly used as a producer cell line for pseudotyping. This choice is due to the Simian Vacuolating Virus SV40 large T-antigen present in the HEK 293T cell line, allowing for the episomal replication of transfected plasmids that carry the SV40 origin of replication. The SV40 large T-antigen is an oncoprotein that drives the amplification of transfected plasmids and transient expression of the desired gene products. Additionally, the HEK 293T cells have high cell growth, transfection efficiency and can be flexibly adapted for adherent or suspension growth [352-355].

Viral vectors such as vesicular stomatitis virus, retroviruses, adenoviruses, adeno-associated viruses, herpes simplex viruses, baculoviruses and poxviruses provide an effective method for transferring genes into cells for transient or permanent gene expression. Retroviral vectors have the advantageous ability to stably integrate the transgene into the host cell genome for its expression. Gamma-retroviral vectors and lentiviral vectors are the main two retroviral vectors that have been developed. However, the ability of lentiviral vectors to pass through the nuclear membrane and transduce nondividing cells is a remarkable difference between lentiviral vectors and retroviral vectors [351, 356]. Transfection involves the delivery of negatively charged nucleic acid into the cell through the negatively charged cell membrane. Masking of the nucleic acid with a positively charged chemical transfection reagent enables its delivery into the cells. These chemical reagents exist as liposomal-based reagents composed of cationic lipids or non-liposomal based reagents such as cationic polymers,

calcium phosphate and lipopoyplex, a lipid and protein/polyamine mixture [357-362]. Chemiluminescence data is derived from measuring the bioluminescence of a group of oxidative enzymes called luciferases, which are commonly used as reporters of gene expression. Luciferase enzymes originate from several organisms, and they include: Gaussia luciferase from the mesopelagic copepod, *Gaussia priceps*, Renilla luciferase from the sea pansy, *Renilla reniformis*, the ATP-independent NanoLuc luciferase from the deep-sea shrimp *Oplophorus gracilirostris* as well as the Firefly luciferase from the big dipper firefly, *Photinus pyralis* [363-365].

In chapter 2, several amino acid changes in the HBsAg were identified from our clinical cohort, and a number of these substitutions have the potential to impact the virus phenotype, hence the need to investigate the *in vitro* impact of these amino acid substitutions. The pseudotyping system offers a way to study the HBsAg and amino acid substitutions that occur in them. It is useful in the study of glycoprotein–receptor interactions and has been significantly used in the study of several viruses, including human immunodeficiency virus (HIV), hepatitis C virus (HCV), and Ebola virus [244, 247, 366, 367]. This chapter focuses on optimising the pseudotyping system to study HBV surface protein in a cost-effective, consistent, rapid high titre pseudotype generation of HBV pseudotypes (HBV pps) to study HBV strain variations and tropism.

3.2 Materials and Methods

3.2.1 Cloning and Plasmid Preparation

HBV DNA extracts representative of genotypes A, B, C, D and G were previously extracted, amplified, and cloned into various pcDNA3.1(+) and pI.18 vectors (Thermofisher Scientific) by a previous member of the laboratory. These were named as follows: genotype A (clone BR1A4), genotype B (clone BR5B6), genotype C (clone BT7C2), genotype D (clone BT10D4), genotype G (clone BT16G2). These clones were transformed into Stellar competent cells (Takara Bio) grown in selective lysogeny broth (LB) (with 100 μg/mL of ampicillin) as bacterial cultures and stored as glycerol stocks at -70 ^{0}C. A loopful of each glycerol stock put on ice was taken as needed, streaked on selective LB agar plates (with 100 μg/mL of ampicillin) and incubated overnight at 37 ^{0}C. Subsequently, one clone from each plate was inoculated into 5 mL of LB broth (with 100 μg/mL of ampicillin) to prepare cultures for either miniprep or midiprep plasmid preparations. The cultures were incubated at 37 ^{0}C in a shaker set at 250 rotations per minute (rpm). Afterwards, plasmids were prepared from the overnight cultures using GenElute Plasmid Miniprep and Midiprep kits (Sigma-Aldrich), according to the manufacturer's protocol. Prepared plasmids were quantified using the Nanodrop 1000 (ThermoFisher) and measured in ng/mL for further use. For optimisation of the pseudotyping system, genotypes B and D were used.

3.2.2 Cell culture

Cell lines used were Human embryonic kidney cells HEK293T [368], Huh7 cells [369], and Huh7.NTCP cells [81, 370]. Huh7.NTCP cells were constructed by Chun Goddard, a colleague in the laboratory. This was done by extracting NTCP-encoding RNA from human hepatocytes and subsequently cloning it into the pHIV-EGFP expression vector, resulting in a pHIV-NTCP-EGFP construct. This construct was delivered into Huh7 cells with the aid of the pCMVR87 packaging

vector and pCMV.VSV.G glycoprotein. Huh7 cells were sorted through the flow cytometer, and cells overexpressing NTCP were selected. These cells were maintained in Dulbecco's Modified Eagle Medium (DMEM) (ThermoFisher Scientific), supplemented with 10 % Fetal Bovine Serum (ThermoFisher Scientific) and 1 % Non-Essential Amino Acids (NEAA) (ThermoFisher Scientific) without antibiotics in a humidified atmosphere at 37 ^{0}C and 5 % CO_2. According to established protocols, cells were passaged and seeded at 1.5-2.0 million cells per T75 flask (Corning) every 2 to 3 days.

3.2.3 Transfection

HEK293T cells were seeded in Primaria-coated 8.5 cm diameter cell culture dishes (Corning) with 10 mL of DMEM and incubated overnight at 37 0C and 5 % CO2. Pseudotypes (pps) were generated in a two-plasmid system with the reporter gene encoded in the viral vector. Optimisation of the pseudotyping system was carried out by optimising the choice of the envelope plasmid expression vector, the viral vector plasmid, viral vector plasmid concentration, envelope plasmid to viral vector plasmid ratio, transfection reagent, cell density, reporter enzyme and the use of fusion enhancer.

HEK 293T cells were seeded overnight before transfection at 0.5, 1.5, 2.5 and 4 million cells per dish to optimise the transfection cell number. Envelope plasmids in expression vectors of 2 µg concentration (which had already been optimised in the laboratory) were added to the viral vector plasmid used, and the mixture was topped up with Opti-MeM. For the envelope plasmid expression vector, we compared pI.18 to pcDNA3.1(+) vectors, while for the viral vector system, we compared the gammaretroviral vector murine leukaemia virus (MLV) vector to a third-generation lentiviral vector with an envelope and rev deletions (pNL4-3.R-E-). In addition, we compared the viral vector pNL4-3.Luc.R-E- with firefly luciferase (NIH AIDS) with pNL4-3.nanoLuc.R-E- with nano luciferase (NIH AIDS). Also, five different amounts (1-5 µg) of the viral vector pNL4-3.Luc.R-E- were compared.

In another tube, the mixture of a stable cationic polymer transfection reagent and Opti-MeM (a reduced-serum medium) was made. We compared four

available transfection reagents using manufacturer's protocols; these were the cationic lipids reagents, K4 (Biontex), and Lipofectamine (Thermofisher), the lipopolyplex reagent TransIT (Mirus Bio) and the cationic polymer reagent Polyethylenimine (Polysciences) transfection reagents.

The manufacturer's protocol for K4 reagent was as follows: 120 µL of K4 Multiplier was added to HEK 293T cells that were seeded overnight and incubated for 30 min. 2 µg each of envelope plasmid and viral vector plasmid were mixed in 600 µL of Opti-MEM while 60 µL of K4 transfection reagent was mixed with 600 µL of Opti-MEM in separate tubes. 600 µL of plasmid solution was then mixed with 600 µL of transfection reagent solution, and the mixture was incubated for 30 min at room temperature. After 30 min, the DNA-reagent mixture was added to the seeded cells and incubated for 6 h at 37 ^{0}C and 5 % CO_2. Transfection medium was then replaced with fresh medium, and the cells were incubated for another 72 h after which the pseudotype-containing cell culture supernatant was filtered using a 0.45 µM PVDF filter and used for downstream experiments.

The manufacturer's protocol for lipofectamine reagent was as follows: 24 µL of lipofectamine 3000 reagent was diluted in 750 µL of Opti-MEM in one tube while 2 µg each of envelope plasmid and viral vector plasmid were mixed along with 10 µL of P3000 reagent in 750 µL of Opti-MEM in a second tube. Both solutions above were mixed in a 1:1 ratio and incubated for 20 min at room temperature. The DNA-lipid complex was then added to overnight pre-seeded HEK 293T cells, and they were incubated for 72 h at 37 ^{0}C and 5 % CO_2, then pseudotypes were harvested using a 0.45 µM PVDF filter for further experiments.

The manufacturer's protocol for TransIT-VirusGEN reagent was as follows: 2 µg of each plasmid was mixed in a tube while 1mL of Opti-MEM was put into another tube. The plasmid mixture was then transferred into the tube containing Opti-MEM and was mixed gently. Subsequently, 25 µL of TransIT-VirusGEN reagent was added to the DNA mixture and incubated for 20 min at room temperature. This was then added to overnight pre-seeded HEK293T cells, and they were incubated for 72 h at 37 ^{0}C and 5 % CO_2, after which the cell culture

supernatant was filtered using a 0.45 μm PVDF filter to harvest the pseudotypes for further experiments.

The manufacturer's protocol for Polyethylenimine (PEI) reagent was as follows: 2 μg of each plasmid was added to 300 μL of Opti-MEM in one tube while 24 μL of Polyethylenimine (PEI) was mixed with 276 μL of Opti-MEM in another tube. Both were mixed and incubated for 1 h at room temperature. The plasmid-PEI mixture was then added to overnight pre-seeded HEK293T cells in 7 mL of fresh Opti-MeM medium and incubated for 6 h at 37 ^{0}C and 5 % CO_2. After 6 h, the Opti-MeM was replaced with 10 mL DMEM and the cells were incubated for 72 h at 37 ^{0}C and 5 % CO_2. After 72 h, the pseudotypes (pps) were harvested by filtering the cell culture supernatant using a 0.45 μM PVDF filter. The pseudotypes contained in the flow-through was then stored at 4 ^{0}C for 2 weeks for further use.

3.2.4 Infection and Luciferase Assay

Cells used for infection assay were: Huh7 cells and Huh7.NTCP cells. Cells were seeded in a sterile flat-bottom 96-well plate and grown in DMEM overnight at 37 ^{0}C and 5 % CO_2. Cells were seeded at 5,000, 10,000, 20,000 and 40,000 cells per well to optimise the infection cell density. Cells were then incubated with 100 μL of the HBV pseudotypes and controls in triplicates for 6 h at 37 ^{0}C and 5 % CO_2. For all experiments, vesicular stomatitis virus glycoprotein (VSV-G) was used as a positive control for transfection efficiency and infection due to its broad cell tropism and high titre pseudotyping generation [371]. The negative control was the no envelope plasmid, deltaE (ΔE) (produced by transfecting cells with only the viral vector). In a separate batch of experiments, we infected the cells with the pseudotypes in the presence and absence of 4 % PEG 8000 and incubated them for 6 h. We added 150 μL of DMEM to the cells after 6 h and incubated the cells at 37 ^{0}C and 5 % CO_2 for 72 h after which luciferase assay was carried out using the luciferase assay system (Promega). A cell viability assay was carried out to determine the cytotoxicity of 4 % PEG 8000 after 6 h of incubation with 4 % PEG 8000 using CellTiter-Blue Cell Viability Assay (Promega) according to the manufacturer's protocol. In the firefly luciferase assay, 50 μL of cell lysis buffer

was added to each well to lyse the cells. The cells were then incubated on a shaker at room temperature for 15 min and then vortexed for 15 sec, whereas, for the nano luciferase assay, 100 μL of cell lysis buffer containing the nano luciferase substrate was added to each well. FLUOstar Omega Filter-based multi-mode chemiluminescence microplate reader (BMG LABTECH) was used to inject 50 μL of the luciferase substrate into the wells for the firefly luciferase experiment. In both cases, the reader measured chemiluminescence from the cells at a machine gain of 3600, giving chemiluminescence values as relative light units (RLU).

3.3 Results

3.3.1 Selection of a Suitable Expression Vector.

To determine which expression vector from the selection available in our laboratory was best for HBV pseudotyping assays, we transiently transfected HEK 293T cells with plasmids expressing HBsAg and controls cloned into pI.18 and pcDNA3.1(+) vectors and harvested pseudotypes. Huh7 and Huh7.NTCP cells were infected with these pseudotypes, incubated for 72 h, lysed, and infectivity was measured by luciferase assay. Relative light unit (RLU) values showed a clear difference in the infectivity of pseudotypes generated from the plasmids in the two expression vectors. HBV BT10D4 cloned into the pcDNA3.1(+) expression vector showed significantly higher infectivity levels than the pI.18 expression vector in both Huh7 ($p < 0.0001$) and Huh7.NTCP ($p < 0.001$) (Figure 3.1). Also, HBV BR5B6 cloned into the pcDNA3.1(+) expression vector demonstrated infectivity levels significantly higher than that of the pI.18 in Huh7.NTCP cells ($p < 0.0001$) and no significant infectivity in Huh7 cells (Figure 3.1). Infectivity RLU values were high for the VSV-G positive control irrespective of the expression vector into which it was cloned in both Huh7 ($p = 0.1291$) and Huh7.NTCP ($p = 0.4927$) (Figure 3.1). Hence, subsequent experiments were carried out with clones in the pcDNA3.1(+) expression vector.
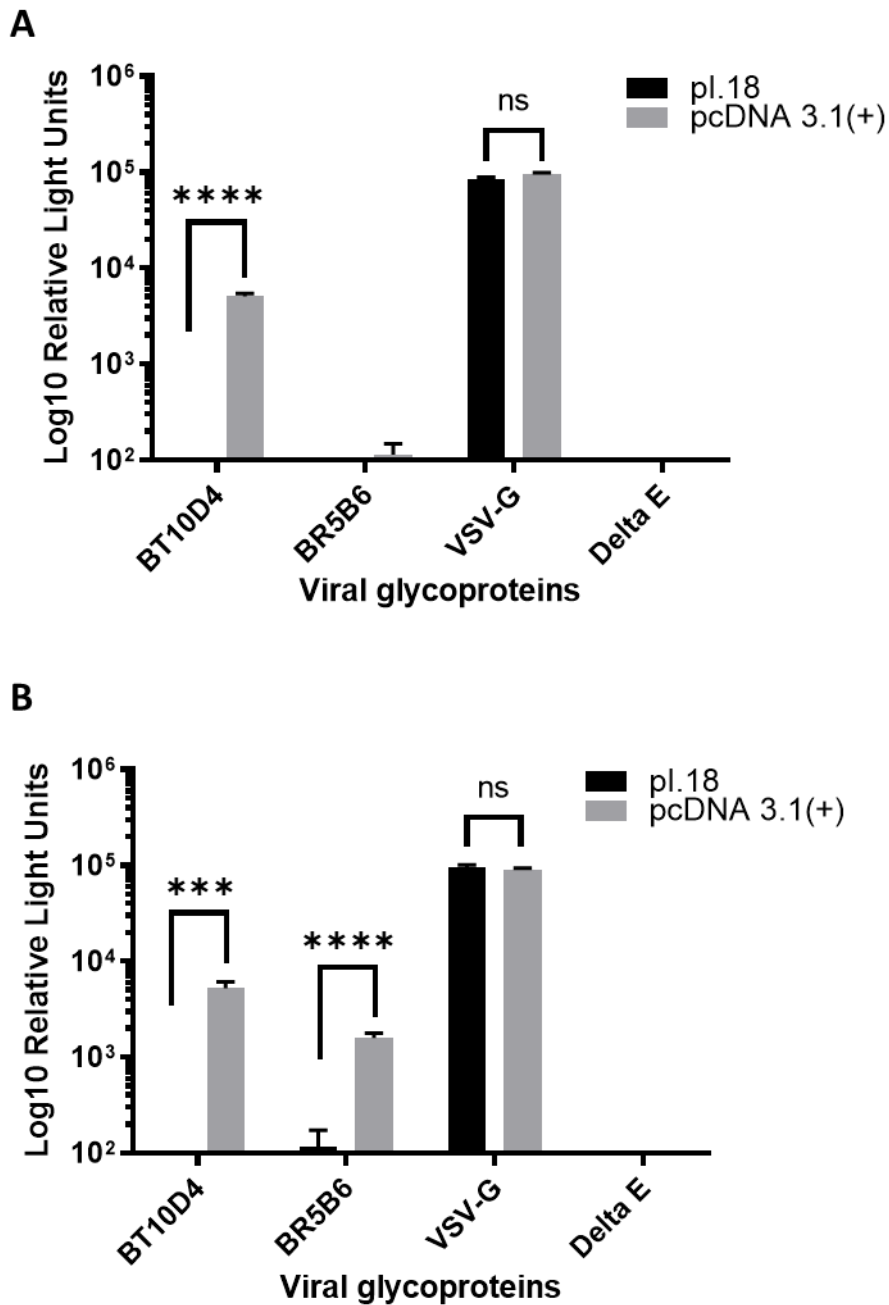
Figure 3.1 Infection of Huh7 and Huh7.NTCP cells with pseudotypes produced from HBV BR5B6 and BT10D4 cloned into pI.18 and pcDNA3.1(+) expression vectors. A. Huh7 and B. Huh7.NTCP cells were infected with HBV pseudotypes and incubated at 37 ^{0}C and 5 % CO_2 for 72 h. VSV-G and ΔE were used as positive and negative controls, respectively. n=3, data are shown as log10 of mean relative light units± Standard deviation (SD). Statistical significance was analysed with an unpaired t-test set at a 95 % confidence interval. **** indicates $p<0.0001$, *** indicates $p<0.001$, ns indicates $p>0.05$.

3.3.2 Selection of a Viral Vector Plasmid for pseudotype production.

In order to identify the viral vector that worked more efficiently for the HBV pseudotyping system, HBV BT10D4, BR5B6 and controls were co-transfected into HEK 293T cells with either the gammaretroviral murine leukaemia virus (MLV) or the lentiviral pNL4-3.Luc.R-E- vectors. We harvested the pseudotypes, infected Huh7 and Huh7.NTCP cells with the pseudotypes and incubated for 72 h, after which cells were lysed and infectivity measured by luciferase assay. RLU values of HBV BT10D4 pseudotype with the pNL4-3.Luc.R-E- vector was significantly higher than the MLV vector in Huh7 ($p<0.0001$) and Huh7.NTCP ($p<0.001$) cells (Figure 3.2). Also, the HBV BR5B6 pseudotype with pNL4-3.Luc.R-E- vector was significantly higher than the MLV vector in Huh7.NTCP ($p<0.0001$) cells and no significant infectivity in Huh7 cells (Figure 3.2). RLU values of the VSV-G control also showed a significant increase in pseudotypes with the pNL4-3.Luc.R-E- vector than the MLV vector in Huh7 ($p<0.0001$) and Huh7.NTCP ($p<0.0001$) cells (Figure 3.2).
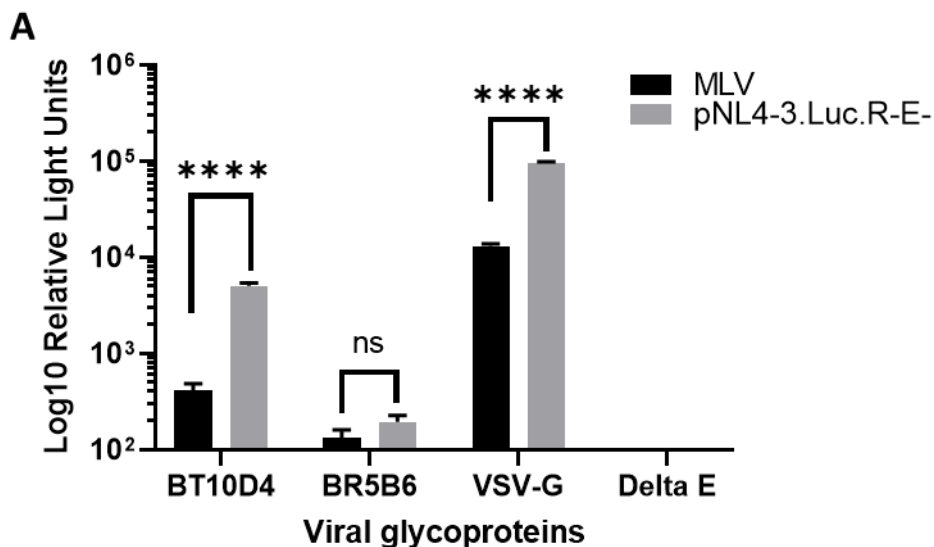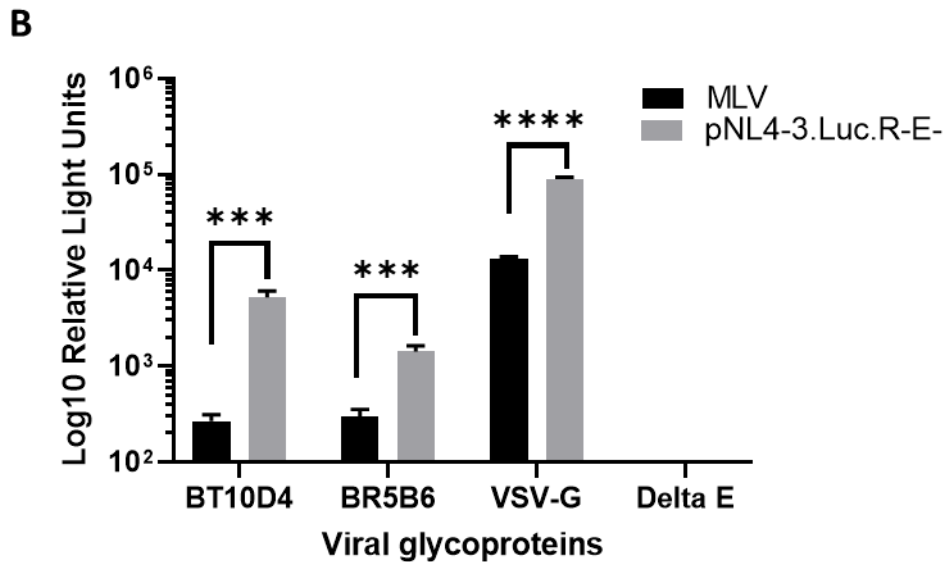
Figure 3.2 Infection of Huh7 and Huh7.NTCP cells with pseudotypes produced from HBV BR5B6 and BT10D4 with different viral vectors. A. Huh7 and B. Huh7.NTCP cells were infected with HBV pseudotypes produced with either lentiviral pNL4-3.Luc.R-E- or MLV viral vector systems incubated at 37 ^{0}C and 5 % CO_2 for 72 h. VSV-G and ΔE were used as positive and negative controls, respectively. n=3, data are shown as log10 of mean relative light units± SD. Statistical significance was analysed with an unpaired t-test set at a 95 % confidence interval. **** indicates $p<0.0001$, *** indicates $p<0.001$, ns indicates $p>0.05$.

3.3.3 Optimising Viral Vector Plasmid Concentration and Envelope Plasmid to Viral Vector Plasmid Ratio.

To optimise the viral vector DNA amount and the envelope plasmid to viral vector plasmid ratio, HEK 293T cells were transfected with 2 μg of HBV and control plasmids together with an increasing amount of pNL4-3.Luc.R-E- lentiviral vector plasmid from 1-5 μg. Huh7 and Huh7.NTCP cells were infected with harvested pseudotypes incubated for 72 h, lysed and infectivity measured by luciferase assay.

There was no significant difference in the RLU values of the HBV BT10D4 in both Huh7 (p=0.9241) and Huh7.NTCP (p=0.8219) when there was an increase in the lentiviral vector concentration (Figure 3.3A). In the HBV BR5B6 infectivity data, using 2 μg of the lentiviral vector generated the HBVpp resulted in a significantly

higher RLU value in Huh7.NTCP cells (p=0.0001) than other concentrations. The HBV BR5B6 showed no significant infectivity above background in Huh7 cells (Figure 3.3B). There was a stepwise decrease in infectivity RLU values of the VSV-G control and a stepwise increase in the RLU values of the delta E control as the lentiviral vector concentration increased (Figure 3.3C, D). The decision to use 2 µg of the lentiviral vector plasmid for subsequent studies resulted from it being the concentration best suit for the HBV BR5B6 clone. Also, we set the ratio of envelope plasmid to lentiviral vector plasmid at 1:1 for subsequent experiments.
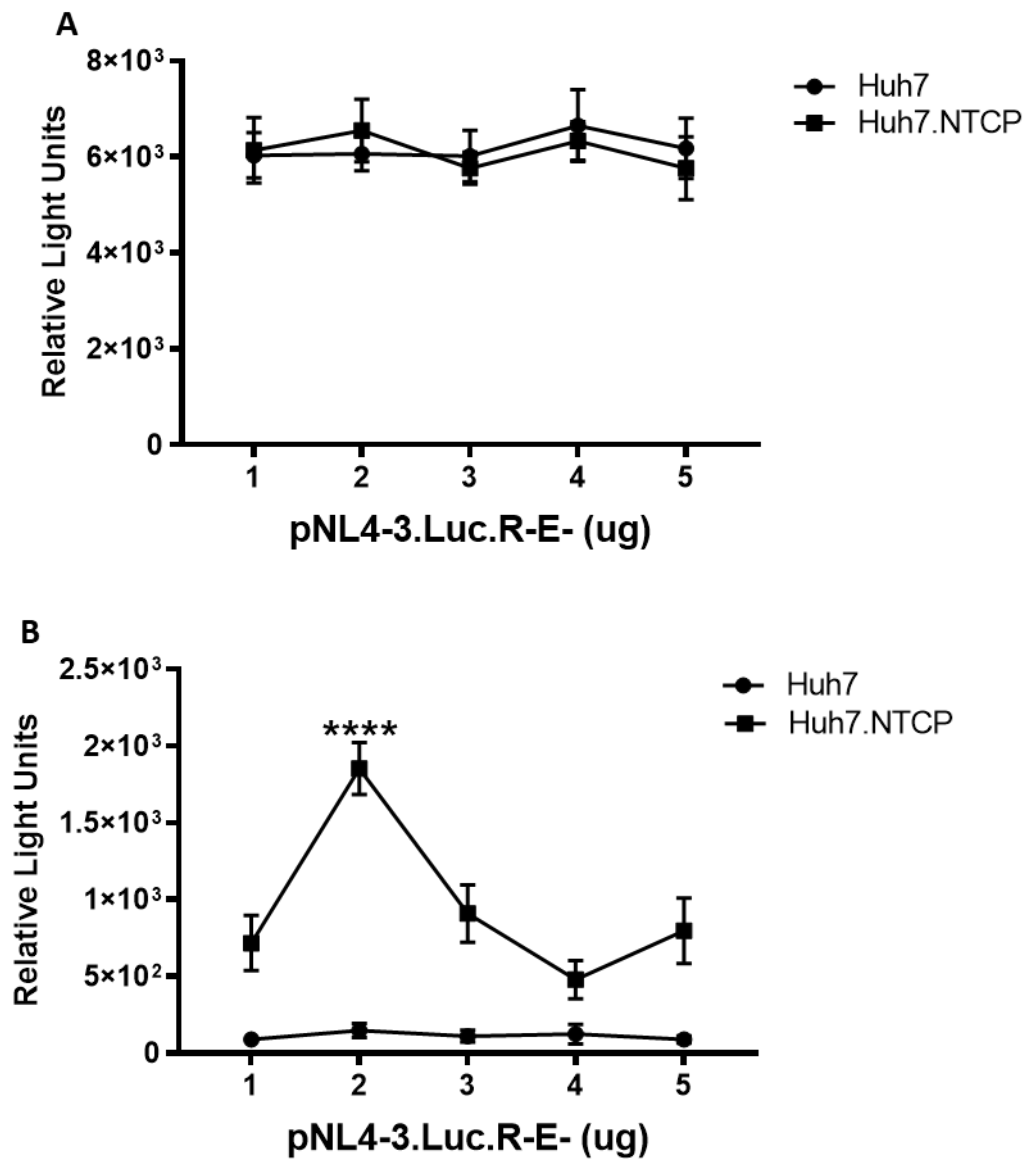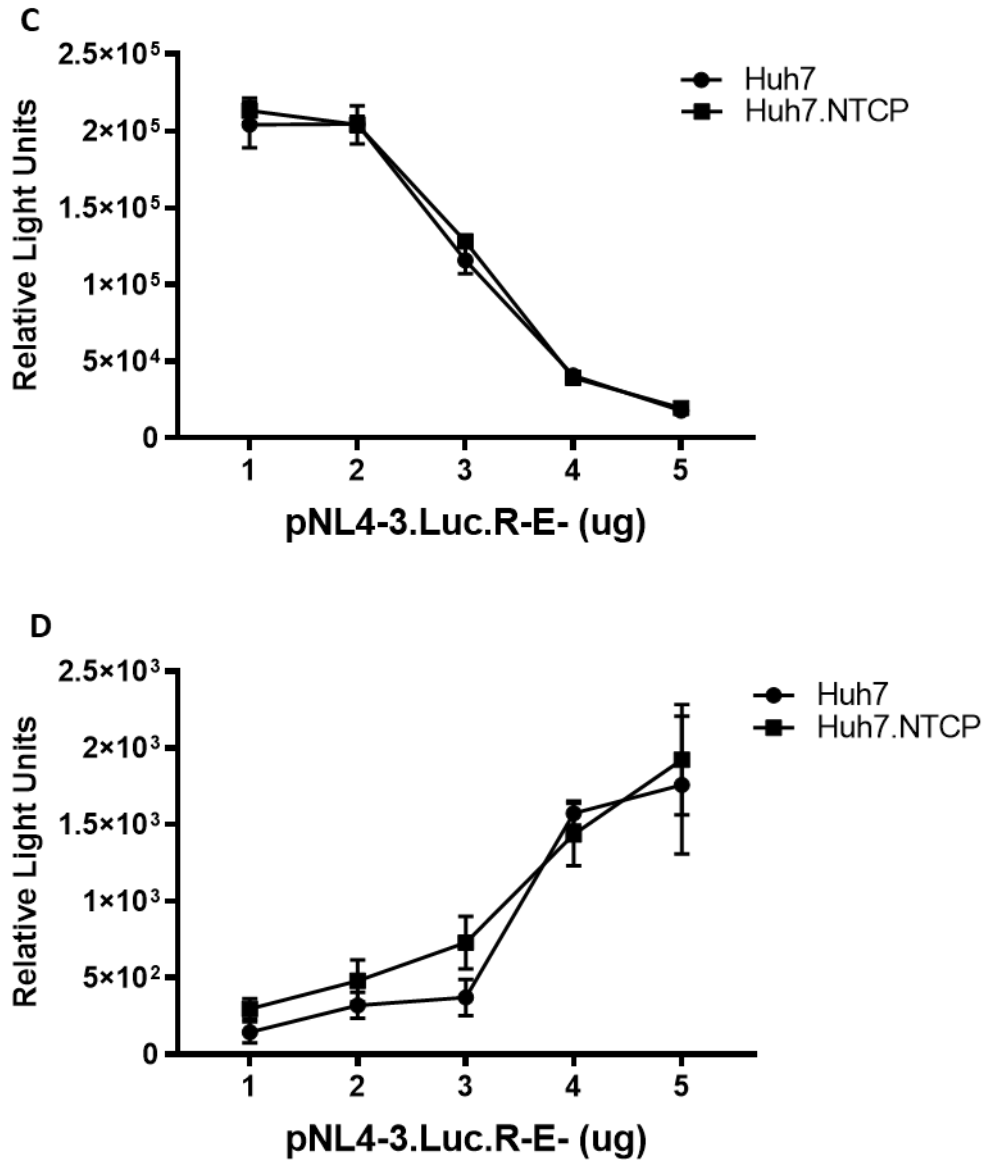
Figure 3.3 Infection of Huh7 and Huh7.NTCP cells with pseudotypes produced from HBV BR5B6 and BT10D4 with an increasing concentration of pNL4-3.Luc.R-E- lentiviral vector. Huh7 and Huh7.NTCP cells were infected with pseudotypes produced with A. BT10D4 B. BR5B6 C. VSV-G D. ΔE and 1-5 μg of pNL4-3.Luc.R-E- lentiviral vector and incubated at 37 ^{0}C and 5 % CO_2 for 72 h. VSV-G and ΔE were used as positive and negative controls, respectively. n=3, data are shown as mean relative light units± SD. Statistical significance was analysed with the ordinary one-way ANOVA and the Tukey's multiple comparisons test set at a 95 % confidence interval. **** indicates p<0.0001.

3.3.4 Optimisation of transfection reagent

To test various chemical reagents, HEK 293T cells were transfected with HBV and control envelope plasmids together with pNL4-3.Luc.R-E- lentiviral vector plasmid using the K4, Lipofectamine, TransIT and Polyethylenimine (PEI) reagents. Huh7 and Huh7.NTCP cells were infected with harvested pps and incubated for 72 h, after which cells were lysed and infectivity measured by luciferase assay. The signal to noise ratio was calculated as the ratio of the RLU values from infectivity in Huh7.NTCP cells of the test samples to that of the ΔE negative control. The transfection reagent with the highest signal to noise ratio would be the transfection system of choice.

The RLU values of pps from the K4 transfection system in Huh7.NTCP cells were significantly lower than the other reagents (p=0.0001). In the Huh7.NTCP cells, HBV BT10D4 (p=0.0731), and BR5B6 (p=0.4212) pps produced with the K4 reagent were not significantly different from the background signal in the assay (p=0.4212), making the K4 system inefficient to use (Figure 3.4, Table 3.1). The Lipofectamine system produced pps with high RLU values; however, the background RLU values were commensurately high, giving a low signal to noise ratio of 5:1 and 2:1 for HBV BT10D4 and BR5B6 in Huh7.NTCP cells, respectively. Hence, the low signal to noise ratio of the Lipofectamine system made it an inappropriate system to use (Figure 3.4, Table 3.1). On the other hand, the TransIT and the PEI transfection systems offered higher efficiency for producing infectious HBVpps. Pseudotypes from the TransIT transfection system showed very high RLU values and a high signal to noise ratio of 42:1 and 8:1 for the HBV BT10D4 and BR5B6 in Huh7.NTCP cells, respectively (Figure 3.4, Table 3.1). Also, the PEI transfection system produced pseudotypes with high RLU values and a high signal to noise ratio of 51:1 for HBV BT10D4 and 21:1 for HBV BR5B6 in Huh7.NTCP cells.

Figure 3.4 Infection of Huh7 and Huh7.NTCP cells with pseudotypes produced from HBV BR5B6 and BT10D4 with different chemical transfection reagents. A. Huh7 and B. Huh7.NTCP cells were infected with pseudotypes produced from BT10D4, BR5B6, VSV-G, and ΔE produced using K4, Lipofectamine, TransIT and PEI transfection reagents incubated at 37 ^{0}C and 5 % CO_2 for 72 h. VSV-G and ΔE were used as positive and negative controls, respectively. n=3, data are shown as log10 of mean relative light units± SD. K4 test sample signal was statistically compared to the background signal using an unpaired t-test set at a 95 % confidence interval.

Table 3.1 Transfection reagent signal to noise ratio. Signal to noise ratio was calculated as the ratio of the RLU values of the test samples to that of the negative control in Huh7.NTCP cells, and a high signal to noise ratio indicates an efficient transfection reagent.

Transfection Reagent / HBV Genotype	K4	Lipofectamine	TransIT	PEI
HBV BT10D4	Not significant	5:1	42:1	51:1
HBV BR5B6	Not significant	2:1	8:1	21:1

3.3.5 Optimising Transfection and Infection Cell Density.

In order to optimise the cell density for transfection, HEK 293T cells seeded in increasing density from 500,000–4 million cells per dish were transfected with HBV and control envelope plasmids together with pNL4-3.Luc.R-E- lentiviral vector plasmid. Harvested pseudotypes were used to infect Huh7 and Huh7.NTCP cells and incubated for 72 h, after which cells were lysed and infectivity measured by luciferase assay. RLU values of all samples and controls showed 1.5 million cells per dish as the optimum cell density required transfection as this was significantly higher than other tested cell densities ($p < 0.0001$) (Figure 3.5).
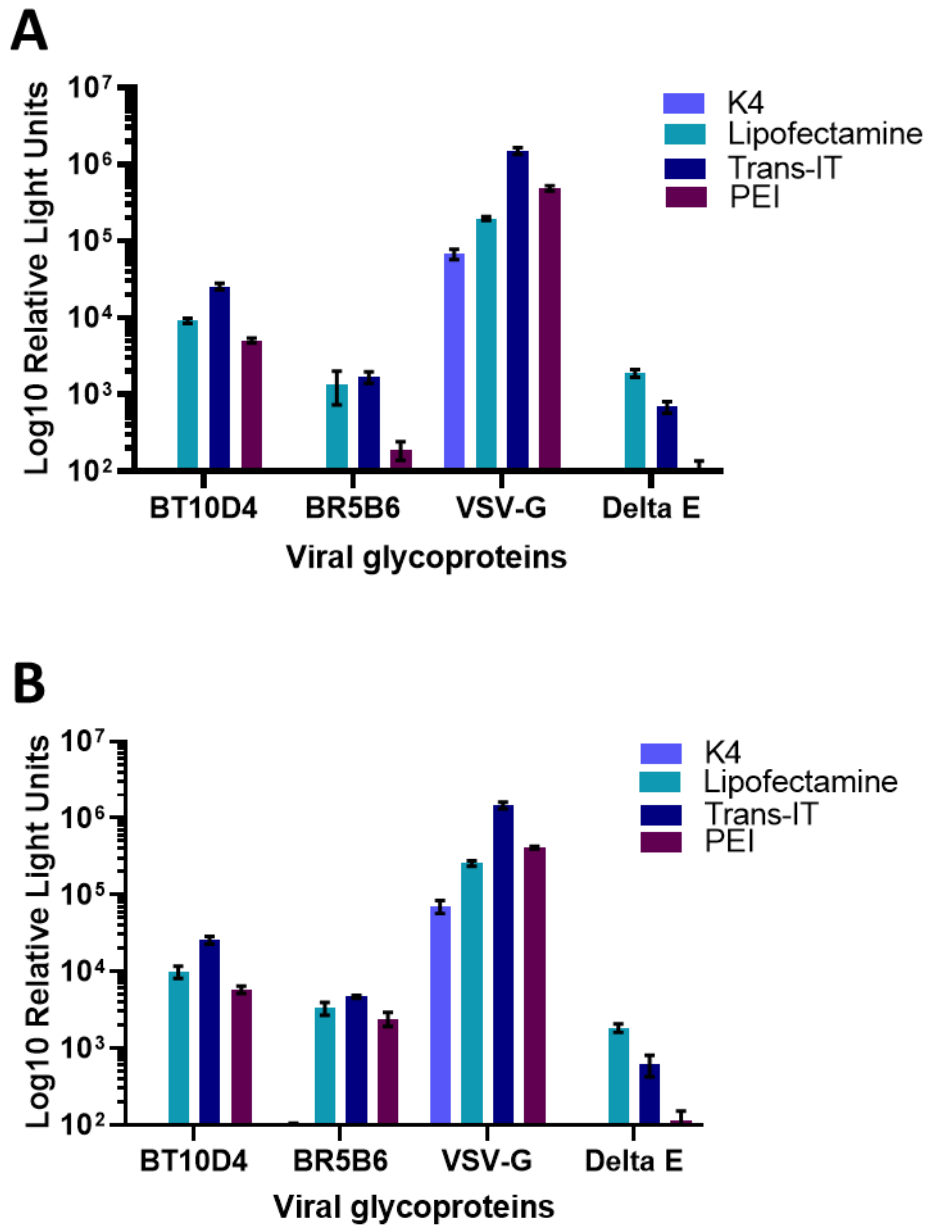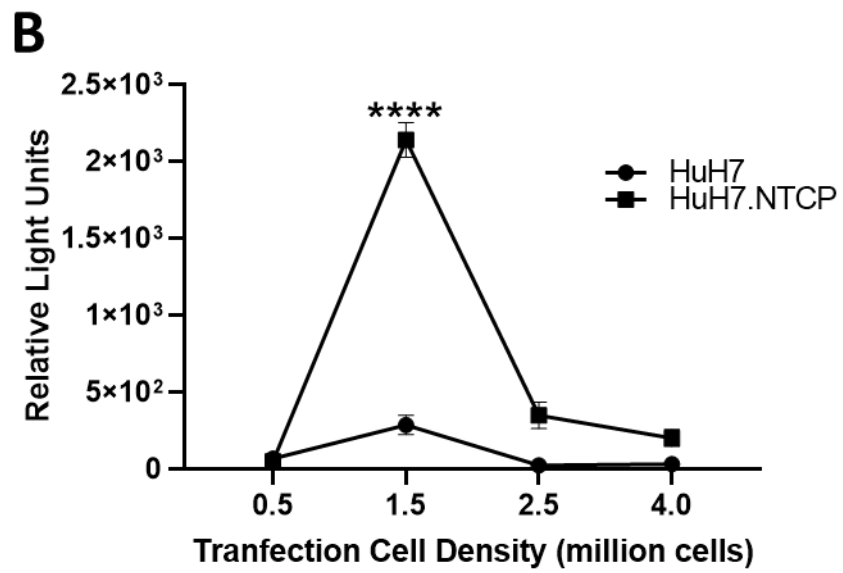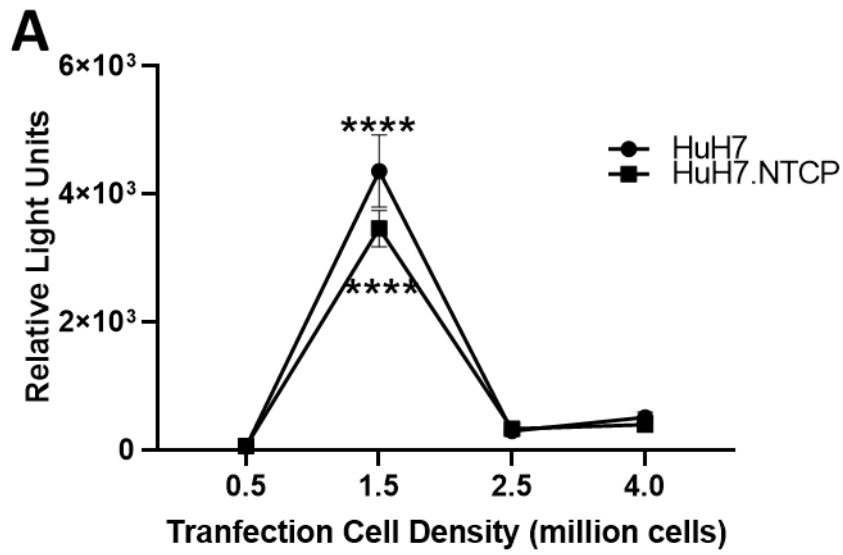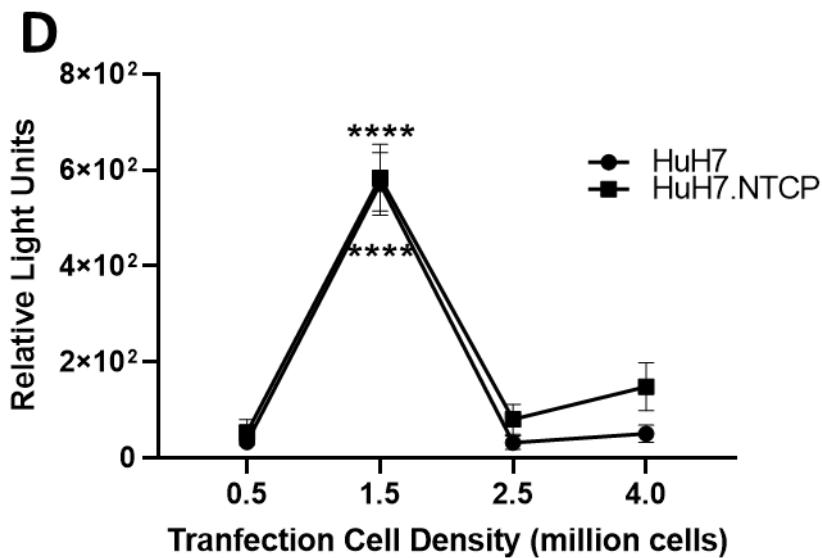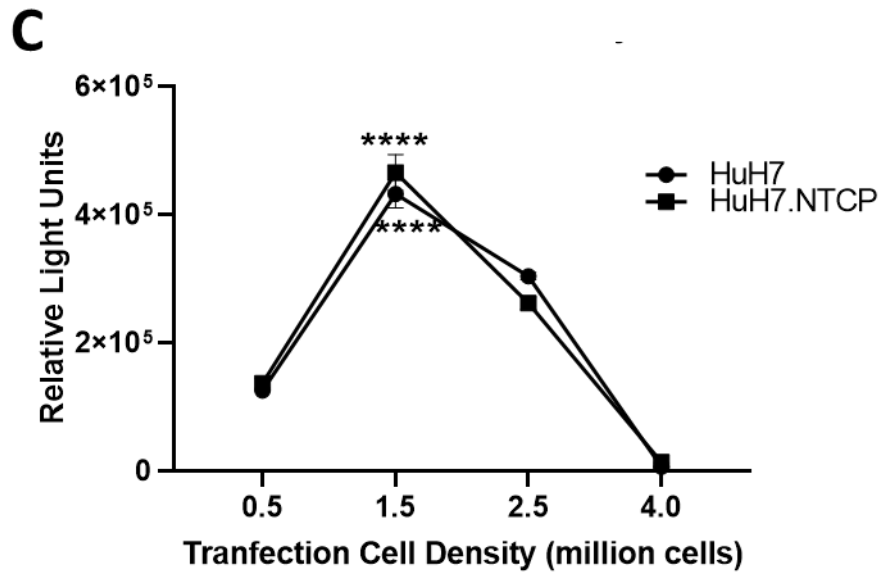
Figure 3.5 Infection of Huh7 and Huh7.NTCP cells with pseudotypes produced from HBV BR5B6 and BT10D4 were transfected into HEK 293T cells at different cell densities. Huh7 and Huh7.NTCP cells were infected with pseudotypes produced from A. BT10D4 B. BR5B6 C. VSV-G D. ΔE transfected in HEK293T cells at densities of 0.5, 1.5, 2.5, and 4 million cells. Infected cells were then incubated at 37 ^{0}C and 5 % CO_2 for 72 h. VSV-G and ΔE were used as positive and negative controls, respectively. n=3, data are shown as mean relative light units± SD. Statistical analysis was done using an ordinary one-way ANOVA and Tukey's multiple comparisons test set at a 95 % confidence interval. **** indicates p<0.0001.

Furthermore, to identify the optimum cell density for infection, Huh7 and Huh7.NTCP cells were seeded at different densities from 5,000–40,000 cells per well, infected with harvested pseudotypes and incubated for 72 h, lysed, and infectivity measured by luciferase assay. Results showed that seeding cells at 20,000 cells per well yielded significantly higher RLU values than other cell densities for HBV BT10D4 (p=0.005), BR5B6 (p<0.0001), VSV-G (p<0.0001) and ΔE (p=0.03). Consequently, based on these results, we seeded cells for transfection at 1.5 million cells per dish and 20,000 cells per well for infection (Figure 3.6).
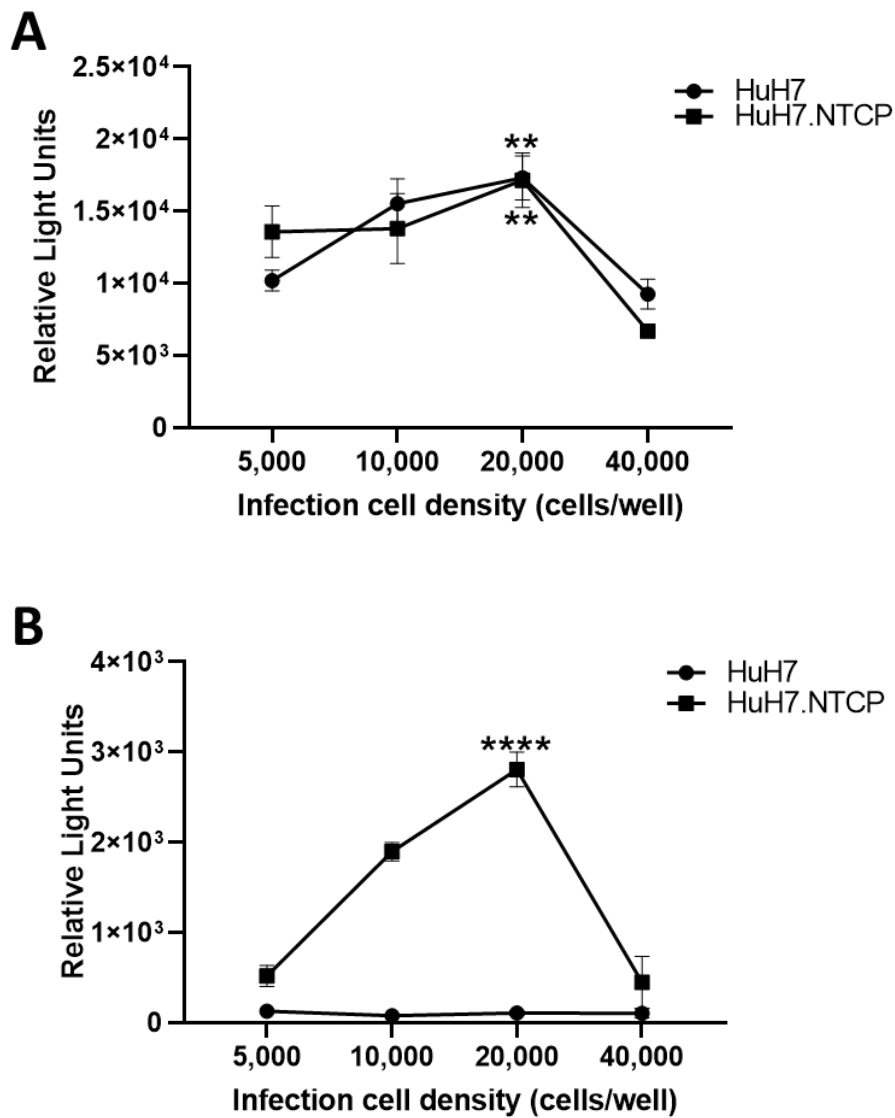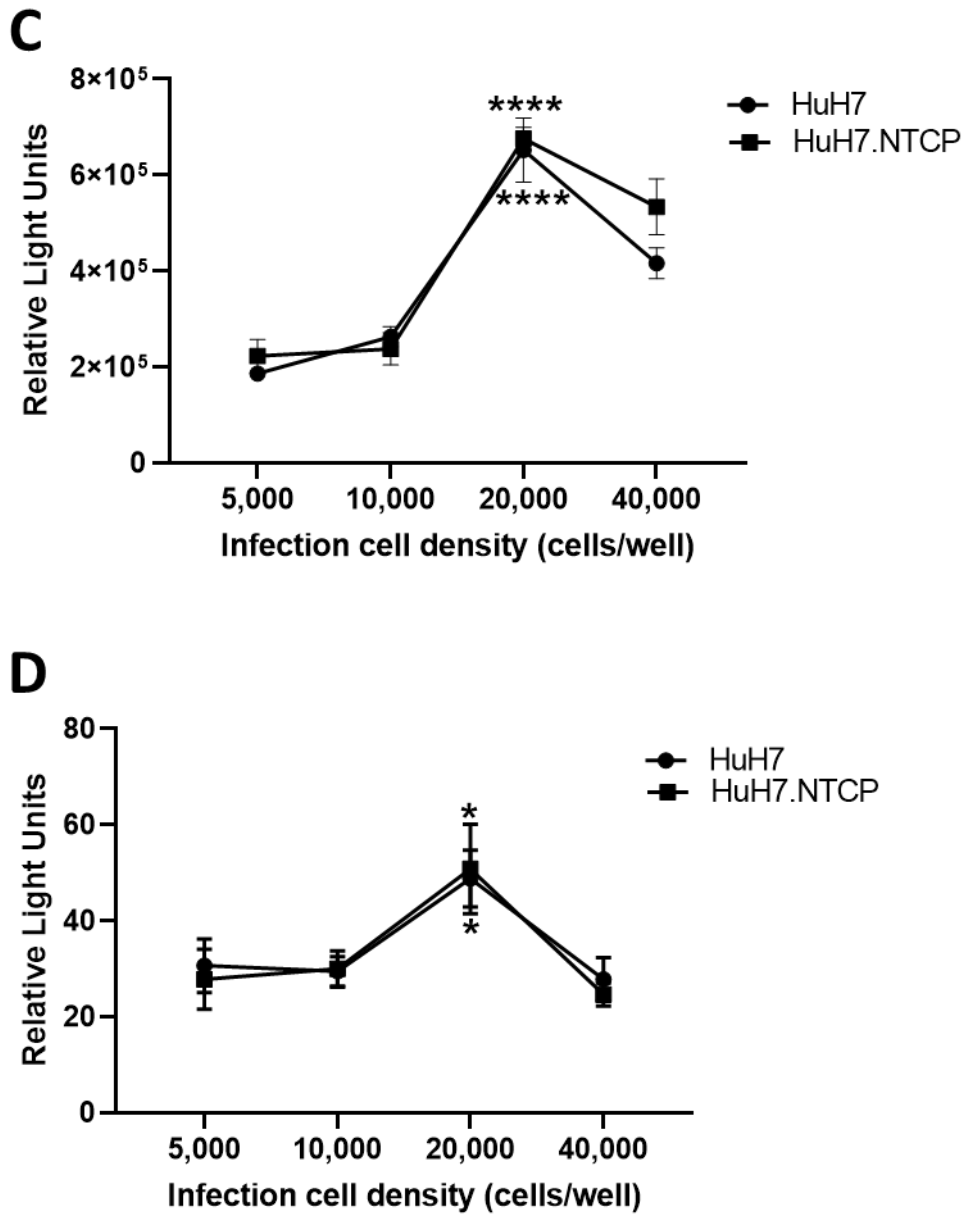
Figure 3.6 Infection of Huh7 and Huh7.NTCP cells seeded at different cell densities with pseudotypes produced from HBV BR5B6 and BT10D4. Huh7 and Huh7.NTCP cells seeded at 5,000, 10,000, 20,000, 40,000 cells per well were infected with pseudotypes produced from A. BT10D4 B. BR5B6 C. VSV-G D. ΔE. Infected cells were incubated at 37 ^{0}C and 5 % CO_2 for 72 h. VSV-G and ΔE were used as positive and negative controls, respectively. n=3, data are shown as mean relative light units± SD. Statistical analysis was done using an ordinary one-way ANOVA and Tukey's multiple comparisons test set at a 95 % confidence interval. **** indicates $p<0.0001$, ** indicates $p<0.01$, * indicates $p<0.05$.

3.3.6 Effect of Polyethylene glycol as a Fusion Enhancer.

In order to find out if PEG 8000 at 4 % was cytotoxic to the cells, Huh7 and Huh7.NTCP cells were incubated with 4 % PEG 8000, and a cell viability assay was performed. Our data showed no significant change in cell viability of Huh7 (p=0.6192) and Huh7.NTCP (p=0.9656) in the presence of 4 % PEG8000 (Figure 3.7). To investigate the effect of PEG 8000 on HBV pseudotype entry, we infected Huh7 and Huh7.NTCP cells pseudotypes in the presence and absence of 4 % PEG and incubated for 72 h, after which cells were lysed and infectivity measured by luciferase assay. When Huh7 and Huh7.NTCP cells were infected with HBV BT10D4 pseudotype in the presence of 4 % PEG; RLU values showed no significant difference in its infectivity in Huh7 (p=0.9261) and Huh7.NTCP (p=0.6492) cells. This was also the case when Huh7 (p=0.2081) and Huh7.NTCP (p=0.1324) cells were infected with VSV-G positive control. However, when Huh7 cells were infected with HBV BR5B6 pseudotype in the presence of 4 % PEG, there was a significant increase in RLU values compared to when they were infected in the absence of PEG (p=0.0011). This was not the case when Huh7.NTCP cells were infected with HBV BR5B6 pseudotype in the presence of 4 % PEG, as there was no significant difference in the RLU values (p=0.4498) compared to when they were infected in the absence of PEG (Figure 3.8).
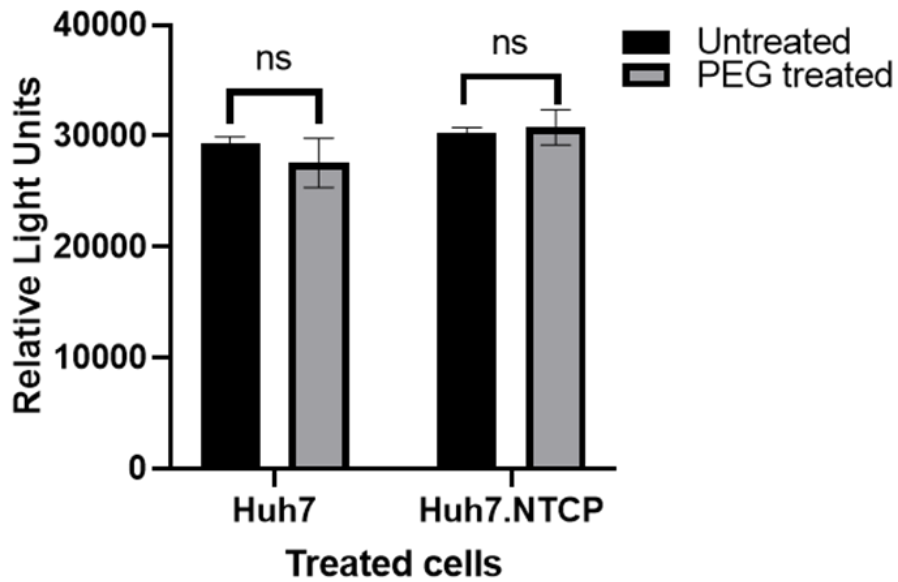
Figure 3.7 Cytotoxic effect of PEG on Huh7 and Huh7.NTCP cells. Huh7 and Huh7.NTCP cells were infected with 4 % PEG8000, and a cell viability assay was carried out. n=3, data are shown as mean relative light units± SD. Statistical significance was analysed with an unpaired t-test set at a 95 % confidence interval. ns indicates p>0.05.

A
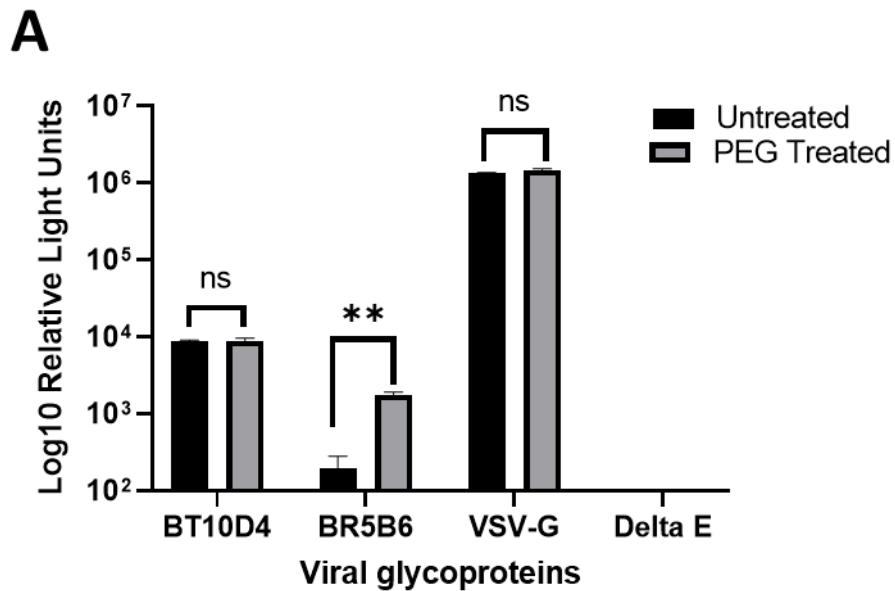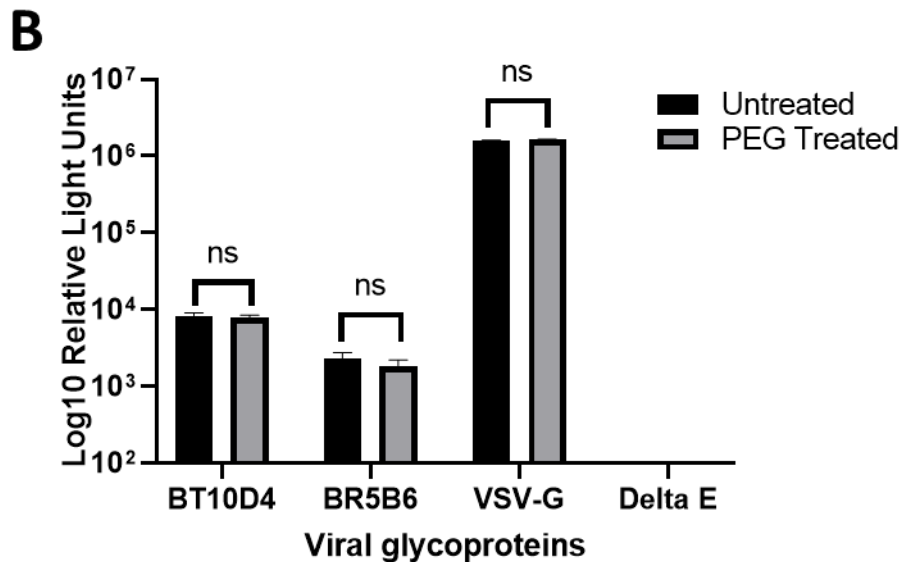
Figure 3.8 Infection of Huh7 and Huh7.NTCP cells in the presence and absence of a fusion enhancer. A. Huh7 and B. Huh7.NTCP cells were infected with HBV BR5B6 and BT10D4 pps in the presence and absence of 4 % PEG 8000. Infected cells were then incubated at 37 ^{0}C and 5 % CO_2 for 72h. VSV-G and ΔE were used as positive and negative controls, respectively. n=3, data are shown as log10 of mean relative light units± SD. Statistical significance was analysed with an unpaired t-test set at a 95 % confidence interval. ** indicates p<0.01, ns indicates p>0.05.

3.3.7 Selection of a suitable Reporter Enzyme.

Furthermore, we compared the commonly used firefly luciferase with the nano luciferase, a more recently designed luciferase enzyme that promises a much higher luminescent activity. Pseudotypes were generated with either pNL4-3.Luc.R-E- lentiviral vector possessing the firefly luciferase gene or pNL4-3.nanoLuc.R-E- lentiviral vector, which contained the nano luciferase gene. Harvested pseudotypes were used to infect Huh7 and Huh7.NTCP cells and incubated for 72 h, after which cells were lysed and infectivity measured by luciferase assay. There was no significant difference between the RLU values of the firefly luciferase and the nano luciferase from the infection of HBV BT10D4 pseudotypes in Huh7 (p=0.0789) and Huh7.NTCP (p=0.4473) cells (Figure 3.9). This was also the case when Huh7 (p=0.6239) and Huh7.NTCP (p=0.1069) cells

were infected with HBV BR5B6. However, there was a significant increase in the nano luciferase RLU values when Huh7 (p<0.0001) and Huh7.NTCP (p=0.0002) cells were infected with VSV-G pps (Figure 3.9).
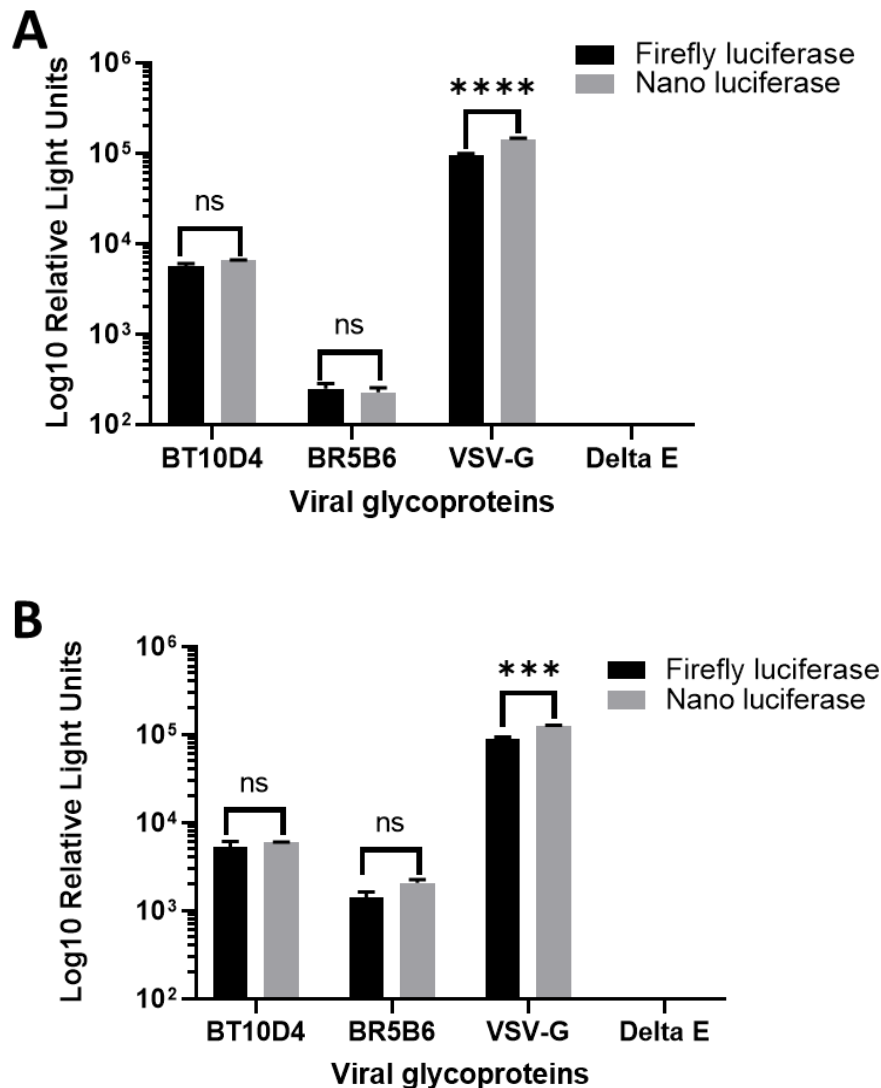
Figure 3.9 Infection of Huh7 and Huh7.NTCP cells with pseudotypes produced from HBV BR5B6 and BT10D4 with different reporter enzymes. A. Huh7 and B. Hu7.NTCP cells were infected with HBV pseudotypes produced with either pNL4-3.Luc.R-E- lentiviral (firefly luciferase) or pNL4-3.nanoLuc.R-E- lentiviral (nano luciferase) and incubated at 37 ^{0}C and 5 % CO_2 for 72 h. VSV-G and ΔE were used as positive and negative controls, respectively. n=3, data are shown as log10 of mean relative light units± SD. Statistical significance was analysed with an unpaired t-test set at a 95 % confidence interval. **** indicates p<0.0001, *** indicates p<0.001, ns indicates p>0.05.

3.4   Discussion

The availability of an efficient *in vitro* study system that supports HBV infection is crucial in studying the HBV entry pathway. HBV entry and infectivity depends on the L and S HBsAg glycoproteins, and despite the identification of the NTCP entry receptor, our understanding of the entry mechanisms is still limited because of the challenge of a suitable cell culture study model [52]. Virus pseudotyping is a powerful tool used to study virus envelope proteins. It is beneficial in characterising the phenotypic consequences of mutations present in the viral glycoproteins and their effects on immunogenicity, tropism, and serology [223]. This chapter is focused on developing a robust pseudotyping system for the study of the HBsAg glycoprotein and HBV entry. Optimising the protocol for this pseudotyping system would facilitate the generation of consistent pseudotype stocks of high titre that would be used in several downstream experiments. There are several mammalian expression vectors, of which pcDNA3.1(+) and pI.18 are examples. Selecting a suitable expression vector for efficient protein expression is pertinent, and in line with this, we compared the pcDNA3.1(+) and pI.18 expression plasmids. Our data revealed that constructs BT10D4 and BR5B6 cloned into pI.18 vector generated pseudotypes that were unable to infect Huh7 and Huh7.NTCP cells, however, this was not the case with the VSV-G glycoprotein. On the other hand, BT10D4, BR5B6, and VSV-G glycoproteins cloned into the pcDNA3.1(+) vector generated pseudotypes that were infectious. Although a comparative study has not been done, several research studies have successfully utilised either the pcDNA3.1(+) or the pI.18 vector, and it is unclear why one is chosen over the other [372-375]. The inability of the pI.18 vector to generate infectious pseudotypes could result from several factors, including non-functional promoter, no transcription of the gene, presence of a cellular inhibitory element, or no secretion of proteins. However, for the purpose of this optimisation and further experiments, the use pI.18 vector was discontinued. Furthermore, the viral vector is another essential factor in achieving an efficient pseudotyping system. We compared the infectivity of pseudotypes produced with the MLV viral vector and those produced with the pNL4-3.Luc.R-E- viral

vector. Our data showed that the infectivity of pseudotypes with the pNL4-3.Luc.R-E- viral vector was significantly higher than of the pseudotypes generated with an MLV vector. An important difference between these two viral vectors is the ability of lentiviral vectors (LV) such as pNL4-3.Luc.R-E- to cross through the nuclear membrane and transduce nondividing cells. This could result in the ability of pNL4-3.Luc.R-E- to transduce Huh7 and Huh7.NTCP cells better [376]. Additionally, several studies showing limitations in the generation of infectious pseudotypes have shown that pseudotyping viral vectors with viral glycoprotein does not necessarily lead to the generation of infectious pseudotypes [377-381]. It appears that the selection of viral vector and glycoprotein combinations have to be compatible for this system to work, and successfully generating infectious pseudotypes can be difficult to predict. This can be attributed to our limited understanding of the mechanisms of assembly of retrovirus pseudotypes. Sandrin, V and colleagues, in their study on the assembly of retroviral pseudotypes, investigated the ability of MLV or LV vectors to incorporate VSV-G, influenza haemagglutinin, HCV E1E2, retroviral MLV Env and RD114 cat virus glycoproteins. Their study showed that the localisation of the glycoproteins and the viral vector within the cell, as well as the ability of the glycoprotein to interact with the viral vector, are significant parameters that influenced the generation of infectious pseudotypes. The cytoplasmic tail of the successfully pseudotyped glycoproteins interact with the viral vector resulting in their colocalisation, packaging and release [382]. From our data, it is unclear why pseudotyping with the MLV vector was unable to generate infectious pseudotypes; however, it is highly plausible that the cytoplasmic tail of the HBV glycoprotein could not efficiently interact with the MLV vector, as seen in several other studies [379-381, 383, 384].

The amount of DNA used for pseudotype genesis was also optimised. The amount of envelope protein expression plasmid, viral pseudotype vector plasmid, and their ratio are crucial for optimal transfection efficiency. Using DNA concentrations below and above the ideal concentration could lower transfection efficiency and possibly cause cell toxicity [385]. Bajgelman, M.C. *et al.,* showed in their study exploring the critical parameters for transient

retrovirus production that a 1:1 ratio was the optimal ratio between the viral and packaging vectors at which they obtained a virus titre peak [386]. From our data, although there was no significant difference in varying the viral vector concentration for HBV BT10D4, however, 2 µg gave the highest infectivity for the HBV BR5B6, which was similar to the amount used by Urbanowicz, R.A., *et al.,* [247]. Similar to the Bajgelman, M.C. *et al.,* study, we used a 1:1 ratio of viral and packaging vectors in subsequent experiments. Furthermore, with the availability of different transfection methods, selecting the method of choice involves considering a cost-effective method that offers high transfection efficiency and low cell toxicity. As a result of the high levels of cell death caused by physical transfection methods such as electroporation, a chemical method of transfection was the method of choice [387]. This study compared the transfection efficiency of the K4, Lipofectamine, TransIT and Polyethylenimine transfection reagents by calculating their signal to noise ratio. Our data showed that the PEI and TransIT systems had higher signal to noise ratios than the K4 and Lipofectamine systems. Also, despite having lower RLU values than the TransIT system, the PEI system still possessed a higher signal to noise ratio. Hence, similar to other studies that have shown the efficiency and cost-effectiveness of the PEI system, subsequent experiments were done using this system [388-390]. In every cell-based experiment, cell health and degree of confluence greatly influence transfection efficiency. Knowing that some degree of cell death will occur during transfection, it is vital to seed the optimum number of cells. Studies have shown that seeding cells to achieve approximately 70 - 90 % confluency at the time of transfection is ideal [391, 392]. Too few cells could result in low cell growth due to poor cell-to-cell contact, while too many cells could inhibit cell growth and cause cell death. These could result in resistance to uptake of foreign DNA, decreased expression of the transfected gene and cell death [391-393]. Similarly, our transfection and infection data showed low efficiency at cell densities lower or higher than the optimum cell density. Consequently, based on these results, optimum transfection cell density was 1.5 million cells per dish, while optimum infection cell density was 20,000 cells per well.

For over 25 years, the use of PEG 8000 to enhance HBV infection in primary human hepatocytes, HepaRG hepatoma cells, and HepG2-NTCP has been shown to result in higher infection efficiency [214, 394, 395]. Gripon, P. *et al.,* in their studies, showed that infection of HBV into primary human hepatocytes was increased and highly reproducible in the presence of PEG 8000, possibly because PEG favoured a better interaction between the viral particles and the cells, resulting in increased internalisation [64, 395]. In the presence of PEG 8000, our data showed no significant increase in the entry of BT10D4 into Huh7 and Huh7.NTCP and a significant increase in the entry of BR5B6 into Huh7 cells. Studies have shown the fusogenic property of PEG 8000 and its ability to enhance membrane fusion [396-399]. Given that we have generated several other data that have confirmed the inability of BR5B6 to infect Huh7 cells, it is highly plausible that the increase in the entry of BR5B6 into Huh7 cells is a result of a non-specific fusion of the BR5B6 pseudotype with the cell membrane. This increase is not significant in BR5B6 entry into Huh7.NTCP cells or BT10D4 entry into both cell lines likely because their entry takes place via a more specific cell receptor mechanism. Although several studies have shown a significant increase in HBV infection with PEG 8000, our data has not shown such an increase. As our results do not show any significant benefit of infecting cells in the presence of 4 % PEG 8000, we carried out further experiments without PEG. Additionally, our data comparing the infectivity of the pseudotypes using the firefly luciferase and the nano luciferase systems showed no significant difference between both systems in the infectivity of the HBV pseudotypes. Hence, to maintain uniformity with previous experiments and the research team, subsequent experiments were carried out using the pNL4-3.Luc.R-E- lentiviral vector, which had the firefly luciferase gene insert.

This chapter has systematically tested a series of experimental conditions to generate an optimised *in vitro* pseudotyping protocol for the efficient pseudotyping of HBV surface protein. Although the individual investigations may not be particularly new, the optimised conditions as set out in this protocol is consistent, reliable, cost-effective, and resulted in a significant increase in the yield of the HBV pseudotyped virus.

Chapter 4

Investigation of Phenotypic Characteristics of

HBV Isolates.

4.1 Introduction

The Hepatitis B virus genome sequence has been studied extensively over the years, with 9 genotypes (A-I) and a putative genotype J, having >8 % nucleotide divergence and at least 35 sub-genotypes, with 4-8 % nucleotide divergence being defined to date. Significant genetic differences among these genotypes have been identified [400]. Consequently, there is a clear connection between HBV genome sequence and their replication, geographical distribution, and clinical outcomes such as therapy and drug resistance. Genotypes A-D are the most widely studied and characterised. Genotypes B and C, which are known to circulate in Asia, also majorly cause chronic infections, with genotype C being more likely to cause cirrhosis and hepatocellular carcinoma (HCC). Genotypes A and D with geographic distribution in Africa and Europe are transmitted mainly by horizontal mode of transmission, with genotype D being a significant cause of acute infection [400-402]. Studies have shown that HBV genotype H has a high incidence of occult HBV and low incidence of liver disease and HCC, while genotype G has led to increased fibrosis in the immunocompromised. These differences can be related to the low replication rate of genotype H and loss of 36-nucleotide insert and the presence of two translational stop codons of the precore/core region in genotype G resulting in its very low HBsAg and no HBeAg secretion [403-407].

Additionally, despite the genome similarity among HBV sub-genotypes, there are peculiar differences in their virological characteristics, mode of transmission and geographical distribution [320, 408]. Genetic recombination, which is a common occurrence in DNA and RNA viruses, plays a vital role in the genetic variability of HBV. The possibility of co-infection and superinfection provides a platform for genetic recombination, and although the mechanism of its occurrence is unclear, the resultant genetic variability drives the current disparity in the pathogenesis of HBV genotypes and sub-genotypes [408, 409].

HBV entry requires a low-affinity interaction with hepatic heparan sulfate proteoglycans (HSPG), which are glycoproteins consisting of two of three heparan sulphate chains covalently bonded together. Positively charged arginine

and lysine at amino acid positions s122 and s141 in the antigenic loop of HBsAg have been shown to interact with negatively charged HSPG in an electrostatic interaction. This interaction is necessary for stabilising the virus and facilitating its binding to NTCP [410-412]. Subsequently, HBV binds with high affinity to sodium taurocholate cotransporting polypeptide (NTCP), a glycoprotein located in the basolateral membrane of hepatocytes. This interaction results in HBV internalisation through endocytosis, although the precise mechanism is still poorly understood [52, 81, 287, 370]. Amino acids (aa) 2-48 in the preS1 region of HBsAg are crucial for HBV infection as they interact with the NTCP [30, 31]. HBsAg S domain contains 14 cysteine residues that form disulphide bridges common to L, M and S-HBsAg proteins, out of which 8 are in the major hydrophilic region (MHR) [58, 59].

Amino acids s99 to s169 constitute the HBsAg MHR containing the 'a' determinant from aa s124-s147. In chronic HBV infections, amino acid substitutions and insertions in HBV occur naturally due to treatment and immune-induced selection. These mutations manifest as immune and diagnostic escape mutants that impede clinical management. Mutations such as sC69*, sE2G and sG145R are the commonly studied and described mutations known to alter the immunogenicity and antigenicity of HBsAg [285, 413, 414]. Several studies have demonstrated diverse consequences of HBsAg mutations *in vitro*, *in vivo*, and clinically and more studies will. In a study by Murayama *et al.,* the deletion of 11 amino acids in the preS1 region of HBsAg resulted in an enhancement of the infectivity of cell culture-generated HBV into HepG2 cells transduced with NTCP [415-417].

In this chapter, we have studied the HBV entry pathway of different genotypes and clinical isolates, exploring how the presence of specific mutations at specific positions can alter HBV entry *in vitro*.

4.2 Materials and Methods

4.2.1 PCR, Cloning, Plasmid preparation and Sequence analysis.

DNA extracts for HBV genotypes A, B, C, D, and G were extracted from patient serum samples by a previous colleague, Gemma Clark, following the manufacturer's protocol of the automated NucliSENS easyMAG® system (Biomérieux Inc) kit. HBsAg sequences for all HBV samples were built using universal primers (HBvseq2b_2819f and HBVM_iR) previously optimised by a previous colleague, Gemma Clark (Table 4.1). The polymerase chain reaction (PCR) was set up following the HotStart Taq DNA Polymerase (Qiagen) protocol and by adding 2.5 µL of template DNA from the DNA extract. PCR thermocycling procedure was as follows: 15 min initial denaturation at 95 ^{0}C, 55 cycles of denaturation at 95 ^{0}C for 20 sec, annealing at 50 ^{0}C for 20 sec, and extension at 72 ^{0}C for 90 sec, followed by a final extension at 72 ^{0}C for 2 min. 2 µL of DNA gel loading dye (Thermo Fisher Scientific) was mixed with 5 µL of the PCR product loaded alongside a DNA ladder (Thermo Fisher Scientific) on a 2 % agarose gel (Thermo Fisher Scientific) containing 0.5 µg/mL ethidium bromide (Thermo Fisher Scientific). The gel electrophoresis was run in Tris-Acetate-EDTA (TAE) (60 mM Tris-acetate 50 mM EDTA, pH 7.8) buffer at 90 volts (V) for 36 min, and DNA bands were visualised by UV transillumination. The samples with positive bands were sequenced by Sanger sequencing (Source Bioscience) and aligned with Mega7 to generate a clean sequence.

Using the generated sequence, in-fusion cloning primers were designed with 15 base-pair extensions and the CACC tag at the 5' end of the primer, both of which are complementary to linearised vector. The CACC Kozak sequence base pairs with the GTGG overhang sequence of the pcDNA 3.1(+) vector (Thermo Fisher Scientific). CACC tag PCR was set up following the LongAmp Hot Start Taq DNA Polymerase (New England Biolabs, NEB) protocol and by adding 1 µL of template DNA from the PCR product. PCR thermocycling procedure was as follows: 30-sec initial denaturation at 94 ^{0}C, 55 cycles of denaturation at 94 ^{0}C for 15 sec, annealing at 51 ^{0}C for 15 sec, and extension at 65 ^{0}C for 70 sec, followed by a final extension at 65 ^{0}C for 10 min. PCR products were analysed on a 2 % agarose

gel, and positive samples were analysed by Sanger sequencing (Source Bioscience) and aligned with MEGA7 to confirm the sequence. All PCR annealing temperatures were derived using the New England Biolabs temperature calculator (NEB).

The PCR product was cleaned up following the Monarch PCR and DNA clean-up protocol (NEB). The pcDNA 3.1(+) vector was linearised at the EcoRI site by the EcoRI restriction enzyme (NEB), using 10 units of the EcoRI restriction enzyme, and incubating for 15 min following the NEB restriction digestion protocol. The purified PCR product was then cloned and transformed into Stellar competent cells using the in-fusion HD cloning and transformation protocol (Takara Bio). The optimal amounts of vector and insert used for the cloning were calculated using the In-Fusion molar ratio calculator (Takara Bio). Transformation mixes were spread on a selective lysogeny broth (LB) agar plate (100 µg/mL of ampicillin) and incubated for 16-18 h at 37 ^{0}C. After this, colonies were screened by PCR with standard T7 forward and bGH reverse primers, run on an agarose gel, and samples with positive bands were Sanger sequenced (Table 4.1). Screened colonies (samples with clean and correct sequences) were grown overnight in LB broth (100 µg/mL of ampicillin). Glycerol stocks were made by adding 300 µL of 100 % glycerol to 700 µL of overnight cultures and stored at -70 ^{0}C. Plasmids were prepared from the overnight cultures using GenElute Plasmid Miniprep and Midiprep kits (Sigma-Aldrich), according to the manufacturer's protocol. We quantified the plasmids using the Nanodrop 1000 (ThermoFisher) at 260 nm wavelength and measured in ng/mL for further use. The purity of the plasmid was measured using the 260/280 wavelength ratio (showed the absence of protein contaminants) and the 260/230 wavelength ratio (showed the absence of salt contaminants). A quality plasmid preparation used had a concentration of >100 ng/mL, a 260/280 ratio range of 1.8-2.0 and a 260/230 ratio range of 2.0-2.2. Furthermore, the BT10D4 clone was screened for contamination with VSV-G and Ebola plasmids. VSV-G and Ebola specific sequencing primers were used to sequence BT10D4 alongside VSV-G and Ebola plasmids as controls. All sequence analyses and comparisons were made using Mega7 software.

Table 4.1 Primers used in this study. Primers 1 and 2 were used to generate parental reference sequences. Primers 3 and 4 were designed to amplify the Large S protein for genotype D. Primers 5 and 6 were used to screen colonies and verify sequence after cloning. Primers 7 to 10 were used to screen the BT10D4 clone of contamination with VSV-G and Ebola plasmid.

Number	Primer name	Description	Primer sequence	Length
1	HBvseq2b_2819f	Forward primer	5'ACCWTATWCYTGGGAACAA3'	19
2	HBVM_iR	Reverse primer	5'GACACACTTTCCAATCAATNGG3'	22
3	HBV gtD in-fusionF	Forward primer	5'CACCATGGGGCAGAATCTTTCCACC3'	25
4	HBV gtD in-fusionR	Reverse primer	5'TTAAATGTATACCCAAAGACAAAAG3'	25
5	T7F sequencing	Forward primer	5'TAATACGACTCACTATAGGG3'	20
6	bGHR sequencing	Reverse primer	5'TAGAAGGCACAGTCGAGG3'	18
7.	VSVG plasmid primerF	Forward primer	5'GTGCCTTTTGTACTTAGCCTTT3'	22
8.	VSVG plasmid primerR	Reverse primer	5'AAGCATGACACATCCAACCG3'	20
9.	Ebola plasmid primerF	Forward primer	5'CCTGGAAATCAAGAAGCCCG3'	20
10.	Ebola plasmid primerR	Reverse primer	5'CACGCCATTGCCTTCCAG3'	18

4.2.2 Restriction Digestion

Single, with BamHI or PvuI (that cut at one point) and double digests with both restriction enzymes (NEB) were performed in a 25 µL reaction mix comprising of 3 µL Fast Digest Buffer, 3 µL of single digest restriction enzyme or 1.5 µL of each restriction enzyme in a double digest, 3 µL bovine serum albumin (BSA), 7 µL DNA Template and 9 µL nuclease-free water. Samples were incubated at 37 ^{0}C for 1 h and then run on an agarose gel. Band sizes were calculated using the DNA ladder guide (Thermo Fisher Scientific).

4.2.3 Site-directed Mutagenesis (SDM)

Primers for site-directed mutagenesis and their respective annealing temperature were designed and obtained using the NEBase changer software (Table 4.2). Substitution mutagenesis PCR was carried out for each selected mutation using the Q5 Site-Directed Mutagenesis protocol (NEB). PCR thermocycling procedure was as follows: 30-sec initial denaturation at 98 ^{0}C, 25 cycles of denaturation at 98 ^{0}C for 10 sec, annealing at 63 ^{0}C for 20 sec, and extension at 72 ^{0}C for 3 min, followed by a final extension at 72 ^{0}C for 4 min. PCR annealing temperature was calculated using the NEB temperature calculator (NEB). The PCR product was treated with kinase, ligase and DpnI enzymes and transformed according to the Q5 KLD reaction and transformation protocol (NEB). The plasmids were prepared from overnight cultures as described in section 4.2.1, and sequence analysis confirmed successful mutagenesis.

Table 4.2 Primers used for Site-directed Mutagenesis. Primers 1 and 2 were used to construct the BT10D4 sR69C mutant. Primers 3 and 4 were used to construct BT10D4 sA96V mutant. Primers 5 and 6 were used to construct BT10D4 sR69C and sA96V double mutant.

Number	Primer name	Description	Primer sequence	Length
1	HBVBT10D4SDMR69CF	Forward primer	5'TCCTCCAACT**TGT**CCTGGTTATC3'	23
2	HBVBT10D4SDMR69CR	Reverse primer	5'CAGGAGGTTGGTGAGTGAT3'	19
3	HBVBT10D4SDMA96VF	Forward primer	5'CTTCTTGTTG**GTT**CTTCTGGACTATC3'	26
4	HBVBT10D4SDMA96VR	Reverse primer	5'ATGAGGCATAGCAGCAGG3'	18
5	HBVBT10D4SDMR69CA96VF	Forward primer	5'TTCCTCTTCATCCTGCTGCTATGCCTCATCTTCTTGTTGGTTCTTCTGGACTATCAGGGTATG3'	63
6	HBVBT10D4SDMR69CA96VR	Reverse primer	5'GATGATAAAACGCCGCAGACACATCCAGCGATAACCAGG**ACA**AGTTGGAGGACAGGAGGT3'	60

4.2.4 Cell culture and transfection

The cell lines human embryonic kidney cells 293T (HEK293T), Huh7, and Huh7.NTCP were maintained as described in section 3.2.2. In order to generate pseudotypes (pps), HEK293T cells were seeded and transfected, as stated in section 3.2.3 and based on the optimised protocol from section 3.2.

4.2.5 Infection and Luciferase assay

Huh7 and Huh7.NTCP cells were infected following the optimised protocol from section 3.2.4. Luciferase assays were performed following the protocol in section 3.2.4.

4.2.6 Neutralisation assays

Cells were seeded and incubated according to established protocols and grown overnight. Monoclonal AP33 anti-HCV antibody [246] was used at a 1:50 concentration as previously established in the laboratory. The aim was to identify any contamination of BT10D4 plasmid with HCV H77 plasmid (a commonly used plasmid in our laboratory); HCV H77 and VSV-G pps were used as controls. In a 96-well V-bottom plate, 30 μL of diluted antibody (and 30 μL Phosphate-Buffered Saline (PBS) for the uninhibited control) was added to 270 μL of pps and incubated for 1 h at room temperature. 100 μL of the pp and antibody mix was added to the cells in triplicates, and cells were incubated for 4-6 h at 37 ^{0}C and 5 % CO_2. After 6 h, 150 μL of DMEM is added to the cells, and the cells were then incubated at 37 ^{0}C and 5 % CO_2 for 72 h. After 72 h, the luciferase assay was carried out as previously described in section 3.2.4.

4.2.7 Bicinchoninic acid assay (BCA assay), Sodium Dodecyl Sulfate–Polyacrylamide Gel Electrophoresis (SDS PAGE) and Western blot

Harvested pps were concentrated by sucrose cushion ultracentrifugation. In this step, 3 mL of 30 % sucrose (prepared in deionised water) was put into a 15 mL ultracentrifugation tube, after which 10 mL of the harvested pps were gently laid over the sucrose cushion. The ultracentrifugation tubes were carefully weighed, balanced out and centrifuged at 40,000 g for 2.5 h. The supernatants were decanted after centrifugation, and 200 µL of PBS was added to each pellet. Pellets were then kept for 24 h at 4 ^{0}C and resuspended for further use. According to the manufacturer's protocol, the total protein concentration of the resuspended pellets was determined using the BCA assay (Pierce BCA Protein Assay Kit). Protein concentration standard curve and calculations were performed using GraphPad Prism version 7. From these preparations, 25 µg of the protein was resuspended in 5x reducing loading buffer (2.5 mL of 0.5 mol/L Tris HCl pH 6.8, 0.39 g Dithiothreitol (DTT), 0.5 g Sodium Dodecyl Sulfate (SDS), 0.025 g Bromophenol Blue, 2.5 mL Glycerine) and heated to 100 ^{0}C for 5 min on a heat block to denature the proteins. Proteins were resolved alongside molecular markers using 10-12 % precast gel (Bio-Rad) and SDS running buffer (15.18 g Tris HCl, 93.85 g Glycine, 50 mL of 20 % SDS) at 120 V for 90 min. Blotting paper and Polyvinylidene difluoride (PVDF) (Amersham) membranes were then soaked in already prepared transfer buffer (5.8 g Tris HCl, 2.9 g Glycine, 1.85 mL of 20 % SDS, 200 mL methanol). Resolved proteins were transferred to PVDF membranes at 100 mA for 60 min using a Trans-Blot transfer system. According to the manufacturer's protocol, protein transfer was confirmed by gel stain with Imperial Protein Stain (Thermo Fisher Scientific) and PVDF membranes stained with Ponceau S stain (Sigma). PVDF membranes were then blocked overnight with freshly prepared PBS, 0.1 % Tween and 10 % skimmed milk (PBSTM) at 4 ^{0}C. The membranes were then washed five times with PBST (with 150 mM NaCl) for 5 min per wash with rocking. The membranes were incubated with 1:1000 of the mouse monoclonal anti-HBsAg primary antibody Ma1694 (Abnova) and mouse

monoclonal anti-HIV1 p24 antibody ab9071 (Abcam) in PBSTM at 4 ^{0}C overnight. They were then washed and incubated with 1:2000 of rabbit anti-mouse Horseradish peroxidase (HRP) secondary antibody (Sigma) for 1 h at room temperature with rocking. The membrane was then treated with Radiance Plus Chemiluminescent HRP substrate reagent (Azure Biosystems) for 5 min, put in a clean, transparent sheet and viewed with a G: BOX F3 gel doc system for gel imaging. Test sample band sizes are compared to the Spectra Multicolour Broad Range Protein Ladder (Thermo Fisher Scientific).

4.3   Results

4.3.1   Infectivity of clones of different HBV genotypes

Detailed understanding of the HBV entry pathway and potential receptors and co-receptors and co-factors involved in this entry and how HBsAg mutations affect HBV cell entry was the aim of this research. We first assessed the infectivity of different clones of different genotypes of HBV in Huh7 and Huh7.NTCP cells. We did this in order to select a specific genotype with which to carry out other downstream experiments. Transient transfection of one representative of each genotype: A (clone BR1A4); B (clone BR5B6); C (clone BT7C2); D (clone BT10D4); and G (clone BT16G2) in HEK293T cells generated a panel of HBV pseudotypes (HBVpp). Huh7 and Huh7.NTCP cells were infected with these pps. RLU values from this infectivity testing showed a significant infectivity increase in HBV genotypes A ($p<0.0001$), B ($p<0.0001$), C ($p<0.0001$) and G ($p<0.0001$) in Huh7.NTCP cells compared to Huh7 cells. However, results showed that the infectivity of HBV genotype D (BT10D4) in both cell lines was significantly higher than the other genotypes ($p<0.0001$) and its infectivity in Huh7 and Huh7.NTCP was not significantly different ($p=0.4245$) (Figure 4.1). This unexpected data indicated that the BT10D4 genotype D isolate was infecting Huh7 cells independent of NTCP expression. As such, there was a need to investigate this clone further to understand the mechanism behind its entry behaviour.
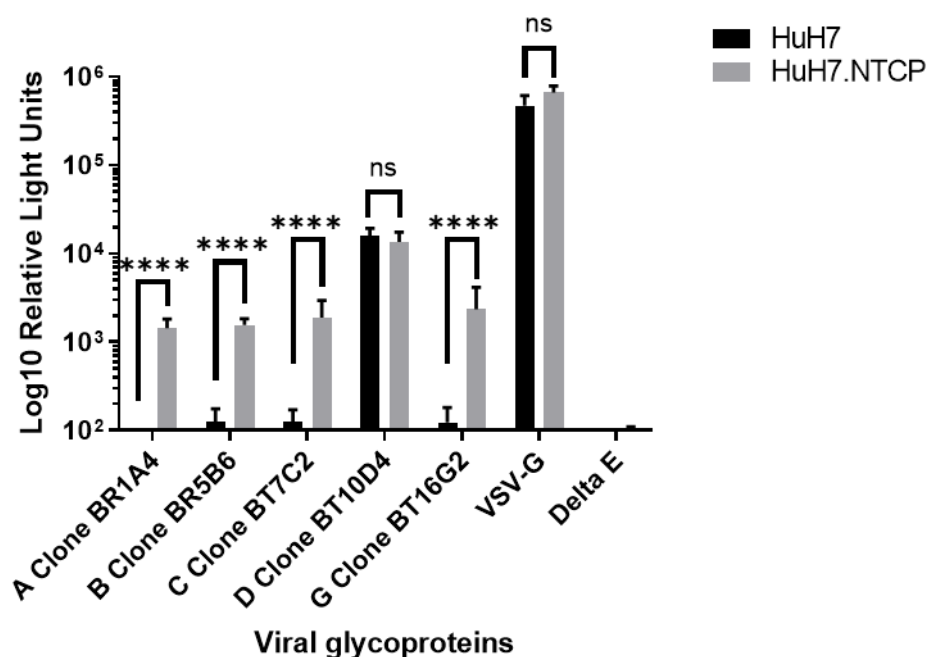
Figure 4.1 Infection of Huh7 and Huh7.NTCP cells with pseudotypes produced from HBV genotypes A (BR1A4), B (BR5B6), C (BT7C2), D (BT10D4), and G (BT16G2). Huh7 and Huh7.NTCP cells were infected with HBV pseudotypes and incubated at 37 ^{0}C and 5 % CO_2 for 72 h. VSV-G and Delta E were used as positive and negative controls, respectively. n = 3, data are shown as means log10 Relative light units± SD. Statistical significance was analysed with an unpaired t-test set at a 95 % confidence interval. **** indicates $p < 0.0001$, ns indicates $p > 0.05$.

4.3.2 Validation of the clone BT10D4

Determination of the order of nucleotides in a specific DNA is achieved by sequencing. It is known as a fast and reliable way to verify the genetic sequence of a plasmid. In line with this, the BT10D4 clone was Sanger sequenced with T7F forward and bGHR reverse sequencing primers. Before this time, all plasmids with cloned viral glycoprotein genes used in the lab were in the pcDNA3.1(+) vector to ensure uniformity and ease in tracing contaminants. The pcDNA3.1(+) vector carries the T7 promoter and the bGH priming sequences, which meant that data from sequencing BT10D4 with primer sequences from them could be analysed to ascertain that its sequence is correct and to identify any contaminating glycoprotein plasmid in the background because the presence of

T7F and bGHR in pcDNA3.1(+) unifies all glycoprotein plasmids used in the lab. The resulting sequence data were trimmed and aligned using MEGA7 to an HBV genotype D reference sequence (FJ904433.1) [418]. This analysis revealed a 99 % uniformity between the BT10D4 sequence and the HBV genotype D reference sequence. The analysis also showed a clean sequence data read with no contaminating background calls. Also, after infectivity levels of all glycoproteins used in the lab were assessed, we determined that the VSV-G and Ebola Makona glycoprotein plasmids were the only plasmids used in the laboratory that could produce pps that generate such high RLU values. We further designed primers specific to Ebola Makona glycoprotein, and VSV-G and Sanger sequenced BT10D4 for Ebola and VSV-G glycoproteins to identify low-level contamination with these. No coherent sequence from BT10D4 was generated using VSV-G and Ebola. Control sequences with plasmids possessing the cloned VSV-G and Ebola Makona glycoprotein showed 100% similarity to its reference sequence. Restriction digestion is a convenient and inexpensive way to screen plasmids, verify the content, and detect possible contamination. The vector backbone pcDNA3.1(+) containing the BT10D4 insert possessed several restriction sites, including BamHI and PvuI. With this understanding, single and double digests of this BT10D4 and BR5B6 (control) were performed with BamHI and PvuI enzymes and compared the fragment sizes with the undigested and no plasmid controls. A gel image of single digestion of BT10D4 and BR5B6 with BamHI and PvuI restriction enzymes showed one band of the linearised plasmid. In the double digestion with both BamHI and PvuI, there were two bands of sizes of 1482 and 5126 base pairs (Figure 4.2).
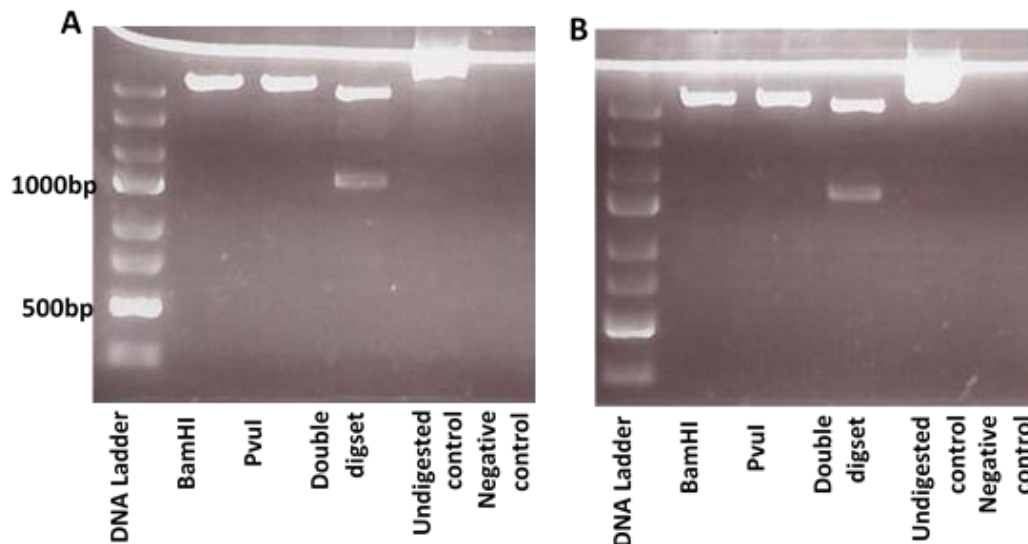
Figure 4.2 Restriction digestion of BT10D4 and BR5B6. A. BT10D4 and B. BR5B6 were digested with BamHI, PvuI individually and together and was resolved on an agarose gel. Bands were viewed under ultraviolet light, and band sizes were determined using the DNA ladder.

Neutralising antibodies prevent viral infection as they potentially bind to the virus, preventing it from binding to the cell and cause an infection. Based on this, we carried out a neutralisation assay in both Huh7 and Huh7.NTCP cells using an anti-Hepatitis C virus (HCV) antibody, a closely related virus studied in the laboratory. This involved infection of Huh7 and Huh7.NTCP with BT10D4 in the presence and absence of monoclonal AP33 anti-HCV antibody [246] using HCV H77 and VSV-G pps as controls. The aim was to identify any contamination of BT10D4 plasmid with HCV H77 plasmid (a commonly used plasmid in our laboratory), in which case the HCV antibody would neutralise the infectivity. These assays showed that no significant neutralisation of BT10D4pp infectivity by the HCV antibody occurred both in Huh7 ($p=0.9829$) and Huh7.NTCP ($p=0.4652$) cells (Figures 4.3). Results showed that the presence of the HCV antibody resulted in a significant neutralisation of the infectivity of HCV H77pp entry in both Huh7 ($p=0.0013$) and Huh7.NTCP ($p=0.0011$). There was also no neutralisation of the VSV-Gpp infectivity in Huh7 ($p=0.6525$) and Huh7.NTCP ($p=0.8749$) (Figures 4.3).
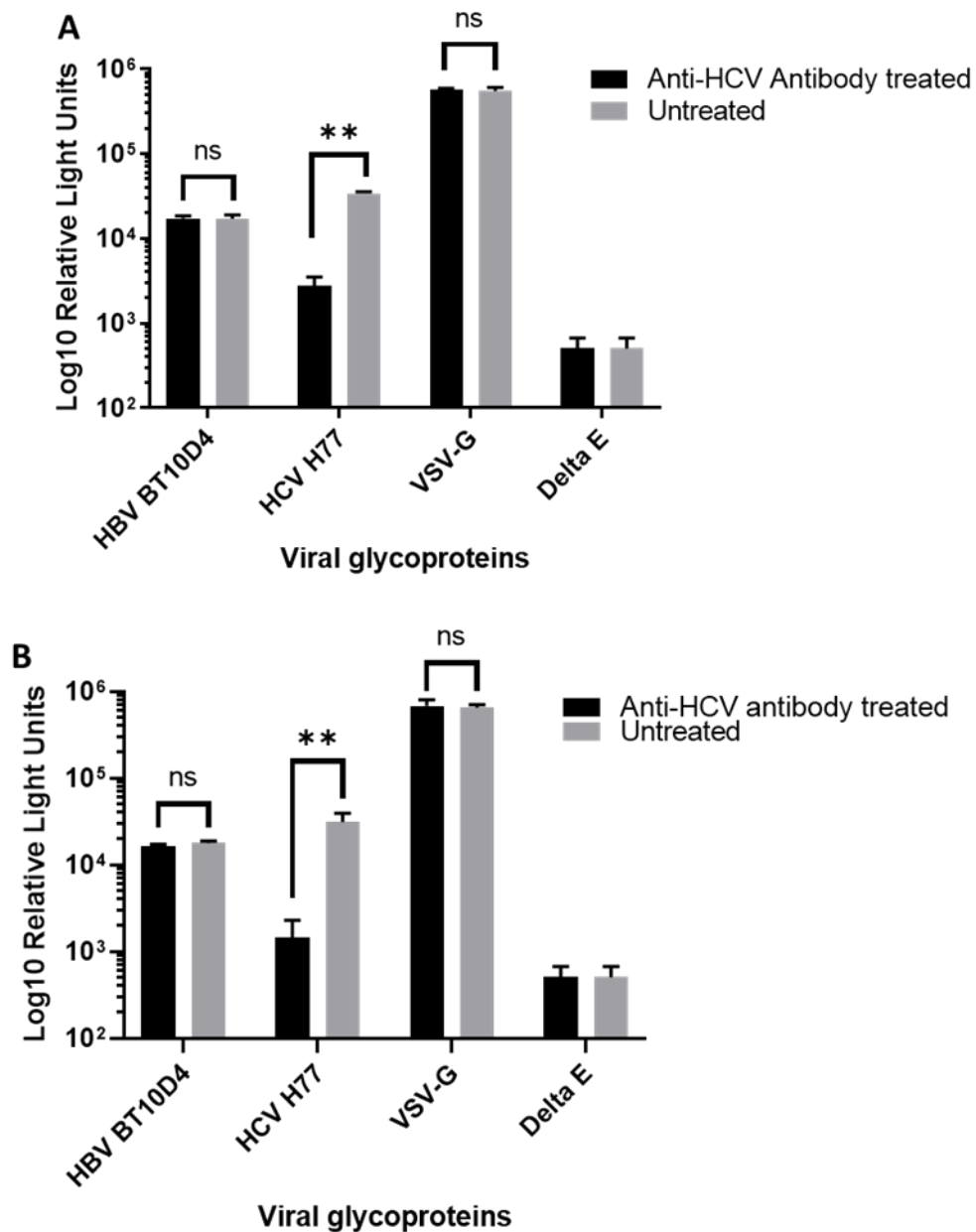
Figure 4.3 Neutralisation of BT10D4 infection in Huh7 and Huh7.NTCP cells using HCV antibody. A. Huh7 and B. Huh7.NTCP cells were infected with BT10D4 and HCV H77 pseudotypes in the presence and absence of monoclonal AP33 anti-HCV antibody and incubated at 37 ^{0}C and 5 % CO_2 for 72 h. VSV-G and ΔE were used as positive and negative controls, respectively. n = 3, data are shown as means log10 Relative light units± SD. Statistical significance was analysed with an unpaired t-test set at a 95 % confidence interval. ** indicates $p < 0.01$, ns indicates $p > 0.05$.

Finally, re-cloning and retransformation of HBV BT10D4 and selecting 2 individual colonies for a repeat of the validation process confirmed the absence of contaminants that could have arisen during cloning, enabling us to ensure that the plasmid preparation we worked with in subsequent experiments was without contamination.

4.3.3 Cloning and testing of other genotype D isolates

Studies have shown that genetic variations among HBV genotypes result in phenotypic differences that have clinical and epidemiological implications. Specific genotypes are known to have genotype-specific characteristics responsible for various clinical outcomes. Putting the unusual behaviour of BT10D4 into perspective and having verified the absence of contamination, the immediate question was to understand if this phenotypic characteristic was genotype-specific or strain-specific.

In order to do this, we cloned the S gene of other genotype D isolates from the same Nottingham cohort as BT10D4. Four DNA extraction samples (D13, D21, D39, D40) with high viral load were selected, amplified, and sequenced. These were subsequently cloned into pcDNA3.1(+) and transformed into competent cells. Plasmid extraction, purification and sequencing were then carried out to prepare the plasmid for further *in vitro* analysis.

In vitro experiments were performed to generate pseudotypes; Huh7 and Huh7.NTCP infected with the pseudotypes. Infectivity data showed infectivity levels for other genotype D isolates to be significantly higher in Huh7.NTCP cells than Huh7 cells for pps ($p<0.0001$) (Figure 4.4). There were also differences in the infectivity of the tested genotypes D isolates in Huh7.NTCP cells; there was no significant difference between the infectivity of D13 and D21 ($p=0.5488$) and between D39 and D40 ($p=0.5327$). However, the infectivity of D13 and D21 were significantly higher than that of D39 and D40 ($p<0.0001$).
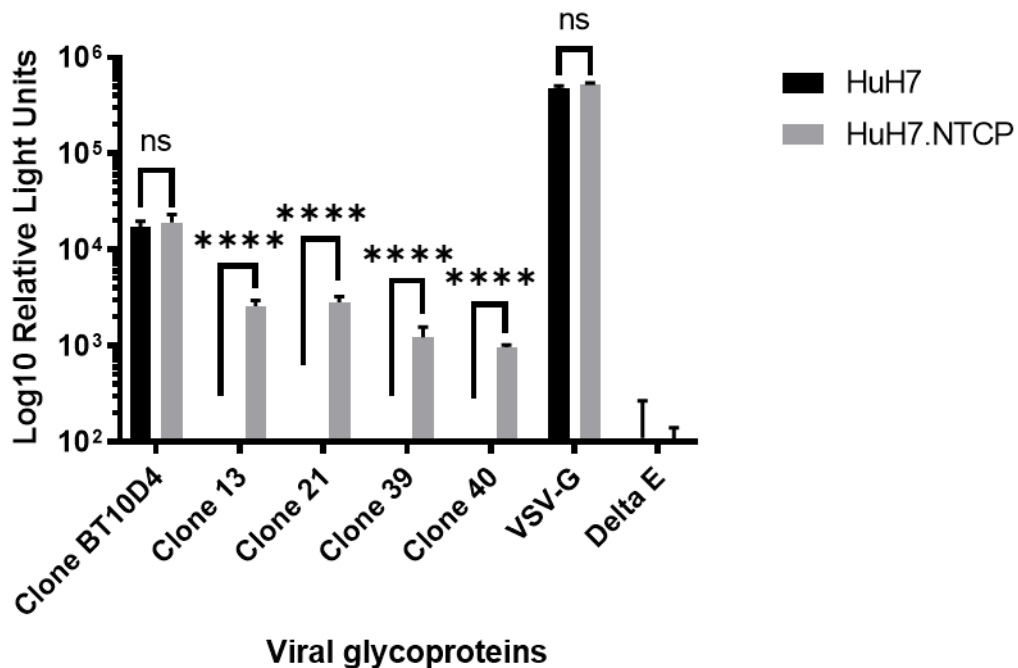
Figure 4.4 Infection of HBV genotype D isolates in Huh7 and Huh7.NTCP cells. Huh7 and Huh7.NTCP cells were infected with HBV BT10D4, D13, D21, D39, D40 pseudotypes and incubated at 37 ^{0}C and 5 % CO_2 for 72 h. VSV-G and ΔE were used as positive and negative controls, respectively. n = 3, data are shown as means log10 Relative light units± SD. Statistical significance was analysed with an unpaired t-test set at a 95 % confidence interval. **** indicates p<0.0001, ns indicates p>0.05.

In addition, pseudotype suspensions were concentrated by sucrose density gradient ultracentrifugation and analysed for HIV p24 capsid protein from the viral vector and HBsAg protein expression by western blotting. The western blot images in Figure 4.5A showed the expression of the HIV p24 capsid and the p55 Gag precursor protein. The western blot images in Figure 4.5B showed the expression of the S-HBsAg (p24 and gp27), M-HBsAg (p33) and L-HBsAg (p39 and gp42) (Figure 4.5). From the western blot images, it was seen that pseudotypes of BT10D4 expressed more p24 and low HBsAg; D13 expressed more HBsAg than p24; D21 expressed more HBsAg than p24; D39 expressed more p24 than HBsAg; D40 expressed an almost similar amount of p24 and HBsAg (Figure 4.5). The western blot images also showed BT10D4 and D39 had the highest p24

114

expression compared to the other clones, while D21 followed by D13 had the highest HBsAg expression, particularly L-HBsAg compared to the other clones (Figure 4.5).
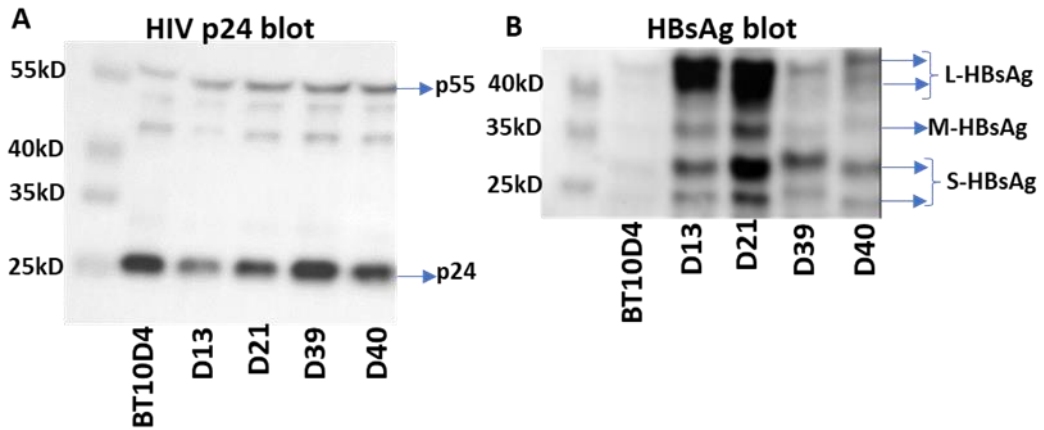
Figure 4.5 Western blot analysis of HBV pseudotypes. HBV pps from BT10D4, D13, D21, D39 and D40 were concentrated, quantified, resolved on SDS PAGE and transferred to a PVDF membrane. The membrane was incubated with 1:1000 of the mouse monoclonal primary antibodies Ma1694 and ab9071 and then incubated with 1:2000 of rabbit anti-mouse Horseradish peroxidase (HRP) secondary antibody (Sigma) and viewed with a G: BOX F3 gel doc system. Spectra Multicolour Broad Range Protein Ladder was used as a molecular marker for comparison.

4.3.4 Sequence Analysis

Given the unusual infectivity of BT10D4 independent of NTCP and the dependence of other genotype D isolates on NTCP for entry, it was imperative to compare the amino acid sequences of all the genotype D isolates. Isolates BT10D4, D13, D21, D39 and D40 were sequenced using T7 forward and bGH reverse sequencing primers. The sequences were queried using the Basic Local Alignment Search Tool (BLAST) to identify their subgenotype. BLAST results showed that D13 and D40 sequences were 99.57 % and 99.32 % similar to HBV subgenotype D1 while BT10D4, D21 and D39 were 98.97 %, 99.40 % and 98.63 % similar to HBV subgenotype D3, respectively. We further aligned these generated sequences in MEGA 7 alongside 16 genotype D sequences from the Nottingham

cohort and 1,520 genotype D sequences sourced from an HBV database [419]. The alignment revealed several single point nucleotide substitutions that were either silent or resulted in amino acid changes at different positions across all the compared sequences. However, we identified a single C to T nucleotide change at positions 695 and 776 respectively present in BT10D4, D39 and JF439696 (C to T in 695 only) from the HBV database only (Fig4.6). These nucleotide changes resulted in a cysteine to arginine amino acid substitution at position 232 (s69) in the cytoplasmic loop and valine to alanine substitution at position 259 (s96) in the second transmembrane domain (Fig 4.6). However, in the overlapping reverse transcriptase of the polymerase gene, the C to T change at position 695 resulted in leucine to serine amino acid substitution (rtL77S) while the C to T change at position 776 was silent (Figure 4.7). The presence of sR69 and sA96 in only 3 out of 1541 compared sequences shows how rare these amino acid substitutions are. As a follow-up and to identify other genetic differences between BT10D4 and D39, we compared their sequences. We identified other nucleotide differences at positions 433, 595, 1060 and 1108 (Figure 4.8). These nucleotide differences resulted in amino acid differences at positions 145 in the preS2, 199 (s36) in the cytoplasmic loop, 354 (s191) in the transmembrane 3 and 370 (s207) in the transmembrane 4 regions (Table 4.3).

Figure 4.6 Representative image of the sequence analysis of BT10D4, D13, D21, D39 and D40 alongside 16 genotype D sequences from the Nottingham cohort and 1,520 genotype D sequences sourced from an HBV database. Red stars highlight cysteine (C) to arginine (R) amino acid substitution at position 232 (s69) and valine (V) to alanine (A) substitution at position 259 (s96) identified in BT10D4, D39 and JF439696 (C to R in 695 only) from the HBV database.

Figure 4.7 Rare amino acid substitution present in BT10D4, D39 and JF439696. The C to T change at position 695 resulted in leucine to serine amino acid substitution (rtL77S), while the C to T change at position 776 was silent.
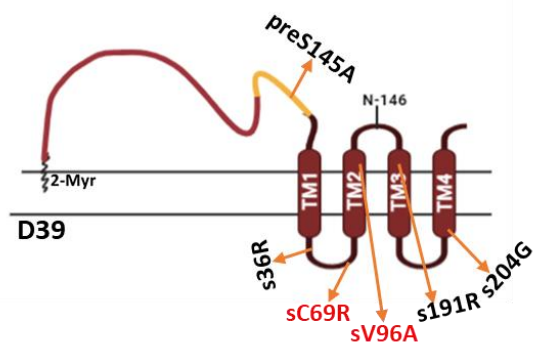
Figure 4.8 Sequence comparison of BT10D4 and D39. The sC69R and sV96A substitutions (in red) were present in both BT10D4 and D39. There were nucleotide differences between BT10D4 and D39 that resulted in amino acid differences at positions 145 in the preS2, 199 (s36) in the cytoplasmic loop, 354 (s191) in the transmembrane 3 and 370 (s207) in the transmembrane 4 regions. The figure was created at http://biorender.com/.
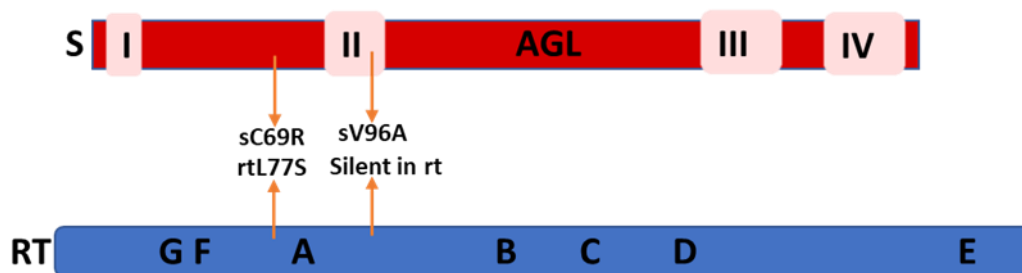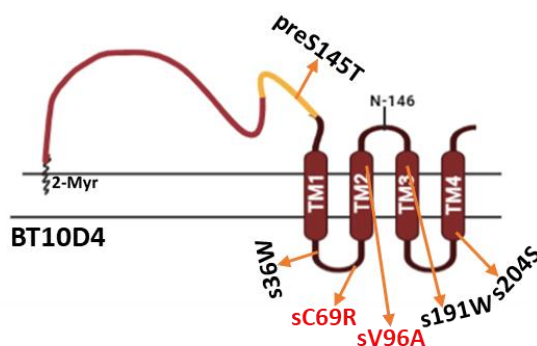
Table 4.3 Comparison of BT10D4 and D39 sequences showing nucleotide changes and the resultant amino acid changes.

Amino acid/Nucleotide position	HBsAg amino acid differences	
	BT10D4	D39
PreS 145/433	Threonine (T) (**A**CT)	Alanine (A) (**G**CT)
199 (s36)/595	Tryptophan (W) (**T**GG)	Arginine (R) (**C**GG)
354 (s191)/1060	Tryptophan (W) (**T**GG)	Arginine (R) (**A**GG)
370 (s207)/1108	Serine (S) (**A**GC)	Glycine (G) (**G**GC)

4.3.5 Infectivity of reverse mutants

To gain a clearer understanding of the effects of the two rare mutations previously identified in BT10D4 on its infectivity, clones bearing the opposite amino acid were created using SDM. In order to achieve this, SDM primers were designed to substitute T with C at amino acids 695 and 776. This substitution reversed the arginine (s69) and alanine (s96) in BT10D4 to cysteine (mutant 1) (s69) and valine (mutant 2) (s96). Single mutants with one substitution and a third mutant (mutant 1+2) that had both substitutions were constructed. After plasmid extraction, purification and sequencing, the plasmids were used for *in vitro* experiments. Subsequently, HEK 293T were co-transfected with each of the BT10D4 mutants and wildtype with pNL4-3.Luc.R-E- to produce pseudotypes. Huh7 and Huh7.NTCP infected with pseudotypes and incubated for 72 h were lysed and infectivity measured by luciferase assay.

The results showed that with the introduction of one of the mutations (mutant 1 or mutant 2) to BT10D4, the NTCP-independent entry was lost. Thus, the infectivity of mutant 1 and mutant 2 into Huh7 cells was significantly lower than their infectivity in Huh7.NTCP (p<0.0001) (Figure 4.9). However, on introducing both mutations (mutant 1+2) into the BT10D4, the NTCP independence was

regained similar to that of BT10D4, there was no significant difference between the infectivity in Huh7 and Huh7.NTCP cells (p=0.7555) (Figure 4.9). However, the level of infectivity of the mutant 1+2 in both Huh7 and Huh7.NTCP cells was significantly reduced compared to BT10D4 (p<0.0001) (Figure 4.9). As seen previously, there was no significant difference between the infectivity of BT10D4 into both Huh7 and Huh7.NTCP (p=0.9136) (Figure 4.9).
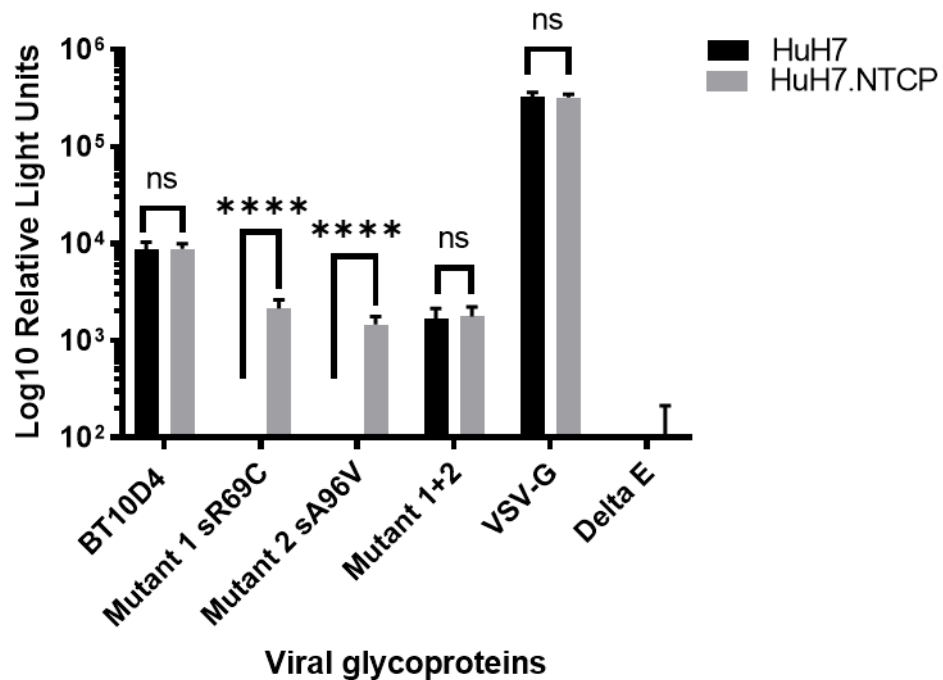
Figure 4.9 Infection of BT10D4 and constructed reverse mutants in Huh7 and Huh7.NTCP cells. Huh7 and Huh7.NTCP cells were infected with pseudotypes from BT10D4, mutant 1 (sR69C), mutant 2 (sA96V) and mutant 1+2, incubated at 37 ^{0}C and 5 % CO_2 for 72 h. VSV-G and ΔE were used as positive and negative controls, respectively. n = 3, data are shown as means log10 Relative light units± SD. Statistical significance was analysed with an unpaired t-test set at a 95 % confidence interval. **** indicates p<0.0001, ns indicates p>0.05.

Also, pseudotype suspensions of BT10D4, mutant 1 (sR69C), mutant 2 (sA96V), and mutant 1+2 were concentrated by sucrose cushion ultracentrifugation and analysed for HIV p24 and HBsAg protein expression by western blotting. The western blot images in Figure 4.10A showed the expression of the HIV p24 capsid

and the p55 Gag precursor protein. The western blot images in Figure 4.10B
showed the expression of the S-HBsAg (p24 and gp27), M-HBsAg (p33 and gp36)
and L-HBsAg (p39 and gp42) (Figure 4.10). Western blot images showed that
pseudotypes from BT10D4 expressed more p24 and low HBsAg; mutant 1, sR69C,
expressed similar amounts of p24 and HBsAg; mutant 2, sA96V, expressed more
p24 and very low HBsAg while mutant 1+2 expressed similar high amounts of p24
and HBsAg (Figure 4.10).
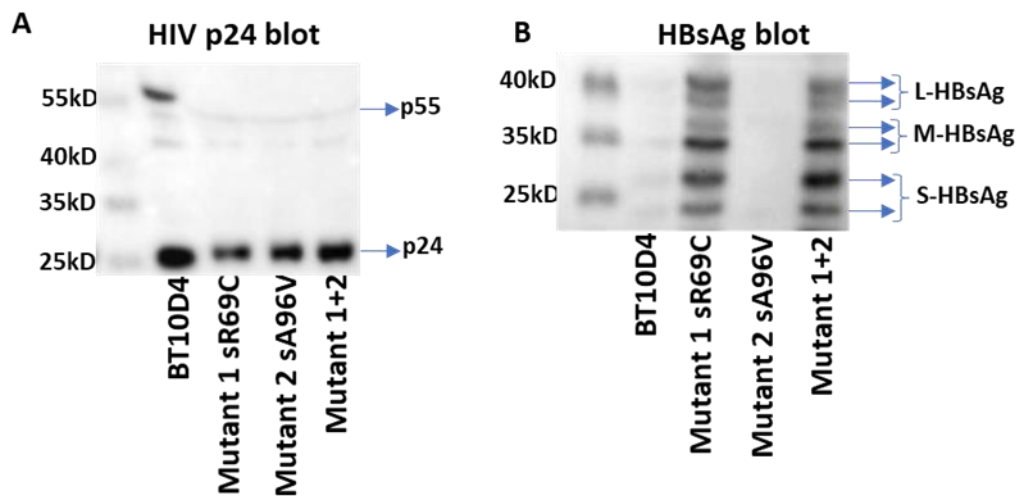
Figure 4.10 Western blot analysis of HBV pseudotypes. HBV pps from BT10D4, mutant 1
sR69C, mutant 2 sA96V, and mutant 1+2 were concentrated, quantified, resolved on SDS
PAGE and transferred to a PVDF membrane. The membrane was incubated with 1:1000
of the mouse monoclonal primary antibodies Ma1694 and ab9071 and then incubated
with 1:2000 of rabbit anti-mouse Horseradish peroxidase (HRP) secondary antibody
(Sigma) and viewed with a G: BOX F3 gel doc system. Spectra Multicolour Broad Range
Protein Ladder was used as a molecular marker for comparison.

4.4 Discussion

The identification of NTCP as a receptor necessary for HBV entry into hepatocytes and preS1 2-48 as the binding domain has revolutionised HBV research, enabling researchers to produce a consistent transformed cell line model for HBV infection [50, 81, 420-422]. This achievement has led to a better understanding of the virus, its entry and tropism. It is now also believed that HSPG cooperatively contributes to the cellular binding and entry of HBV at the molecular level, although the mechanism through which this happens is still unclear. Previous studies have shown the multi-step entry pathway of HBV, which begins with a low-affinity interaction to HSPG and then a high-affinity binding that leads to HBV entry by endocytosis [410, 411, 423]. In this study, we sought to identify and understand the use of other co-receptors and co-factors in HBV entry. Infection of Huh7 and Huh7.NTCP with pseudotypes from several HBV genotypes was a preliminary step to test all genotypes as well as show the change in infectivity in the presence of NTCP. However, early experiments indicated that HBV genotype D (isolate BT10D4) infected cells irrespective of NTCP expression was both unexpected and intriguing, hence the immediate need to validate the clone by ruling out the presence of any contaminants.

Sanger sequencing of BT10D4 with T7 forward and bGH reverse primers revealed a clean and correct sequence, thus indicating that BT10D4 was indeed an HBV genotype D isolate and that there was no contaminating plasmid sequence detected. Careful investigation of all plasmids available within our laboratory revealed Ebola, VSV-G and HCV plasmids as possible contaminants. Further Sanger sequencing with specific Ebola and VSV-G primers used to sequence the BT10D4 clone ruled out the presence of both plasmids as contaminants. Restriction digest confirms plasmid sizes and can predict the characteristics of the plasmid according to the predicted sizes. The presence of more DNA fragments than expected or fragments of unexpected sizes would indicate a contaminating plasmid. Restriction digestion of BT10D4 clone and BR5B6 control revealed the expected number of bands of the right sizes with no unexpected bands. This result further establishes the purity of the plasmid. Previous research

from our team and other groups have shown that monoclonal antibody AP33 can neutralise HCV infection by interacting with the E2 domain [246, 424, 425]. In the experiments performed here, AP33 resulted in significant neutralisation of HCV infection and no neutralisation of infection when using the HBV BT10D4 clone. This supported previous studies and confirmed the absence of the HCV H77 plasmid contaminant [246, 424, 425]. Finally, recloning and retransformation of HBV BT10D4 and selection of 2 individual colonies for a repeat of the validation process confirmed the absence of contaminants that could have arisen during cloning, enabling us to make sure that the plasmid preparation we worked with in subsequent experiments was without contamination and to demonstrate that the phenotype was not just associated with one batch of the plasmid.

In this study, our data showed the NTCP dependence of clones representing genotypes A, B, C, D, and G; however, we did not identify any significant difference in the infectivity pattern of genotypes A, B, C, and G. Interestingly, we identified unusual infectivity in genotype D isolate BT10D4 which made its infectivity higher than other genotypes and independent of NTCP. In these experiments, a pseudotyping system was used to understand the HBV entry in better detail, and although this system interrogates the function of HBsAg only, there are apparent phenotypic differences that could result from their genetic differences. Comparative studies of HBV genotypes and variants have revealed striking phenotypic differences between them. Genetic variations in HBV genotypes have profound effects on the viral prognosis, pathogenesis, viral detection, immune response, and drug therapy. *In vitro* studies analysing the characteristics of various HBV genotypes have found that genetic variations have a role in modulating replication and gene expression [403, 426-428]. In one study of HBV infections of Africans living in Australia, genotypes D and E were identified as the most typical genotypes associated with poor clinical prognosis, lowered vaccine efficiency, and a more rapid disease progression to liver cancer [429]. Also, data from a study by Sozzi *et al.,* showed that significant differences in replication and gene expression exist between the genotypes. Using several *in vitro* experiments, they showed that genotypes A, C, and D have the highest

replicative capacity while genotypes B and J had the least [426]. A similar study from Sozzi *et al.* described occult HBV and less severe disease pathogenesis seen in HBV genotype H clinical manifestations due *to* its low replication capability indicated by low HBV DNA levels and HBeAg expression [403].

As we further investigated the entry of other HBV genotype D strains in comparison with the unusual BT10D4 strain, it was found that other genotype D isolates were NTCP-dependent, as reported in previous studies [223]. Our data also showed differences in the infectivity of all the HBV genotype D clones, with clones D13 and D21 having higher infectivity values than D39 and D40. In addition, analysis of protein expression by western blotting showed that D13 and D21 expressed the highest amount of HBsAg. High expression of HBsAg in D13 and D21 implies a higher amount of secreted HBsAg-containing pseudotype particles capable of entry into Huh7.NTCP cells, which explains the higher infectivity values compared to D39 and D40. These two showed lower HBsAg expression, likely indicating reduced secretion of infectious pseudotypes capable of entry into Huh7.NTCP cells. Hence, these data suggest that HBV D13 and D21 clones expressed and secreted HBsAg more efficiently than D39 and D40. The fact that these HBV genotype D isolates were acquired from different patients and are of different subgenotypes highlight their varying genetic sequences, which could explain the differences in their expression and secretion of HBsAg [320]. This has also been shown by Bannister, E. *et al.,* in a study that showed that HBV D3 replicated more efficiently than A1, D2 and D6, whereas A1 expressed and secreted the HBsAg more efficiently [430]. On the other hand, HBV BT10D4 showed higher infectivity in both Huh7 and Huh7.NTCP cells but had the lowest level of HBsAg. There are two plausible explanations for this observation: firstly, BT10D4 could be secreting low levels of HBsAg that are more efficient in entry and infection of Huh7 and Huh7.NTCP cells through an unknown mechanism. Secondly, it could be that BT10D4 secretes HBsAg efficiently; however, the anti-HBsAg antibody used for detection in the western blot is unable to properly interact or recognise it as a result of an alteration on its antigenicity likely caused by amino acid changes. The high infectivity as shown by the luciferase assay and high expression of p24 protein in BT10D4 pseudotype as

shown by western blot image suggests efficient secretion of infectious pseudotype particles, which indicates that the second explanation is more probable. This is not a new phenomenon as it has also been observed in several other studies that the presence of certain amino acid changes alters the antigenicity of HBsAg, resulting in low detection in western blots [413, 431-433]. The lack of proofreading ability in HBV polymerase, in addition to the overlapping characteristics of its genome, implies that mutations present in the polymerase gene could result in corresponding mutations in the surface gene. Data from *in vitro*, *in vivo,* and clinical studies, show that the presence of mutations in HBsAg can alter the synthesis and expression of viral proteins and clinical manifestations such as occult HBV [346, 434]. Our alignment of the HBsAg genetic sequences of BT10D4 alongside D13, D21, D39, D40 and 1,536 sequences of HBV genotypes D assessed from our cohort samples, and the HBV database [419] was carried out to identify the genetic differences between all our sequences and other sequences available in the database. Our findings showed sequence differences in all the compared sequences. However, the rarity of the aa232(s69) cysteine to arginine substitution and aa259(s96) valine to alanine substitution present in BT10D4 and D39 was interesting. A careful interrogation of the phenotypic features of BT10D4 and D39, as shown by luciferase assay and western blotting, highlighted specific differences and similarities between them. Western blot images showed a similarity between the protein expression of HBsAg and p24 in BT10D4 and D39 pseudotypes. However, infectivity data showed that BT10D4 was able to enter both Huh7 and Huh7.NTCP, whereas D39 was not. It also showed that the infectivity of BT10D4 to be a lot higher than that of D39. Also significant is the presence of several other amino acid differences between BT10D4 and D39 genetic sequences. These differences are present in functionally important regions of HBsAg, including the cytoplasmic loop 1, as well as the transmembrane domains 3 and 4. Previous studies have shown that amino acid changes in transmembrane domains 3 and 4 do not affect HBsAg protein assembly and secretion; however, virion stability was affected by amino acid changes in cytoplasmic loop 1. Similarities in the protein expression between BT10D4 and D39 contrasted with the differences in their entry and infectivity

implies that the amino acid differences do not affect HBsAg secretion but affects viral entry. This could mean that any or all of the amino acids present in BT10D4 and not in D39 could contribute to its unique entry ability [413, 430, 435, 436]. Structural studies of proteins have shown that changes to some amino acid residues influence protein structure and function more than others. To better understand the aa232(s69) cysteine to arginine and aa259(s96) valine to alanine substitutions in BT10D4, we tried to understand the characteristics of the amino acids in question and their location within the protein. The S region of HBsAg contains 14 cysteine residues that form disulphide bonds, with 8 of them in the antigenic loop, the "a" determinant. Disulphide bonds are crucial for protein folding, stability and secretion. They stabilise protein folding thermodynamically by decreasing the entropy of the unfolded protein form. Studies have shown cysteines at positions s121, s124, and s137 to be involved in disulphide bond formation and are essential for HBsAg conformation [437-440]. In a study investigating the relevance of the antigenic loop cysteine residues on Hepatitis D virus entry (HDV), Georges Abou-Jaoudé and Camille Sureau showed that mutations of these cysteines result in conformational changes that adversely affect HDV entry. Also, conformational changes can result in changes in epitope recognition residues to antibodies, as shown in a serological analysis done by El Chaar, M. *et al.,* [438, 439]. The presence and relevance of disulphide bonds have also been described in other HBV proteins asides from HBsAg. The conserved cysteine residues present in HBV capsid protein contribute to the capsid's stability, as shown by Siliang Zhou and David N. Standring, while Kim, S. *et al.,* showed that cysteine residues present in the HBV RNA are critical for HBV pregenomic RNA encapsidation [441, 442]. Studies have shown that cysteine s69 is conserved across all hepadnaviruses, is involved in inter-molecular disulphide crosslink and is necessary for the secretion of the 20 nm subviral particles [61, 344]. This makes it particularly crucial in understanding what effect a substitution at that position would have on the protein. The position and importance of the cysteine s69 indicate that the cysteine to arginine mutation would most probably have a drastic impact on the protein structure and function. It is plausible that the absence of a cysteine at position s69 results in

the absence of the disulphide bond usually formed at that position, thus altering the integrity of the protein conformation. In contrast with earlier studies investigating the impact of cysteine mutations, where the mutations adversely affected viral entry and infectivity, our results showed that the cysteine to arginine mutation present in BT10D4 was associated with increased viral entry and infectivity. These studies focused on cysteine mutations within the antigenic loop, whereas s69 is in the HBsAg protein's cytosolic domain; thus, different environments in which the disulphide bonds are formed could influence the outcomes of the absence of these bonds. Constance M. T. Mangold and Rolf E. Streeck showed in their study that mutation of cysteine s69 to serine or alanine adversely affected the assembly and secretion of the S protein as detected by western blotting [61, 440]. However, as stated earlier, our infectivity data suggests low detection of secreted protein, possibly due to a change in conformation. In the case of BT10D4, this mutation has a favourable effect on viral entry, and this could be a direct effect that enables it to bind to other membrane proteins present in Huh7 cells or other indirect effects that could arise from an altered protein conformation [61, 344, 440].

Furthermore, differences in the properties of amino acids mean that amino acid replacement from a different category could have more impact on protein structure and function. In as much as valine and alanine have similar properties, cysteine and arginine do not have similar properties. Cysteine is a small, non-polar and neutral amino acid, whereas arginine is a large, polar, and highly basic amino acid; hence, considering the bonds and interaction which a cysteine would usually form in its position, it is safe to say that a cysteine to arginine substitution would most likely affect protein structure and possibly function. This is supported by Bang, G. *et al.,* in their study, which reported that mutation of the cysteine in HBeAg by arginine blocks virion secretion, whereas mutation with alanine, serine, phenylalanine, or aspartic acid does not [443]. A cysteine to arginine mutation in HBsAg is quite rare, as seen from our data, and although El Chaar, M. *et al.,* reported its presence at position s147 in HBsAg from a patient's sample, its implication on protein structure and function has not been previously studied. The loss of NTCP independence when the s69 arginine in BT10D4 was

reversed to a cysteine showed that the unusual entry phenotype of BT10D4 is influenced by its C to R mutation. Our western blot data also indicated that the presence of arginine in the place of a cysteine at s69 is associated with low HBsAg detection, which as earlier stated, is more likely to be as a result of poor recognition by the antibody rather than poor protein secretion [439, 443]. Additionally, the valine to alanine substitution at position s96 occurs with the transmembrane II (TM2) of HBsAg, required for subviral particles formation, interaction, and oligomerisation [55, 435]. The loss of NTCP independence when the s96 alanine in BT10D4 was substituted with valine also indicated that this substitution plays a role in the entry phenotype of BT10D4 but may not play a role in antibody recognition of the protein as the western blot images do not suggest this.

Also, the change in infectivity and protein expression as the mutations are reversed individually and together is intriguing. Wildtype BT10D4 is characterised by a high level of infectivity/entry and NTCP independence; however, the back mutagenesis of either s69 (R to C) or s96 (A to V) mutations led to a loss of NTCP independence and over four times reduction in infectivity. Back mutagenesis of both mutations resulted in over four times reduction of infectivity while NTCP independence was retained. Our data suggest an epistatic interaction between amino acids at positions s69 and s96. It has previously been shown that drug resistance mutations in the HBV genome are involved in epistatic interaction; it is highly plausible for epistatic interactions to occur in HBsAg, which fully overlaps HBV polymerase [444-446]. The fact that back mutations at both positions do not alter the NTCP independence but reduces its infectivity strongly indicates that one or more other amino acid positions interact epistatically with s69 and s96 to achieve the NTCP independence phenotype. The arginine at position s69 and alanine at position s96 interact synergistically to enable BT10D4 wildtype high infectivity as replacement of either of them by cysteine or valine or both respectively reduces its infectivity ability. The proximity of these amino acids to each other is supported by studies showing that epistatic mutations tend to occur close to each other as their interactions possibly affect the protein shape [447, 448]. We hypothesise that the conformation of BT10D4 which gives it an

infectivity advantage in both Huh7 and Huh7.NTCP is influenced by epistatic interactions between the s69 arginine, s96 valine and one or more unknown amino acids in the HBsAg. We also hypothesise that the unknown amino acid(s) are likely unfit, hence the need for the occurrence of s69 cysteine to arginine and s96 alanine to valine mutations confer high infectivity ability. This contributes to the fitness of the BT10D4 variant, possibly enabling it to be naturally selected from the quasispecies. Similar interactions between amino acid mutations in proteins have been previously recorded in HBsAg [413, 433] and other viral proteins such as vesicular stomatitis virus and influenza virus [449, 450].

In this study, we have isolated HBV BT10D4 isolate, which has the phenotypic ability to infect Huh7 *in vitro* in the absence of the NTCP receptor. Sequence analysis and subsequent mutagenesis experiments revealed several mutations that could be associated with this phenotype; however, the mechanism by which this occurs is still unclear. We propose that these mutations interact with each other and with other unknown amino acid positions to give BT10D4 give a conformation that favours its interaction with one or more unknown Huh7 cell receptors. Future experiments would seek to understand its entry mechanism, other factors involved in its entry, its antigenicity, and its cell tropism.

Chapter 5

Characterisation of HBV Entry Properties

5.1 Introduction

Hepatitis B virus entry is a multi-step process that begins with its attachment, binding to cell receptors and internalisation. The events involved at this early stage of infection include the attachment to a low-affinity co-receptor, binding to a high-affinity cell receptor, followed by internalisation by endocytosis. It is now known that HBV interacts with low affinity to heparan sulfate proteoglycans (HSPGs), members of the glycosaminoglycan family present in the extracellular matrix of cells, closely related to heparin, and have been previously implicated in the entry of several other viruses [451]. HBV then binds with high affinity to sodium taurocholate cotransporting polypeptide (NTCP), a protein found mainly on the basolateral membrane of hepatocytes, encoded by the SLC10A1 gene, which functions as a transporter of conjugated bile acids from the blood into the liver [81]. HBV interaction with highly sulfated HSPGs found on hepatocytes and the exclusive expression of NTCP in the liver are significant factors for the strict hepatotropism of HBV [81, 227, 370, 410, 411].

The preS1 region and the antigenic loop are the two known infectivity determinants of HBsAg that interact with cell receptors at different points of HBV entry. The preS1 region interacts with NTCP, whereas the antigenic loop is believed to be involved in fusion [52]. Entry inhibitors have the ability to interfere with HBV entry at various entry stages, thus inhibiting HBV infection. Human hepatitis B immunoglobulin (HBIG) is a purified pool of anti-HBsAg antibodies from convalescent or vaccinated individuals used in postexposure prophylaxis [452, 453]. HBIG and other monoclonal antibody preparations can interact and bind to HBV infectivity determinants in the antigenic loop, thus inhibiting entry and infection. On the other hand, Myrcludex B, a synthetic preS1 peptide, is able to bind to NTCP, thus inhibiting HBV entry and has now been approved for medical use [452-455].

Epidermal growth factor receptor (EGFR) is a transmembrane protein found in epithelial tissues and plays crucial roles in morphogenesis, differentiation, and homeostasis. EGFR is activated by ligands such as epidermal growth factor (EGF) and transforming growth factor (TGF). EGFR transits to an active dimer on activation and autophosphorylation, resulting in the stimulation of intracellular

protein-tyrosine kinases such as mitogen-activated protein kinase (MAPK) and phosphatidylinositol 3-kinase MAPK (PI3K) that lead to cell survival and proliferation [89]. It has been shown that several viruses utilise the EGFR signalling pathway to transit the plasma membrane and enter host cells. They include viruses such as Hepatitis C virus (HCV), Hepatitis B virus (HBV), Human cytomegalovirus (HCMV), Herpes simplex virus (HSV), Epstein–Barr virus (EBV), Influenza A virus (IAV) and several others. For some viruses such as HCMV and HSV, virus-induced EGFR-mediated actin remodelling and reorganisation enables viral entry into cells and further enhances post-entry processes. Some other viruses, such as HCV and HBV, take advantage of the continuous endocytosis followed by complex downstream signals that work for the benefit of the virus, enabling virus endocytosis [456-465].

Following the initial binding steps, HBV is then internalised by endocytosis, the cellular process through which the cell takes up external substances. There have been conflicting reports as to which endocytosis pathway HBV is internalised. Several studies support clathrin-mediated endocytosis, which involves viral uptake through clathrin-coated pits. In contrast, other studies suggest caveolin-dependent endocytosis, which involves HBV being taken up via caveolin-rich microdomains present in the plasma membrane [87, 286, 466]. Continuing down the endocytosis pathway, HBV is taken up into early endosomes and subsequently to the late endosomes. It is thought that membrane fusion occurs, resulting in the transportation of the nucleocapsid into the nuclear pore complex and the release of the viral genome into the nucleus. However, the site of HBV fusion, the conditions surrounding HBV fusion and nucleocapsid release remain unclear.

In chapter 4, an HBV isolate, BT10D4, was recovered from our clinical cohort and identified to have an unusual entry ability into Huh7 cells in the absence of NTCP and amino acid changes within the surface antigen that could contribute to this phenotype. This study seeks to characterise the entry properties of BT10D4 further and provide answers to questions surrounding its immunogenicity, entry, and infectivity.

5.2 Materials and Methods

5.2.1 Cell culture and transfection

The hepatic cell lines Hep3B, HepG2, HepG2.NTCP, Huh7.5, Huh7, and
Huh7.NTCP as well as the non-hepatic cell lines human embryonic kidney cells
293T (HEK293T), adenocarcinoma human alveolar basal epithelial cells (A549),
human lung epithelial cells (BEAS), were maintained as described in section 3.2.2.
In order to generate pseudotypes, HEK293T cells were seeded and transfected,
as described in section 3.2.3, based on the optimised protocol from section 3.2.

5.2.2 Infection and Luciferase assay

Hep3B, HepG2, HepG2.NTCP, Huh7, Huh7.NTCP, HEK293T, A549 and BEAS cells
were infected following the optimised protocol from section 3.2.4. In addition,
luciferase assays were performed following the protocol in section 3.2.4. Results
were analysed using GraphPad Prism and shown as relative light units.

5.2.3 Human serum samples and Neutralisation assays

Patient serum samples used included: two serum samples (taken in 2007 and
2019) from the chronic HBV patient from which BT10D4 was derived, anti-HBsAg
positive convalescent sera and anti-HBsAg negative sera were used. Serum
samples were processed in a class I cabinet and heat-inactivated at 56 ^{0}C for 30
min before use according to WHO standards. Cells were seeded and incubated
according to established protocols and grown overnight. Hyperimmune hepatitis
B immune globulin (HBIG) derived specifically from blood donors with high levels
of antibody to HBV (gift from Public Health England collaborators), Hepatitis B
(anti-HBsAg) monoclonal antibody (Ma1694, Abnova) and all anti-HBsAg sera
were used at a 1:50 concentration as previously established in the laboratory.
Antibody preparations were diluted, incubated with pseudotypes and added to
cells as described in section 4.2.6. Cells were then incubated, and a luciferase
assay was carried out as previously described.

5.2.4 Chemical Inhibition and Competition Assay

Different steps of HBV entry into Huh7 and Huh7.NTCP cells were studied (Figure 5.1) to investigate the how BT10D4 utilises each of these entry receptors. Huh7 and Huh7.NTCP cells were seeded overnight as previously described, then incubated for 1 h at 37 ^{0}C with 500 µg/mL heparin (Sigma) or 1 µM of Myrcludex B (MyrB; Creative Peptides Inc.). The cells were then infected following the optimised protocol from section 3.2.4, and the medium containing inhibitor was removed after 6 h and replaced with fresh medium. Luciferase assays were performed following the protocol in section 3.2.4. HCV H77 pseudotype generated as previously described was used as a control for the heparin experiments. To identify the cytotoxicity of the chemical inhibitors, Huh7 and Huh7.NTCP cells were seeded overnight as previously described, then treated for 6 h at 37 ^{0}C with 1 µM brefeldin A (BFA; Sigma), 10 mM methyl-β-cyclodextrin (MCD; Sigma), 10 µg/mL chlorpromazine (CPZ; Sigma), 25 nM of bafilomycin A1 (Baf; Sigma), 100 ng/mL recombinant human epidermal growth factor (hEGF; R&DSystems), or 10 µM of the EGFR inhibitor, gefitinib (Sigma) [87]. Cell viability assay was carried out after 6 h of cell incubation with each inhibitor using CellTiter-Blue Cell Viability Assay (Promega) according to the manufacturer's protocol. To understand the effect of the inhibitor chlorpromazine on HBV endocytosis, Huh7 and Huh7.NTCP cells were seeded overnight as previously described, incubated with 10 µg/mL chlorpromazine (CPZ; Sigma) for 1 h at 37 ^{0}C. The cells were then infected following the optimised protocol from section 3.2.4, and the medium containing inhibitor was removed after 6 h and replaced with a fresh medium. Luciferase assays were performed following the protocol in section 3.2.4. Ebola glycoprotein pseudotype generated as previously described was used as a control in the chemical inhibition experiments. To understand the role of EGFR in HBV entry, Huh7 and Huh7.NTCP cells were seeded overnight as previously described, then incubated for 1 h at 37 ^{0}C with 100 ng/mL recombinant human epidermal growth factor (hEGF; R&DSystems), 200 ng/mL recombinant human epidermal growth factor receptor (hEGFR; R&DSystems), or 10 µM of the EGFR inhibitor, Gefitinib (Sigma) [88, 89, 467]. The cells were then infected following the optimised protocol from section 3.2.4, and the medium

containing EGF, EGFR or gefitinib was removed after 6 h and replaced with a fresh medium. Luciferase assays were performed following the protocol in section 3.2.4. VSV-G utilises its type III viral fusion protein for a VSV-G protein-mediated membrane fusion entry mechanism; thus its entry was unaffected by the inhibitors used in this study, making it a good cell viability control in all assays [468, 469].
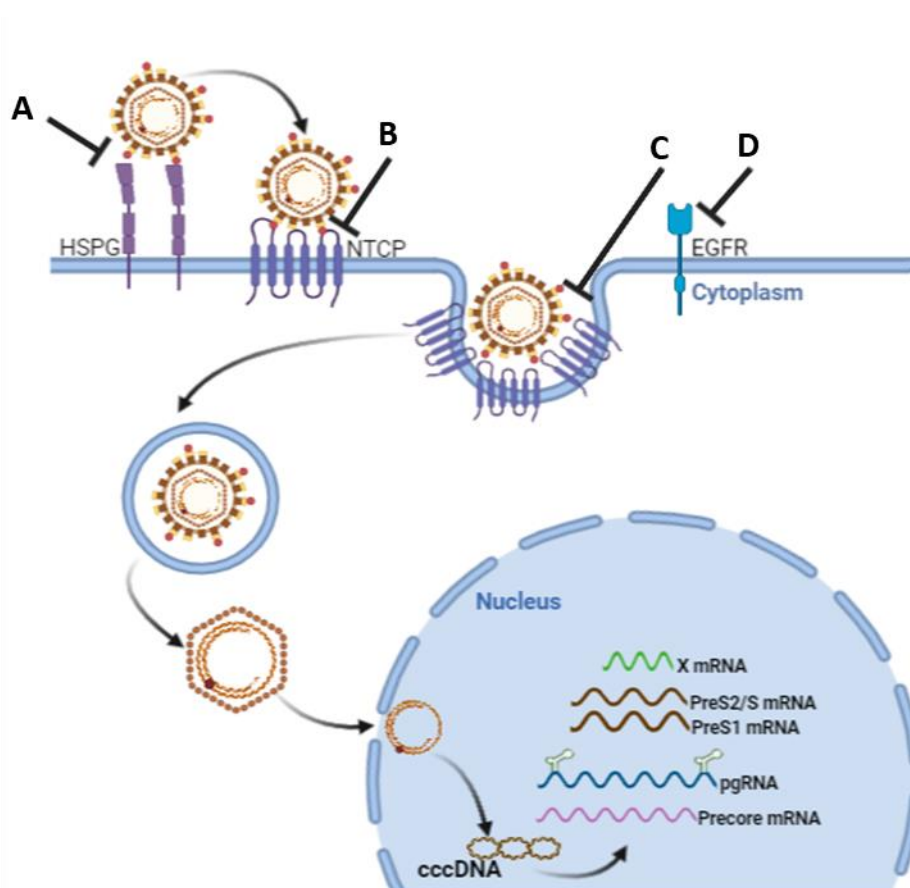
Figure 5.1 Different steps of HBV entry into Huh7 and Huh7.NTCP cells that were studied to investigate the how BT10D4 utilises each of these entry receptors. A. HBsAg interaction with HSPG was investigated by heparin inhibition assay. B. HBsAg interaction with NTCP was investigated by Myrcludex B inhibition assay. C. HBsAg endocytosis mechanism was investigated by chlorpromazine inhibition assay. D. Role of EGFR in HBV entry was investigated by EGF stimulation, EGFR competition and gefitinib inhibition assays. The figure was created at http://biorender.com/.

5.2.5 Site-directed Mutagenesis (SDM)

Primers for site-directed mutagenesis were designed and obtained using the NEBase changer software (Table 4.2). The deletion mutagenesis primers were CAGTGTGGTGGAATTCACCGCTGGAGCATTCGGGCTGGG (forward) and GATATCTGCAGAATTTTAAATGTATACCCAAAGACAAAAG (reverse). The mutagenesis PCR was carried out using the Q5 Site-Directed Mutagenesis protocol (New England Biolab). PCR thermocycling procedure was as follows: 30-sec initial denaturation at 98 ^{0}C, 25 cycles of denaturation at 98 ^{0}C for 10 sec, annealing at 68 ^{0}C for 20 sec, and extension at 72 ^{0}C for 3 min, followed by a final extension at 72 ^{0}C for 4 min. PCR annealing temperature was calculated using the NEB calculator (NEB). The PCR product was treated with kinase, ligase and DpnI (KLD) enzymes and transformed according to the Q5 KLD reaction and transformation protocol (NEB). The plasmid prep was prepared from overnight cultures as described in section 3.2.1, and sequence analysis confirmed successful mutagenesis.

5.3 Results

5.3.1 Antibody neutralisation of HBV entry.

Virus-neutralising antibodies are crucial in preventing viral entry and infection due to their ability to bind to multiple regions in a viral protein, hence blocking infection. However, the fact that antibody reactivity is specific to certain viral epitopes indicates that a change in the viral epitope could render the antibodies inefficacious. The entry characteristics of BT10D4 led us to query its interaction with anti-HBsAg antibodies and their ability to neutralise its infectivity. To this end, we attempted to neutralise the infectivity of BT10D4 using a commercially-produced monoclonal antibody, polyclonal HBIG, and anti-HBsAg positive sera. The anti-HBsAg antibodies in these preparations should recognise and interact with HBsAg resulting in the inability of HBsAg to carry out entry and infectivity. Huh7 and Huh7.NTCP were infected with pseudotypes generated from BT10D4 and D13 isolates in the presence and absence of the commercially-produced monoclonal antibody (Ma1694) and incubated for 72 h at 37 ^{0}C and 5 % CO_2, after which luciferase assay was carried out. Results showed that the infection of the cells in the presence of Ma1694 showed low-level neutralisation of BT10D4 in both Huh7 (p=0.0447) and Huh7.NTCP cells (p=0.0107) (Figure 5.2). There was also significant neutralisation of D13 infection by Ma1694 in Huh7.NTCP cells ($p<0.0001$) (Figure 5.2).

Also, Huh7 and Huh7.NTCP were infected with BT10D4 and D13 isolates in the presence and absence of HBIG. Neutralisation of BT10D4 infection of Huh7 ($p=0.4358$) and Huh7.NTCP ($p=0.4135$) in the presence of HBIG was not significant, whereas results showed a significant neutralisation in infectivity of D13 by HBIG in Huh7.NTCP cells ($p<0.0001$) (Figure 5.2).
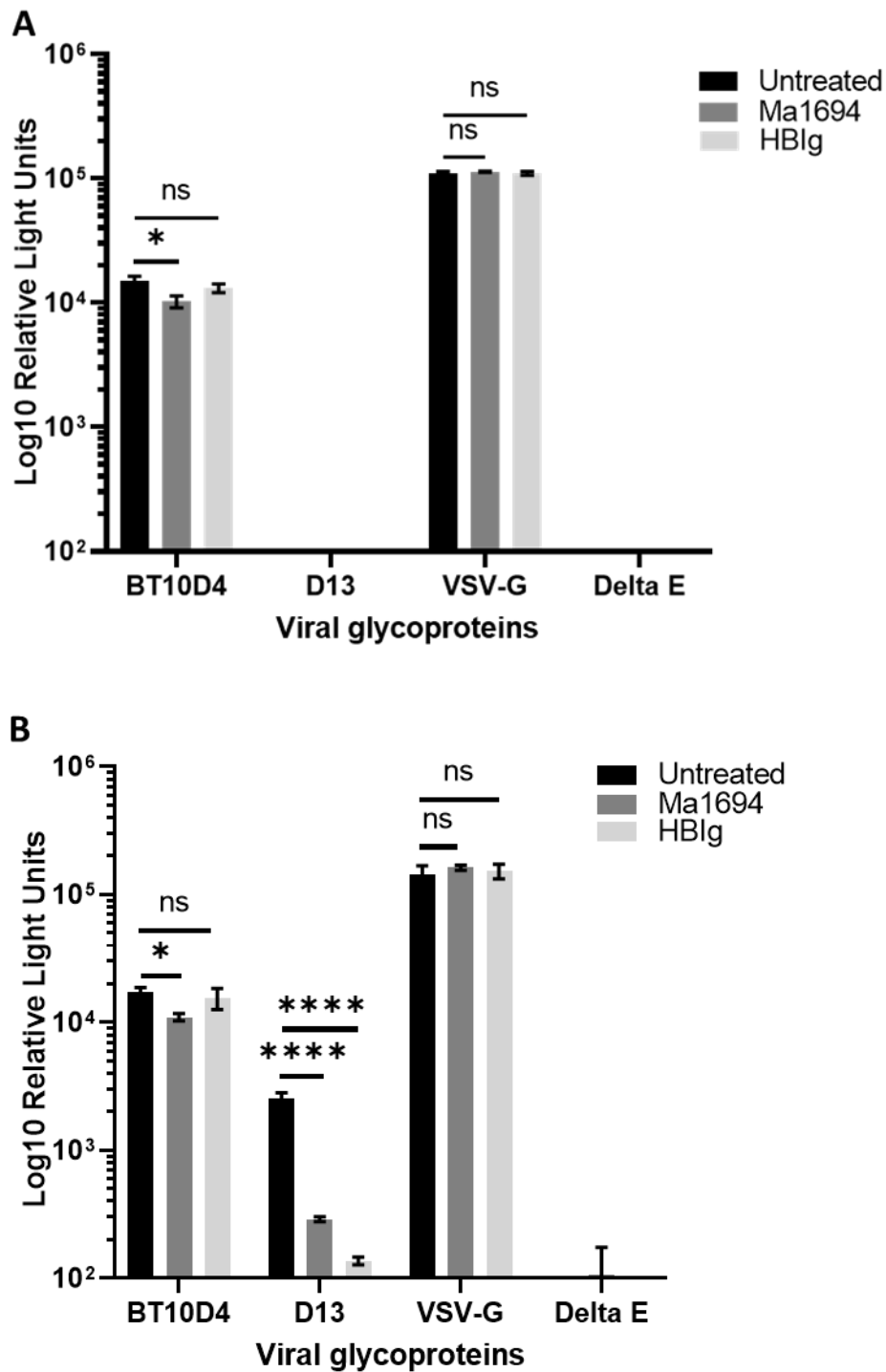
Figure 5.2 Neutralisation of BT10D4 infection in Huh7 and Huh7.NTCP cells with Ma1694 and HBIG. A. Huh7 and B. Huh7.NTCP cells were infected with BT10D4 and D13 pseudotypes in the presence and absence of Ma1694 and HBIG and incubated at 37 ^{0}C and 5 % CO_2 for 72 h. VSV-G and ΔE were used as positive and negative controls, respectively. n = 3, data are shown as means relative light units± SD. Statistical analysis was done using an ordinary one-way ANOVA. **** indicates $p < 0.0001$, * indicates $p < 0.05$, ns indicates $p > 0.05$.

The inability of HBIG to effectively neutralise infectivity of BT10D4 and the low-level neutralisation of BT10D4 infection by Ma1694 prompted the use of inactivated anti-HBsAg positive patient serum for further neutralisation tests. We used two different anti-HBsAg positive serum samples from the patient from whom BT10D4 was derived, collected at different times (2007 and 2019) in addition to anti-HBsAg positive and negative sera from other patients as controls for further neutralisation of BT10D4 and D13 infectivity. Results showed a significant inhibition in BT10D4 infection in the presence of the first and second BT10D4 patient sera both in Huh7 (p=0.0003 and p=0.0003) and Huh7.NTCP cells (p=0.0004 and p=0.0003) (Figure 5.3). There was also a significant inhibition of BT10D4 infection in both Huh7 (p=0.0004) and Huh7.NTCP (p=0.0003) cells in the presence of the anti-HBsAg positive control serum (p=0.0003) (Figure 5.3). Also, a significant decrease in D13 pseudotype infection in Huh7.NTCP cells was observed in the presence of the anti-HBsAg positive serum (p=0.0003) as well as the first (p=0.0004) and second (p=0.0001) BT10D4 patient sera (p<0.0001). Infection in the presence of the anti-HBsAg negative serum results showed no significant difference for BT10D4 in Huh7 (p=0.5345) and Huh7.NTCP (p=0.6428) (Figure 5.3).
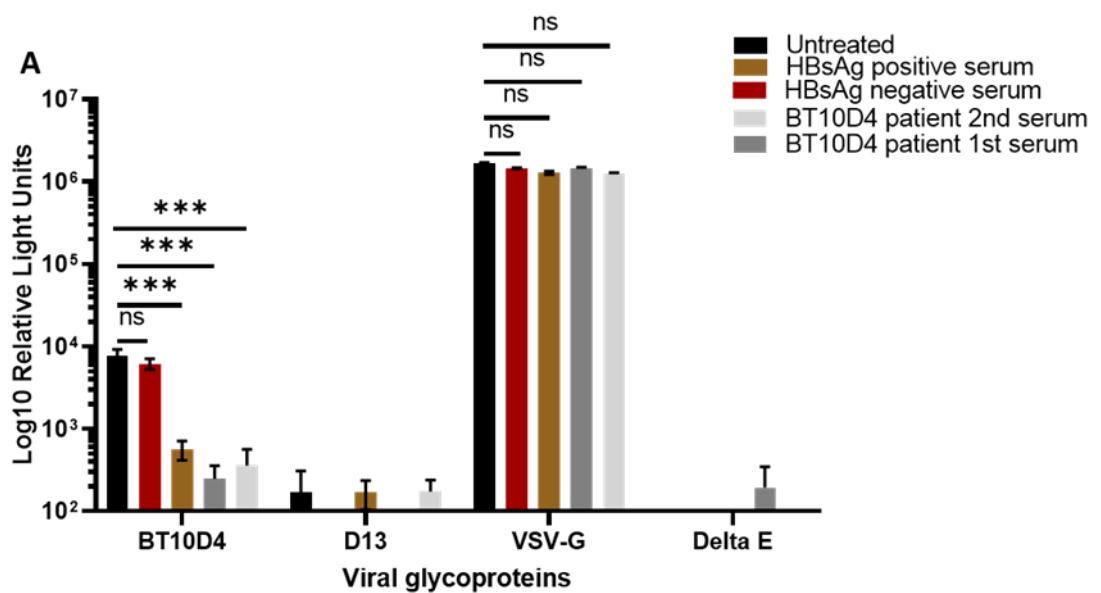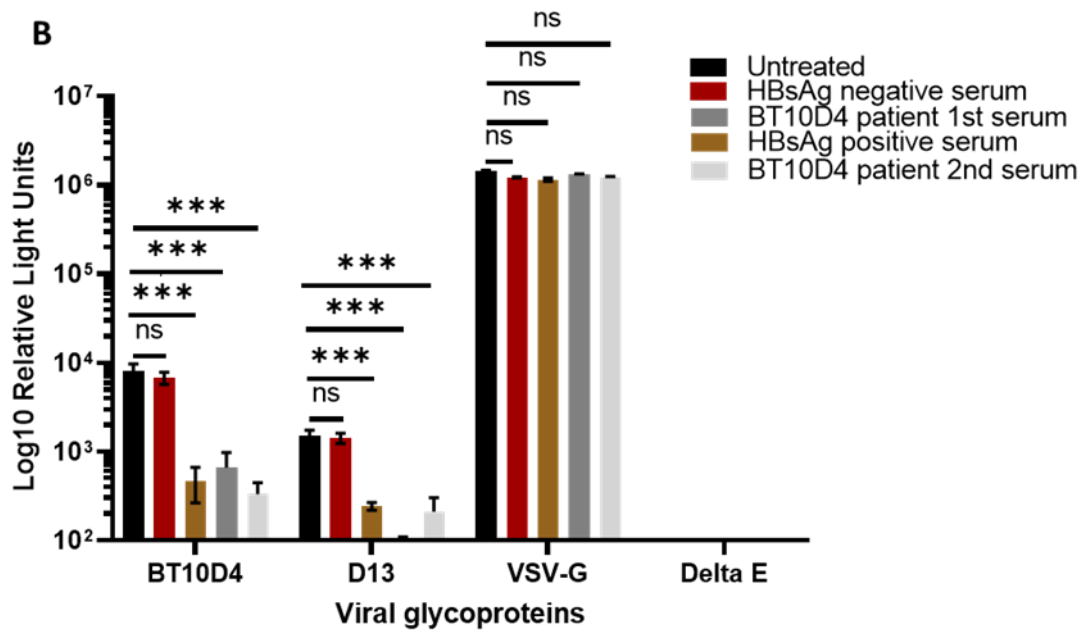
Figure 5.3 Neutralisation of BT10D4 entry in Huh7 and Huh7.NTCP cells with sera from the patient from whom BT10D4 was derived in addition to anti-HBsAg positive and negative sera from other patients. A. Huh7 and B. Huh7.NTCP cells were infected with BT10D4 and D13 pseudotypes in the presence and absence of sera from the patient from whom BT10D4 was derived in addition to anti-HBsAg positive and negative sera from other patients and incubated at 37 ^{0}C and 5 % CO_2 for 72 h. VSV-G and ΔE were used as positive and negative controls, respectively. n = 3, data are shown as means relative light units± SD. Statistical analysis was done using an ordinary one-way ANOVA. *** indicates $p < 0.001$, ns indicates $p > 0.05$.

5.3.2 Investigating BT10D4 cell tropism.

The unusual nature of the BT10D4 isolate has brought to question the possibility of its entry and infection into other hepatic and non-hepatic cell lines. To answer this question, we carried out *in vitro* infectivity experiments of BT10D4 and D13 pseudotypes in the hepatic-derived cell lines (HepG2, HepG2.NTCP, Hep 3B and Huh7.5) and the non-hepatic cell lines (A549, BEAS and HEK293T). These cells were infected with pseudotypes and incubated for 72 h and were lysed for infectivity measurement by luciferase assay. Results showed that when the hepatic-derived cell lines were infected with BT10D4 pseudotype, there was a significant increase in infection into HepG2.NTCP cells compared to HepG2 cells

(p=0.0051), results also showed a significant increase in infection into Huh7.5 cells compared to HepG2, HepG2.NTCP and Hep3B cells (p<0.0001) (Figure 5.4). However, there was no significant difference between BT10D4 infection in Hep3B compared to that of HepG2 (p=0.5163) and HepG2.NTCP (p=0.0998) (Figure 5.4). Also, RLU values from infection of hepatic-derived cell lines with D13 pseudotype showed a significant increase in infection into HepG2.NTCP cells compared to HepG2 (p<0.0001), Hep3B (p<0.0001) and Huh7.5 (p=0.0006) (Figure 5.4). There was no significant difference in D13 infection into HepG2 (p=0.9980), Hep3B (p=0.7974) and Huh7.5 (p=0.6986) (Figure 5.15). On the contrary, data from the infection of BT10D4 and D13 in non-hepatic cell lines (A549, BEAS, and 293T) showed very low RLU values that were not significant (Figure 5.4).
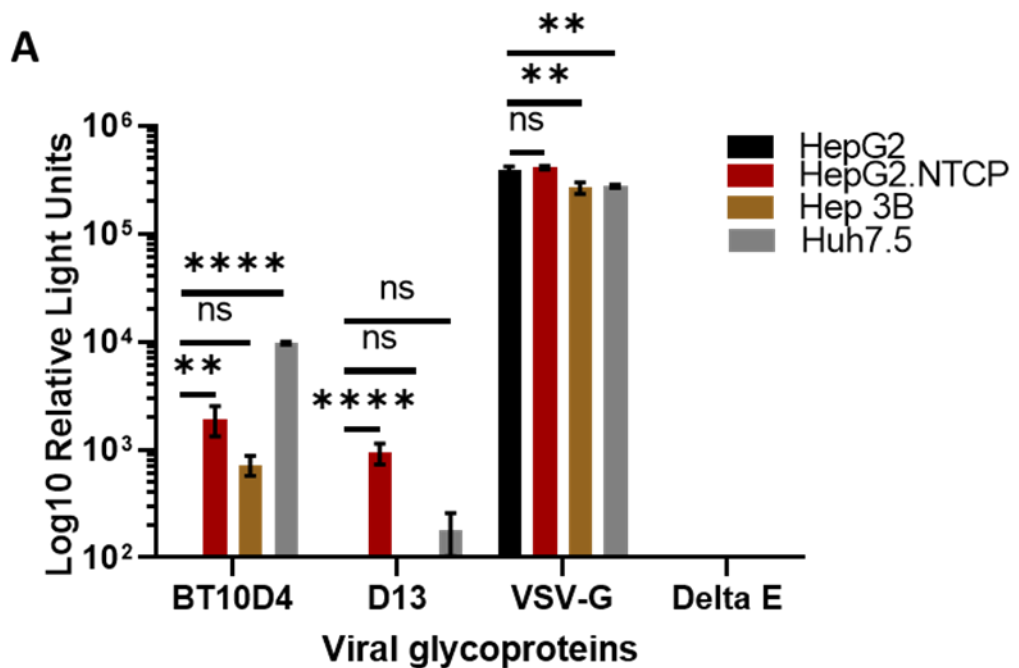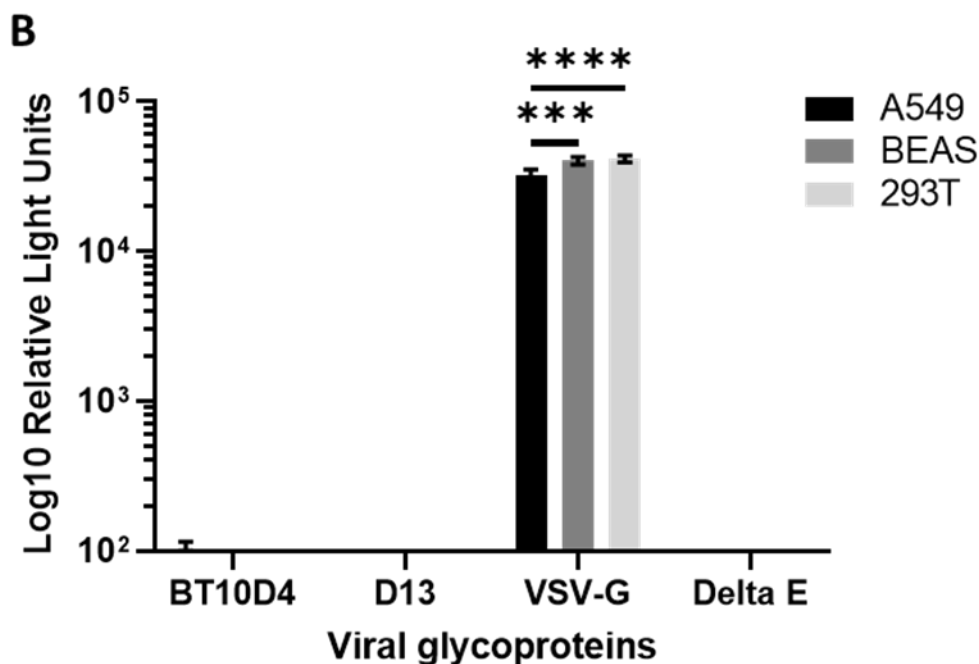
Figure 5.4 Infection of HBV in hepatic and non-hepatic cell lines. A. HepG2, HepG2.NTCP, Hep3B and Huh7.5 cells and B. A549, BEAS and 293T cells were infected with BT10D4 and D13 pseudotypes and incubated at 37 ^{0}C and 5 % CO_2 for 72 h. VSV-G and ΔE were used as positive and negative controls, respectively. n = 3, data are shown as means relative light units± SD. Statistical analysis was done using an ordinary one-way ANOVA. **** indicates $p<0.0001$, *** indicates $p<0.001$, ** indicates $p<0.01$, ns indicates $p>0.05$.

5.3.3 Investigation of Interaction with Heparan sulfate proteoglycan (HSPG).

Heparan sulfate proteoglycans (HSPGs) have been shown to play an essential role in HBV entry by acting as a low-affinity receptor for the virus. In line with this, we investigated the role of HSPG in the entry of BT10D4 into Huh7 and Huh7.NTCP. Studies have shown that heparin, a polysaccharide with structural similarities to HSPGs, can competitively inhibit HBV entry into hepatocytes by interacting with HSPGs, making it unavailable for HBV to bind [411]. Based on this, we used heparin as a competitive inhibitor of BT10D4 and D13 entry into Huh7 and Huh7.NTCP cells to examine the dependence of BT10D4 and D13 on HSPG and compare the differences in the interaction of BT10D4 with HSPG with

142

another genotype D represented by D13. A dose-dependent experiment of published heparin concentrations was tested to identify the suitable concentration to be used [411, 451, 470, 471]. Huh7 and Huh7.NTCP cells were pre-treated with 0, 5, 50, 100 and 500 µg/mL of heparin and subsequently infected with BT10D4 pseudotype produced using previously described protocols and incubated for 72 h at 37 ^{0}C and 5 % CO_2, after which luciferase assay was carried out. Incubation of cells with 5 µg/mL of heparin resulted in a significant increase in BT10D4 infectivity in Huh7 ($p=0.0002$) and Huh7.NTCP cells ($p<0.0001$) (Figure 5.5). There was no significant change in infectivity when Huh7 and Huh7.NTCP cells were pre-treated with 50 µg/mL ($p=0.3003$ and $p=0.4348$) and 100 µg/mL ($p=0.0741$ and $p=0.5588$) of heparin; there was no significant change in the infectivity, whereas pre-treating Huh7 and Huh7.NTCP cells with 500 µg/mL resulted in significant inhibition of infectivity ($p<0.0001$) (Figure 5.5).
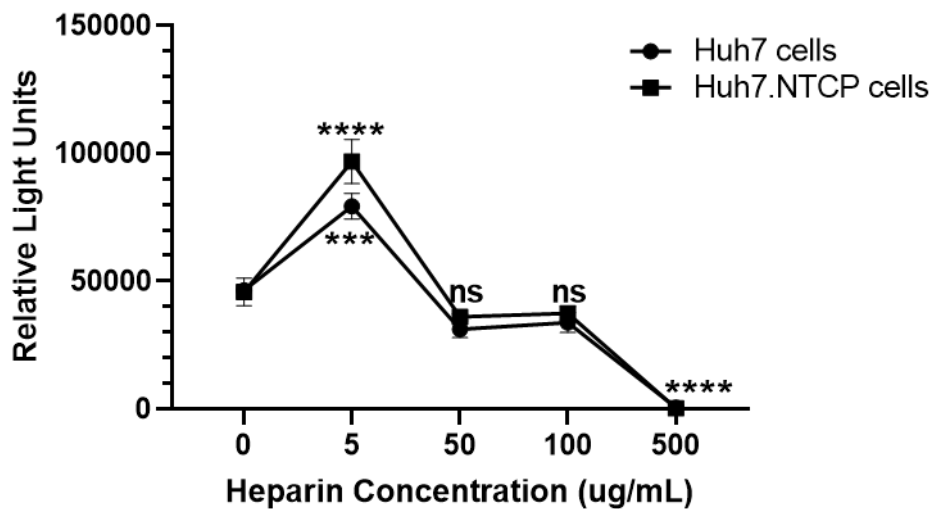
Figure 5.5 Optimisation for heparin concentration. Huh7 and Huh7.NTCP cells were pre-treated with 0, 5, 50, 100, and 500 µg/mL of heparin, infected with BT10D4 pseudotype and incubated at 37 ^{0}C and 5 % CO_2 for 72 h. n = 3, data are shown as means relative light units± SD. Statistical analysis was done using an ordinary one-way ANOVA. **** indicates $p<0.0001$, *** indicates $p<0.001$, ns indicates $p>0.05$.

To investigate any cytotoxic effect on cells from the pre-treatment with 500 µg/mL of heparin, Huh7 and Huh7.NTCP were treated with 500 µg/mL of heparin, and cell viability was assessed using the CellTiter-Blue Cell Viability Assay. Results showed that treating cells with 500 µg/mL of heparin did not result in any significant cell death in Huh7 cells (p=0.1149) and Huh7.NTCP cells (p=0.1800) (Figure 5.6). Hence, further experiments were carried out using 500 µg/mL as heparin concentration.
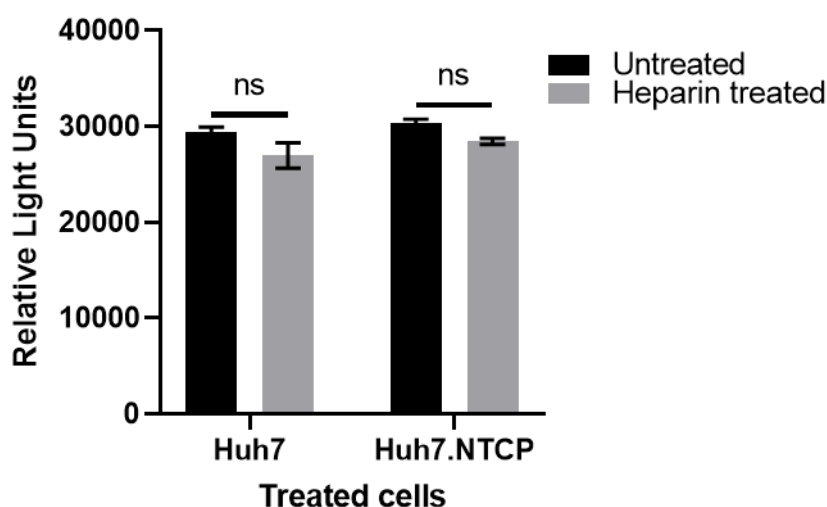
Figure 5.6 Investigating the cytotoxic effect of 500 µg/mL of heparin. Huh7 and Huh7.NTCP cells were treated with 500 µg/mL of heparin, incubated at 37 ^{0}C and 5 % CO_2 for 4 h, after which cell viability was assessed using the CellTiter-Blue Cell Viability Assay. n = 3, data are shown means relative light units± SD. Statistical significance was analysed with an unpaired t-test set at a 95 % confidence interval. ns indicates p>0.05.

Consequently, in further inhibition experiments, Huh7 and Huh7.NTCP cells were pre-treated with 500 µg/mL of heparin and then infected with pseudotypes of HBV BT10D4 and D13 with HCV H77 (a positive control previously shown to be dependent on HSPG for entry), VSV-G and delta E as the controls. Results showed that pre-treatment of Huh7 cells with heparin and subsequent infection with BT10D4 (p=0.0007) and HCV H77 (p<0.0001) pseudotypes significantly inhibited their infectivity (Figure 5.6). Also, pre-treatment of Huh7.NTCP cells with heparin significantly inhibited its infection with BT10D4 (p<0.0001), D13 (p=0.0005) and

HCV H77 (p=0.0002) pseudotypes. Infection of the Huh7 and Huh7.NTCP cells with VSV-G pseudotype (cell viability control) was not significantly inhibited by the presence of heparin at 500 µg/mL (p=0.9169 and p=0.9994) (Figure 5.7).
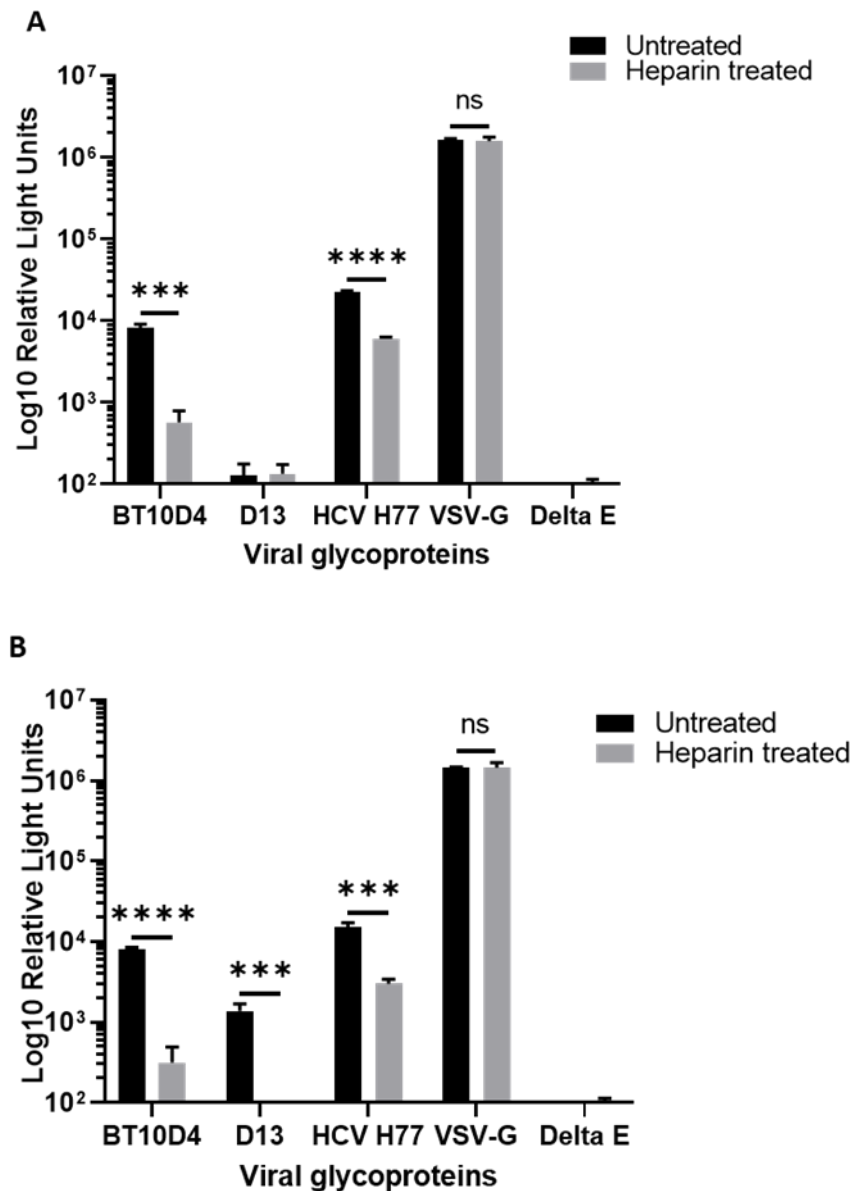
Figure 5.7 Heparin inhibition of HBV interaction with HSPG. A. Huh7 and B. Huh7.NTCP cells were pre-treated with 500 µg/mL of heparin, infected with BT10D4, D13, and HCV H77 pseudotypes and incubated at 37 ^{0}C and 5 % CO_2 for 72 h. VSV-G and ΔE were used as positive and negative controls, respectively. n = 3, data are shown as means relative light units± SD. Statistical significance was analysed with an unpaired t-test set at a 95 % confidence interval. **** indicates $p<0.0001$, *** indicates $p<0.001$, ns indicates $p>0.05$.

5.3.4 Investigation of HBsAg PreS2-48 interaction with Sodium Taurocholate Cotransporting Polypeptide (NTCP).

Sodium taurocholate cotransporting polypeptide, a bile acid transporter exclusively expressed in the liver, is known as an entry receptor for HBV. The synthetic peptide Myrcludex B is designed to mimic the PreS1 NTCP-binding domain of HBsAg, resulting in its ability to inhibit HBV NTCP-mediated entry. It was important to investigate the interaction of the PreS12-48 region of BT10D4 and D13 with NTCP using Myrcludex B as a competitor. In line with this, Huh7 and Huh7.NTCP cells were pre-treated with 1 μM of Myrcludex B (MyrB) for 1 h at 37 ^{0}C, infected with BT10D4 and D13 isolates and incubated for 72 h as previously described, after which luciferase assay was carried out.

Pre-treatment of Huh7 and Huh7.NTCP cells with MyrB before the infection with BT10D4 resulted in a significant reduction in BT10D4 infectivity in Huh7 (p=0.0011) and Huh7.NTCP (p=0.0001) cells (Figure 5.8). Also, pre-treatment of Huh7.NTCP with MyrB before infection with D13 resulted in a reduction of its infectivity into Huh7.NTCP cells (p=0.0013) (Figure 5.8). The presence of MyrB did not significantly inhibit the infectivity of the VSV-G (cell viability control) in Huh7 (p=0.9847) and Huh7.NTCP (p=0.3079) cells (Figure 5.8).
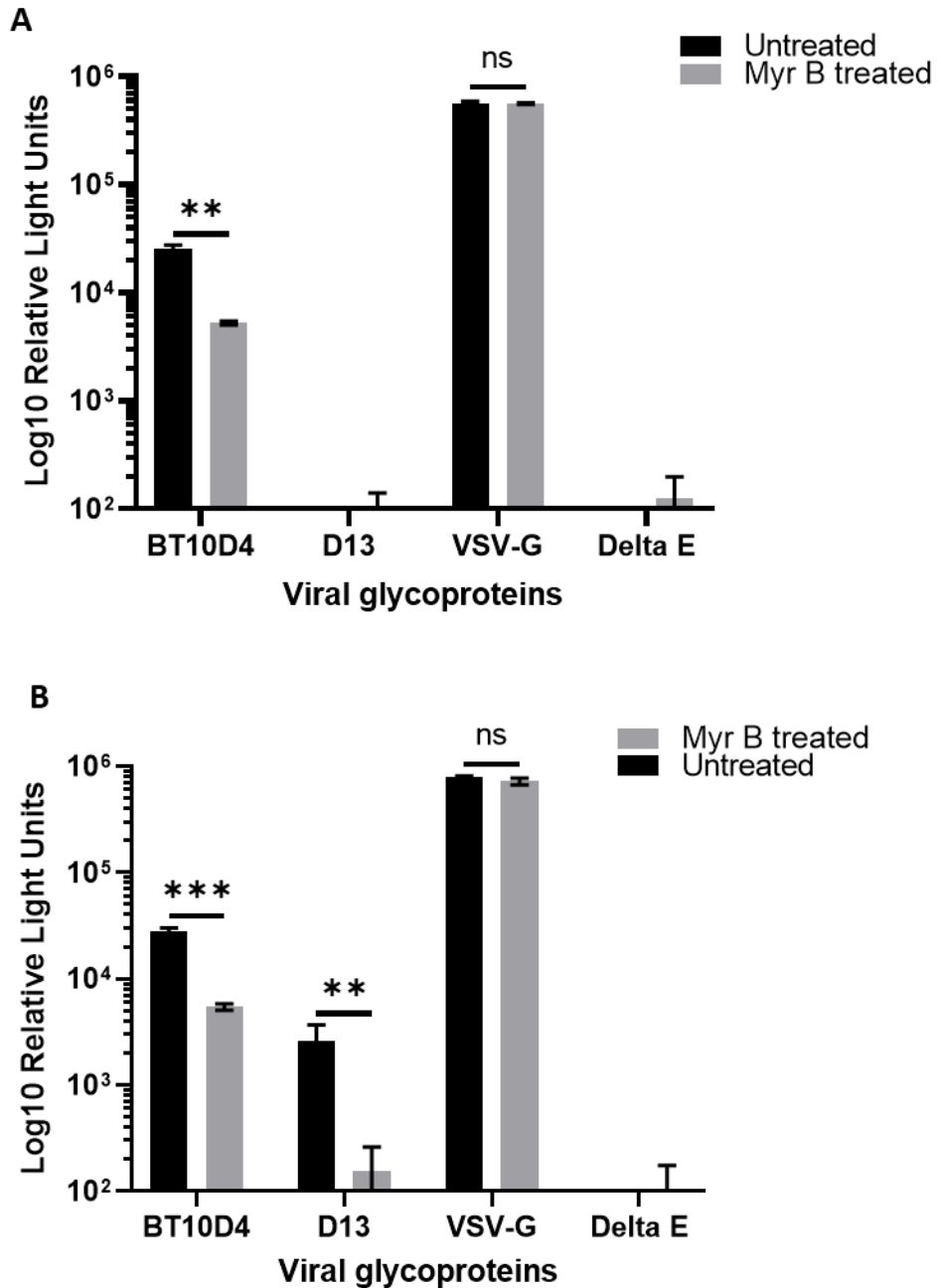
Figure 5.8 Myrcludex B inhibition of HBV entry. A. Huh7 and B. Huh7.NTCP cells were pre-treated with 1 μM of MyrB, infected with BT10D4, D13 pseudotypes and incubated at 37 ^{0}C and 5 % CO_2 for 72 h. VSV-G and ΔE were used as positive and negative controls, respectively. n = 3, data are shown as means relative light units± SD. Statistical significance was analysed with an unpaired t-test set at a 95 % confidence interval. *** indicates $p < 0.001$, ** indicates $p < 0.01$, ns indicates $p > 0.05$.

5.3.5 Functionality of HBsAg PreS1 2-48

Studies have shown that the PreS1 region, particularly amino acids 2-48, are indispensable in HBV infection. It is known that this region interacts with the high-affinity receptor to facilitate viral entry. Results from previous experiments showed that the PreS1 2-48 mimic peptide MyrB could inhibit infectivity. To move further from this, we decided to confirm the functionality of PreS1 2-48 in BT10D4 and its role in BT10D4 entry by testing a deletion mutant (BT10D4 PreSdel). Site-directed mutagenesis deletion primers were designed and used to construct a BT10D4 mutant with PreS1 2-48 deletion. After plasmid extraction, purification and sequencing, the correct mutagenesis sequence was confirmed. The plasmid was then used to produce pseudotypes as previously described. Huh7 and Huh7.NTCP were infected with BT10D4 wildtype and PreS1 2-48 deletion mutant pseudotypes and incubated for 72 h, after which luciferase assay was performed. RLU values from infectivity experiments showed that deletion of PreS1 2-48 amino acids resulted in a 100 % loss of entry ability and infectivity in Huh7 and Huh7.NTCP cells (Figure 5.9).
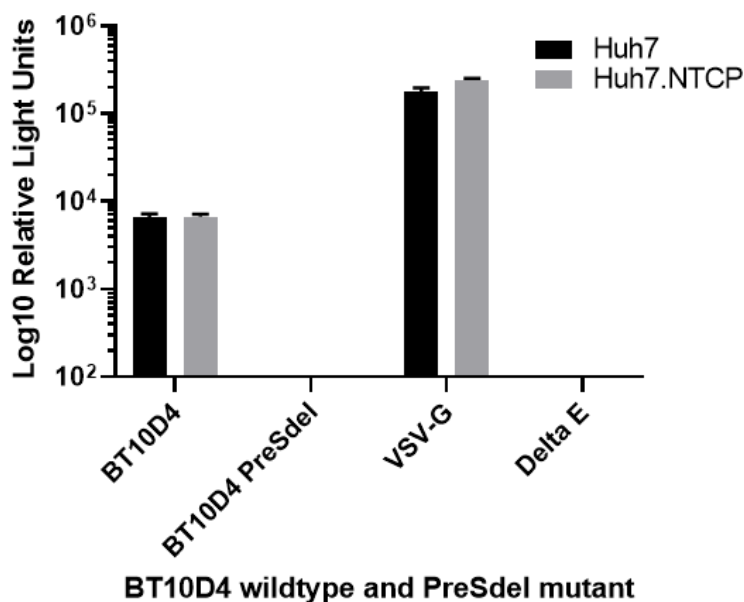
Figure 5.9 Infection of BT10D4 PreS deletion mutant. Huh7 and Huh7.NTCP cells were infected with BT10D4 and BT10D4 PreSdel pseudotypes and incubated at 37 ^{0}C and 5 % CO_2 for 72 h. VSV-G and ΔE were used as positive and negative controls, respectively. n = 3, data are shown as log10 of means relative light units± SD.

5.3.6 Investigation of the endocytosis entry pathway and its role in HBV entry.

Following receptor binding, HBV has been shown to enter cells through an endocytosis-mediated pathway. Studies have shown that the entry of HBV is potentially through a clathrin-mediated endocytosis pathway, although a few conflicting studies point to caveola-mediated endocytosis [87, 286, 466]. To investigate whether BT10D4 entry was dependent on clathrin-mediated endocytosis and compare the BT10D4 entry pathway with that of BR5B6, another HBV genotype other than genotype D, we carried out inhibition experiments using inhibitors that are known to block different steps in the endocytosis pathway. The inhibitors were: chlorpromazine (CPZ), which inhibits clathrin-mediated endocytosis by inhibiting the assembly of clathrin-coated lattices at the cell membrane and on the endosomes, methyl-β-cyclodextrin (MCD), which is an inhibitor of caveola-mediated endocytosis by depletion of cell membrane cholesterol, bafilomycin A1 (Baf-A1), which inhibits endocytosis by specifically inhibiting the vacuolar-type H+-ATPase (V-ATPase), and brefeldin A (Bref A), which is an inhibitor of clathrin-mediated exocytosis brings about the changes in the golgi structure and further inhibits movement of cytosolic clathrin adaptors to golgi membranes.

At first, we examined the cytotoxic effect of these inhibitors on cells. Huh7 and Huh7.NTCP cells were treated with 10 μg/mL CPZ, 10 mM MCD, 25 nM Baf A1, 1 μM Bref A, and cell viability was assessed using the CellTiter-Blue Cell Viability Assay. Results showed that when Huh7 and Huh7.NTCP cells were treated with CPZ; there was no significant change in the viability of Huh7 ($p=0.8493$) and Huh7.NTCP ($p=0.1735$) (Figure 5.10). However, treating Huh7 and Huh7.NTCP cells with MCD, Baf A1, and Bref A resulted in significant cell death ($p<0.0001$) (Figure 5.10). Hence, MCD, Baf A1 and Bref A were excluded from further experiments, and only CPZ was used.
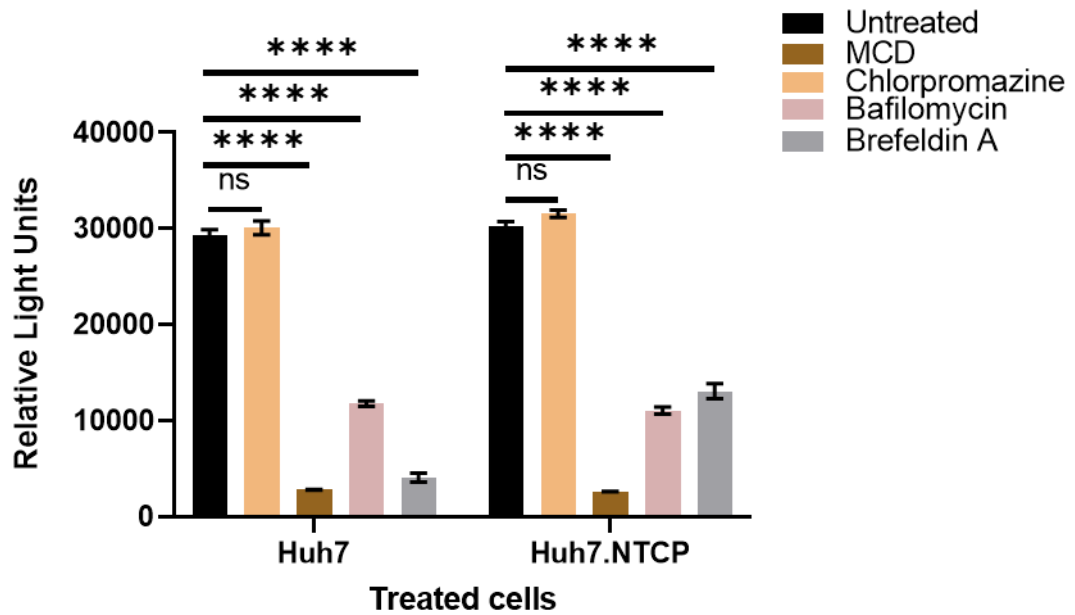
Figure 5.10 Investigating the cytotoxic effect of 10 µg/mL chlorpromazine, 10 mM methyl-β-cyclodextrin, 25 nM bafilomycin A1 and 1 µM brefeldin A. Huh7 and Huh7.NTCP cells were treated with them, incubated at 37 ^{0}C and 5 % CO_2 for 6 h after which cell viability was assessed using the CellTiter-Blue Cell Viability Assay. n = 3, data are shown as means relative light units± SD. Statistical significance was analysed using repeated measures one-way ANOVA with the Geisser-Greenhouse correction and the Dunnett's multiple comparisons test. **** indicates $p<0.0001$, ns indicates $p>0.05$.

Subsequently, Huh7 and Huh7.NTCP cells were pre-treated with CPZ and then infected with pseudotypes from HBV BT10D4, BR5B6, Ebola glycoprotein (a positive control previously shown to use the clathrin-mediated pathway for entry) [472], VSV-G and delta E as the controls. Cells were incubated for 72 h at 37 ^{0}C and 5 % CO_2, after which luciferase assay was performed. The resulting data showed pre-treatment of Huh7 cells with CPZ led to a significant decrease in infectivity of BT10D4 ($p=0.0011$) and Ebola ($p=0.0002$) (Figure 5.11). Also, pre-treatment of Huh7.NTCP cells with CPZ led to a significant decrease in infectivity of BT10D4 ($p=0.0002$), BR5B6 ($p=0.0004$) and Ebola ($p<0.0001$). into them ($p<0.0001$) (Figure 5.11). However, there was no significant inhibition in VSV-G

(cell viability control) infectivity in Huh7 ($p = 0.9230$) and Huh7.NTCP ($p = 0.6813$) cells (Figure 5.11).
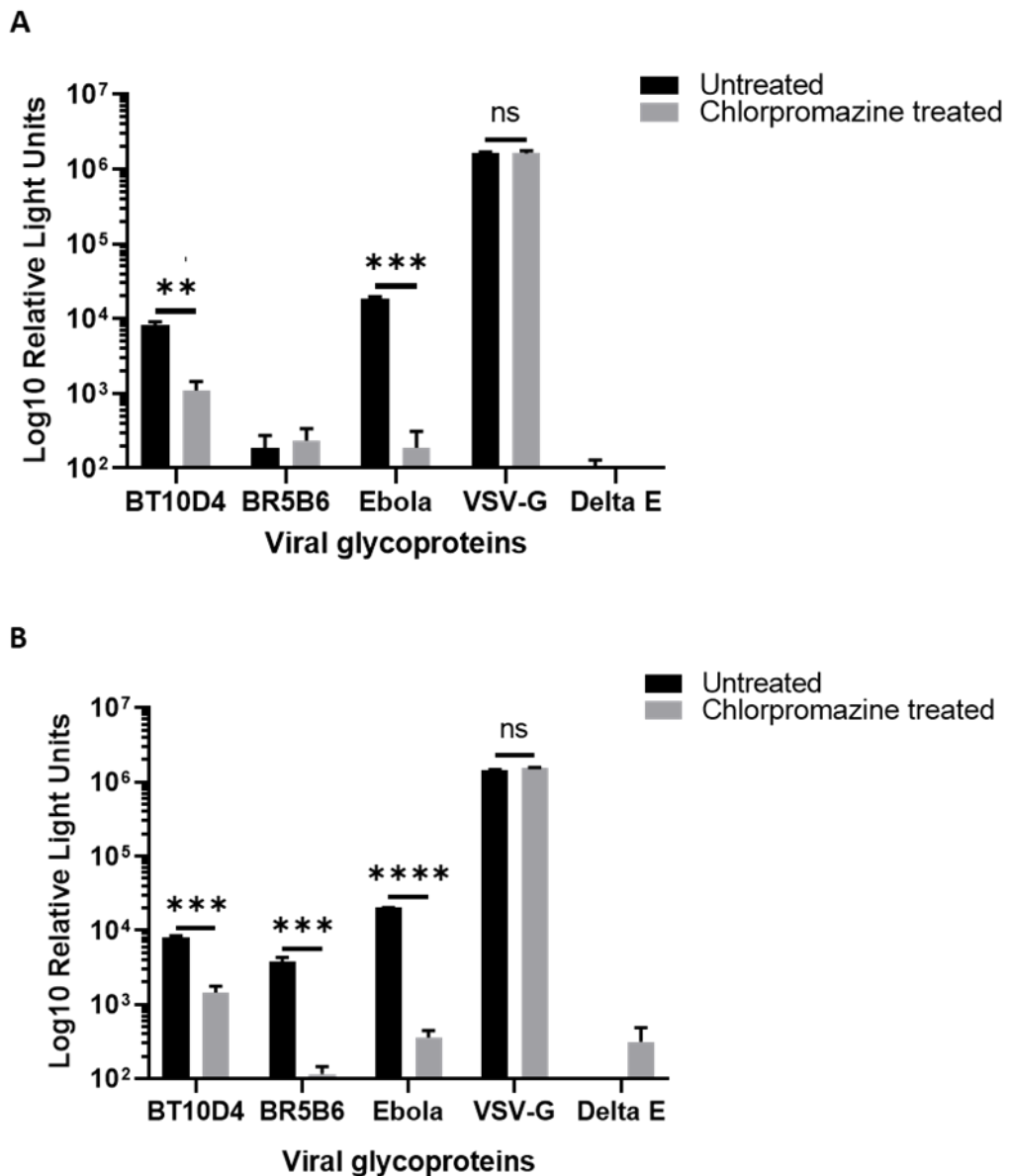
Figure 5.11 Chlorpromazine inhibition of HBV entry. A. Huh7 and B. Huh7.NTCP cells were pre-treated with 10 μg/mL of CPZ, infected with BT10D4, BR5B6 and Ebola pseudotypes and incubated at 37 ^{0}C and 5 % CO_2 for 72 h. VSV-G and ΔE were used as positive and negative controls, respectively. n = 3, data are shown as means relative light units± SD. Statistical significance was analysed with an unpaired t-test set at a 95 % confidence interval. *** indicates $p<0.001$, ** indicates $p<0.01$, ns indicates $p>0.05$.

5.3.7 The Function of Epidermal Growth Factor Receptor (EGFR) in HBV entry.

Several studies investigating viral entry have identified EGFR as a host factor promoting viral internalisation via the clathrin-mediated endocytosis pathway. The function of EGFR in viral internalisation has been studied in several viruses, including HBV. So far, our previous data, which showed significant inhibition of entry by chlorpromazine, suggests the internalisation of BT10D4 via the clathrin-mediated endocytosis pathway. Therefore, we examined the contribution of EGFR to the internalisation of BT10D4 compared to another HBV genotype represented by genotype B, BR5B6. Epidermal growth factor (EGF), a known EGFR ligand that binds to activate EGFR, was used to investigate further the role of EGFR in the entry of BT10D4. Firstly, the cytotoxicity of EGF in Huh7 and Huh7.NTCP was determined by incubating the cells with recombinant human EGF protein and assessing cell viability using the CellTiter-Blue Cell Viability Assay. Results showed that treating Huh7 and Huh7.NTCP cells with 100 ng/mL EGF resulted in no significant change in the viability of Huh7 ($p = 0.2188$) and Huh7.NTCP ($p = 0.1624$) cells (Figure 5.12).

Figure 5.12 Investigating the cytotoxic effect of recombinant human EGF protein. Huh7 and Huh7.NTCP cells were pre-treated with 100 ng/mL of recombinant human EGF protein, incubated at 37 ^{0}C and 5 % CO_2 for 6 h, after which cell viability was assessed using the CellTiter-Blue Cell Viability Assay. n = 3, data are shown as means relative light units± SD. Statistical significance was analysed with an unpaired t-test set at a 95 % confidence interval. ns indicates $p > 0.05$.

After establishing that EGF is not toxic to the cells, Huh7 and Huh7.NTCP cells were stimulated with EGF prior to infection with pseudotypes. Cells were then infected with pseudotypes of HBV BT10D4 and BR5B6 with HCV H77 (previously shown to utilise EGFR as an entry co-factor) [88], VSV-G and delta E as the controls and incubated for 72 h at 37 ^{0}C and 5 % CO_2, after which luciferase assay was carried out. Results showed a significant reduction in infectivity of HBV BT10D4 when Huh7 (p=0.0028) and Huh7.NTCP (p=0.0006) cells were stimulated with EGF and then infected with BT10D4 pseudotype (p=0.0037) (Figure 5.13). Also, there was a significant decrease in infectivity of HBV BR5B6 when Huh7.NTCP cells were stimulated with EGF prior to infection with BR5B6 pseudotype (p=0.0008) (Figure 5.13). The infectivity of HCV H77 in Huh7 (p=0.6930) and Huh7.NTCP (p=0.8773) cells was not significantly inhibited by the presence of EGF (Figure 5.13).

153
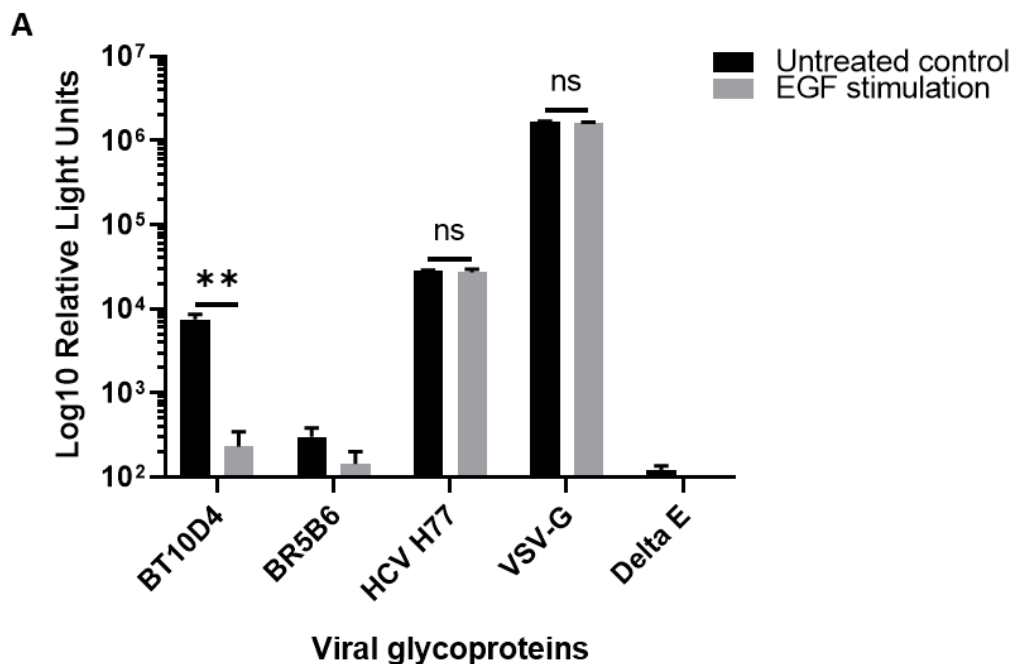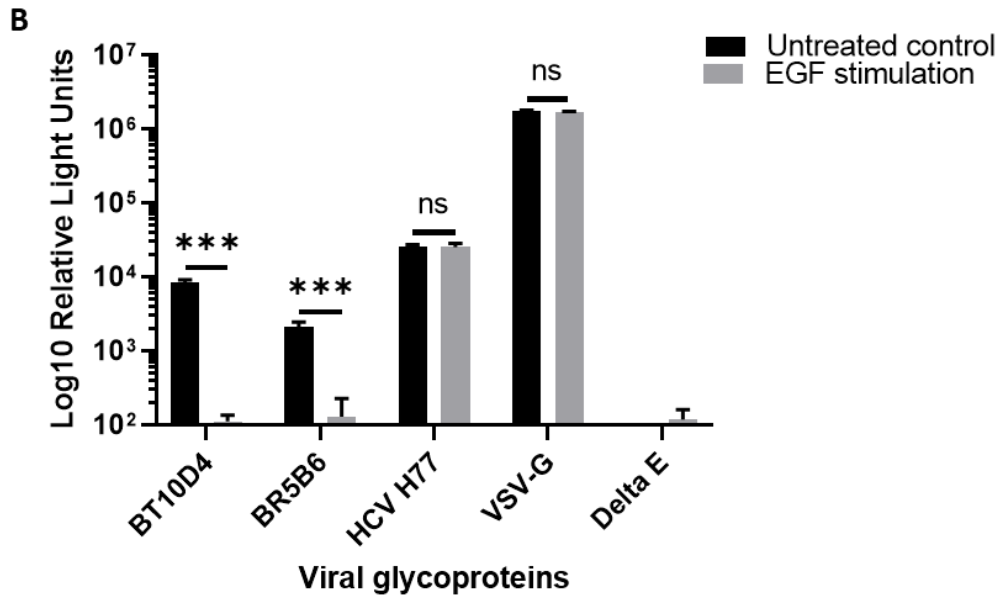
Figure 5.13 EGF stimulation of Huh7 and Huh7.NTCP cells. A. Huh7 and B. Huh7.NTCP cells were pre-treated with 100 ng/mL of recombinant human EGF protein, infected with BT10D4, BR5B6 and HCV H77 pseudotypes and incubated at 37 ^{0}C and 5 % CO_2 for 72 h. VSV-G and ΔE were used as positive and negative controls, respectively. n = 3, data are shown as means relative light units± SD. Statistical significance was analysed with an unpaired t-test set at a 95 % confidence interval. *** indicates $p<0.001$, ** indicates $p<0.01$, ns indicates $p>0.05$.

Furthermore, we carried out a competition assay using recombinant human EGFR protein to compete with the cellular EGFR. In this experiment, recombinant human EGFR was incubated with HBV BT10D4, BR5B6 and HCV H77 pseudotypes prior to their use in infecting Huh7 and Huh7.NTCP cells. Chemiluminescence data showed that infection of Huh7 in the presence of recombinant human EGFR pre-treated with the pseudotypes led to a significant increase in infectivity of BR5B6 ($p=0.0006$) and HCV H77 ($p=0.0002$). However, there was no significant change in the infectivity of BT10D4 ($p=0.2634$) (Figure 5.14). Also, the infection of Huh7.NTCP in the presence of recombinant human EGFR pre-treated with the pseudotypes led to a significant increase in infectivity of BR5B6 ($p=0.0031$) and HCV H77 ($p=0.0007$) and no significant change in BT10D4 infectivity ($p=0.1937$) (Figure 5.14).
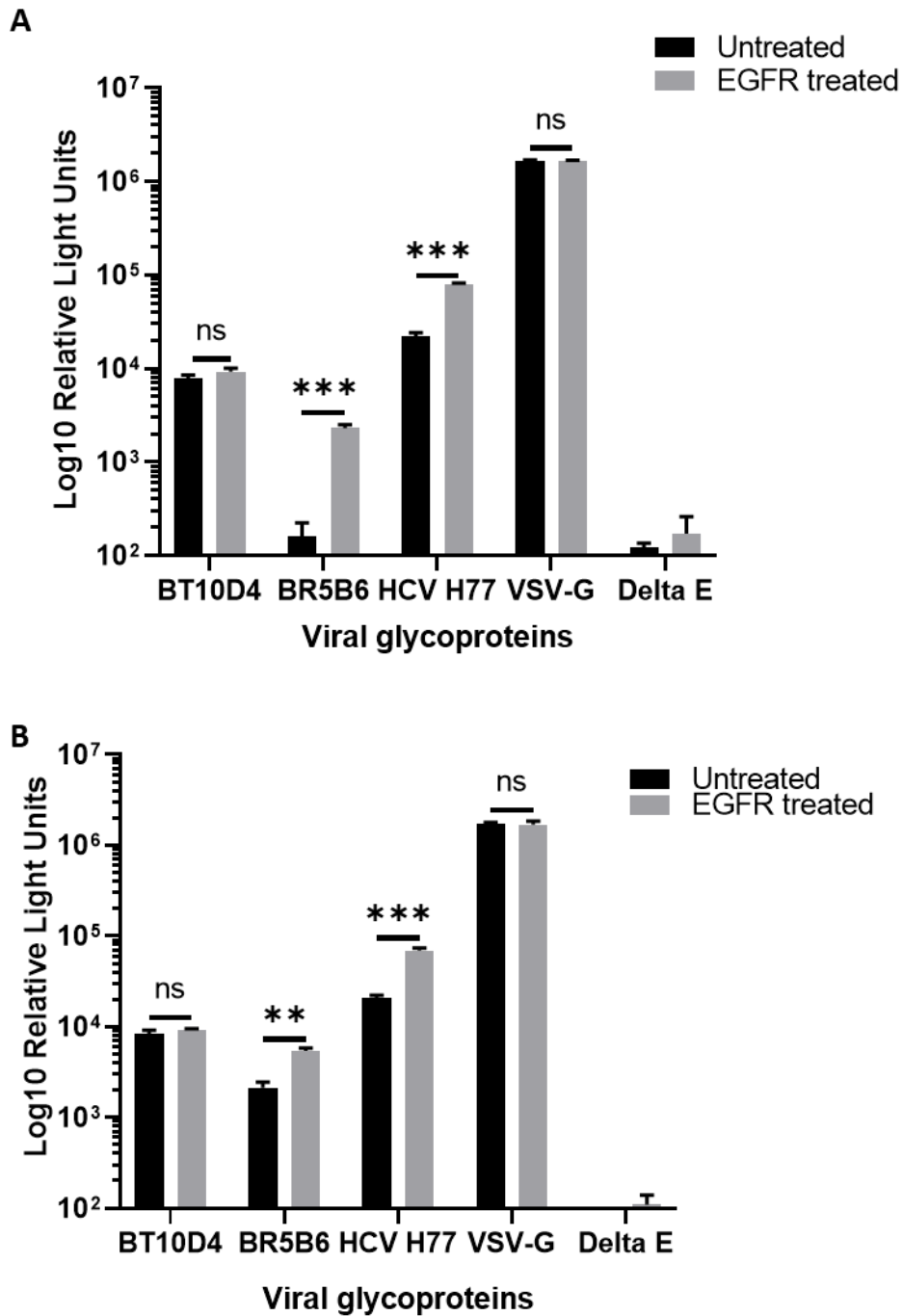
Figure 5.14 Competition assay using recombinant human EGFR protein to compete with the cellular EGFR. A. Huh7 and B. Huh7.NTCP cells were infected with BT10D4, BR5B6 and HCV H77 pseudotypes preincubated with 200 ng/mL of recombinant human EGFR and were incubated at 37 ^{0}C and 5 % CO_2 for 72 h. VSV-G and ΔE were used as positive and negative controls, respectively. n = 3, data are shown as means relative light units± SD. Statistical significance was analysed with an unpaired t-test set at a 95 % confidence interval. *** indicates $p<0.001$, ** indicates $p<0.01$, ns indicates $p>0.05$.

Subsequently, to investigate the role of EGFR in BT10D4 entry, we carried out an inhibition assay using gefitinib, an inhibitor of EGFR autophosphorylation. In order to ascertain if incubation of cells with gefitinib resulted in cytotoxicity, Huh7 and Huh7.NTCP were incubated with gefitinib, and cell viability was assessed using the CellTiter-Blue Cell Viability Assay. Results showed that treating Huh7 and Huh7.NTCP cells with gefitinib resulted in no significant change in cell viability of Huh7 ($p_=0.9299$) and Huh7.NTCP ($p_=0.9475$) (Figure 5.15).
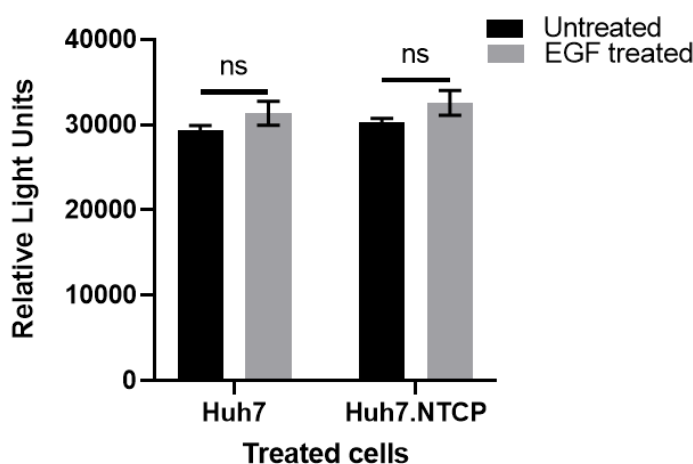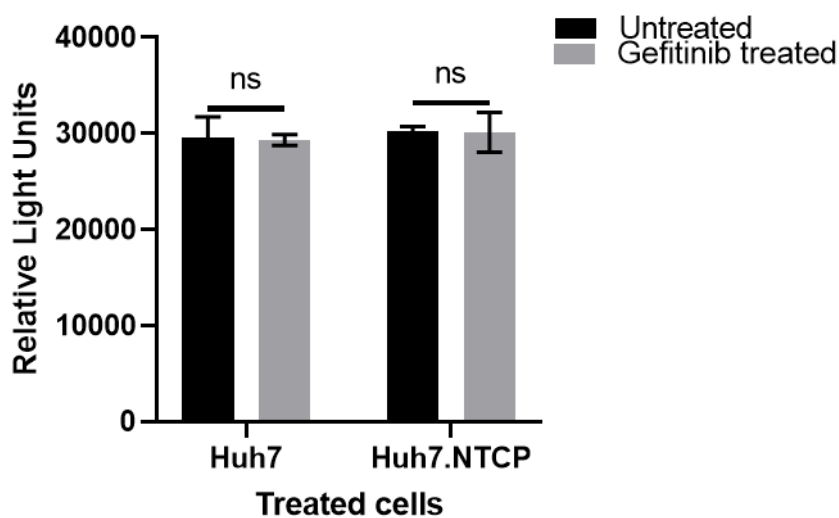

Figure 5.15 Investigating the cytotoxic effect of gefitinib. Huh7 and Huh7.NTCP cells were pre-treated with 10 µM of gefitinib, incubated at 37 ^{0}C and 5 % CO_2 for 6 h, after which cell viability was assessed using the CellTiter-Blue Cell Viability Assay. VSV-G and ΔE were used as positive and negative controls, respectively. n = 3, data are shown as log10 of means relative light units± SD. Statistical significance was analysed with an unpaired t-test set at a 95 % confidence interval. ns indicates $p>0.05$.

In the absence of any toxicity from gefitinib on Huh7 and Huh7.NTCP cells, the cells were then stimulated with gefitinib and infected with pseudotypes of HBV BT10D4 and BR5B6 with HCV H77, VSV-G and delta E as the controls and incubated for 72 h at 37 ^{0}C and 5 % CO_2,after which luciferase assay was carried out. Results showed that when Huh7 cells were stimulated with gefitinib and

then infected with pseudotypes, there was a significant reduction in infectivity of HBV BT10D4 (p=0.0007) and HCV H77 (p=0.0014) (Figure 5.16). Also, when Huh7.NTCP cells were stimulated with gefitinib prior to infection with pseudotypes; there was a significant decrease in infectivity of HBV BT10D4 (p=0.0004), BR5B6 (p=0.0003) and HCV H77 (p=0.0044) (Figure 5.16).
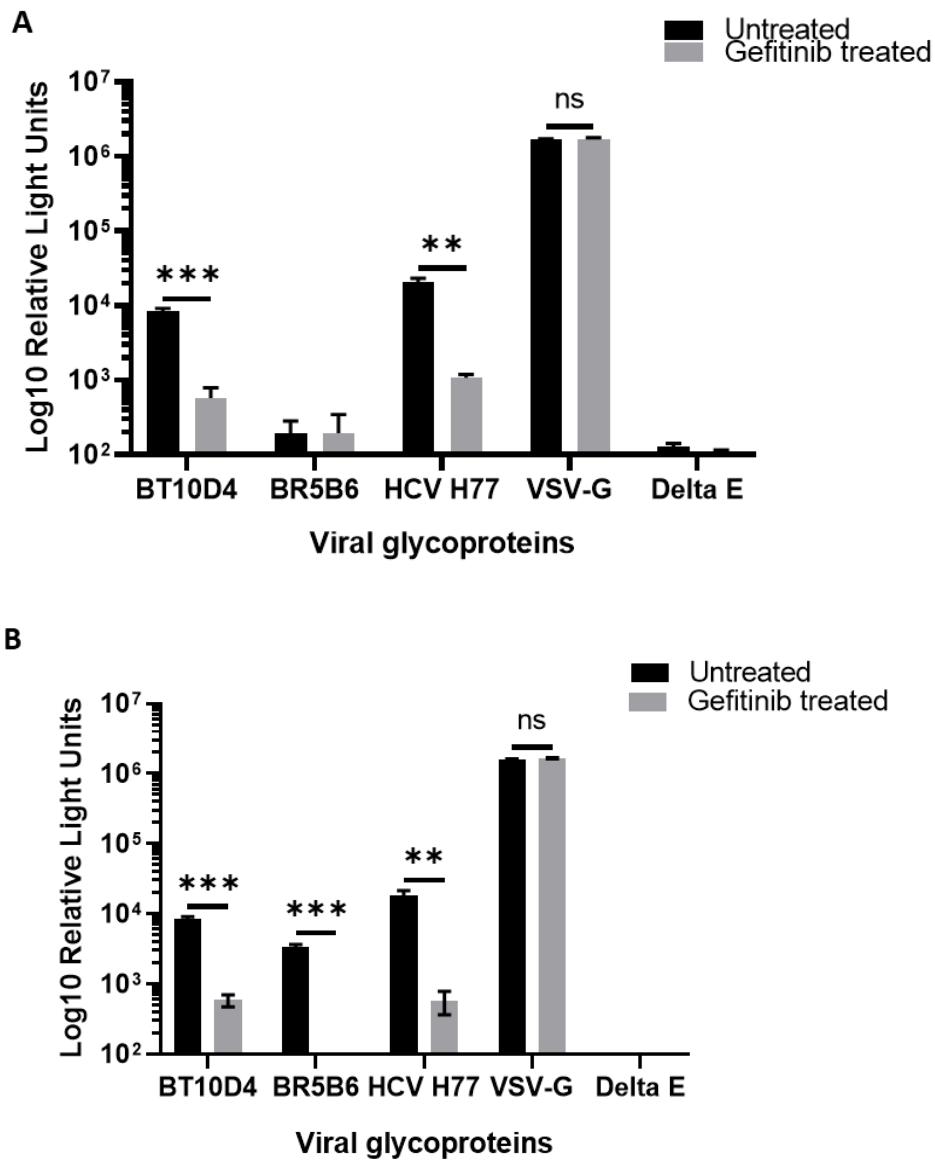
Figure 5.16 Gefitinib inhibition of HBV entry. A. Huh7 and B. Huh7.NTCP cells were pre-treated with 10 µM of gefitinib, infected with BT10D4, BR5B6 and HCV H77 pseudotypes and incubated at 37 ^{0}C and 5 % CO_2 for 72 h. VSV-G and ΔE were used as positive and negative controls, respectively. n = 3, data are shown as means relative light units± SD. Statistical significance was analysed with an unpaired t-test set at a 95 % confidence interval. *** indicates p<0.001, ** indicates p<0.01, ns indicates p>0.05.

5.4   Discussion

Viral infection and subsequent replication in cells are primarily dependent on viral entry into susceptible cells. On the other hand, the presence or absence of suitable entry receptors, co-receptors and co-factors greatly determines the susceptibility of cells to viral infections as well as viral tropism. Several long-standing questions and limitations in HBV research are beginning to get answers and clarity due to the discovery of NTCP as an HBV receptor. The unusual entry characteristics of BT10D4 into Huh7 and Huh7.NTCP in a similar manner, thus indicating NTCP independence infection, and raiseing more questions than answers. Identifying a plausible relationship between specific amino acid changes and the BT10D4 entry behaviour makes it even more exciting. Considering the implications of an NTCP-independent entry possibly influenced by amino acid changes on our understanding of HBV pathogenesis, there is a great need to understand the entry properties of BT10D4. Hence, this study is focused on understanding the entry characteristics of BT10D4, particularly in comparison with other HBV genotypes D and B. We also sought to acquire more information about its antigenicity, tropism, and other factors involved in its entry.

HBV antigenic loop (AGL) has been identified as a second infectivity determinant in HBsAg as mutational analysis revealed entry inhibition. This is also supported by the neutralisation of infection with antibodies targeted at the S region of HBsAg, known to interact with the AGL [52, 473, 474]. To interrogate the role of AGL in BT10D4 entry characteristics, it was important to understand the role of the AGL in its entry and infectivity; hence we carried out neutralisation experiments with antibodies targeting the AGL. The commercially-produced antibody (Ma1694) successfully neutralised the entry and infection of the D13 isolate but not that of BT10D4. In our second attempt, HBIG was used, which showed similar results as Ma1694 by neutralising D13 and showing no significant neutralisation of BT10D4. There are two plausible reasons why an antibody that can neutralise infection of one HBV isolate cannot neutralise another isolate of the same genotype. Firstly, both Ma1694 and HBIG may interact and bind to the

AGL region of BT10D4 as they do with other isolates, but if BT10D4 does not require the AGL region for entry, then this binding would not result in infection neutralisation. Secondly, considering that Ma1694 is a commercially-produced mouse monoclonal antibody, it may be unable to interact with the BT10D4. On the other hand, the HBIG preparation used is a pooled antibody preparation from vaccinated plasma donors. The HBV vaccine is designed to generate an antibody respose against the s-HBsAg only, thus, HBIG which is from vaccinated plasma donors will have antibody targeted against the s-HBsAg. This implies that an absence of anti-PreS antibody in the HBIG preparation would very likely mean that entry is not neutralised as the PreS1 domain which is the known primary receptor-binding domain is not inhibited. This also suggests that BT10D4 unlike D13 is not heavily dependent on the entry domain present in the antigenic loop of the s-HBsAg for entry as neutralisation of the s-HBsAg by the HBIG does not result in a neutralisation of BT10D4 entry. An immunoprecipitation experiment would need to be performed to demonstrate an interaction between BT10D4 HBsAg and the anti-HBs in these antibody preparations. An inability to interact could be because the antibody preparations were induced by HBV genotypes other than genotype D or other subgenotypes genetically different from BT10D4. If BT10D4 has an unusual entry phenotype, it is not surprising that it could have an unusual antibody-binding phenotype. The inability of Ma1694 to neutralise BT10D4 infectivity further supports the western blot data that showed low detection of BT10D4 using the Ma1694 antibody in the western blot data from the previous chapter. Moving forward to narrow down the reasons for the above observations, further neutralisation experiments were performed using three anti-HBs positive sera, two of which were from the patient from which BT10D4 was isolated. All three anti-HBs positive sera were able to neutralise BT10D4 infectivity. This supports the second hypothesis that both Ma1694 could not interact and bind to BT10D4, possibly due to genetic differences in the genotypes and/or strains from which they were produced. On the other hand, two of the three anti-HBs positive sera which neutralised BT10D4 infection were from the patient from which BT10D4 was isolated, and the third serum was a convalescent serum from a seroconverted patient at the same hospital. In as much as the HBV

genotype from which the convalescent serum was generated is unknown, its ability to neutralise BT10D4 suggests a genetic similarity, thus validating that similar HBV strains circulate within distinct geographical regions [475]. Although we cannot say at this point that BT10D4 is an immune-escape mutant strain, we can say that its immunogenicity characteristic is similar to that of vaccine-escape mutants such as sG145R, which have been shown to result in diagnostics and vaccination failures [413, 476-478].

Viral tropism is influenced by a balance of positive and negative factors in target cells that provide a suitable environment for viral replication and survival. This is a crucial characteristic of viral infection and pathogenesis as viral pathogenicity depends on host cell factors such as cell receptors and co-factors. HBV, just like other hepadnaviruses, is known to have a strict hepatotropic characteristic, as shown by previous studies [479]. Our study investigated the entry ability of BT10D4 into other hepatic and non-hepatic cell lines. Expectedly, our data show that BT10D4 was unable to enter and infect A549, BEAS and 293T cells which are non-hepatic cells. Similar to the study by Meredith, L.W., *et al.,* our results support the already known hepatotropic characteristic of HBV [223].

Unsurprisingly, the high infectivity of BT10D4 and low infectivity D13 isolate in Huh7.5 was similar to that of Huh7, as Huh7.5 is a clone of Huh7 [480]. BT10D4 infectivity in the hepatic cells lines differ; there was no significant infectivity in Hep 3B; there was significant infectivity in HepG2.NTCP cells, whereas there was no infectivity in HepG2 cells. Infectivity of HBV D13 was consistent with its dependence on NTCP for entry and infection. It is important to note that although these cell lines are of hepatic origin, they are transformed cell lines that differ in their protein expression profiles. For instance, studies have shown remarkable differences in the p53 gene of these cell lines. Bressac, B., *et al.,* in their study, showed that HepG2 had a normal p53 expression, Huh7 had an increased p53 expression, while Hep3B had an undetectable p53 expression. These differences have been related to the fact that HepG2 carries the wildtype p53, while Huh7 and Hep3B carry point and null mutations, respectively, at codon 220 of p53 [481]. Tsai, T.J., *et al.,* compared Hep3B, Huh7 and HepG2 and showed that HepG2 cells had the lowest mRNA and protein levels of CapG

protein, which remodels the actin filaments and shapes the cell cytoskeleton [482]. Also, Guo, L., *et al.,* in their comparison of these three cell lines, showed that Huh7 and Hep3B are similar in drug metabolising enzymes expression patterns, whereas HepG2 differed from both [483, 484]. It is unclear at this point the specific reasons for the differences in the infectivity of BT10D4 in the hepatic cell lines; however, considering that they have differences, any of these could be responsible for our findings. It is rather intriguing to see that BT10D4 does not infect HepG2 cells in the absence of NTCP, unlike how it infects Huh7 cells. This strongly suggests that the unknown cell receptor BT10D4 interacts with for entry is absent or lowly expressed in HepG2 cells.

Glycosaminoglycans are crucial entry factors used by several pathogens as they are known to be an essential part of the initial attachment of pathogens to host cells [485]. Previous studies have shown HBV to be one of the viruses that utilise HSPG, a glycosaminoglycan, as an initial attachment receptor. Our study showed that infection of BT10D4 and D13 isolates was inhibited by heparin. This suggests that BT10D4 and D13 isolates indispensably use HSPG as an entry receptor similar to what has been shown by many other studies [451, 486]. Leistner, C.M., *et al.,* showed a 100 % inhibition of HBV infection into primary Tupaia hepatocytes using 100 μg/mL of heparin [410]. We achieved 100% inhibition of HBV infection into Huh7 and Huh7.NTCP cells using 500 μg/mL, and the concentration difference could be due to the inherent differences between the cells used. In as much as primary Tupaia hepatocytes are susceptible to human HBV infection, not being a human hepatocyte could mean the binding of HBV to its HSPG is not as strong as its binding to HSPG on the human hepatocyte cell surface; hence this interaction can be inhibited with a lower concentration of heparin [410]. Schulze, *et al.,* achieved a 100 % inhibition of HBV infection in HepaRG cells using 100 μg/mL of heparin [411]. However, their extended incubation of cells with heparin for 16 h could mean that more inhibition is achieved with a lower concentration for a longer time [214]. Interestingly, our data showed that at 5 μg/mL, there is an increase in infectivity of BT10D4 in Huh7 and Huh7.NTCP cells. This is supported by the study of Choijilsuren, *et al.,* where they observed that heparin at a physiological concentration of 5 μg/mL

could enhance HBV infection *in vitro* [471]. The hypothesis is that the binding of heparin at a low concentration to HBV drives a facilitated interaction with NTCP, thus enhancing entry possibly by inducing conformational changes to better expose the receptor-binding domains. In this case, heparin at this concentration could also be driving the entry of BT10D4 into Huh7 and Huh7.NTCP through the unknown entry mechanism [471].

Consequently, it was necessary to investigate the interaction between BT10D4 and NTCP using Myrcludex B. Our results showed inhibition of HBV entry in the presence of Myrcludex B, which many studies have confirmed [50, 370, 487]. In their study to evaluate and identify hepatitis B virus entry inhibitors using HepG2.NTCP cells, Iwamoto, M., *et al.,* demonstrated that at 1 µM, Myrcludex could block HBV entry and infection [488]. Also, Shimura, S., *et al.,* while investigating whether HBV entry inhibitors interfere with NTCP transporter activity, showed that 100 nM of PreS peptide inhibited HBV infection into HepG2-hNTCP-C4 [489]. The use of a lower concentration to achieve HBV entry inhibition could result from differences in PreS peptide preparations [489]. As much as our data align with previous studies, it is crucial to understand what this could mean as it pertains to BT10D4. Although Myrcludex B inhibition of HBV entry of other genotype D isolates supports the hypothesis of their use of NTCP for entry, the case is not the same for BT10D4. Inhibition of BT10D4 entry and infection in both Huh7 and Huh7.NTCP cells by Myrcludex B suggests that the unknown entry mechanism of BT10D4 requires the use of PreS1 aa2-48, which supports previous studies that showed that HBV entry is dependent on PreS1 aa2-48 interaction with cell receptors [62]. We have further confirmed this by showing that deletion of PreS1 aa2-48 ultimately renders BT10D4 non-infectious. This implies that BT10D4 depends on PreS1 aa2-48 for entry either directly by its interaction with entry receptors or indirectly by its presence, enabling a conformation that favours interaction of other domains with entry receptors. However, our MyrB inhibition data support a direct involvement, although having both direct and indirect involvements at the same time is plausible [62, 422, 490]. It is important to note that just as BT10D4 infection was similar in both Huh7 and Huh7.NTCP cells, Myrcludex B inhibition, was also similar in both cells;

in other words, it can be said that the presence of NTCP entry mechanism in addition to its unknown mechanism does not increase BT10D4 infectivity. This suggests that BT10D4 in the presence of NTCP in Huh7.NTCP cells either utilises this unknown mechanism of entry or utilises only the NTCP entry pathway, and both pathways result in infectivity level similar to when BT10D4 utilises the unknown entry mechanism in Huh7 cells. Whether this implies that BT10D4 has a higher affinity for the unknown mechanism cannot be said at this point, although an altered conformation that better suits the unknown mechanism is plausible. Previous studies have also shown the ability of HBV PreS1 21-47 to interact with several other cell receptors such as Asialoglycoprotein and HBV-binding protein. We could hypothesise that Myrcludex B, which is made of PreS1 2-48, could interact with NTCP as well as other cell receptors, any of which could be used by BT10D4 for entry [491-493].

The internalisation of viruses into cells is a crucial part of their infection process, and for enveloped viruses, this can be through a range of endocytic pathways such as caveolar-mediated, clathrin-mediated, macropinocytosis and clathrin- and caveolae-independent endocytosis. Soon after HBV interacts with its receptors and co-receptors, it enters the cells via endocytosis, and several studies support a clathrin-mediated endocytosis pathway [87, 286, 494]. This study sought to understand the endocytosis pathway utilised by HBV genotype D BT10D4 compared to HBV genotype B BR5B6. The chlorpromazine inhibition assay data revealed that the presence of chlorpromazine resulted in an inhibition of infection of both HBV and Ebola. Similar to our study, Huang, H.-C., *et al.,* in their study investigating the mechanism of HBV infection using HuS-E/2, which are immortalised human primary hepatocytes, showed that chlorpromazine inhibition of HBV infection indicated that HBV was dependent on clathrin endocytosis [87]. Also, Herrscher, C., *et al.,* showed in their study using Pitstop 2 and dynasore to investigate HBV endocytosis mechanism into HepG2.NTCP cells that HBV entry into HepG2.NTCP cells required clathrin-mediated endocytosis [286]. Our study supports these and other previous studies suggesting that the entry of HBV into Huh7 and Huh7.NTCP cells is dependent on clathrin-mediated endocytosis [472, 494].

Over the years, research has shown that growth factor receptors such as EGFR are not only involved in cell differentiation and proliferation but have also been implicated in virus entry and infection. Interaction of growth factor EGF with its receptor EGFR results in receptor-mediated endocytosis that internalises the ligand-receptor complex providing an essential portal for virus entry. Studies have shown that viruses such as human cytomegalovirus (HCMV), Influenza A virus and HCV require the activation of EGFR for cell entry [464, 495, 496]. In our study, Huh7 and Huh7.NTCP stimulation with EGF before their infection with HBV pseudotypes resulted in an inhibition of entry and infection. This could be explained by the fact that EGF, the natural ligand of EGFR, interacts with it, leading to its internalisation. Studies have shown that the binding of EGF to EGFR results in efficient phosphorylation of EGFR, its internalisation, and lysosomal degradation [497, 498]. Wang, X., *et al.,* in their study on the cellular trafficking of EGFR, described from their data that EGF incubation of Huh7 cells expressing NTCP-sfGFP resulted in the internalisation and co-trafficking of EGFR and NTCP that led to a depletion of EGFR after 1 h of 100 ng/mL EGF incubation. Their data showed that NTCP and EGFR interact and are internalised into common endocytic vesicles, after which they are separated as NTCP is recycled back to the cell surface while EGF-EGFR traffics into lysosomes and is degraded [499]. Sigismund, S., *et al.,* demonstrated in their papers that depending on ligand dose, EGFR endocytosis can occur via either clathrin-mediated and clathrin-independent endocytosis. They established that at low doses of EGF (1-5 ng/mL), EGFR is dominantly endocytosed via the clathrin-mediated endocytosis pathway and is recycled to the cell surface, whereas at high doses of EGF (25-100 ng/mL), EGFR is endocytosed via clathrin-independent endocytosis, and is trafficked for degradation [500, 501]. Also, Iwamoto, M., *et al.,* in their study on EGFR as a host-entry co-factor for HBV, showed that the HBV binding to NTCP leads to its recruitment to the NTCP-EGFR complex and subsequently an internalisation of HBV-NTCP-EGFR complex [89]. Taken together, it is plausible that our EGF stimulation of Huh7.NTCP cells resulted in the internalisation of NTCP alongside the EGF-EGFR complex, making EGFR and/or NTCP unavailable for HBV binding and entry (Figure 5.17). This explains the complete elimination of HBV infection

after the Huh7.NTCP cells were stimulated with EGF because, from the findings of Iwamoto, M., *et al.,* the unavailability of EGFR for NTCP interaction eliminated HBV entry. Interestingly, other studies such as Chen, S.-W., *et al.,* and Iwamoto, M., *et al.,* in their studies, confirmed the modulatory effect of EGF on HBV infection as a result of its effect on EGFR. Similar to our data, they showed that EGF at low dose enhanced HBV infection while at high dose, it suppressed HBV infection [88, 467]. Chen, S.-W., *et al.,* suggested that the suppression of HBV infection at a high dose of EGF could result from HBV degradation alongside the EGF-EGFR complex [467]. However, in their study, Wang, X., *et al.,* showed that depletion of EGFR 1 h after EGF stimulation does not lead to depletion of NTCP, suggesting the use of different endocytic routes after internalisation. Hence, in our study and as a result of the interaction of EGF at 100 ng/mL, EGFR was endocytosed, and degraded and NTCP may have been recycled; however, the depletion of EGFR and/or NTCP at the point of HBV entry could be the reason for our findings (Figure 5.17). Elimination of HBV genotype D BT10D4 infection similar to HBV genotype B BR5B6 further supports previous studies that EGFR is indispensable for HBV entry [88, 89]. Also, entry of the HCV control is not inhibited by EGF stimulation because its entry is more dependent on the activation of EGFR tyrosine kinases activated by EGF binding to EGFR [502].
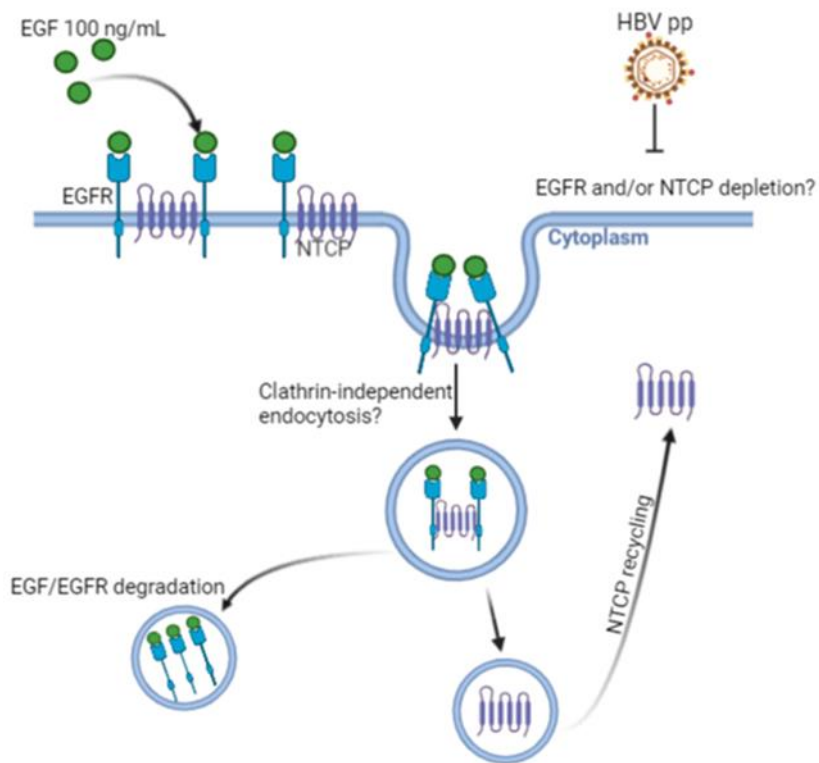
Figure 5.17 Hypothetical effect of EGF stimulation on HBV pseudotype entry. EGF stimulation of Huh7.NTCP cells could have resulted in the internalisation of NTCP alongside the EGF-EGFR complex, making EGFR and/or NTCP unavailable for HBV binding and entry. The figure was created at http://biorender.com/.

Furthermore, we carried out a competition assay of HBV infection using recombinant human EGFR. Rather than a competitive decrease in HBV infection, our data revealed an increase in HBV BR5B6 and HCV H77 infection in Huh7 and Huh7.NTCP. For the BR5B6 pseudotype, the infectivity increase was significantly more in Huh7 cells than in Huh7.NTCP cells, whereas the infectivity increase for HCV pseudotypes was not significantly different in both cells. Studies have described the occurrence of a ligand-independent activation and endocytosis that can occur in the presence of overexpression of EGFR [503-505]. The possibility of this occurrence could explain some of our observations. The presence of the recombinant human EGFR leads to an excess of EGFR, a scenario similar to the overexpression of EGFR; hence, there could be an activation of EGFR via the ligand-independent pathway. For BR5B6 pseudotypes, it is plausible that the interaction between the transmembrane EGFR and the soluble

recombinant EGFR results in the ligand-independent internalisation of EGFR that drives the non-specific internalisation of BR5B6 into Huh7 (Figure 5.18). In Huh7.NTCP cells, this effect could be happening in addition to the NTCP-dependent entry. This is not the case with BT10D4, as there is very little increase in infectivity in both cells in the presence of recombinant EGFR. This is unsurprising as BT10D4 has been shown repeatedly to possess a specific alternative entry mechanism into Huh7 cells; thus, the ligand-independent internalisation of EGFR does not drive a non-specific internalisation. Studies have shown that the ligand-independent activation of EGFR leads to non-canonical signalling that does not involve the activation of the tyrosine kinase pathway [504, 506]. In line with this, the non-specific internalisation seen in BR5B6 as a result of the ligand-independent EGFR activation could also be the case for the HCV entry which could be happening in addition to the receptor specific HCV entry in both Huh7 and Huh7.NTCP cells. Additionally, similar to several other studies, HBV and HCV infection was inhibited in the presence of gefitinib which inhibits EGFR tyrosine kinase signalling and endocytosis [496, 507]. All these put together confirm that EGFR is a co-factor for HBV entry and internalisation though previous studies suggest it does not bind to EGFR but binds to NTCP in an NTCP-EGFR complex [88, 89].
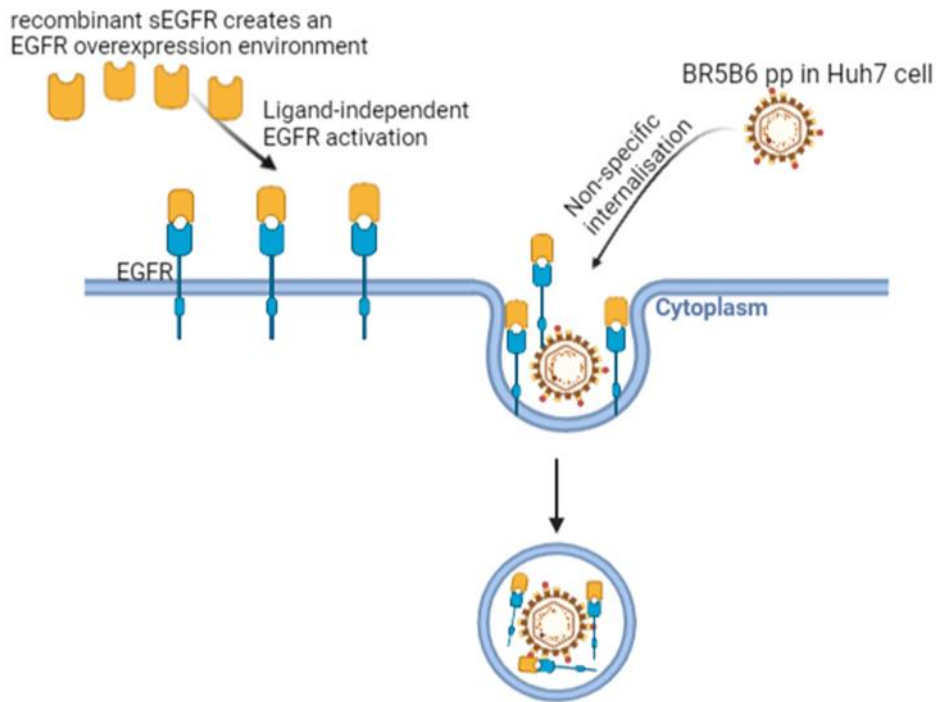
Figure 5.18 Hypothetical effect of the presence of recombinant sEGFR stimulation on BR5B6 pseudotype entry. The presence of the recombinant sEGFR could lead to an excess of EGFR, a scenario similar to the overexpression of EGFR; hence, there could be an activation of EGFR via the ligand-independent pathway. It is plausible that the interaction between the transmembrane EGFR and the recombinant sEGFR results in the ligand-independent internalisation of EGFR that drives the non-specific internalisation of BR5B6 into Huh7. The figure was created at http://biorender.com/.

Our study has highlighted the entry properties of HBV BT10D4 and how it differs from other HBV isolates (genotypes B and D). In addition, our data is suggestive of conformational changes in HBV BT10D4 that could alter its immunogenicity. However, BT10D4 is similar to other HBV isolates in its use of HSPG, PreS1 aa2-48, EGFR and clathrin-mediated endocytosis for entry. On the other hand, our data suggest that whatever alternative receptor BT10D4 uses in Huh7 cells is not expressed in HepG2 cells, and although the mechanism through which BT10D4 infects Huh7 cells and what entry receptors it uses is still unclear, this could be the basis for more research required to provide these answers.

Chapter 6

Diagnostic Characterisation of clinically

relevant mutations.

6.1 Introduction

The infectious human hepatitis B virus (HBV) exists as a 42 nm spherical particle with an icosahedral capsid and a partially double-stranded genome that encodes the P, C, X and S genes. This particle is known as the Dane particle. The S gene is expressed as the large, middle and small HBsAg protein, which is the surface protein responsible for viral entry. HBV surface protein is also assembled as empty subviral particles without the HBV nucleic acid and capsid [128, 132]. The subviral particles, which exist as 22 nm spheres and elongated filaments, are secreted 1,000- to 100,000-fold more than the infectious virions. These subviral particles, which outnumber the infectious viral particles and flood the system, subsequently reduce the activity of the immune system by acting as decoys that bind to antibodies that would otherwise bind to infectious viral particles [508-510]. It has also been shown that the presence of subviral particles could enhance viral replication and gene expression, although the mechanism behind this is not clearly understood [511].

The excess secretion of HBsAg subviral particles in an infected patient makes HBsAg a crucial and sensitive marker for HBV infection. The major hydrophilic region (MHR) of the HBsAg, a cluster of B-cell epitopes, is the primary target of anti-HBsAg antibodies in a patients' circulation. It is also the focus for vaccines, therapeutic immunoglobulin (HBIG) and conventional diagnostic assays. Long-term antiviral therapy, low proofreading ability of the HBV polymerase, and the HBV genome's overlapping nature result in a high frequency of mutations introduced in the HBV polymerase gene during therapy, leading to mutations in the overlapping S gene. Consequently, these mutations can alter the HBsAg epitopes, potentially affecting neutralisation of infection and resulting in diagnostic assay escape [267, 512-514].

In our previous last chapters, we have generated data identifying and characterising amino acid mutations in HBsAg isolated from patient samples. Our *in vitro* pseudotype assays have shown that certain amino acid changes in HBsAg are potentially implicated in several novel phenotypic characteristics of HBV. In line with these data, it is pertinent to understand the implication of these mutations in clinical diagnostics. The HBsAg assay is the first-line screen for HBV

in blood and organ donations, and therefore a highly sensitive screening assay is needed to reduce the risk of transfusion-associated HBV infection.

This chapter focuses on characterising the phenotype of selected mutations in a clinical diagnostic system to find out if the presence of the selected mutations affects the ability of the assay to detect the HBsAg.

6.2   Materials and Methods

6.2.1   Mutation selection and Site-directed Mutagenesis (SDM)

The most frequently occurring mutations from our clinical patients' serum samples previously sequenced were selected for this study (Table 6.1); each of these mutations was then inserted into the BT10D4 as the backbone strain and then compared with the BT10D4 wildtype. The sG145R was not a mutation present among our samples but was included because it is a widely studied mutation, and it would be interesting to see how it compares to the naturally occurring diversity in our sample set. SDM primer design and assay were carried out as previously described in section 4.2.3. Plasmid preps were prepared from overnight cultures as described in section 4.2.1, and sequence analysis confirmed successful mutagenesis.

Table 6.1 Selected HBsAg mutations showing their numbering in the L and S HBsAg proteins.

Number	L-HBsAg position	S-HBsAg position
1.	Mutant 1+2 (R232C+A259V)	Mutant 1+2 (sR69C+sA96V)
2.	Mutant 1 (R232C)	Mutant 1 (sR69C)
3.	Mutant 2 (A259V)	Mutant 2 (sA96V)
4.	L272P	sL109P
5.	G308R	sG145R
6.	T352I	sT189I
7.	S356L	sS193L
8.	S367R	sS204R
9.	S370R	sS207R
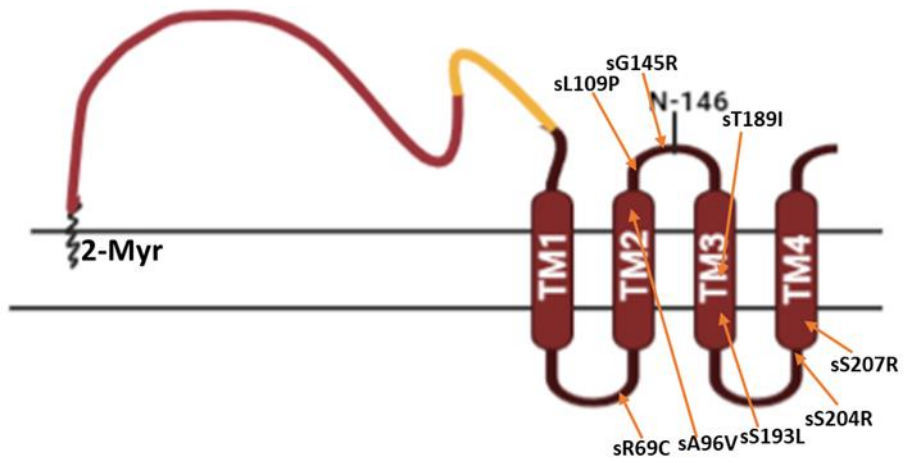
Figure 6.1 Structure of HBsAg showing the positions of the selected mutations. The figure was created at http://biorender.com/.

Table 6.2 Site-directed mutagenesis primers.

Number	Primer name	Description	Primer sequence	Length
1.	L272P	Forward primer	5'CGTTTGTCCTCCAATTCCAGGATC3'	24
		Reverse primer	5'GGCAACATACCCTGATAG3'	18
2.	G308R	Forward primer	5'ACCTTCGGACCGAAATTGCACCT3'	23
		Reverse primer	5'TTGGTACAGCAACAGGAG3'	18
3.	T352I	Forward primer	5'GCTCTCCCCCATTGTTTGGCTTT3'	23
		Reverse primer	5'CCTACGAACCACTGAACAAATG3'	22
4.	S356L	Forward primer	5'TGTTTGGCTTttaGTTATATGGATGATGTGGTATTG3'	36
		Reverse primer	5'GTGGGGGAGAGCCCTACG3'	18
5.	S367R	Forward primer	5'TTGGGGGCCAAGACTGTACAGCA3'	23
		Reverse primer	5'TACCACATCATCCATATAACTGAAAGC3'	27
6.	S370R	Forward primer	5'AAGTCTGTACCGCATCTTGAGTCC3'	24
		Reverse primer	5'GGCCCCCAATACCACATC3'	18

6.2.2 Cell culture and transfection

The hepatic cell lines Huh7 and Huh7.NTCP were maintained as described in section 3.2.2. In order to generate pseudotypes and subviral particles, HEK293T cells were seeded and transfected, as described in section 3.2.3, based on the optimised protocol from section 3.2. Subviral particles were generated by transfecting HEK293T cells without the lentiviral vector pNL4-3Luc.R-E-. Subviral particles were an expression of HBsAg produced by transfecting only with the plasmid, which contains the S gene (with appropriate point mutations).

6.2.3 Infection and Luciferase assay

Huh7 and Huh7.NTCP cells were infected following the optimised protocol from section 3.2.4. Luciferase assays were performed following the protocol in section 3.2.4.

6.2.4 Concentration of Cell culture and Qualitative detection of HBsAg

After 72 h of transfection, cell culture supernatants from HEK293T cells containing the generated pseudotypes and subviral particles were harvested and concentrated using the Amicon Ultra-15 Centrifugal Filter Unit (Merck) with a 10K molecular weight cut-off, according to the manufacturer's protocol. For the qualitative detection of HBsAg and following the manufacturer's protocols, the concentrated supernatants were passed through the ADVIA Centaur HBsAgII assay system, a sandwich immunoassay using direct, chemiluminometric technology.

6.2.5 Bicinchoninic acid assay (BCA assay), Sodium Dodecyl Sulfate–Polyacrylamide Gel Electrophoresis (SDS PAGE) and western blot

The BCA assay, SDS PAGE and western blot were carried out on the concentrated cell culture supernatants according to the protocol described in section 4.2.7.

6.3   Results

6.3.1 Infectivity of selected clinically relevant mutants.

In order to test the effect of several other selected amino acid changes on the BT10D4 phenotype, site-directed mutagenesis (SDM) was performed on the pcDNA 3.1 (+) vector with the HBV BT10D4 isolate. To do this, amino acid changes were selected from our previously studied clinical samples, and SDM primers were designed to substitute the specific amino acid required for the substitution mutagenesis to generate mutant constructs. The constructs were subsequently cloned and transformed into competent cells. Plasmid extraction, purification and sequencing were then carried out to prepare the plasmid for further *in vitro* analysis. To test the infectivity of the mutants, *in vitro* experiments were performed. In the *in vitro* experiments, HEK 293T were co-transfected with each BT10D4 mutant plasmid and pNL4-3.Luc.R-E- vector to produce mutant pseudotypes. Subsequently, Huh7 and Huh7.NTCP infected with the HBV pseudotypes, incubated for 72 h, lysed and infectivity measured by luciferase assay.

Our results showed that BT10D4 (p=0.1936), and Mutant 1+2 (sR69C+sA96V) (p=0.7555) showed NTCP independence as seen in chapter 4, while Mutant 1 (sR69C) (p<0.0001), and Mutant 2 (sA96V) (p<0.0001) showed NTCP dependence as seen in chapter 4. Other mutants showed NTCP-dependent entry similar to that of sR69C and sA96V mutants (p<0.0001) (Figure 6.2).
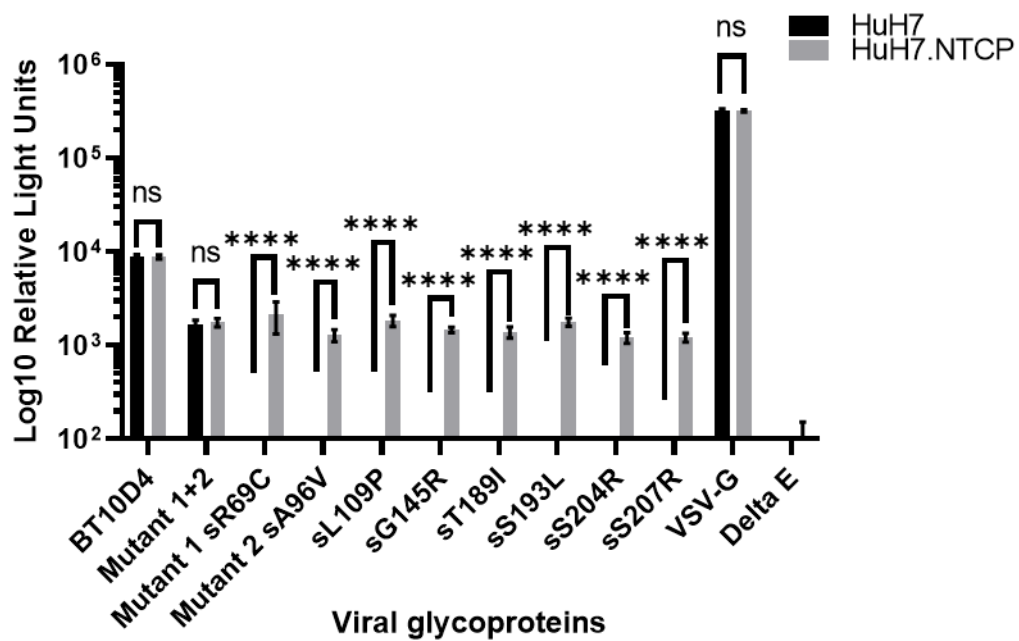
Figure 6.2 Infection of Huh7 and Huh7.NTCP cells with pseudotypes produced from BT10D4 and selected clinically relevant mutants. Huh7 and Huh7.NTCP cells were infected with pseudotypes and incubated at 37 ^{0}C and 5 % CO_2 for 72 h. VSV-G and ΔE were used as positive and negative controls, respectively. n = 3, data are shown as means log10 Relative light units± SD. Statistical significance was analysed with an unpaired t-test set at a 95 % confidence interval. **** indicates p<0.0001, ns indicates p>0.05.

6.3.2 Qualitative detection of BT10D4 mutants

As demonstrated previously in Chapter 4, amino acid mutations present in HBsAg can potentially have several impacts on its phenotype *in vitro*. These impacts can have far-reaching consequences on the clinical behaviour of HBV, facilitating the development of antibody detection escape and affecting the downstream management of HBV infection. In line with this, we tested the ability of the qualitative diagnostic assay to detect the presence of BT10D4 and the selected mutants. In order to mimic a clinical infection in which the virus can release large amounts of subviral particles devoid of the HBV DNA, we carried out *in vitro* experiments to generate particles made just from the surface antigen. HBV pseudotypes (carrying the lentiviral vector) of BT10D4 and all the selected mutants were produced, and their infectivity was tested as shown in section

6.3.1. Subviral HBV particles (lacking the lentiviral vector) were produced using the same protocol, and HBsAg expression was confirmed by western blotting. The western blotting image showed a varying HBsAg expression among BT10D4 and the mutants (Figure 6.3).
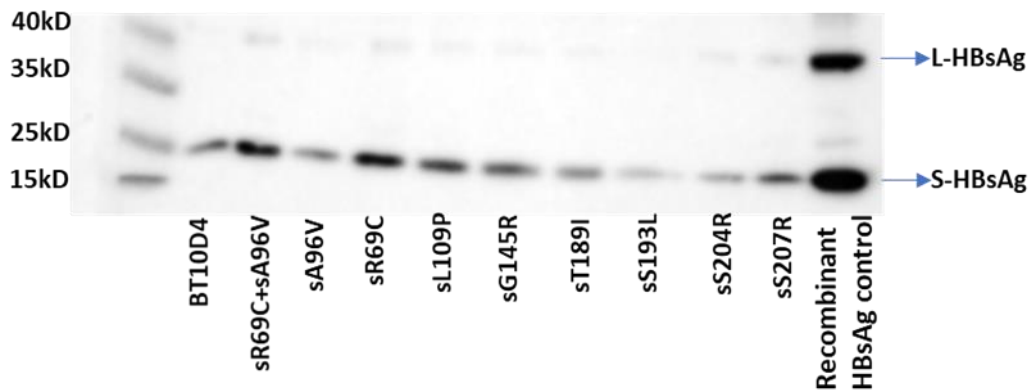
Figure 6.3 Western blot image of BT10D4 and its mutants. Concentrated cell culture supernatants were run on a 12 % SDS Page gel and transferred to a PVDF membrane. The membrane was incubated with a 1:1000 dilution mouse anti-HBsAg primary antibody and 1:2000 rabbit anti-mouse HRP secondary antibody. Images were taken using the G: BOX F3 gel doc system.

Subsequently, an HBsAg qualitative detection test was performed; cell supernatants containing the pseudotypes and subviral particles were concentrated by ultrafiltration and passed through the ADVIA Centaur HBsAgII (HBsII) regularly for diagnostic assays. From our results given as relative light units (RLU), we compared the data for the HBV pseudotypes BT10D4 and the selected mutants. Our results showed that compared to the BT10D4 wildtype, the RLU value of: sR69C (p=0.0046) and sR69C+sA96V (p=0.0223) were significantly higher (Figure 6.4). Our data also showed that compared to the BT10D4 wildtype, the RLU value of: sA96V (p=0.0005), sL109P (p=0.0003), sG145R (p=0.0007), sT189I (P=0.0465), sS193L (p=0.0237), sS204R (p=0.0013) were significantly lower while sS207R (p=0.4494) did not show any significant difference with the BT10D4 wildtype (Figure 6.4).
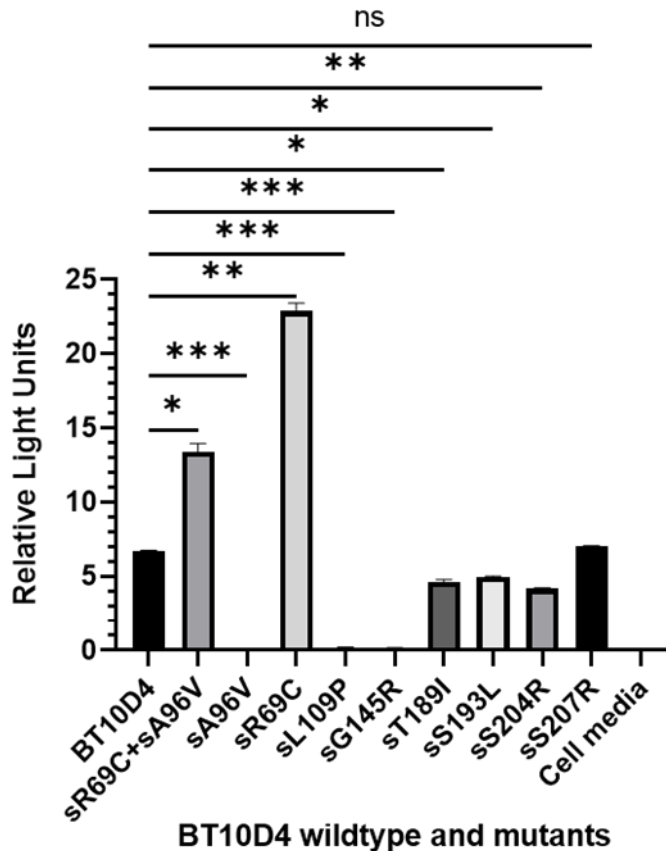
Figure 6.4 Qualitative detection of HBsAg in pseudotyped particles produced from BT10D4 wildtype and the selected mutants. Concentrated cell culture supernatants were passed through the ADVIA Centaur HBsAgII assay system. n = 3, data are shown as means of Relative light units± SD. Statistical significance was analysed using a repeated measures one-way ANOVA with the Geisser-Greenhouse correction and the Dunnett's multiple comparisons test, and each mutant was compared to the BT10D4 wildtype. *** indicates $p<0.001$, ** indicates $p<0.01$, * indicates $p>0.05$, ns indicates $p>0.05$.

We further compared the RLU values of the subviral particles produced from BT10D4 and the selected mutants. Our results showed that compared to the BT10D4 wildtype, the RLU value of: sR69C ($p=0.0091$) and sR69C+sA96V ($p=0.0147$) were significantly higher (Figure 6.5). Our data also showed that compared to the BT10D4 wildtype, the RLU value of: sA96V ($p=0.0025$), sL109P ($p=0.0025$), sG145R ($p=0.0023$), sS207R ($P=0.0025$), were significantly lower

while sT189I (p=0.8879), sS193L (p=0.1374), and sS204R (p=0.1087) did not show any significant difference with the BT10D4 wildtype (Figure 6.5)
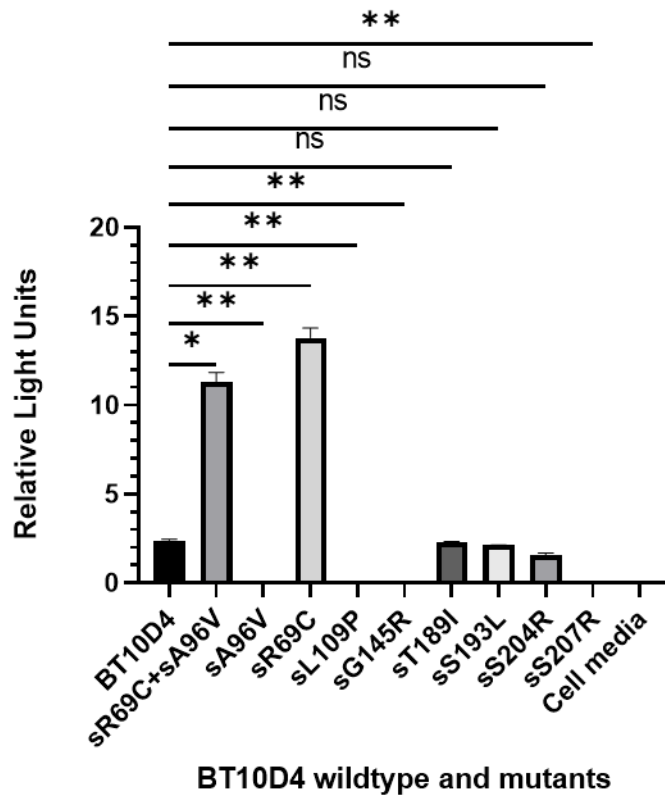
Figure 6.5 Qualitative detection of HBsAg in subviral particles produced from BT10D4 wildtype and the selected mutants. Concentrated cell culture supernatants were passed through the ADVIA Centaur HBsAgII assay system. n = 3, data are shown as means of Relative light units± SD. Statistical significance was analysed using a repeated measures one-way ANOVA with the Geisser-Greenhouse correction and the Dunnett's multiple comparisons test, and each mutant was compared to the BT10D4 wildtype. ** indicates p<0.01, * indicates p<0.05, ns indicates p>0.05.

Furthermore, comparing the RLU values of the pseudotyped particles and the subviral particles showed that the RLU of the subviral particles of BT10D4 wildtype, sR69C+sA96V, sR69C, sT189I, sS193L, sS204R and sS207R were significantly lower than that of the pseudotyped particles (Figure 6.6). The

sA96V, sL109P and sG145R were undetectable as pseudotyped particles and subviral particles (Figure 6.6).
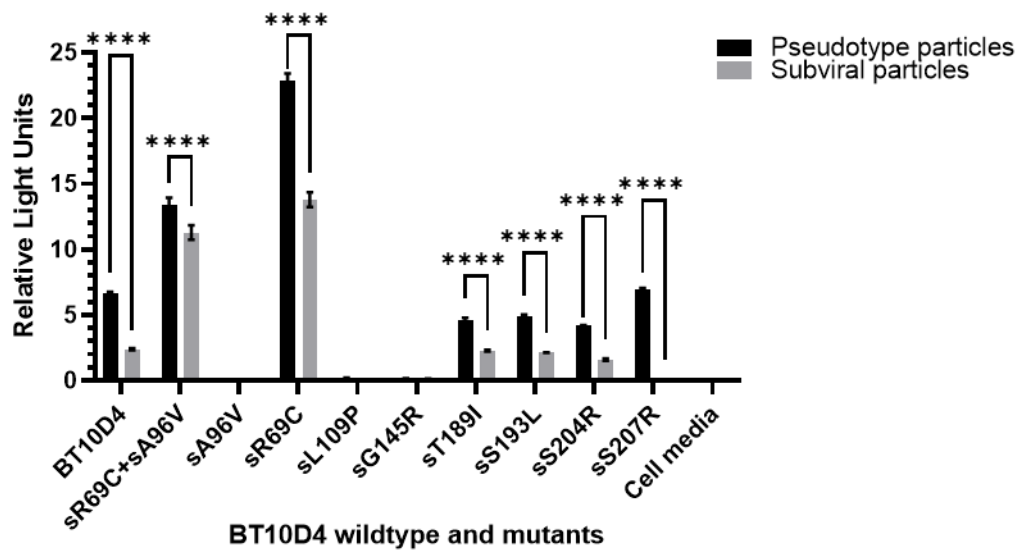
Figure 6.6 Qualitative detection of HBsAg in pseudotyped and subviral particles produced from BT10D4 wildtype and the selected mutants. Concentrated cell culture supernatants were passed through the ADVIA Centaur HBsAgII assay system. n = 3, data are shown as means of Relative light units± SD. Statistical significance was analysed with an unpaired t-test set at a 95 % confidence interval. **** indicates $p<0.0001$.

6.4   Discussion

HBsAg is known as the first serological marker of infection and presents a determining characteristic of HBV infection; thus, its detection is critical in diagnosing and managing HBV infection. Clinically, immunoassays are used routinely to detect HBsAg in diagnosing HBV and the screening of donated blood and organs. In as much as the nucleic acid amplification tests (NAATs) are ideal for diagnosing HBV infection, there are several parts of the world in which this is not the case. In these parts of the world, mainly because of the cost involved in running NAATs, HBsAg diagnosis is used as the standard for detecting HBV infection [515, 516]. Our previous chapters demonstrated that amino acid mutations present in HBsAg could potentially influence phenotypic characteristics of the protein, which could alter the antigenicity and immunogenicity of HBV. This study was aimed at understanding the diagnostic implications of clinically relevant amino acid mutations.

The MHR region of HBsAg is a region containing highly conformational B-cell epitopes, making it the primary target of antibodies and a region recognised in diagnostic assays, and changes in this region could impact diagnosis [517, 518]. In line with our previous results, we investigated the impact of several clinically isolated mutations on the diagnostic phenotype of BT10D4 by running BT10D4 wildtype and the mutants constructed on the BT10D4 backbone through a qualitative clinical diagnostic system. Our data showed that the sA96V mutant was non-reactive, indicating low HBsAg secretion or poor detection by the diagnostic system. On the other hand, the sR69C+sA96V mutant had a higher detection RLU value than the wildtype BT10D4, and the sR69C had the highest detection value. Interestingly, these results are similar to the western blot data we have generated in previous chapter 4. In line with our previous data (chapter 4), these data also showed that arginine at position s69 found in BT10D4 plays a role in the low HBsAg detection. Replacing this arginine with cysteine, as seen in other strains, increased the ability of HBsAg to be detected. As previously postulated, we hypothesise that a conformational change resulting from the cysteine to arginine mutation in BT10D4 possibly leads to poor antibody

182

recognition of BT10D4. We have also shown that this mutation alters the entry phenotype of BT10D4.

The data presented here demonstrate that the presence of alanine in the place of valine at position s96 increased the detection of virus particles, suggesting an enhancing effect by the presence of alanine. We have previously stated that the alanine at s96 may not be involved directly with antibody recognition of BT10D4 but plays a role in its entry phenotype. From our data, it is plausible that the alanine at s96 tends to reverse the possible conformation change resulting from the presence of arginine at s69, which led to poor antibody recognition of BT10D4. This would imply that the presence of alanine at amino acid s96 would make BT10D4 more detectable. This is supported by our western blot data from the previous chapter, which showed a very low detection of HBsAg when alanine was replaced with valine at s96 and arginine was present at s69. However, our infectivity data have shown that BT10D4 requires the arginine at s69 and the alanine at s96 to achieve its high infectivity. Thus, recent data now suggest that s96 alanine possibly has a stabilising effect on BT10D4 such that while it enhances BT10D4 entry and infectivity, it also enhances its ability to be detected. This could mean that the BT10D4 strain is more infectious but not particularly refractive to detection or antibody therapy.

Going further in this study, we looked at several other mutations present in our previously analysed clinical samples and of clinical interest. It is important to highlight how introducing each of these mutations completely reverses the NTCP-independent entry phenotype of BT10D4. More importantly, the HBV population in an infected patient is known to exist as quasispecies that continue to interact to favour viral fitness in not easily predictable ways [331, 335, 336]. This data indicates how the effect of amino acid substitutions can change the phenotype of the virus strain. Interestingly, from our data, the sL109P and the sG145R mutations show undetectable RLU values in the qualitative diagnostic system. These mutations are both present in the MHR of the HBsAg, a region particularly targeted by antibodies in diagnostic tests. The glycine to arginine mutation at position s145 in the second antigenic loop is a well-described escape mutant. This mutation has been shown to cause conformational changes in the

HBsAg antigenic loop, reducing the HBsAg immunogenic activity. Carman, W.F., *et al.,* identified the sG145R mutation in 1990 among individuals with HBV infection despite their previous active and passive immunisation [251]. Carman, W.F., *et al.,* also described this mutation in their 1995 study, which identified the sG145R mutation in the case of HBV reactivation in a vaccinated patient in Indonesia [519]. Both studies have described this mutation as stable, resulting in the loss of the 'a' determinant and reduction in the binding of HBV monoclonal antibody. Rezaee, R., *et al.,* in their study using computational analysis to investigate the impact of the sG145R mutation on the structure and immunogenic activity of HBsAg, reported that this mutation leads to the insertion of a new beta-strand in the HBsAg 'a' determinant. They stated that this insertion increases the rigidity of the 'a' determinant, making the HBsAg more compact and stable, leading to a reduction in the monoclonal antibody affinity [414]. It is also striking that Jammeh, S., *et al.,* showed in the study on the replicative competence of HBsAg variants *in vitro* that the sG145R mutation did not affect the HBV replication as the sG145R mutant has a replication efficiency equal to the wildtype [520]. Over the years, this mutation has been extensively studied and associated with immune escape, vaccination, and diagnostic failures [267, 268, 413, 521-523]. Similar to these studies, the undetectable RLU value of the sG145R mutant in our study supports previous studies, suggesting that this mutation could affect antibody recognition of HBsAg and lead to diagnostic failure. Similarly, from our data, the sL109P mutation also showed a low signal in the diagnostic assay. Although this mutation has not been extensively studied, it has been reported in several other studies [300, 309, 524-528]. This mutation, also located in the MHR of HBsAg, could contribute to conformational changes in the HBsAg epitopes that led to its undetectable phenotype.

In our study, the sT189I, sS193L, sS204R mutations showed a significant reduction in detection RLU values compared to the BT10D4 wildtype. Several studies have identified these mutations among clinical samples in different parts of the world [300, 310, 526, 529-534]. Olinger, C.M., *et al.,* evaluated the efficiency of HBsAg detection assays in detecting HBV genotype E from Nigerian samples and reported that sT189I mutation in HBsAg genotype E was associated

with a reduction in detection signals [305]. In as much as our samples were representatives of genotype D, we have seen a similar reduction in detection signals in the presence of sT189I mutation. Also, Kırdar, S., *et al.,* [535] and Kazim, S.N., *et al.,* [536] in studies identified and characterised the polymerase and surface gene mutations prevalent in chronic HBV patients receiving long-term nucleoside/nucleotide analogues treatment. These studies identified the sS193L mutant among other mutations from HCC patients and characterised this mutation as an antiviral drug-associated potential vaccine-escape mutant [535, 536]. It is plausible that replacing polar amino acids threonine at position s189 and serine at position s193 with non-polar amino acids isoleucine and leucine, respectively, alters the propensity for HBsAg secretion or the ability of antibodies to recognise the HBsAg, resulting in a reduced detection signal. Additionally, Jing, Z.-T., *et al.,* in their study investigating the effect of HBsAg in enhancing the sensitivity of hepatocytes to Fas-mediated apoptosis, found intracellular retention of HBsAg and a reduction in secreted HBsAg in the presence of sS204R mutation [537]. Sterneck, M., *et al.,* also reported this in their study, stating an HBsAg secretion defect of about 60 % in the presence of sS204R mutation among other mutations [538, 539]. Our study has also shown a reduction in the detection signal of the sS204R mutant. Although it is unclear if this reduction is a result of HBsAg retention, it is highly plausible that the replacement of the small, polar, uncharged serine at amino acid s204 with the large, positively charged arginine could affect viral particle release causing a reduction in the detection signal. On the other hand, the sS207R mutant pseudotype showed no difference in its detection signal compared to the BT10D4 wildtype. Although this mutation has been identified in various other studies, its phenotypic characteristics have not been stated [300, 526, 540-542]. Our data suggest that the presence of the sS207R mutation has no effect on the secretion and antibody recognition of HBsAg, or another amino acid at a different position compensates its effect. Furthermore, there was a significant difference between the pseudotyped and the subviral HBV particles detection signals, which is very likely related to their release mechanism from the host cell. The release of pseudotyped particles depends on several factors, including the virus's glycoprotein ability to interact

with the retroviral core [382]. Hence, it can be said that the pseudotyped particles were released via the retroviral pathway, while the subviral particles in the absence of a retroviral vector were released via the HBV release pathway. The differences seen between the pseudotyped and the subviral particles could mean that the release of the pseudotyped particles is more efficient in this system, possibly because of the presence of the viral vector.

In this chapter, our study has generated data showing the impact of several clinically relevant HBsAg mutations on the qualitative detection of the pseudotyped and subviral particles using a clinical diagnostic system. It is important to note that the clinical samples from which these mutations were identified had quantifiable positive HBsAg; hence our data only shows the effect of these mutations on the BT10D4 wildtype. However, it is also crucial to note that our results do not indicate whether or not the variation in detection signals of the mutants compared to the wildtype results from a secretion or antibody recognition defect. In future studies, it would be important to quantify the HBsAg titre for each mutant to give a clearer picture of how the presence of the mutations could impact clinical diagnosis. It would also be interesting to compare the intracellular and extracellular HBsAg to give an insight into the effect of the mutations on secretion and antibody recognition of HBsAg. Additionally, as amino acid mutations on real-life infections do not occur individually but in groups, it would be interesting to investigate the effect of these mutations as they occurred in patients' samples from which they were isolated.

Chapter 7

Conclusion and Future Work

In conclusion, our study has generated several unusual data particularly focused on the BT10D4 unusual entry phenotype and the rare amino acid substitutions associated with it. Therefore, it is imperative to consider its implication on the clinical management of HBV. With the findings from our study and prior knowledge that anti-HBs antibodies in diagnostics and immune therapy are dependent on the interaction with the HBsAg conformational epitopes, it raises the question of how this could impact clinical diagnosis and immune therapy, especially with the previously described sG145R mutant [347, 520, 523]. If the conformation of the HBsAg protein is altered from the presence of the arginine and alanine mutations, it is plausible that this could adversely affect its antibody recognition in diagnosis and immune therapy. Additionally, in the context of HBV/HDV co-infection, there is the question of how the HDV entry is affected in the presence of potentially conformation-altering mutations associated with unusual entry phenotype. It is also particularly important to consider how the possibility of this occurrence could impact the therapeutic management of HBV/HDV using entry inhibitors, especially the very promising recently approved Myrcludex and others being developed [202, 453].

Our data has raised more questions than we were able to answer within this study. Many questions have remained unanswered as to how BT10D4 infects Huh7 cells independent of the known receptor, NTCP; however, one thing is for sure; this is not unheard-of among viruses. Distinctive differences in entry among virus strains have been described for other viruses in the past. A classic example is the Human Immunodeficiency Virus (HIV), which has been studied extensively across the globe. HIV entry generally occurs by binding its gp120 protein to the CD4 cell receptor followed by conformational changes that enable gp120 interaction with the CCR5 co-receptor or CXCR4 co-receptor, as seen in late-stage patients [543]. Interestingly, a few isolates of HIV-1, such as the CXCR4-tropic NDK HIV-1 virus, have been shown to directly infect CD4-negative cells using CXCR4 or CCR5 while still retaining their CD4 lymphocyte tropism. Further studies showed that several spontaneous mutations in gp120 are associated with this phenotype [544-547]. Also, Saha *et al.,* have previously described HIV-1 strains from patient isolates that infect cells using the CD8 cell receptor in the absence

of either CCR5 or CXCR4 co-receptors. This phenotype has also been attributed to selective pressure mutation in the advanced stages of the infection [548, 549]. Another example is the vaccinia virus; in a study comparing the differences in cell attachment and entry of 5 vaccinia virus strains, Bengali, Z. *et al.,* identified that three out of the five compared strains were less dependent on low pH endosomal pathway and more reliant on the use of glycosaminoglycans for cell attachment resulting in differences in the entry pathways. Sequence comparison further indicated that specific viral determinants could be responsible for the entry properties [550-552].

In this study, we have identified HBV BT10D4 from a patient isolate that has the phenotypic ability to infect Huh7 *in vitro* without the NTCP receptor. Sequence analysis and subsequent mutagenesis experiments revealed sC69R and sV96A mutations that could be associated with this phenotype; however, the mechanism by which this occurs is still unclear. These rare mutations were identified only in HBV genotype D isolates; in the future, it would be interesting to investigate the existence of these mutations in other HBV genotypes as well as compare the *in vitro* phenotype resulting from the presence of these mutations in other HBV genotypes. This study showed that the sR69 and sA96 amino acids interact epistatically with each other and possibly with one or more other amino acid positions to achieve the unusual phenotype. Sequence comparison of BT10D4 with D39 showed that sR69 and sA96 alone does not give the NTCP-independent phenotype. Hence, focusing on the amino acid differences between BT10D4 and D39, it would be important to carry out further mutational analysis to identify other amino acid positions interacting with sR69 and sA96 amino acids to produce the NTCP-independent phenotype. Also, it is important to explore if any other mutations frequently occur alongside these two in the clinic. It has been shown that the preS domain of L is in the cytosol of the ER membrane, which is in the internal-preS (i-preS) conformation during translation. However, after translation, translocational changes occur in about 50 % of the L proteins changing their conformation to the external-preS (e-preS) conformation in which the preS domain is in the ER lumen [117, 120-122]. The two topologies of L-HBsAg achieve two different roles at the interior and exterior sides of the

viral envelope. The i-preS conformation of L-HBsAg enables the interaction with the HBV capsid during virion assembly and subsequent virion envelopment while the e-preS conformation of L-HBsAg interacts with the viral cell receptor for entry and infectivity [119, 553]. It is plausible that the presence of these mutations in the cytosolic and transmembrane 1 domains could alter the translocation of the L-HBsAg, possibly by altering the percentage of translocated L-HBsAg in such a way that favours receptor interaction and entry. Consequently, it would be interesting to question the percentage of e-PreS in the BT10D4 HBV isolate. This can be done by immunoprecipitation using an antibody that recognises regions in the preS1 (preS1 because the target is the L-HBsAg) and subsequent western blotting similar to the study by Bruss, V., *et al.,* on the "post-translational alterations in the transmembrane topology of the hepatitis B virus large envelope protein" [121]. Also, a protein tag such as a GFP-tag or His-tag can be added to the preS1 region of L-HBsAg, which can be detected by fluorescence, immunoprecipitation, or western blotting.

Furthermore, this study revealed strikingly notable data regarding the cellular tropism of BT10D4. Our study showed that the BT10D4 entry phenotype is peculiar to Huh7 and Huh7.5 and is not seen to occur in HepG2 cells. This data is remarkable on its own because it tells us that the receptor which BT10D4 could be interacting with for entry is highly expressed in Huh7 cells, has some expression in Hep3B cells and has a very low expression in HepG2 cells, thus pointing us in the right direction for future studies. Shi, J., *et al.,* in their study on the comparison of protein expression between human livers and the hepatic cell lines HepG2, Hep3B, and Huh7 using mass spectrometry and other proteomics techniques, generated some interesting comparison data. Their data showed Annexin 2 (ANXA2) as the protein that fits the above-stated requirements and shows prospects for further investigation [484]. It is also plausible that more than one factor is involved; however, working with ANXA2 would be a good start. Annexin 2 is a pleiotropic protein encoded by the ANXA2 gene [554]. It is a multifunctional calcium- and lipid-binding protein broadly expressed in nearly all human tissues implicated in multiple human diseases, immune function, and viral infection. It has been associated with binding, endocytosis, and egress stages of

different viral infections, including HCV and the Influenza A virus [555-558]. One of the first and probably the most straightforward test to perform would be to block the ANXA2 protein with an anti-ANXA2 antibody prior to infection with BT10D4. This would immediately give information as to whether the presence of ANXA2 contributes to the entry of BT10D4. Alternatively, carrying out a siRNA knockdown of the ANXA2 protein in the Huh7 cells prior to BT10D4 infection should provide similar information as the antibody blocking assay. However, both assays should serve as confirmatory tests to each other. Also, cloning the ANXA2 gene into HepG2 cells and subsequent infection with BT10D4 would also be an informative experiment to do. Although this has a higher degree of complexity, it would not only provide information as to the relevance of ANXA2; it would also provide information with regards to whether ANXA2 is the only factor involved in BT10D4 entry into Huh7 cells. Another experiment to do would be tracking the expression of the ANXA2 protein over a period post-infection with BT10D4. It is expected that the binding of BT10D4 to the ANXA2 protein should involve its endocytosis alongside the bound virus, potentially reducing the expressed protein just after infection. Although this is not a definitive test as it is based on the hypothesis of endocytosis nonetheless, this would provide some insight into the activity of the ANXA2 protein after BT10D4 infection. This study shows that EGFR is an essential factor for BT10D4 infection; it would be interesting to investigate if the ANXA2 protein works together with EGFR for BT10D4 infection. These can be done similar to Martin, D.N. and colleagues who previously carried out a similar investigation in their study on the "Identification of transferrin receptor 1 as a hepatitis C virus entry factor" [559].

From this study, therefore, we propose a hypothetical model of the BT10D4 isolate. We propose that the presence of the mutations discussed above, which interact with each other, alter the conformation of the L-HBsAg, possibly increasing the percentage of e-PreS in such a way that favours its interaction with one or more unknown Huh7 cell receptors, possibly Annexin 2 (ANXA2) (Figure 7.1). Consequently, future work will explore this hypothetical model to provide the much-needed answers about the BT10D4 isolate. Further work should also be done to investigate the possibility of an increased affinity of

BT10D4 for vely low level NTCP expression in the Huh7 cells. This can be done first by quantifying the NTCP mRNA levels present in the Huh7 cells; completely knocking down the NTCP expression and subsequently infecting the Huh7 cells with BT10D4. In all, this study has looked at the phenotypic characteristics of HBsAg using the pseudotyping system, which gives information only about the characteristics of the S gene. Therefore, it is vital to consider the overlapping nature of the HBV genome and what that could mean in studying the effect of mutations in HBsAg. This study does not give information on the characteristics of the corresponding polymerase gene mutations and the visibility of the resulting virus. Hence, it is unclear the effect of these mutations in a full HBV genome *in vitro*, *in vivo* and in a clinical infection; this would be an important future research area.

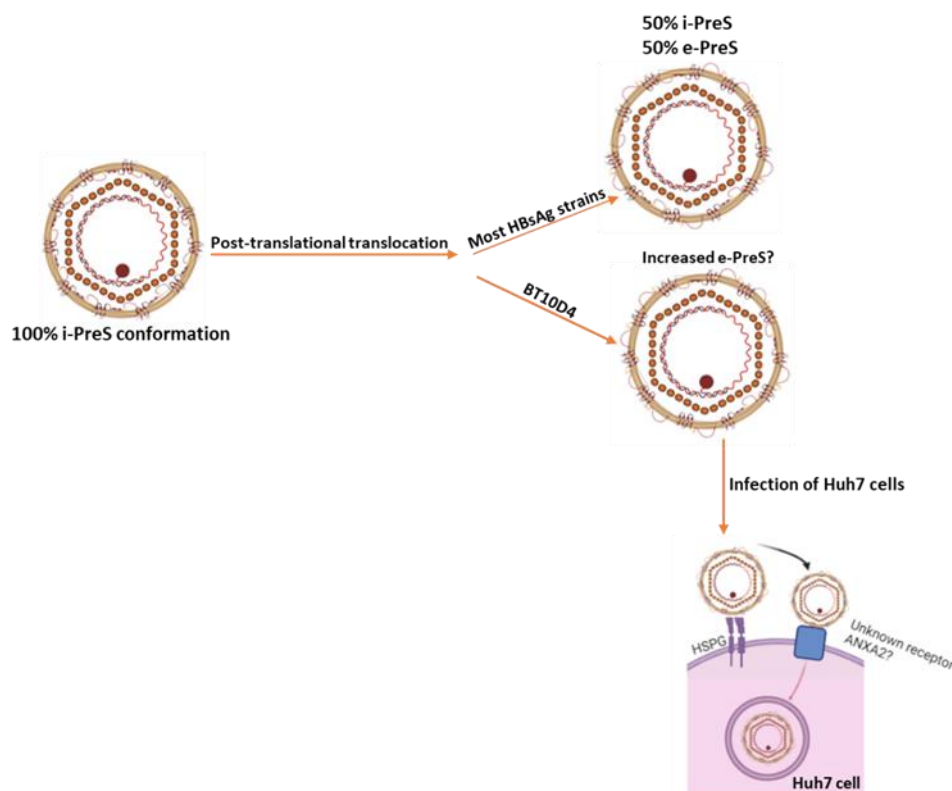**Figure 7.1** Hypothetical model of BT10D4 conformation and entry into Huh7 cells. We propose that the presence of the mutations discussed above which interact with each other alter the conformation of the L-HBsAg possibly increasing the percentage of e-PreS in such a way that favours its interaction with one or more unknown Huh7 cell receptors, possibly Annexin 2 (ANXA2). The figure was created at http://biorender.com/.

References

1.   Modi, A.A. and T.J. Liang, *Hepatitis C: a clinical review.* Oral Dis, 2008. **14**(1): p. 10-4.
2.   Lee, G.Y., et al., *Hepatitis E virus infection: Epidemiology and treatment implications.* World J Virol, 2015. **4**(4): p. 343-55.
3.   Cuthbert, J.A., *Hepatitis A: Old and New.* Clinical Microbiology Reviews, 2001. **14**(1): p. 38.
4.   Wiktor, S.Z. and Y.J. Hutin, *The global burden of viral hepatitis: better estimates to guide hepatitis elimination efforts.* Lancet, 2016. **388**(10049): p. 1030-1031.
5.   Liang, T.J., *Hepatitis B: the virus and disease.* Hepatology, 2009. **49**(5 Suppl): p. S13-21.
6.   Datta, S., et al., *Molecular biology of the hepatitis B virus for clinicians.* Journal of clinical and experimental hepatology, 2012. **2**(4): p. 353-365.
7.   MacCallum, F.O., *1971 International Symposium on Viral Hepatitis. Historical perspectives.* Canadian Medical Association journal, 1972. **106**(Spec Issue): p. 423-426.
8.   Seeff, L.B., et al., *A Serologic Follow-up of the 1942 Epidemic of Post-Vaccination Hepatitis in the United States Army.* New England Journal of Medicine, 1987. **316**(16): p. 965-970.
9.   Fonseca, J.C.F.d., *Histórico das hepatites virais.* Revista da Sociedade Brasileira de Medicina Tropical, 2010. **43**: p. 322-330.
10.   Blumberg, B.S., *Australia antigen and the biology of hepatitis B.* Science, 1977. **197**(4298): p. 17.
11.   Blumberg, B.S., et al., *A Serum Antigen (Australia Antigen) in Down's Syndrome, Leukemia, and Hepatitis.* Annals of Internal Medicine, 1967. **66**(5): p. 924-931.
12.   Krugman, S., J.P. Giles, and J. Hammond, *Infectious Hepatitis: Evidence for Two Distinctive Clinical, Epidemiological, and Immunological Types of Infection.* JAMA, 1967. **200**(5): p. 365-373.
13.   Blumberg, B.S. and H.J. Alter, *A "New" Antigen in Leukemia Sera.* JAMA, 1965. **191**(7): p. 541-546.
14.   Dane, D.S., C.H. Cameron, and M. Briggs, *Virus-like particles in serum of patients with Australia-antigen-associated hepatitis.* Lancet, 1970. **1**(7649): p. 695-8.
15.   Patterson Ross, Z., et al., *The paradox of HBV evolution as revealed from a 16th century mummy.* PLOS Pathogens, 2018. **14**(1): p. e1006750.
16.   Gust, I.D., et al., *Taxonomic classification of human hepatitis B virus.* Intervirology, 1986. **25**(1): p. 14-29.
17.   Mason, W.S., G. Seal, and J. Summers, *Virus of Pekin ducks with structural and biological relatedness to human hepatitis B virus.* J Virol, 1980. **36**(3): p. 829-36.
18.   Chang, S.F., et al., *A new avian hepadnavirus infecting snow geese (Anser caerulescens) produces a significant fraction of virions containing single-stranded DNA.* Virology, 1999. **262**(1): p. 39-54.
19.   Naumann, H., et al., *Identification of a new hepatitis B virus (HBV) genotype from Brazil that expresses HBV surface antigen subtype adw4.* J Gen Virol, 1993. **74 (Pt 8)**: p. 1627-32.
20.   Nie, F.-Y., et al., *Extensive diversity and evolution of hepadnaviruses in bats in China.* Virology, 2018. **514**: p. 88-97.
21.   Warren, K.S., et al., *A new group of hepadnaviruses naturally infecting orangutans (Pongo pygmaeus).* Journal of virology, 1999. **73**(9): p. 7860-7865.
22.   Testut, P., et al., *A new hepadnavirus endemic in arctic ground squirrels in Alaska.* Journal of virology, 1996. **70**(7): p. 4210-4219.
23.   Vaudin, M., et al., *The complete nucleotide sequence of the genome of a hepatitis B virus isolated from a naturally infected chimpanzee.* J Gen Virol, 1988. **69 (Pt 6)**: p. 1383-9.

24.	Norder, H., et al., *Complete sequencing of a gibbon hepatitis B virus genome reveals a unique genotype distantly related to the chimpanzee hepatitis B virus.* Virology, 1996. **218**(1): p. 214-23.

25.	Lanford, R.E., et al., *Isolation of a hepadnavirus from the woolly monkey, a New World primate.* Proc Natl Acad Sci U S A, 1998. **95**(10): p. 5757-61.

26.	Schaefer, S., *Hepatitis B virus taxonomy and hepatitis B virus genotypes.* World journal of gastroenterology, 2007. **13**(1): p. 14-21.

27.	Paronetto, F. and B.C. Tennant, *Woodchuck hepatitis virus infection: a model of human hepatic diseases and hepatocellular carcinoma.* Prog Liver Dis, 1990. **9**: p. 463-83.

28.	Ganem, D. and H.E. Varmus, *The molecular biology of the hepatitis B viruses.* Annu Rev Biochem, 1987. **56**: p. 651-93.

29.	Roggendorf, M. and T.K. Tolle, *The woodchuck: an animal model for hepatitis B virus infection in man.* Intervirology, 1995. **38**(1-2): p. 100-12.

30.	Gerlich, W.H. and W.S. Robinson, *Hepatitis B virus contains protein attached to the 5' terminus of its complete DNA strand.* Cell, 1980. **21**(3): p. 801-9.

31.	Gavilanes, F., J.M. Gonzalez-Ros, and D.L. Peterson, *Structure of hepatitis B surface antigen. Characterization of the lipid components and their association with the viral proteins.* Journal of Biological Chemistry, 1982. **257**(13): p. 7770-7777.

32.	Lamontagne, R.J., S. Bagga, and M.J. Bouchard, *Hepatitis B virus molecular biology and pathogenesis.* Hepatoma research, 2016. **2**: p. 163-186.

33.	Seeger, C., D. Ganem, and H.E. Varmus, *Biochemical and genetic evidence for the hepatitis B virus replication strategy.* Science, 1986. **232**(4749): p. 477-84.

34.	Hatton, T., S. Zhou, and D.N. Standring, *RNA- and DNA-binding activities in hepatitis B virus capsid protein: a model for their roles in viral replication.* J Virol, 1992. **66**(9): p. 5232-41.

35.	Gavilanes, F., J.M. Gonzalez-Ros, and D.L. Peterson, *Structure of hepatitis B surface antigen. Characterization of the lipid components and their association with the viral proteins.* J Biol Chem, 1982. **257**(13): p. 7770-7.

36.	Radziwill, G., W. Tucker, and H. Schaller, *Mutational analysis of the hepatitis B virus P gene product: domain structure and RNase H activity.* Journal of virology, 1990. **64**(2): p. 613-620.

37.	Weber, M., et al., *Hepadnavirus P protein utilizes a tyrosine residue in the TP domain to prime reverse transcription.* Journal of virology, 1994. **68**(5): p. 2994-2999.

38.	Zoulim, F. and C. Seeger, *Reverse transcription in hepatitis B viruses is primed by a tyrosine residue of the polymerase.* Journal of virology, 1994. **68**(1): p. 6-13.

39.	Jones, S.A., et al., *Comparative analysis of hepatitis B virus polymerase sequences required for viral RNA binding, RNA packaging, and protein priming.* Journal of virology, 2014. **88**(3): p. 1564-1572.

40.	Wang, G.H. and C. Seeger, *The reverse transcriptase of hepatitis B virus acts as a protein primer for viral DNA synthesis.* Cell, 1992. **71**(4): p. 663-70.

41.	Bartenschlager, R. and H. Schaller, *The amino-terminal domain of the hepadnaviral P-gene encodes the terminal protein (genome-linked protein) believed to prime reverse transcription.* Embo j, 1988. **7**(13): p. 4185-92.

42.	Summers, J. and W.S. Mason, *Replication of the genome of a hepatitis B--like virus by reverse transcription of an RNA intermediate.* Cell, 1982. **29**(2): p. 403-15.

43.	Quarleri, J., *Core promoter: a critical region where the hepatitis B virus makes decisions.* World journal of gastroenterology, 2014. **20**(2): p. 425-435.

44. Milich, D. and T.J. Liang, *Exploring the biological basis of hepatitis B e antigen in hepatitis B virus infection.* Hepatology, 2003. **38**(5): p. 1075-86.

45. Wang, J., A.S. Lee, and J.H. Ou, *Proteolytic conversion of hepatitis B virus e antigen precursor to end product occurs in a postendoplasmic reticulum compartment.* J Virol, 1991. **65**(9): p. 5080-3.

46. Diab, A., et al., *The diverse functions of the hepatitis B core/capsid protein (HBc) in the viral life cycle: Implications for the development of HBc-targeting antivirals.* Antiviral Research, 2018. **149**: p. 211-220.

47. Chen, M.T., et al., *A function of the hepatitis B virus precore protein is to regulate the immune response to the core antigen.* Proc Natl Acad Sci U S A, 2004. **101**(41): p. 14913-8.

48. Eble, B.E., V.R. Lingappa, and D. Ganem, *The N-terminal (pre-S2) domain of a hepatitis B virus surface glycoprotein is translocated across membranes by downstream signal sequences.* J Virol, 1990. **64**(3): p. 1414-9.

49. Eble, B.E., et al., *Multiple topogenic sequences determine the transmembrane orientation of the hepatitis B surface antigen.* Mol Cell Biol, 1987. **7**(10): p. 3591-601.

50. Gripon, P., I. Cannie, and S. Urban, *Efficient Inhibition of Hepatitis B Virus Infection by Acylated Peptides Derived from the Large Viral Surface Protein.* Journal of Virology, 2005. **79**(3): p. 1613.

51. Jiang, B., et al., *The N-Terminus Makes the Difference: Impact of Genotype-Specific Disparities in the N-Terminal Part of The Hepatitis B Virus Large Surface Protein on Morphogenesis of Viral and Subviral Particles.* Cells, 2020. **9**(8).

52. Urban, S., et al., *Strategies to inhibit entry of HBV and HDV into hepatocytes.* Gastroenterology, 2014. **147**(1): p. 48-64.

53. Gilbert, R.J.C., et al., *Hepatitis B small surface antigen particles are octahedral.* Proceedings of the National Academy of Sciences of the United States of America, 2005. **102**(41): p. 14783.

54. Lepère-Douard, C., et al., *The First Transmembrane Domain of the Hepatitis B Virus Large Envelope Protein Is Crucial for Infectivity.* Journal of Virology, 2009. **83**(22): p. 11819.

55. Siegler, V.D. and V. Bruss, *Role of transmembrane domains of hepatitis B virus small surface proteins in subviral-particle biogenesis.* Journal of virology, 2013. **87**(3): p. 1491-1496.

56. Stirk, H.J., J.M. Thornton, and C.R. Howard, *A topological model for hepatitis B surface antigen.* Intervirology, 1992. **33**(3): p. 148-58.

57. Venkatakrishnan, B. and A. Zlotnick, *The Structural Biology of Hepatitis B Virus: Form and Function.* Annual review of virology, 2016. **3**(1): p. 429-451.

58. Lee, J., et al., *N-Linked Glycosylation Is Not Essential for Sodium Taurocholate Cotransporting Polypeptide To Mediate Hepatitis B Virus Infection <em>In Vitro</em&gt.* Journal of Virology, 2018. **92**(15): p. e00732-18.

59. Abou-Jaoudé, G. and C. Sureau, *Entry of hepatitis delta virus requires the conserved cysteine residues of the hepatitis B virus envelope protein antigenic loop and is blocked by inhibitors of thiol-disulfide exchange.* Journal of virology, 2007. **81**(23): p. 13057-13066.

60. Niedre-Otomere, B., et al., *Posttranslational modifications and secretion efficiency of immunogenic hepatitis B virus L protein deletion variants.* Virology Journal, 2013. **10**(1): p. 63.

61. Mangold, C.M. and R.E. Streeck, *Mutational analysis of the cysteine residues in the hepatitis B virus small envelope protein.* Journal of virology, 1993. **67**(8): p. 4588-4597.

62. Blanchet, M. and C. Sureau, *Infectivity Determinants of the Hepatitis B Virus Pre-S Domain Are Confined to the N-Terminal 75 Amino Acid Residues.* Journal of Virology, 2007. **81**(11): p. 5841.

63. Gripon, P., et al., *Myristylation of the hepatitis B virus large surface protein is essential for viral infectivity.* Virology, 1995. **213**(2): p. 292-9.

64. Gripon, P., et al., *Infection of a human hepatoma cell line by hepatitis B virus.* Proc Natl Acad Sci U S A, 2002. **99**(24): p. 15655-60.

65. Le Duff, Y., M. Blanchet, and C. Sureau, *The Pre-S1 and Antigenic Loop Infectivity Determinants of the Hepatitis B Virus Envelope Proteins Are Functionally Independent.* Journal of Virology, 2009. **83**(23): p. 12443.

66. Le Seyec, J., et al., *Role of the Pre-S2 Domain of the Large Envelope Protein in Hepatitis B Virus Assembly and Infectivity.* Journal of Virology, 1998. **72**(7): p. 5573.

67. Sureau, C., B. Guerra, and H. Lee, *The middle hepatitis B virus envelope protein is not necessary for infectivity of hepatitis delta virus.* Journal of Virology, 1994. **68**(6): p. 4063.

68. Sureau, C., B. Guerra, and R.E. Lanford, *Role of the large hepatitis B virus envelope protein in infectivity of the hepatitis delta virion.* Journal of Virology, 1993. **67**(1): p. 366.

69. Rawat, S. and M.J. Bouchard, *The hepatitis B virus (HBV) HBx protein activates AKT to simultaneously regulate HBV replication and hepatocyte survival.* Journal of virology, 2015. **89**(2): p. 999-1012.

70. Chung, T.-W., Y.-C. Lee, and C.-H. Kim, *Hepatitis B viral HBx induces matrix metalloproteinase-9 gene expression through activation of ERKs and PI-3K/AKT pathways: Involvement of invasive potential.* The FASEB Journal, 2004. **18**(10): p. 1123-1125.

71. Iyer, S. and J.D. Groopman, *Interaction of mutant hepatitis B X protein with p53 tumor suppressor protein affects both transcription and cell survival.* Molecular carcinogenesis, 2011. **50**(12): p. 972-980.

72. Hsieh, A., et al., *Hepatitis B viral X protein interacts with tumor suppressor adenomatous polyposis coli to activate Wnt/β-catenin signaling.* Cancer Letters, 2011. **300**(2): p. 162-172.

73. Kim, J.H. and H.M. Rho, *Activation of the human transforming growth factor alpha (TGF-α) gene by the hepatitis B viral X protein (HBx) through AP-2 sites.* Molecular and Cellular Biochemistry, 2002. **231**(1): p. 155-161.

74. Tanaka, Y., et al., *The hepatitis B virus X protein enhances AP-1 activation through interaction with Jab1.* Oncogene, 2006. **25**(4): p. 633-642.

75. Arbuthnot, P., A. Capovilla, and M. Kew, *Putative role of hepatitis B virus X protein in hepatocarcinogenesis: Effects on apoptosis, DNA repair, mitogen-activated protein kinase and JAK/STAT pathways.* Journal of Gastroenterology and Hepatology, 2000. **15**(4): p. 357-368.

76. Bouchard, M.J. and R.J. Schneider, *The enigmatic X gene of hepatitis B virus.* Journal of virology, 2004. **78**(23): p. 12725-12734.

77. Lucifora, J., et al., *Hepatitis B virus X protein is essential to initiate and maintain virus replication after infection.* Journal of Hepatology, 2011. **55**(5): p. 996-1003.

78. Elfassi, E., et al., *Evidence of extrachromosomal forms of hepatitis B viral DNA in a bone marrow culture obtained from a patient recently infected with hepatitis B virus.* Proceedings of the National Academy of Sciences, 1984. **81**(11): p. 3526.

79. Noonan, C.A., et al., *Extrachromosomal sequences of hepatitis B virus DNA in peripheral blood mononuclear cells of acquired immune deficiency syndrome patients.* Proceedings of the National Academy of Sciences of the United States of America, 1986. **83**(15): p. 5698-5702.

80. Hosoda, K., et al., *Extrahepatic replication of duck hepatitis b virus: More than expected.* Hepatology, 1990. **11**(1): p. 44-48.

81. Yan, H., et al., *Sodium taurocholate cotransporting polypeptide is a functional receptor for human hepatitis B and D virus.* eLife, 2012. **1**: p. e00049-e00049.

82. Watashi, K., et al., *NTCP and Beyond: Opening the Door to Unveil Hepatitis B Virus Entry.* International Journal of Molecular Sciences, 2014. **15**(2).

83. Li, W., *The Hepatitis B Virus Receptor.* Annual Review of Cell and Developmental Biology, 2015. **31**(1): p. 125-147.

84. Köck, J., et al., *Efficient Infection of Primary Tupaia Hepatocytes with Purified Human and Woolly Monkey Hepatitis B Virus.* Journal of Virology, 2001. **75**(11): p. 5084.

85. Ye, X., et al., *Efficient Inhibition of Hepatitis B Virus Infection by a preS1-binding Peptide.* Scientific Reports, 2016. **6**(1): p. 29391.

86. Yan, H., et al., *Molecular determinants of hepatitis B and D virus entry restriction in mouse sodium taurocholate cotransporting polypeptide.* J Virol, 2013. **87**(14): p. 7977-91.

87. Huang, H.-C., et al., *Entry of hepatitis B virus into immortalized human primary hepatocytes by clathrin-dependent endocytosis.* Journal of virology, 2012. **86**(17): p. 9443-9453.

88. Iwamoto, M., et al., *The machinery for endocytosis of epidermal growth factor receptor coordinates the transport of incoming hepatitis B virus to the endosomal network.* The Journal of biological chemistry, 2020. **295**(3): p. 800-807.

89. Iwamoto, M., et al., *Epidermal growth factor receptor is a host-entry cofactor triggering hepatitis B virus internalization.* Proceedings of the National Academy of Sciences, 2019. **116**(17): p. 8487.

90. Fukano, K., et al., *Troglitazone Impedes the Oligomerization of Sodium Taurocholate Cotransporting Polypeptide and Entry of Hepatitis B Virus Into Hepatocytes.* Frontiers in Microbiology, 2019. **9**(3257).

91. Rabe, B., et al., *Nuclear entry of hepatitis B virus capsids involves disintegration to protein dimers followed by nuclear reassociation to capsids.* PLoS Pathog, 2009. **5**(8): p. e1000563.

92. Guo, H., et al., *Characterization of the Intracellular Deproteinized Relaxed Circular DNA of Hepatitis B Virus: an Intermediate of Covalently Closed Circular DNA Formation.* Journal of Virology, 2007. **81**(22): p. 12472.

93. Molnar-Kimber, K.L., et al., *Protein covalently bound to minus-strand DNA intermediates of duck hepatitis B virus.* Journal of Virology, 1983. **45**(1): p. 165.

94. Wang, G.-H. and C. Seeger, *The reverse transcriptase of hepatitis B virus acts as a protein primer for viral DNA synthesis.* Cell, 1992. **71**(4): p. 663-670.

95. Kitamura, K., et al., *Flap endonuclease 1 is involved in cccDNA formation in the hepatitis B virus.* PLOS Pathogens, 2018. **14**(6): p. e1007124.

96. Qi, Y., et al., *DNA Polymerase κ Is a Key Cellular Factor for the Formation of Covalently Closed Circular DNA of Hepatitis B Virus.* PLOS Pathogens, 2016. **12**(10): p. e1005893.

97. Sheraz, M., et al., *Cellular DNA Topoisomerases Are Required for the Synthesis of Hepatitis B Virus Covalently Closed Circular DNA.* Journal of Virology, 2019. **93**(11): p. e02230-18.

98. Tang, L., et al., *DNA Polymerase alpha is essential for intracellular amplification of hepatitis B virus covalently closed circular DNA.* PLOS Pathogens, 2019. **15**(4): p. e1007742.

99. Long, Q., et al., *The role of host DNA ligases in hepadnavirus covalently closed circular DNA formation.* PLOS Pathogens, 2017. **13**(12): p. e1006784.

100. Lucifora, J., et al., *Specific and Nonhepatotoxic Degradation of Nuclear Hepatitis B Virus cccDNA.* Science, 2014. **343**(6176): p. 1221.

101. Xia, Y., et al., *Interferon-γ and Tumor Necrosis Factor-α Produced by T Cells Reduce the HBV Persistence Form, cccDNA, Without Cytolysis.* Gastroenterology, 2016. **150**(1): p. 194-205.

102. Belloni, L., et al., *Nuclear HBx binds the HBV minichromosome and modifies the epigenetic regulation of cccDNA function.* Proceedings of the National Academy of Sciences, 2009. **106**(47): p. 19975.

103. Luo, L., et al., *Hepatitis B virus X protein modulates remodelling of minichromosomes related to hepatitis B virus replication in HepG2 cells.* Int J Mol Med, 2013. **31**(1): p. 197-204.

104. Rivière, L., et al., *HBx relieves chromatin-mediated transcriptional repression of hepatitis B viral cccDNA involving SETDB1 histone methyltransferase.* J Hepatol, 2015. **63**(5): p. 1093-102.

105. Bill, C.A. and J. Summers, *Genomic DNA double-strand breaks are targets for hepadnaviral DNA integration.* Proceedings of the National Academy of Sciences of the United States of America, 2004. **101**(30): p. 11135.

106. Yang, W. and J. Summers, *Integration of Hepadnavirus DNA in Infected Liver: Evidence for a Linear Precursor.* Journal of Virology, 1999. **73**(12): p. 9710.

107. Edman, J.C., et al., *Integration of hepatitis B virus sequences and their expression in a human hepatoma cell.* Nature, 1980. **286**(5772): p. 535-538.

108. Waris, G. and A. Siddiqui, *Regulatory mechanisms of viral hepatitis B and C.* J Biosci, 2003. **28**(3): p. 311-21.

109. Antonucci, T.K. and W.J. Rutter, *Hepatitis B virus (HBV) promoters are regulated by the HBV enhancer in a tissue-specific manner.* Journal of virology, 1989. **63**(2): p. 579-583.

110. Nassal, M. and A. Rieger, *A bulged region of the hepatitis B virus RNA encapsidation signal contains the replication origin for discontinuous first-strand DNA synthesis.* J Virol, 1996. **70**(5): p. 2764-73.

111. Loeb, D.D., R.C. Hirsch, and D. Ganem, *Sequence-independent RNA cleavages generate the primers for plus strand DNA synthesis in hepatitis B viruses: implications for other reverse transcribing elements.* Embo j, 1991. **10**(11): p. 3533-40.

112. Lewellyn, E.B. and D.D. Loeb, *Base pairing between cis-acting sequences contributes to template switching during plus-strand DNA synthesis in human hepatitis B virus.* J Virol, 2007. **81**(12): p. 6207-15.

113. Wu, T.T., et al., *In hepatocytes infected with duck hepatitis B virus, the template for viral RNA synthesis is amplified by an intracellular pathway.* Virology, 1990. **175**(1): p. 255-61.

114. Summers, J., P.M. Smith, and A.L. Horwich, *Hepadnavirus envelope proteins regulate covalently closed circular DNA amplification.* J Virol, 1990. **64**(6): p. 2819-24.

115. Tuttleman, J.S., C. Pourcel, and J. Summers, *Formation of the pool of covalently closed circular viral DNA in hepadnavirus-infected cells.* Cell, 1986. **47**(3): p. 451-60.

116. Bruss, V., *Hepatitis B virus morphogenesis.* World journal of gastroenterology, 2007. **13**(1): p. 65-73.

117. Guo, J.T. and J.C. Pugh, *Topology of the large envelope protein of duck hepatitis B virus suggests a mechanism for membrane translocation during particle morphogenesis.* Journal of virology, 1997. **71**(2): p. 1107-1114.

118. Swameye, I. and H. Schaller, *Dual topology of the large envelope protein of duck hepatitis B virus: determinants preventing pre-S translocation and glycosylation.* Journal of virology, 1997. **71**(12): p. 9434-9441.

119. Bruss, V. and K. Vieluf, *Functions of the internal pre-S domain of the large surface protein in hepatitis B virus particle morphogenesis.* Journal of virology, 1995. **69**(11): p. 6652-6657.

120. Ostapchuk, P., P. Hearing, and D. Ganem, *A dramatic shift in the transmembrane topology of a viral envelope glycoprotein accompanies hepatitis B viral morphogenesis.* The EMBO journal, 1994. **13**(5): p. 1048-1057.

121. Bruss, V., et al., *Post-translational alterations in transmembrane topology of the hepatitis B virus large envelope protein.* The EMBO journal, 1994. **13**(10): p. 2273-2279.

122. Prange, R. and R.E. Streeck, *Novel transmembrane topology of the hepatitis B virus envelope proteins.* The EMBO journal, 1995. **14**(2): p. 247-256.

123. Huovila, A.P., A.M. Eder, and S.D. Fuller, *Hepatitis B surface antigen assembles in a post-ER, pre-Golgi compartment.* J Cell Biol, 1992. **118**(6): p. 1305-20.

124. Patzer, E.J., et al., *Intracellular assembly and packaging of hepatitis B surface antigen particles occur in the endoplasmic reticulum.* J Virol, 1986. **58**(3): p. 884-92.

125. Gerelsaikhan, T., J.E. Tavis, and V. Bruss, *Hepatitis B virus nucleocapsid envelopment does not occur without genomic DNA synthesis.* J Virol, 1996. **70**(7): p. 4269-74.

126. Yuan, T.T., et al., *The mechanism of an immature secretion phenotype of a highly frequent naturally occurring missense mutation at codon 97 of human hepatitis B virus core antigen.* J Virol, 1999. **73**(7): p. 5731-40.

127. Watanabe, T., et al., *Involvement of host cellular multivesicular body functions in hepatitis B virus budding.* Proc Natl Acad Sci U S A, 2007. **104**(24): p. 10205-10.

128. Patient, R., et al., *Hepatitis B virus subviral envelope particle morphogenesis and intracellular trafficking.* Journal of virology, 2007. **81**(8): p. 3842-3851.

129. Bruss, V. and D. Ganem, *The role of envelope proteins in hepatitis B virus assembly.* Proceedings of the National Academy of Sciences, 1991. **88**(3): p. 1059.

130. Kuroki, K., R. Russnak, and D. Ganem, *Novel N-terminal amino acid sequence required for retention of a hepatitis B virus glycoprotein in the endoplasmic reticulum.* Molecular and cellular biology, 1989. **9**(10): p. 4459-4466.

131. Gazina, E., A. Gallina, and G. Milanesi, *Common localization of retention determinants in hepatitis B virus L protein from different strains.* J Gen Virol, 1996. **77 (Pt 12)**: p. 3069-75.

132. Patient, R., C. Hourioux, and P. Roingeard, *Morphogenesis of hepatitis B virus and its subviral envelope particles.* Cellular microbiology, 2009. **11**(11): p. 1561-1570.

133. Lambert, C., T. Döring, and R. Prange, *Hepatitis B virus maturation is sensitive to functional inhibition of ESCRT-III, Vps4, and gamma 2-adaptin.* J Virol, 2007. **81**(17): p. 9050-60.

134. Hoffmann, J., et al., *Identification of α-taxilin as an essential factor for the life cycle of hepatitis B virus.* J Hepatol, 2013. **59**(5): p. 934-41.

135. Jiang, B., et al., *Subviral Hepatitis B Virus Filaments, like Infectious Viral Particles, Are Released via Multivesicular Bodies.* Journal of virology, 2015. **90**(7): p. 3330-3341.

136. Schmit, N., et al., *The global burden of chronic hepatitis B virus infection: comparison of country-level prevalence estimates from four research groups.* International Journal of Epidemiology, 2021. **50**(2): p. 560-569.

137. World Health, O., *Global hepatitis report 2017*. 2017, Geneva: World Health Organization.

138. Hou, J., Z. Liu, and F. Gu, *Epidemiology and Prevention of Hepatitis B Virus Infection.* International journal of medical sciences, 2005. **2**(1): p. 50-57.

139. Chen, C.J., L.Y. Wang, and M.W. Yu, *Epidemiology of hepatitis B virus infection in the Asia-Pacific region.* J Gastroenterol Hepatol, 2000. **15 Suppl**: p. E3-6.

140. Lavanchy, D., *Hepatitis B virus epidemiology, disease burden, treatment, and current and emerging prevention and control measures.* Journal of Viral Hepatitis, 2004. **11**(2): p. 97-107.

141. MacLachlan, J.H. and B.C. Cowie, *Hepatitis B virus epidemiology.* Cold Spring Harbor perspectives in medicine, 2015. **5**(5): p. a021410-a021410.

142. Velkov, S., et al., *The Global Hepatitis B Virus Genotype Distribution Approximated from Available Genotyping Data.* Genes, 2018. **9**(10): p. 495.

143. Gust, I.D., *Epidemiology of hepatitis B infection in the Western Pacific and South East Asia.* Gut, 1996. **38 Suppl 2**(Suppl 2): p. S18-23.

144. Allain, J.P., *Epidemiology of Hepatitis B virus and genotype.* J Clin Virol, 2006. **36 Suppl 1**: p. S12-7.

145. Sakamoto, T., et al., *Novel subtypes (subgenotypes) of hepatitis B virus genotypes B and C among chronic liver disease patients in the Philippines.* J Gen Virol, 2006. **87**(Pt 7): p. 1873-1882.

146. Biswas, A., et al., *Shift in the hepatitis B virus genotype distribution in the last decade among the HBV carriers from eastern India: possible effects on the disease status and HBV epidemiology.* J Med Virol, 2013. **85**(8): p. 1340-7.

147. Sunbul, M., *Hepatitis B virus genotypes: global distribution and clinical importance.* World journal of gastroenterology, 2014. **20**(18): p. 5427-5434.

148. Huang, C.C., et al., *One single nucleotide difference alters the differential expression of spliced RNAs between HBV genotypes A and D.* Virus Res, 2013. **174**(1-2): p. 18-26.

149. Chang, M.-H., *Hepatitis B virus infection.* Seminars in Fetal and Neonatal Medicine, 2007. **12**(3): p. 160-167.

150. Allain, J.P., et al., *Infectivity of blood products from donors with occult hepatitis B virus infection*, in *Transfusion*. 2013.

151. Glebe, D. and S. Urban, *Viral and cellular determinants involved in hepadnaviral entry.* World Journal of Gastroenterology : WJG, 2007. **13**(1): p. 22-38.

152. Grek, A. and L. Arasi, *Acute Liver Failure.* AACN Advanced Critical Care, 2016. **27**(4): p. 420-429.

153. Trepo, C. and L.c. Guillevin, *Polyarteritis Nodosa and Extrahepatic Manifestations of HBV Infection: The Case Against Autoimmune Intervention in Pathogenesis.* Journal of Autoimmunity, 2001. **16**(3): p. 269-274.

154. Dienstag, J.L., *Hepatitis B as an Immune Complex Disease.* Semin Liver Dis, 1981. **1**(01): p. 45-57.

155. Shiffman, M.L., *Management of Acute Hepatitis B.* Clinics in Liver Disease, 2010. **14**(1): p. 75-91.

156. Hoofnagle, J.H., et al., *Fulminant hepatic failure: Summary of a workshop.* Hepatology, 1995. **21**(1): p. 240-252.

157. Galbraith, R.M., et al., *Fulminant hepatic failure in leukaemia and choriocarcinoma related to withdrawal of cytotoxic drug therapy.* Lancet, 1975. **2**.

158. Liang, T.J., *Hepatitis B: The Virus and Disease.* Hepatology (Baltimore, Md.), 2009. **49**(5 Suppl): p. S13-S21.

159. Said, Z.N.A., *An overview of occult hepatitis B virus infection.* World Journal of Gastroenterology : WJG, 2011. **17**(15): p. 1927-1938.

160.   Hu, K.-Q., *Occult hepatitis B virus infection and its clinical implications.* Journal of Viral Hepatitis, 2002. **9**(4): p. 243-257.

161.   Conjeevaram, H.S. and A.S.-F. Lok, *Management of chronic hepatitis B.* Journal of Hepatology, 2003. **38**: p. 90-103.

162.   Seto, W.-K., et al., *Chronic hepatitis B virus infection.* The Lancet, 2018. **392**(10161): p. 2313-2324.

163.   Mangia, A., et al., *Pathogenesis of chronic liver disease in patients with chronic hepatitis B virus infection without serum HBeAg.* Digestive Diseases and Sciences, 1996. **41**(12): p. 2447-2452.

164.   Tang, L.S.Y., et al., *Chronic Hepatitis B Infection: A Review.* Jama, 2018. **319**(17): p. 1802-1813.

165.   Pramoolsinsup, C., *Management of viral hepatitis B.* Journal of Gastroenterology and Hepatology, 2002. **17**: p. S125-S145.

166.   *EASL 2017 Clinical Practice Guidelines on the management of hepatitis B virus infection.* J Hepatol, 2017. **67**(2): p. 370-398.

167.   Lok, A.S.F. and B.J. McMahon, *Chronic hepatitis B.* Hepatology, 2001. **34**(6): p. 1225-1241.

168.   Croagh, C.M.N. and J.S. Lubel, *Natural history of chronic hepatitis B: Phases in a complex relationship.* World Journal of Gastroenterology : WJG, 2014. **20**(30): p. 10395-10404.

169.   Lampertico, P., et al., *EASL 2017 Clinical Practice Guidelines on the management of hepatitis B virus infection.* Journal of Hepatology. **67**(2): p. 370-398.

170.   Pita, I., et al., *Hepatitis B inactive carriers: An overlooked population?* GE Portuguese Journal of Gastroenterology, 2014. **21**(6): p. 241-249.

171.   Netter, H.J., et al., *Hepatitis Delta Virus (HDV) and Delta-Like Agents: Insights Into Their Origin.* Frontiers in Microbiology, 2021. **12**(1448).

172.   Negro, F., *Hepatitis D virus coinfection and superinfection.* Cold Spring Harbor perspectives in medicine, 2014. **4**(11): p. a021550-a021550.

173.   Koh, C., B.L. Da, and J.S. Glenn, *HBV/HDV Coinfection: A Challenge for Therapeutics.* Clinics in liver disease, 2019. **23**(3): p. 557-572.

174.   Urban, S., C. Neumann-Haefelin, and P. Lampertico, *Hepatitis D virus in 2021: virology, immunology and new treatment approaches for a difficult-to-treat disease.* Gut, 2021. **70**(9): p. 1782.

175.   Peeling, R.W., et al., *The future of viral hepatitis testing: innovations in testing technologies and approaches.* BMC infectious diseases, 2017. **17**(Suppl 1): p. 699-699.

176.   Konstantinou, D. and M. Deutsch, *The spectrum of HBV/HCV coinfection: epidemiology, clinical characteristics, viralinteractions and management.* Annals of gastroenterology, 2015. **28**(2): p. 221-228.

177.   Shih, Y.-F. and C.-J. Liu, *Hepatitis C Virus and Hepatitis B Virus Co-Infection.* Viruses, 2020. **12**(7): p. 741.

178.   Mavilia, M.G. and G.Y. Wu, *HBV-HCV Coinfection: Viral Interactions, Management, and Viral Reactivation.* Journal of clinical and translational hepatology, 2018. **6**(3): p. 296-305.

179.   Singh, K.P., et al., *HIV-hepatitis B virus coinfection: epidemiology, pathogenesis, and treatment.* AIDS (London, England), 2017. **31**(15): p. 2035-2052.

180.   Dharel, N. and R.K. Sterling, *Hepatitis B Virus-HIV Coinfection: Forgotten but Not Gone.* Gastroenterology & hepatology, 2014. **10**(12): p. 780-788.

181.   Thibault, V., et al., *Performance of HBsAg quantification assays for detection of Hepatitis B virus genotypes and diagnostic escape-variants in clinical samples.* Journal of Clinical Virology, 2017. **89**: p. 14-21.

182. Lee , W.M., *Hepatitis B Virus Infection.* New England Journal of Medicine, 1997. **337**(24): p. 1733-1745.

183. Krajden, M., G. McNabb, and M. Petric, *The laboratory diagnosis of hepatitis B virus.* The Canadian Journal of Infectious Diseases & Medical Microbiology, 2005. **16**(2): p. 65-72.

184. Dienstag , J.L., *Hepatitis B Virus Infection.* New England Journal of Medicine, 2008. **359**(14): p. 1486-1500.

185. Tang, C.-M., T.O. Yau, and J. Yu, *Management of chronic hepatitis B infection: Current treatment guidelines, challenges, and new developments.* World Journal of Gastroenterology : WJG, 2014. **20**(20): p. 6262-6278.

186. Belloni, L., et al., *IFN-α inhibits HBV transcription and replication in cell culture and in humanized mice by targeting the epigenetic regulation of the nuclear cccDNA minichromosome.* The Journal of clinical investigation, 2012. **122**(2): p. 529-537.

187. Woo, A.S.J., R. Kwok, and T. Ahmed, *Alpha-interferon treatment in hepatitis B.* Annals of translational medicine, 2017. **5**(7): p. 159-159.

188. Tan, G., et al., *When Hepatitis B Virus Meets Interferons.* Frontiers in Microbiology, 2018. **9**(1611).

189. Taylor, J.L. and S.E. Grossberg, *The effects of interferon-alpha on the production and action of other cytokines.* Semin Oncol, 1998. **25**(1 Suppl 1): p. 23-9.

190. Xia, Y. and U. Protzer, *Control of Hepatitis B Virus by Cytokines.* Viruses, 2017. **9**(1): p. 18.

191. Yang, I., et al., *Modulation of major histocompatibility complex Class I molecules and major histocompatibility complex-bound immunogenic peptides induced by interferon-alpha and interferon-gamma treatment of human glioblastoma multiforme.* J Neurosurg, 2004. **100**(2): p. 310-9.

192. Fung, J., et al., *Nucleoside/nucleotide analogues in the treatment of chronic hepatitis B.* Journal of Antimicrobial Chemotherapy, 2011. **66**(12): p. 2715-2725.

193. Perrillo, R., *Benefits and risks of interferon therapy for hepatitis B.* Hepatology, 2009. **49**(S5): p. S103-S111.

194. *EASL clinical practice guidelines: Management of chronic hepatitis B virus infection.* J Hepatol, 2012. **57**(1): p. 167-85.

195. Lok, A.S. and B.J. McMahon, *Chronic hepatitis B: update 2009.* Hepatology, 2009. **50**(3): p. 661-2.

196. Jardi, R., et al., *Hepatitis B virus polymerase variants associated with entecavir drug resistance in treatment-naive patients.* Journal of Viral Hepatitis, 2007. **14**(12): p. 835-840.

197. Zhang, X., et al., *Potential resistant mutations within HBV reverse transcriptase sequences in nucleos(t)ide analogues-experienced patients with hepatitis B virus infection.* Scientific Reports, 2019. **9**(1): p. 8078.

198. Choi, Y.M., S.Y. Lee, and B.J. Kim, *Naturally occurring hepatitis B virus reverse transcriptase mutations related to potential antiviral drug resistance and liver disease progression.* World J Gastroenterol, 2018. **24**(16): p. 1708-1724.

199. Pacheco, S.R., et al., *Genotyping of HBV and tracking of resistance mutations in treatment-naïve patients with chronic hepatitis B.* Infection and drug resistance, 2017. **10**: p. 201-207.

200. Soriano, V., et al., *Advances in hepatitis B therapeutics.* Therapeutic Advances in Infectious Disease, 2020. **7**: p. 2049936120965027.

201. Loglio, A., et al., *Excellent safety and effectiveness of high-dose myrcludex-B monotherapy administered for 48 weeks in HDV-related compensated cirrhosis: A case report of 3 patients.* J Hepatol, 2019. **71**(4): p. 834-839.

202. Cheng, D., et al., *Clinical effects of NTCP-inhibitor myrcludex B.* Journal of Viral Hepatitis, 2021. **28**(6): p. 852-858.

203. Schinazi, R.F., et al., *Towards HBV curative therapies.* Liver international : official journal of the International Association for the Study of the Liver, 2018. **38 Suppl 1**(Suppl 1): p. 102-114.

204. Kim, W.R., *Emerging Therapies Toward a Functional Cure for Hepatitis B Virus Infection.* Gastroenterology & hepatology, 2018. **14**(7): p. 439-442.

205. World Health, O., *Hepatitis B vaccines: WHO position paper, July 2017 – Recommendations.* Vaccine, 2019. **37**(2): p. 223-225.

206. Galle, P.R., et al., *In vitro experimental infection of primary human hepatocytes with hepatitis B virus.* Gastroenterology, 1994. **106**(3): p. 664-673.

207. Hu, J., et al., *Cell and Animal Models for Studying Hepatitis B Virus Infection and Drug Development.* Gastroenterology, 2019. **156**(2): p. 338-354.

208. Shlomai, A., et al., *Modeling host interactions with hepatitis B virus using primary and induced pluripotent stem cell-derived hepatocellular systems.* Proceedings of the National Academy of Sciences of the United States of America, 2014. **111**(33): p. 12193-12198.

209. Rijntjes, P.J., H.J. Moshage, and S.H. Yap, *In vitro infection of primary cultures of cryopreserved adult human hepatocytes with hepatitis B virus.* Virus Res, 1988. **10**(1): p. 95-109.

210. Gripon, P., et al., *Hepatitis B virus infection of adult human hepatocytes cultured in the presence of dimethyl sulfoxide.* Journal of virology, 1988. **62**(11): p. 4136-4143.

211. Godoy, P., et al., *Recent advances in 2D and 3D in vitro systems using primary hepatocytes, alternative hepatocyte sources and non-parenchymal liver cells and their use in investigating mechanisms of hepatotoxicity, cell signaling and ADME.* Archives of Toxicology, 2013. **87**(8): p. 1315-1530.

212. Glebe, D., et al., *Pre-S1 antigen-dependent infection of Tupaia hepatocyte cultures with human hepatitis B virus.* Journal of Virology, 2003. **77**(17): p. 9511-9521.

213. Hantz, O., et al., *Persistence of the hepatitis B virus covalently closed circular DNA in HepaRG human hepatocyte-like cells.* J Gen Virol, 2009. **90**(Pt 1): p. 127-35.

214. Schulze, A., P. Gripon, and S. Urban, *Hepatitis B virus infection initiates with a large surface protein–dependent binding to heparan sulfate proteoglycans.* Hepatology, 2007. **46**(6): p. 1759-1768.

215. Shen, F., et al., *Hepatitis B virus sensitivity to interferon-α in hepatocytes is more associated with cellular interferon response than with viral genotype.* Hepatology, 2018. **67**(4): p. 1237-1252.

216. Luangsay, S., et al., *Early inhibition of hepatocyte innate responses by hepatitis B virus.* Journal of Hepatology, 2015. **63**(6): p. 1314-1322.

217. Qiu, G.-H., et al., *Distinctive pharmacological differences between liver cancer cell lines HepG2 and Hep3B.* Cytotechnology, 2015. **67**(1): p. 1-12.

218. Acs, G., et al., *Hepatitis B virus produced by transfected Hep G2 cells causes hepatitis in chimpanzees.* Proceedings of the National Academy of Sciences of the United States of America, 1987. **84**(13): p. 4641-4644.

219. Sureau, C., et al., *Production of hepatitis B virus by a differentiated human hepatoma cell line after transfection with cloned circular HBV DNA.* Cell, 1986. **47**(1): p. 37-47.

220. Ladner, S.K., et al., *Inducible expression of human hepatitis B virus (HBV) in stably transfected hepatoblastoma cells: a novel system for screening potential*

inhibitors of HBV replication. Antimicrob Agents Chemother, 1997. **41**(8): p. 1715-20.

221.   Glebe, D., et al., *Optimised conditions for the production of hepatitis B virus from cell culture.* Intervirology, 2001. **44**(6): p. 370-378.

222.   Tsurimoto, T., A. Fujiyama, and K. Matsubara, *Stable expression and replication of hepatitis B virus genome in an integrated state in a human hepatoma cell line transfected with the cloned viral DNA.* Proceedings of the National Academy of Sciences of the United States of America, 1987. **84**(2): p. 444-448.

223.   Meredith, L.W., et al., *Lentiviral hepatitis B pseudotype entry requires sodium taurocholate co-transporting polypeptide and additional hepatocyte-specific factors.* The Journal of general virology, 2016. **97**(1): p. 121-127.

224.   Luo, J., et al., *Identification of an Intermediate in Hepatitis B Virus Covalently Closed Circular (CCC) DNA Formation and Sensitive and Selective CCC DNA Detection.* Journal of virology, 2017. **91**(17): p. e00539-17.

225.   Long, Q., et al., *The role of host DNA ligases in hepadnavirus covalently closed circular DNA formation.* PLoS pathogens, 2017. **13**(12): p. e1006784-e1006784.

226.   Nkongolo, S., et al., *Cyclosporin A inhibits hepatitis B and hepatitis D virus entry by cyclophilin-independent interference with the NTCP receptor.* J Hepatol, 2014. **60**(4): p. 723-31.

227.   Verrier, E.R., et al., *A targeted functional RNA interference screen uncovers glypican 5 as an entry factor for hepatitis B and D viruses.* Hepatology, 2016. **63**(1): p. 35-48.

228.   Michailidis, E., et al., *A robust cell culture system supporting the complete life cycle of hepatitis B virus.* Sci Rep, 2017. **7**(1): p. 16616.

229.   Yan, R., et al., *Spinoculation Enhances HBV Infection in NTCP-Reconstituted Hepatocytes.* PloS one, 2015. **10**(6): p. e0129889-e0129889.

230.   King, B., et al., *Troubleshooting methods for the generation of novel pseudotyped viruses.* Future Virology, 2016.

231.   Sanders, D.A., *No false start for novel pseudotyped vectors.* Current Opinion in Biotechnology, 2002. **13**(5): p. 437-442.

232.   Hanafusa, H., T. Hanafusa, and H. Rubin, *The defectiveness of Rous sarcoma virus.* Proceedings of the National Academy of Sciences of the United States of America, 1963. **49**(4): p. 572-580.

233.   Rous, P., *A SARCOMA OF THE FOWL TRANSMISSIBLE BY AN AGENT SEPARABLE FROM THE TUMOR CELLS.* The Journal of experimental medicine, 1911. **13**(4): p. 397-411.

234.   Rubin, H., *Genetic control of cellular susceptibility to pseudotypes of rous sarcoma virus.* Virology, 1965. **26**(2): p. 270-276.

235.   Lortal, B., et al., *Preclinical study of an ex vivo gene therapy protocol for hepatocarcinoma.* Cancer Gene Therapy, 2009. **16**(4): p. 329-337.

236.   Chen, T.-L., et al., *Highly Effective <i>Ex Vivo</i> Gene Manipulation to Study Kidney Development Using Self-Complementary Adenoassociated Viruses.* The Scientific World Journal, 2014. **2014**: p. 682189.

237.   Corti, D., et al., *Prophylactic and postexposure efficacy of a potent human monoclonal antibody against MERS coronavirus.* Proc Natl Acad Sci U S A, 2015. **112**(33): p. 10473-8.

238.   Qian, Z., S.R. Dominguez, and K.V. Holmes, *Role of the Spike Glycoprotein of Human Middle East Respiratory Syndrome Coronavirus (MERS-CoV) in Virus Entry and Syncytia Formation.* PLOS ONE, 2013. **8**(10): p. e76469.

239.   Zhao, G., et al., *A safe and convenient pseudovirus-based inhibition assay to detect neutralizing antibodies and screen for viral entry inhibitors against the novel human coronavirus MERS-CoV.* Virology Journal, 2013. **10**(1): p. 266.

240. Perera, R.A., et al., *Seroepidemiology for MERS coronavirus using microneutralisation and pseudoparticle virus neutralisation assays reveal a high prevalence of antibody in dromedary camels in Egypt, June 2013.* Euro Surveill, 2013. **18**(36): p. pii=20574.
241. Long, J., et al., *Antiviral therapies against Ebola and other emerging viral diseases using existing medicines that block virus entry*. 2015, F1000Res.
242. Côté, M., et al., *Small molecule inhibitors reveal Niemann-Pick C1 is essential for Ebola virus infection.* Nature, 2011. **477**(7364): p. 344-8.
243. Basu, A., et al., *Novel Small Molecule Entry Inhibitors of Ebola Virus.* J Infect Dis, 2015. **212 Suppl 2**(Suppl 2): p. S425-34.
244. Urbanowicz, R.A., et al., *Human Adaptation of Ebola Virus during the West African Outbreak.* Cell, 2016. **167**(4): p. 1079-1087.e5.
245. Lavillette, D., et al., *Characterization of host-range and cell entry properties of the major genotypes and subtypes of hepatitis C virus.* Hepatology, 2005. **41**(2): p. 265-74.
246. Tarr, A.W., et al., *Characterization of the hepatitis C virus E2 epitope defined by the broadly neutralizing monoclonal antibody AP33.* Hepatology, 2006. **43**(3): p. 592-601.
247. Urbanowicz, R.A., et al., *Novel functional hepatitis C virus glycoprotein isolates identified using an optimized viral pseudotype entry assay.* J Gen Virol, 2016. **97**(9): p. 2265-2279.
248. Zheng, A., et al., *Claudin-6 and claudin-9 function as additional coreceptors for hepatitis C virus.* J Virol, 2007. **81**(22): p. 12465-71.
249. Bartosch, B., et al., *Cell entry of hepatitis C virus requires a set of co-receptors that include the CD81 tetraspanin and the SR-B1 scavenger receptor.* J Biol Chem, 2003. **278**(43): p. 41624-30.
250. Evans, M.J., et al., *Claudin-1 is a hepatitis C virus co-receptor required for a late step in entry.* Nature, 2007. **446**(7137): p. 801-805.
251. Carman, W.F., et al., *Vaccine-induced escape mutant of hepatitis B virus.* Lancet, 1990. **336**(8711): p. 325-9.
252. Kuang, S.Y., et al., *Specific mutations of hepatitis B virus in plasma predict liver cancer development.* Proc Natl Acad Sci U S A, 2004. **101**(10): p. 3575-80.
253. Chan, H.L., M. Hussain, and A.S. Lok, *Different hepatitis B virus genotypes are associated with different mutations in the core promoter and precore regions during hepatitis B e antigen seroconversion.* Hepatology, 1999. **29**(3): p. 976-84.
254. Friedt, M., et al., *Mutations in the basic core promotor and the precore region of hepatitis B virus and their selection in children with fulminant and chronic hepatitis B.* Hepatology, 1999. **29**(4): p. 1252-8.
255. Aritomi, T., et al., *Association of mutations in the core promoter and precore region of hepatitis virus with fulminant and severe acute hepatitis in Japan.* J Gastroenterol Hepatol, 1998. **13**(11): p. 1125-32.
256. Nishizono, A., et al., *Mutations in the Core Promoter/Enhancer II Regions of Naturally Occurring Hepatitis B Virus Variants and Analysis of the Effects on Transcription Activities.* Intervirology, 1995. **38**(5): p. 290-294.
257. Takahashi, K., et al., *The precore/core promoter mutant (T1762A1764) of hepatitis B virus: clinical significance and an easy method for detection.* J Gen Virol, 1995. **76 (Pt 12)**: p. 3159-64.
258. Günther, S., et al., *Naturally occurring variants of hepatitis B virus.* Adv Virus Res, 1999. **52**: p. 25-137.
259. Angus, P., et al., *Resistance to adefovir dipivoxil therapy associated with the selection of a novel mutation in the HBV polymerase.* Gastroenterology, 2003. **125**(2): p. 292-7.

260. Delaney, W.E.t., et al., *The hepatitis B virus polymerase mutation rtV173L is selected during lamivudine therapy and enhances viral replication in vitro.* J Virol, 2003. **77**(21): p. 11833-41.

261. Das, K., et al., *Molecular modeling and biochemical characterization reveal the mechanism of hepatitis B virus polymerase resistance to lamivudine (3TC) and emtricitabine (FTC).* J Virol, 2001. **75**(10): p. 4771-9.

262. Lok, A.S., et al., *Monitoring drug resistance in chronic hepatitis B virus (HBV)-infected patients during lamivudine therapy: evaluation of performance of INNO-LiPA HBV DR assay.* J Clin Microbiol, 2002. **40**(10): p. 3729-34.

263. Stuyver, L.J., et al., *Nomenclature for antiviral-resistant human hepatitis B virus mutations in the polymerase region.* Hepatology, 2001. **33**(3): p. 751-7.

264. Datta, S., et al., *Analysis of hepatitis B virus X gene phylogeny, genetic variability and its impact on pathogenesis: implications in Eastern Indian HBV carriers.* Virology, 2008. **382**(2): p. 190-8.

265. Chong-Jin, O., et al., *Identification of hepatitis B surface antigen variants with alterations outside the "a" determinant in immunized Singapore infants.* J Infect Dis, 1999. **179**(1): p. 259-63.

266. Moerman, B., et al., *Evaluation of sensitivity for wild type and mutant forms of hepatitis B surface antigen by four commercial HBsAg assays.* Clin Lab, 2004. **50**(3-4): p. 159-62.

267. Coleman, P.F., Y.C. Chen, and I.K. Mushahwar, *Immunoassay detection of hepatitis B surface antigen mutants.* J Med Virol, 1999. **59**(1): p. 19-24.

268. Seddigh-Tonekaboni, S., et al., *Hepatitis B surface antigen variants in vaccinees, blood donors and an interferon-treated patient.* J Viral Hepat, 2001. **8**(2): p. 154-8.

269. Hsu, H.Y., et al., *Changes of hepatitis B surface antigen variants in carrier children before and after universal vaccination in Taiwan.* Hepatology, 1999. **30**(5): p. 1312-7.

270. Zuckerman, J.N. and A.J. Zuckerman, *Mutations of the surface protein of hepatitis B virus.* Antiviral Res, 2003. **60**(2): p. 75-8.

271. Salpini, R., et al., *Hepatitis B surface antigen genetic elements critical for immune escape correlate with hepatitis B virus reactivation upon immunosuppression.* Hepatology, 2015. **61**(3): p. 823-33.

272. Cassini, R., et al., *A novel stop codon mutation within the hepatitis B surface gene is detected in the liver but not in the peripheral blood mononuclear cells of HIV-infected individuals with occult HBV infection.* J Viral Hepat, 2013. **20**(1): p. 42-9.

273. Jaramillo, C.M. and M.-C. Navas, *Variantes de escape del virus de la hepatitis B.* Revista chilena de infectología, 2015. **32**: p. 190-197.

274. Su, I.J., et al., *Ground glass hepatocytes contain pre-S mutants and represent preneoplastic lesions in chronic hepatitis B virus infection.* J Gastroenterol Hepatol, 2008. **23**(8 Pt 1): p. 1169-74.

275. He, C., et al., *Prevalence of vaccine-induced escape mutants of hepatitis B virus in the adult population in China: a prospective study in 176 restaurant employees.* J Gastroenterol Hepatol, 2001. **16**(12): p. 1373-7.

276. Ngui, S.L., et al., *Low detection rate and maternal provenance of hepatitis B virus S gene mutants in cases of failed postnatal immunoprophylaxis in England and Wales.* J Infect Dis, 1997. **176**(5): p. 1360-5.

277. Lee, K.M., et al., *Emergence of vaccine-induced escape mutant of hepatitis B virus with multiple surface gene mutations in a Korean child.* J Korean Med Sci, 2001. **16**(3): p. 359-62.

278. Lee, S.-A., et al., *Male-specific W4P/R mutation in the pre-S1 region of hepatitis B virus, increasing the risk of progression of liver diseases in chronic patients.* Journal of clinical microbiology, 2013. **51**(12): p. 3928-3936.

279. Biswas, S., D. Candotti, and J.-P. Allain, *Specific Amino Acid Substitutions in the S Protein Prevent Its Excretion In Vitro and May Contribute to Occult Hepatitis B Virus Infection.* Journal of Virology, 2013. **87**(14): p. 7882-7892.

280. Waters, J.A., et al., *Loss of the common "A" determinant of hepatitis B surface antigen by a vaccine-induced escape mutant.* J Clin Invest, 1992. **90**(6): p. 2543-7.

281. Weinberger, K.M., et al., *High genetic variability of the group-specific a-determinant of hepatitis B virus surface antigen (HBsAg) and the corresponding fragment of the viral polymerase in chronic virus carriers lacking detectable HBsAg in serum.* J Gen Virol, 2000. **81**(Pt 5): p. 1165-74.

282. Karthigesu, V.D., et al., *A novel hepatitis B virus variant in the sera of immunized children.* J Gen Virol, 1994. **75 (Pt 2)**: p. 443-8.

283. Harrison, T.J., et al., *Independent emergence of a vaccine-induced escape mutant of hepatitis B virus.* J Hepatol, 1991. **13 Suppl 4**: p. S105-7.

284. Salpini, R., et al., *Novel HBsAg mutations correlate with hepatocellular carcinoma, hamper HBsAg secretion and promote cell proliferation in vitro.* Oncotarget, 2017. **8**(9): p. 15704-15715.

285. Bi, X. and S. Tong, *Impact of immune escape mutations and N-linked glycosylation on the secretion of hepatitis B virus virions and subviral particles: Role of the small envelope protein.* Virology, 2018. **518**: p. 358-368.

286. Herrscher, C., et al., *Hepatitis B virus entry into HepG2-NTCP cells requires clathrin-mediated endocytosis.* Cellular Microbiology, 2020. **22**(8): p. e13205.

287. Herrscher, C., P. Roingeard, and E. Blanchard, *Hepatitis B Virus Entry into Cells.* Cells, 2020. **9**(6): p. 1486.

288. Shiffman, M.L., *Management of acute hepatitis B.* Clin Liver Dis, 2010. **14**(1): p. 75-91; viii-ix.

289. Schaefer, S., *Hepatitis B virus taxonomy and hepatitis B virus genotypes.* World J Gastroenterol, 2007. **13**(1): p. 14-21.

290. Ono-Nita, S.K., et al., *YMDD motif in hepatitis B virus DNA polymerase influences on replication and lamivudine resistance: A study by in vitro full-length viral DNA transfection.* Hepatology, 1999. **29**(3): p. 939-45.

291. Jones, S.A. and J. Hu, *Hepatitis B virus reverse transcriptase: diverse functions as classical and emerging targets for antiviral intervention.* Emerging Microbes & Infections, 2013. **2**(1): p. 1-11.

292. Girones, R. and R.H. Miller, *Mutation rate of the hepadnavirus genome.* Virology, 1989. **170**(2): p. 595-7.

293. Orito, E., et al., *Host-independent evolution and a genetic classification of the hepadnavirus family based on nucleotide sequences.* Proceedings of the National Academy of Sciences of the United States of America, 1989. **86**(18): p. 7059-7062.

294. Buti, M., et al., *Hepatitis B virus genome variability and disease progression: the impact of pre-core mutants and HBV genotypes.* Journal of Clinical Virology, 2005. **34**: p. S79-S82.

295. Osiowy, C., et al., *Molecular Evolution of Hepatitis B Virus over 25 Years.* Journal of Virology, 2006. **80**(21): p. 10307-10314.

296. Massey, S.E., et al., *Characterizing positive and negative selection and their phylogenetic effects.* Gene, 2008. **418**(1): p. 22-26.

297. Sheldon, J., et al., *Selection of hepatitis B virus polymerase mutations in HIV-coinfected patients treated with tenofovir.* Antivir Ther, 2005. **10**(6): p. 727-34.

298. Sheldon, J., et al., *Selection of Hepatitis B Virus (HBV) Vaccine Escape Mutants in HBV-Infected and HBV/HIV-Coinfected Patients Failing Antiretroviral Drugs With Anti-HBV Activity.* JAIDS Journal of Acquired Immune Deficiency Syndromes, 2007. **46**(3).

299. Sheldon, J., et al., *Mutations affecting the replication capacity of the hepatitis B virus.* J Viral Hepat, 2006. **13**(7): p. 427-34.

300. Hosseini, S.Y., et al., *Association of HBsAg mutation patterns with hepatitis B infection outcome: Asymptomatic carriers versus HCC/cirrhotic patients.* Annals of Hepatology, 2019. **18**(4): p. 640-645.

301. Kumar, S., G. Stecher, and K. Tamura, *MEGA7: Molecular Evolutionary Genetics Analysis Version 7.0 for Bigger Datasets.* Mol Biol Evol, 2016. **33**(7): p. 1870-4.

302. McNaughton, A.L., et al., *Analysis of genomic-length HBV sequences to determine genotype and subgenotype reference sequences.* The Journal of general virology, 2020. **101**(3): p. 271-283.

303. Hall, T. *BIOEDIT: A USER-FRIENDLY BIOLOGICAL SEQUENCE ALIGNMENT EDITOR AND ANALYSIS PROGRAM FOR WINDOWS 95/98/ NT*. 1999.

304. Yao, Q.Q., et al., *Hepatitis B virus surface antigen (HBsAg)-positive and HBsAg-negative hepatitis B virus infection among mother-teenager pairs 13 years after neonatal hepatitis B virus vaccination.* Clin Vaccine Immunol, 2013. **20**(2): p. 269-75.

305. Olinger, C.M., et al., *Hepatitis B virus genotype E surface antigen detection with different immunoassays and diagnostic impact of mutations in the preS/S gene.* Medical Microbiology and Immunology, 2007. **196**(4): p. 247-252.

306. Dunford, L., et al., *A multicentre molecular analysis of hepatitis B and blood-borne virus coinfections in Viet Nam.* PLoS One, 2012. **7**(6): p. e39027.

307. Darmawan, E., et al., *Seroepidemiology and occult hepatitis B virus infection in young adults in Banjarmasin, Indonesia.* J Med Virol, 2015. **87**(2): p. 199-207.

308. Colagrossi, L., et al., *Immune-escape mutations and stop-codons in HBsAg develop in a large proportion of patients with chronic HBV infection exposed to anti-HBV drugs in Europe.* BMC Infectious Diseases, 2018. **18**(1): p. 251.

309. Ababneh, N.A., et al., *Patterns of hepatitis B virus S gene escape mutants and reverse transcriptase mutations among genotype D isolates in Jordan.* PeerJ, 2019. **7**: p. e6583-e6583.

310. Abdelnabi, Z., et al., *Subgenotypes and mutations in the s and polymerase genes of hepatitis B virus carriers in the West Bank, palestine.* PloS one, 2014. **9**(12): p. e113821-e113821.

311. Anastasiou, O.E., et al., *Clinical and Virological Aspects of HBV Reactivation: A Focus on Acute Liver Failure.* Viruses, 2019. **11**(9): p. 863.

312. Gomes-Gouvêa, M.S., et al., *HBV carrying drug-resistance mutations in chronically infected treatment-naive patients.* Antivir Ther, 2015. **20**(4): p. 387-95.

313. Salpini, R., et al., *Characterization of drug-resistance mutations in HBV D-genotype chronically infected patients, naïve to antiviral drugs.* Antiviral Res, 2011. **92**(2): p. 382-5.

314. Huang, C.J., et al., *Impact of genetic heterogeneity in polymerase of hepatitis B virus on dynamics of viral load and hepatitis B progression.* PLoS One, 2013. **8**(7): p. e70169.

315. Yamani, L.N., et al., *Profile of Mutations in the Reverse Transcriptase and Overlapping Surface Genes of Hepatitis B Virus (HBV) in Treatment-Naïve Indonesian HBV Carriers.* Jpn J Infect Dis, 2017. **70**(6): p. 647-655.

316. Zhang, X., et al., *Pre-existing mutations related to tenofovir in chronic hepatitis B patients with long-term nucleos(t)ide analogue drugs treatment by ultra-deep pyrosequencing.* Oncotarget, 2016. **7**(43): p. 70264-70275.

317. Singla, B., et al., *Hepatitis B virus reverse transcriptase mutations in treatment Naïve chronic hepatitis B patients.* Journal of Medical Virology, 2013. **85**(7): p. 1155-1162.

318. Kim, J.H., et al., *Molecular diagnosis and treatment of drug-resistant hepatitis B virus.* World J Gastroenterol, 2014. **20**(19): p. 5708-20.

319. Nowak, M.A., et al., *Viral dynamics in hepatitis B virus infection.* Proc Natl Acad Sci U S A, 1996. **93**(9): p. 4398-402.

320. Kramvis, A., *Genotypes and genetic variability of hepatitis B virus.* Intervirology, 2014. **57**(3-4): p. 141-50.

321. Lago, B.V., et al., *Hepatitis B Virus Subgenotype A1: Evolutionary Relationships between Brazilian, African and Asian Isolates.* PLOS ONE, 2014. **9**(8): p. e105317.

322. Sugauchi, F., et al., *Epidemiological and sequence differences between two subtypes (Ae and Aa) of hepatitis B virus genotype A.* Journal of General Virology, 2004. **85**(4): p. 811-820.

323. Sharma, S., et al., *Clinical significance of genotypes and precore/basal core promoter mutations in HBV related chronic liver disease patients in North India.* Dig Dis Sci, 2010. **55**(3): p. 794-802.

324. Fan, Y.F., et al., *Prevalence and significance of hepatitis B virus (HBV) pre-S mutants in serum and liver at different replicative stages of chronic HBV infection.* Hepatology, 2001. **33**(1): p. 277-86.

325. Sugauchi, F., et al., *Influence of hepatitis B virus genotypes on the development of preS deletions and advanced liver disease.* J Med Virol, 2003. **70**(4): p. 537-44.

326. Kao, J.H., et al., *Hepatitis B virus genotypes and spontaneous hepatitis B e antigen seroconversion in Taiwanese hepatitis B carriers.* J Med Virol, 2004. **72**(3): p. 363-9.

327. Chu, C.J., M. Hussain, and A.S. Lok, *Hepatitis B virus genotype B is associated with earlier HBeAg seroconversion compared with hepatitis B virus genotype C.* Gastroenterology, 2002. **122**(7): p. 1756-62.

328. Kao, J.H., et al., *Hepatitis B genotypes and the response to interferon therapy.* J Hepatol, 2000. **33**(6): p. 998-1002.

329. Shi, Y.H., *Correlation between hepatitis B virus genotypes and clinical outcomes.* Jpn J Infect Dis, 2012. **65**(6): p. 476-82.

330. Malmström, S., et al., *Genotype impact on long-term virological outcome of chronic hepatitis B virus infection.* J Clin Virol, 2012. **54**(4): p. 321-6.

331. Xiao, Y., et al., *Quasispecies characteristic in "a" determinant region is a potential predictor for the risk of immunoprophylaxis failure of mother-to-child-transmission of sub-genotype C2 hepatitis B virus: a prospective nested case–control study.* Gut, 2020. **69**(5): p. 933.

332. Cao, L., et al., *Coexistence of hepatitis B virus quasispecies enhances viral replication and the ability to induce host antibody and cellular immune responses.* Journal of virology, 2014. **88**(15): p. 8656-8666.

333. Zhou, T.-C., et al., *Evolution of full-length genomes of HBV quasispecies in sera of patients with a coexistence of HBsAg and anti-HBs antibodies.* Scientific reports, 2017. **7**(1): p. 661-661.

334. Cortese, M.F., et al., *Sophisticated viral quasispecies with a genotype-related pattern of mutations in the hepatitis B X gene of HBeAg-ve chronically infected patients.* Scientific Reports, 2021. **11**(1): p. 4215.

335. Nishijima, N., et al., *Dynamics of Hepatitis B Virus Quasispecies in Association with Nucleos(t)ide Analogue Treatment Determined by Ultra-Deep Sequencing.* PLOS ONE, 2012. **7**(4): p. e35052.

336. Liang, Y., et al., *Early changes in quasispecies variant after antiviral therapy for chronic hepatitis B.* Mol Med Rep, 2018. **17**(4): p. 5528-5537.

337. Sloan, R., et al., *Genotyping of acute HBV isolates from England, 1997-2001.* Journal of Clinical Virology, 2009. **44**: p. 157-60.

338. Tedder, R.S., et al., *The Diversity and Management of Chronic Hepatitis B Virus Infections in the United Kingdom: A Wake-up Call.* Clinical Infectious Diseases, 2013. **56**(7): p. 951-960.

339. Chong-Jin, O., et al., *Identification of Hepatitis B Surface Antigen Variants with Alterations outside the "a" Determinant in Immunized Singapore Infants.* The Journal of Infectious Diseases, 1999. **179**(1): p. 259-263.

340. Harris, B.J., et al., *Hepatitis B genotypes and surface antigen mutants present in Pakistani blood donors.* PLOS ONE, 2017. **12**(6): p. e0178988.

341. Ko, K., et al., *Existence of hepatitis B virus surface protein mutations and other variants: demand for hepatitis B infection control in Cambodia.* BMC Infectious Diseases, 2020. **20**(1): p. 305.

342. Hu, A.-q., et al., *Overt and occult hepatitis B infection after neonatal vaccination: mother-to-infant transmission and HBV vaccine effectiveness.* International Journal of Infectious Diseases, 2021. **104**: p. 601-609.

343. Kim, J.H., et al., *Hepatitis B viral surface mutations in patients with adefovir resistant chronic hepatitis B with A181T/V polymerase mutations.* Journal of Korean medical science, 2010. **25**(2): p. 257-264.

344. Mangold, C.M., et al., *Analysis of intermolecular disulfide bonds and free sulfhydryl groups in hepatitis B surface antigen particles.* Arch Virol, 1997. **142**(11): p. 2257-67.

345. Shaw, T., A. Bartholomeusz, and S. Locarnini, *HBV drug resistance: Mechanisms, detection and interpretation.* Journal of Hepatology, 2006. **44**(3): p. 593-606.

346. Xiang, K.-H., et al., *Effects of amino acid substitutions in hepatitis B virus surface protein on virion secretion, antigenicity, HBsAg and viral DNA.* Journal of hepatology, 2017. **66**(2): p. 288-296.

347. Ito, K., et al., *Impairment of hepatitis B virus virion secretion by single-amino-acid substitutions in the small envelope protein and rescue by a novel glycosylation site.* J Virol, 2010. **84**(24): p. 12850-61.

348. Steffen, I. and G. Simmons, *Pseudotyping Viral Vectors With Emerging Virus Envelope Proteins.* Curr Gene Ther, 2016. **16**(1): p. 47-55.

349. Duvergé, A. and M. Negroni, *Pseudotyping Lentiviral Vectors: When the Clothes Make the Virus.* Viruses, 2020. **12**(11).

350. Bentley, E.M., S.T. Mather, and N.J. Temperton, *The use of pseudotypes to study viruses, virus sero-epidemiology and vaccination.* Vaccine, 2015. **33**(26): p. 2955-2962.

351. Cronin, J., X.-Y. Zhang, and J. Reiser, *Altering the tropism of lentiviral vectors through pseudotyping.* Current gene therapy, 2005. **5**(4): p. 387-398.

352. Merten, O.W., et al., *Large-scale manufacture and characterization of a lentiviral vector produced for clinical ex vivo gene therapy application.* Hum Gene Ther, 2011. **22**(3): p. 343-56.

353. Merten, O.-W., M. Hebben, and C. Bovolenta, *Production of lentiviral vectors.* Molecular therapy. Methods & clinical development, 2016. **3**: p. 16017-16017.

354. Butel, J.S., *SV40 large T-antigen: dual oncogene.* Cancer Surv, 1986. **5**(2): p. 343-65.

355. Gama-Norton, L., et al., *Lentivirus production is influenced by SV40 large T-antigen and chromosomal integration of the vector in HEK293 cells.* Hum Gene Ther, 2011. **22**(10): p. 1269-79.

356. Sinn, P.L., et al., *Lentiviral Vectors Pseudotyped with Filoviral Glycoproteins.* Methods in molecular biology (Clifton, N.J.), 2017. **1628**: p. 65-78.

357. Bofinger, R., et al., *Development of lipopolyplexes for gene delivery: A comparison of the effects of differing modes of targeting peptide display on the structure and transfection activities of lipopolyplexes.* Journal of Peptide Science, 2018. **24**(12): p. e3131.

358. Pirona, A.C., et al., *Process for an efficient lentiviral cell transduction.* Biology methods & protocols, 2020. **5**(1): p. bpaa005-bpaa005.

359. Mali, S., *Delivery systems for gene therapy.* Indian J Hum Genet, 2013. **19**(1): p. 3-8.

360. Valetti, S., et al., *Rational design for multifunctional non-liposomal lipid-based nanocarriers for cancer management: theory to practice.* J Nanobiotechnology, 2013. **11 Suppl 1**(Suppl 1): p. S6.

361. Guo, L., et al., *Optimizing conditions for calcium phosphate mediated transient transfection.* Saudi J Biol Sci, 2017. **24**(3): p. 622-629.

362. Kim, T.K. and J.H. Eberwine, *Mammalian cell transfection: the present and the future.* Anal Bioanal Chem, 2010. **397**(8): p. 3173-8.

363. De Niz, M., et al., *An ultrasensitive NanoLuc-based luminescence system for monitoring Plasmodium berghei throughout its life cycle.* Malaria Journal, 2016. **15**(1): p. 232.

364. Loh, J.M.S. and T. Proft, *Comparison of firefly luciferase and NanoLuc luciferase for biophotonic labeling of group A Streptococcus.* Biotechnology Letters, 2014. **36**(4): p. 829-834.

365. Hall, M.P., et al., *Engineered Luciferase Reporter from a Deep Sea Shrimp Utilizing a Novel Imidazopyrazinone Substrate.* ACS Chemical Biology, 2012. **7**(11): p. 1848-1857.

366. Siegert, S., et al., *Assessment of HIV-1 entry inhibitors by MLV/HIV-1 pseudotyped vectors.* AIDS Research and Therapy, 2005. **2**(1): p. 7.

367. Steeds, K., et al., *Pseudotyping of VSV with Ebola virus glycoprotein is superior to HIV-1 for the assessment of neutralising antibodies.* Scientific Reports, 2020. **10**(1): p. 14289.

368. Yu, H. and Y.J. Kwon, *Preparation and quantification of pseudotyped retroviral vector.* Methods Mol Biol, 2008. **433**: p. 1-16.

369. Sun, D. and M. Nassal, *Stable HepG2- and Huh7-based human hepatoma cell lines for efficient regulated expression of infectious hepatitis B virus.* J Hepatol, 2006. **45**(5): p. 636-45.

370. Ni, Y., et al., *Hepatitis B and D Viruses Exploit Sodium Taurocholate Co-transporting Polypeptide for Species-Specific Entry into Hepatocytes.* Gastroenterology, 2014. **146**(4): p. 1070-1083.e6.

371. Hastie, E., et al., *Understanding and altering cell tropism of vesicular stomatitis virus.* Virus Research, 2013. **176**(1): p. 16-32.

372. Carnell, G., et al., *The bat influenza H17N10 can be neutralized by broadly-neutralizing monoclonal antibodies and its neuraminidase can facilitate viral egress.* bioRxiv, 2018: p. 499947.

373. Hu, D., et al., *Chikungunya Virus Glycoproteins Pseudotype with Lentiviral Vectors and Reveal a Broad Spectrum of Cellular Tropism.* PLOS ONE, 2014. **9**(10): p. e110893.

374. Fe Medina, M., et al., *Lentiviral vectors pseudotyped with minimal filovirus envelopes increased gene transfer in murine lung.* Molecular Therapy, 2003. **8**(5): p. 777-789.

375. Scott, S.D., et al., *The Optimisation of Pseudotyped Viruses for the Characterisation of Immune Responses to Equine Influenza Virus.* Pathogens (Basel, Switzerland), 2016. **5**(4): p. 68.

376. Naldini, L., et al., *In vivo gene delivery and stable transduction of nondividing cells by a lentiviral vector.* Science, 1996. **272**(5259): p. 263-7.

377. Takeuchi, Y., et al., *Retroviral pseudotypes produced by rescue of a Moloney murine leukemia virus vector by C-type, but not D-type, retroviruses.* Virology, 1992. **186**(2): p. 792-4.

378. Sandrin, V., et al., *Lentiviral vectors pseudotyped with a modified RD114 envelope glycoprotein show increased stability in sera and augmented transduction of primary lymphocytes and CD34+ cells derived from human and nonhuman primates.* Blood, 2002. **100**(3): p. 823-832.

379. Mammano, F., et al., *Truncation of the human immunodeficiency virus type 1 envelope glycoprotein allows efficient pseudotyping of Moloney murine leukemia virus particles and gene transfer into CD4+ cells.* Journal of virology, 1997. **71**(4): p. 3341-3345.

380. Lindemann, D., et al., *Efficient pseudotyping of murine leukemia virus particles with chimeric human foamy virus envelope proteins.* Journal of virology, 1997. **71**(6): p. 4815-4820.

381. Christodoulopoulos, I. and P.M. Cannon, *Sequences in the cytoplasmic tail of the gibbon ape leukemia virus envelope protein that prevent its incorporation into lentivirus vectors.* Journal of virology, 2001. **75**(9): p. 4129-4138.

382. Sandrin, V. and F.-L. Cosset, *Intracellular Versus Cell Surface Assembly of Retroviral Pseudotypes Is Determined by the Cellular Localization of the Viral Glycoprotein, Its Capacity to Interact with Gag, and the Expression of the Nef Protein *.* Journal of Biological Chemistry, 2006. **281**(1): p. 528-542.

383. Manrique, J.M., et al., *Positive and negative modulation of virus infectivity and envelope glycoprotein incorporation into virions by amino acid substitutions at the N terminus of the simian immunodeficiency virus matrix protein.* J Virol, 2003. **77**(20): p. 10881-8.

384. Saad, J.S., et al., *Structural basis for targeting HIV-1 Gag proteins to the plasma membrane for virus assembly.* Proc Natl Acad Sci U S A, 2006. **103**(30): p. 11364-9.

385. Chen, Y., W.M. Miller, and A. Aiyar, *Transduction efficiency of pantropic retroviral vectors is controlled by the envelope plasmid to vector plasmid ratio.* Biotechnology progress, 2005. **21**(1): p. 274-282.

386. Bajgelman, M.C., E. Costanzi-Strauss, and B.E. Strauss, *Exploration of critical parameters for transient retrovirus production.* Journal of Biotechnology, 2003. **103**(2): p. 97-106.

387. Batista Napotnik, T., T. Polajžer, and D. Miklavčič, *Cell death due to electroporation – A review.* Bioelectrochemistry, 2021. **141**: p. 107871.

388. Toledo, J.R., et al., *Polyethylenimine-Based Transfection Method as a Simple and Effective Way to Produce Recombinant Lentiviral Vectors.* Applied Biochemistry and Biotechnology, 2009. **157**(3): p. 538-544.

389. Tang, Y., et al., *Optimization of lentiviral vector production using polyethylenimine-mediated transfection.* Oncol Lett, 2015. **9**(1): p. 55-62.

390. Yang, S., et al., *Optimized PEI-based Transfection Method for Transient Transfection and Lentiviral Production.* Current Protocols in Chemical Biology, 2017. **9**(3): p. 147-157.

391.   Chu, C., et al., *A simple protocol for producing high-titer lentivirus.* Acta Biochimica et Biophysica Sinica, 2013. **45**(12): p. 1079-1082.

392.   Thomas, P. and T.G. Smart, *HEK293 cell line: A vehicle for the expression of recombinant proteins.* Journal of Pharmacological and Toxicological Methods, 2005. **51**(3): p. 187-200.

393.   Kuroda, H., et al., *Simplified lentivirus vector production in protein-free media using polyethylenimine-mediated transfection.* J Virol Methods, 2009. **157**(2): p. 113-21.

394.   Michailidis, E., et al., *A robust cell culture system supporting the complete life cycle of hepatitis B virus.* Scientific Reports, 2017. **7**(1): p. 16616.

395.   Gripon, P., C. Diot, and C. Guguen-Guillouzo, *Reproducible High Level Infection of Cultured Adult Human Hepatocytes by Hepatitis B Virus: Effect of Polyethylene Glycol on Adsorption and Penetration.* Virology, 1993. **192**(2): p. 534-540.

396.   Li, L.H. and S.W. Hui, *Characterization of PEG-mediated electrofusion of human erythrocytes.* Biophys J, 1994. **67**(6): p. 2361-6.

397.   Ross, P.C. and S.W. Hui, *Polyethylene glycol enhances lipoplex-cell association and lipofection.* Biochimica et Biophysica Acta (BBA) - Biomembranes, 1999. **1421**(2): p. 273-283.

398.   Tabarin, T., et al., *Poly-ethylene glycol induced super-diffusivity in lipid bilayer membranes.* Soft Matter, 2012. **8**(33): p. 8743-8751.

399.   Yang, J. and M.H. Shen, *Polyethylene glycol-mediated cell fusion.* Methods Mol Biol, 2006. **325**: p. 59-66.

400.   Rajoriya, N., et al., *How viral genetic variants and genotypes influence disease and treatment outcome of chronic hepatitis B. Time for an individualised approach?* Journal of Hepatology, 2017. **67**(6): p. 1281-1297.

401.   Kuhnhenn, L., et al., *Impact of HBV genotype and mutations on HBV DNA and qHBsAg levels in patients with HBeAg-negative chronic HBV infection.* Alimentary Pharmacology & Therapeutics, 2018. **47**(11): p. 1523-1535.

402.   Kramvis, A., et al., *Relationship of serological subtype, basic core promoter and precore mutations to genotypes/subgenotypes of hepatitis B virus.* Journal of Medical Virology, 2008. **80**(1): p. 27-46.

403.   Sozzi, V., et al., *In vitro studies identify a low replication phenotype for hepatitis B virus genotype H generally associated with occult HBV and less severe liver disease.* Virology, 2018. **519**: p. 190-196.

404.   Hassemer, M., et al., *Comparative characterization of hepatitis B virus surface antigen derived from different hepatitis B virus genotypes.* Virology, 2017. **502**: p. 1-12.

405.   Peiffer, K.-H., et al., *Intracellular accumulation of subviral HBsAg particles and diminished Nrf2 activation in HBV genotype G expressing cells lead to an increased ROI level.* Journal of Hepatology, 2015. **62**(4): p. 791-798.

406.   Sugiyama, M., et al., *Early dynamics of hepatitis B virus in chimeric mice carrying human hepatocytes monoinfected or coinfected with genotype G.* Hepatology, 2007. **45**(4): p. 929-937.

407.   Dao, D.Y., et al., *Hepatitis B virus genotype G: Prevalence and impact in patients co-infected with human immunodeficiency virus.* Journal of Medical Virology, 2011. **83**(9): p. 1551-1558.

408.   Tong, S. and P. Revill, *Overview of hepatitis B viral replication and genetic variability.* Journal of hepatology, 2016. **64**(1 Suppl): p. S4-S16.

409.   Araujo, N.M., *Hepatitis B virus intergenotypic recombinants worldwide: An overview.* Infection, Genetics and Evolution, 2015. **36**: p. 500-510.

410.   Leistner, C.M., S. Gruen-Bernhard, and D. Glebe, *Role of glycosaminoglycans for binding and infection of hepatitis B virus.* Cell Microbiol, 2008. **10**(1): p. 122-33.

411. Schulze, A., P. Gripon, and S. Urban, *Hepatitis B virus infection initiates with a large surface protein-dependent binding to heparan sulfate proteoglycans.* Hepatology, 2007. **46**(6): p. 1759-68.

412. Sureau, C. and J. Salisse, *A conformational heparan sulfate binding site essential to infectivity overlaps with the conserved hepatitis B virus A-determinant.* Hepatology, 2013. **57**(3): p. 985-994.

413. Hossain, M.G. and K. Ueda, *Investigation of a Novel Hepatitis B Virus Surface Antigen (HBsAg) Escape Mutant Affecting Immunogenicity.* PLOS ONE, 2017. **12**(1): p. e0167871.

414. Rezaee, R., et al., *Impacts of the G145R Mutation on the Structure and Immunogenic Activity of the Hepatitis B Surface Antigen: A Computational Analysis.* Hepatitis monthly, 2016. **16**(7): p. e39097-e39097.

415. Yu, D.M., et al., *N-glycosylation mutations within hepatitis B virus surface major hydrophilic region contribute mostly to immune escape.* J Hepatol, 2014. **60**(3): p. 515-22.

416. Tian, Y., et al., *The Amino Acid Residues at Positions 120 to 123 Are Crucial for the Antigenicity of Hepatitis B Surface Antigen.* Journal of Clinical Microbiology, 2007. **45**(9): p. 2971.

417. Murayama, A., et al., *N-terminal PreS1 Sequence Regulates Efficient Infection of Cell Culture-generated Hepatitis B Virus.* Hepatology. **n/a**(n/a).

418. Gnaneshan, S., et al., *HepSEQ: International Public Health Repository for Hepatitis B.* Nucleic Acids Res, 2007. **35**(Database issue): p. D367-70.

419. Hayer, J., et al., *HBVdb: a knowledge database for Hepatitis B Virus.* Nucleic Acids Research, 2012. **41**(D1): p. D566-D570.

420. Glebe, D., et al., *Mapping of the hepatitis B virus attachment site by use of infection-inhibiting preS1 lipopeptides and tupaia hepatocytes.* Gastroenterology, 2005. **129**(1): p. 234-45.

421. Barrera, A., et al., *Mapping of the Hepatitis B Virus Pre-S1 Domain Involved in Receptor Recognition.* Journal of Virology, 2005. **79**(15): p. 9786.

422. Schulze, A., et al., *Fine mapping of pre-S sequence requirements for hepatitis B virus large envelope protein-mediated receptor interaction.* J Virol, 2010. **84**(4): p. 1989-2000.

423. Lamas Longarela, O., et al., *Proteoglycans act as cellular hepatitis delta virus attachment receptors.* PloS one, 2013. **8**(3): p. e58340-e58340.

424. Haberstroh, A., et al., *Neutralizing host responses in hepatitis C virus infection target viral entry at postbinding steps and membrane fusion.* Gastroenterology, 2008. **135**(5): p. 1719-1728.e1.

425. Desombere, I., et al., *A novel neutralizing human monoclonal antibody broadly abrogates hepatitis C virus infection in vitro and in vivo.* Antiviral Research, 2017. **148**: p. 53-64.

426. Sozzi, V., et al., *In Vitro Studies Show that Sequence Variability Contributes to Marked Variation in Hepatitis B Virus Replication, Protein Expression, and Function Observed across Genotypes.* Journal of Virology, 2016. **90**(22): p. 10054.

427. Sugiyama, M., et al., *Influence of hepatitis B virus genotypes on the intra- and extracellular expression of viral DNA and antigens.* Hepatology, 2006. **44**(4): p. 915-924.

428. Qin, Y., et al., *Hepatitis B Virus Genotype C Isolates with Wild-Type Core Promoter Sequence Replicate Less Efficiently than Genotype B Isolates but Possess Higher Virion Secretion Capacity.* Journal of Virology, 2011. **85**(19): p. 10167.

429. Bannister, E.G., et al., *Molecular characterization of hepatitis B virus (HBV) in African children living in Australia identifies genotypes and variants associated with poor clinical outcome.* Journal of General Virology, 2018. **99**(8): p. 1103-1114.

430. Bannister, E., et al., *Analysis of the in vitro replication phenotype of African hepatitis B virus (HBV) genotypes and subgenotypes present in Australia identifies marked differences in DNA and protein expression.* Virology, 2020. **540**: p. 97-103.

431. Hossain, M.G., et al., *PreS1 Mutations Alter the Large HBsAg Antigenicity of a Hepatitis B Virus Strain Isolated in Bangladesh.* Int J Mol Sci, 2020. **21**(2).

432. Wu, C., et al., *Biological significance of amino acid substitutions in hepatitis B surface antigen (HBsAg) for glycosylation, secretion, antigenicity and immunogenicity of HBsAg and hepatitis B virus replication.* J Gen Virol, 2010. **91**(Pt 2): p. 483-92.

433. Zhang, M., et al., *Decreased antigenicity profiles of immune-escaped and drug-resistant hepatitis B surface antigen (HBsAg) double mutants.* Virology journal, 2013. **10**: p. 292-292.

434. Hossain, M.G., et al., *PreS1 Mutations Alter the Large HBsAg Antigenicity of a Hepatitis B Virus Strain Isolated in Bangladesh.* International journal of molecular sciences, 2020. **21**(2): p. 546.

435. Berkower, I., et al., *Hepatitis B virus surface antigen assembly function persists when entire transmembrane domains 1 and 3 are replaced by a heterologous transmembrane sequence.* Journal of virology, 2011. **85**(5): p. 2439-2448.

436. Blanchet, M. and C. Sureau, *Analysis of the Cytosolic Domains of the Hepatitis B Virus Envelope Proteins for Their Function in Viral Particle Assembly and Infectivity.* Journal of Virology, 2006. **80**(24): p. 11935.

437. Cao, J., S. Luo, and Y. Xiong, *The Variability of Amino Acid Sequences in Hepatitis B Virus.* Virologica Sinica, 2019. **34**(1): p. 42-49.

438. Jaoudé, G.A. and C. Sureau, *Role of the antigenic loop of the hepatitis B virus envelope proteins in infectivity of hepatitis delta virus.* Journal of virology, 2005. **79**(16): p. 10460-10466.

439. El Chaar, M., et al., *Impact of hepatitis B virus surface protein mutations on the diagnosis of occult hepatitis B virus infection.* Hepatology, 2010. **52**(5): p. 1600-1610.

440. Mangold, C.M., et al., *Secretion and antigenicity of hepatitis B virus small envelope proteins lacking cysteines in the major antigenic region.* Virology, 1995. **211**(2): p. 535-43.

441. Zhou, S. and D.N. Standring, *Cys residues of the hepatitis B virus capsid protein are not essential for the assembly of viral core particles but can influence their stability.* Journal of virology, 1992. **66**(9): p. 5393-5398.

442. Kim, S., J. Lee, and W.-S. Ryu, *Four Conserved Cysteine Residues of the Hepatitis B Virus Polymerase Are Critical for RNA Pregenome Encapsidation.* Journal of Virology, 2009. **83**(16): p. 8032.

443. Bang, G., et al., *Effect of mutating the two cysteines required for HBe antigenicity on hepatitis B virus DNA replication and virion secretion.* Virology, 2005. **332**(1): p. 216-224.

444. Betz-Stablein, B.D., et al., *Single-Molecule Sequencing Reveals Complex Genome Variation of Hepatitis B Virus during 15 Years of Chronic Infection following Liver Transplantation.* Journal of Virology, 2016. **90**(16): p. 7171.

445. Teppa, E., et al., *Coevolution analysis of amino-acids reveals diversified drug-resistance solutions in viral sequences: a case study of hepatitis B virus.* Virus Evolution, 2020. **6**(1).

446. Ahn, S.H., et al., *Substitution at rt269 in Hepatitis B Virus Polymerase Is a Compensatory Mutation Associated with Multi-Drug Resistance.* PloS one, 2015. **10**(8): p. e0136728-e0136728.

447. Davis, B.H., A.F.Y. Poon, and M.C. Whitlock, *Compensatory mutations are repeatable and clustered within proteins.* Proceedings. Biological sciences, 2009. **276**(1663): p. 1823-1827.

448. Poon, A., B.H. Davis, and L. Chao, *The coupon collector and the suppressor mutation: estimating the number of compensatory mutations by maximum likelihood.* Genetics, 2005. **170**(3): p. 1323-32.

449. Li, W., et al., *Complementary Mutations in the N and L Proteins for Restoration of Viral RNA Synthesis.* Journal of Virology, 2018. **92**(22): p. e01417-18.

450. Liu, H., M.L. Grantham, and A. Pekosz, *Mutations in the Influenza A Virus M1 Protein Enhance Virus Budding To Complement Lethal Mutations in the M2 Cytoplasmic Tail.* Journal of virology, 2017. **92**(1): p. e00858-17.

451. Cagno, V., et al., *Heparan Sulfate Proteoglycans and Viral Attachment: True Receptors or Adaptation Bias?* Viruses, 2019. **11**(7).

452. Galun, E., et al., *Clinical evaluation (phase I) of a combination of two human monoclonal antibodies to HBV: safety and antiviral properties.* Hepatology, 2002. **35**(3): p. 673-9.

453. Volz, T., et al., *The entry inhibitor Myrcludex-B efficiently blocks intrahepatic virus spreading in humanized mice previously infected with hepatitis B virus.* Journal of Hepatology, 2013. **58**(5): p. 861-867.

454. Hong, H.J., et al., *In vivo neutralization of hepatitis B virus infection by an anti-preS1 humanized antibody in chimpanzees.* Virology, 2004. **318**(1): p. 134-41.

455. Ryu, C.J., et al., *In vitro neutralization of hepatitis b virus by monoclonal antibodies against the viral surface antigen.* Journal of Medical Virology, 1997. **52**(2): p. 226-233.

456. Diehl, N. and H. Schaal, *Make yourself at home: viral hijacking of the PI3K/Akt signaling pathway.* Viruses, 2013. **5**(12): p. 3192-212.

457. Wheeler, D.L., E.F. Dunn, and P.M. Harari, *Understanding resistance to EGFR inhibitors-impact on future treatment strategies.* Nat Rev Clin Oncol, 2010. **7**(9): p. 493-507.

458. Wang, X., et al., *Epidermal growth factor receptor is a cellular receptor for human cytomegalovirus.* Nature, 2003. **424**(6947): p. 456-61.

459. Bentz, G.L. and A.D. Yurochko, *Human CMV infection of endothelial cells induces an angiogenic response through viral binding to EGF receptor and beta1 and beta3 integrins.* Proc Natl Acad Sci U S A, 2008. **105**(14): p. 5531-6.

460. Liang, Y., A. Kurakin, and B. Roizman, *Herpes simplex virus 1 infected cell protein 0 forms a complex with CIN85 and Cbl and mediates the degradation of EGF receptor from cell surfaces.* Proc Natl Acad Sci U S A, 2005. **102**(16): p. 5838-43.

461. Zheng, K., et al., *Epidermal Growth Factor Receptor-PI3K Signaling Controls Cofilin Activity To Facilitate Herpes Simplex Virus 1 Entry into Neuronal Cells.* mBio, 2014. **5**(1): p. e00958-13.

462. Dawson, C.W., et al., *Epstein-Barr virus latent membrane protein 1 (LMP1) activates the phosphatidylinositol 3-kinase/Akt pathway to promote cell survival and induce actin filament remodeling.* J Biol Chem, 2003. **278**(6): p. 3694-704.

463. Kung, C.P., D.G. Meckes, Jr., and N. Raab-Traub, *Epstein-Barr virus LMP1 activates EGFR, STAT3, and ERK through effects on PKCdelta.* J Virol, 2011. **85**(9): p. 4399-408.

464. Eierhoff, T., et al., *The epidermal growth factor receptor (EGFR) promotes uptake of influenza A viruses (IAV) into host cells.* PLoS pathogens, 2010. **6**(9): p. e1001099-e1001099.

465.	Karlas, A., et al., *Genome-wide RNAi screen identifies human host factors crucial for influenza virus replication.* Nature, 2010. **463**(7282): p. 818-22.

466.	Macovei, A., et al., *Hepatitis B virus requires intact caveolin-1 function for productive infection in HepaRG cells.* J Virol, 2010. **84**(1): p. 243-53.

467.	Chen, S.-W., et al., *Modulation of hepatitis B virus infection by epidermal growth factor secreted from liver sinusoidal endothelial cells.* Scientific Reports, 2020. **10**(1): p. 14349.

468.	Harrison, S.C., *Viral membrane fusion.* Nature Structural & Molecular Biology, 2008. **15**(7): p. 690-698.

469.	Ci, Y., et al., *Vesicular stomatitis virus G protein transmembrane region is crucial for the hemi-fusion to full fusion transition.* Scientific Reports, 2018. **8**(1): p. 10669.

470.	Leistner, C.M., S. Gruen-Bernhard, and D. Glebe, *Role of glycosaminoglycans for binding and infection of hepatitis B virus.* Cellular Microbiology, 2008. **10**(1): p. 122-133.

471.	Choijilsuren, G., et al., *Heparin at physiological concentration can enhance PEG-free in vitro infection with human hepatitis B virus.* Scientific Reports, 2017. **7**(1): p. 14461.

472.	Bhattacharyya, S., et al., *Ebola virus uses clathrin-mediated endocytosis as an entry pathway.* Virology, 2010. **401**(1): p. 18-28.

473.	Cerino, A., et al., *Human Monoclonal Antibodies as Adjuvant Treatment of Chronic Hepatitis B Virus Infection.* Frontiers in Immunology, 2019. **10**(2290).

474.	Li, W. and S. Urban, *Entry of hepatitis B and hepatitis D virus into hepatocytes: Basic insights and clinical implications.* Journal of Hepatology, 2016. **64**(1, Supplement): p. S32-S40.

475.	Saha, D., et al., *Molecular Characterization of HBV Strains Circulating among the Treatment-Naive HIV/HBV Co-Infected Patients of Eastern India.* PLOS ONE, 2014. **9**(2): p. e90432.

476.	Ye, Q., S.-Q. Shang, and W. Li, *A new vaccine escape mutant of hepatitis B virus causes occult infection.* Human vaccines & immunotherapeutics, 2015. **11**(2): p. 407-410.

477.	Purdy, M.A., *Hepatitis B virus S gene escape mutants.* Asian journal of transfusion science, 2007. **1**(2): p. 62-70.

478.	Grethe, S., et al., *Characterization of Unusual Escape Variants of Hepatitis B Virus Isolated from a Hepatitis B Surface Antigen-Negative Subject.* Journal of Virology, 1998. **72**(9): p. 7692.

479.	Schieck, A., et al., *Hepatitis B virus hepatotropism is mediated by specific receptor recognition in the liver and not restricted to susceptible hosts.* Hepatology, 2013. **58**(1): p. 43-53.

480.	Feigelstock, D.A., et al., *Increased susceptibility of Huh7 cells to HCV replication does not require mutations in RIG-I.* Virology Journal, 2010. **7**(1): p. 44.

481.	Bressac, B., et al., *Abnormal structure and expression of p53 gene in human hepatocellular carcinoma.* Proc Natl Acad Sci U S A, 1990. **87**(5): p. 1973-7.

482.	Tsai, T.J., et al., *Gelsolin-like Actin-capping Protein (CapG) Overexpression in the Cytoplasm of Human Hepatocellular Carcinoma, Associated with Cellular Invasion, Migration and Tumor Prognosis.* Anticancer Res, 2018. **38**(7): p. 3943-3950.

483.	Guo, L., et al., *Similarities and differences in the expression of drug-metabolizing enzymes between human hepatic cell lines and primary human hepatocytes.* Drug metabolism and disposition: the biological fate of chemicals, 2011. **39**(3): p. 528-538.

484.   Shi, J., et al., *Comparison of protein expression between human livers and the hepatic cell lines HepG2, Hep3B, and Huh7 using SWATH and MRM-HR proteomics: Focusing on drug-metabolizing enzymes.* Drug metabolism and pharmacokinetics, 2018. **33**(2): p. 133-140.

485.   Aquino, R.S. and P.W. Park, *Glycosaminoglycans and infection.* Frontiers in bioscience (Landmark edition), 2016. **21**: p. 1260-1277.

486.   Watashi, K., et al., *Cyclosporin A and its analogs inhibit hepatitis B virus entry into cultured hepatocytes through targeting a membrane transporter, sodium taurocholate cotransporting polypeptide (NTCP).* Hepatology, 2014. **59**(5): p. 1726-1737.

487.   Meier, A., et al., *Myristoylated PreS1-domain of the hepatitis B virus L-protein mediates specific binding to differentiated hepatocytes.* Hepatology, 2013. **58**(1): p. 31-42.

488.   Iwamoto, M., et al., *Evaluation and identification of hepatitis B virus entry inhibitors using HepG2 cells overexpressing a membrane transporter NTCP.* Biochemical and Biophysical Research Communications, 2014. **443**(3): p. 808-813.

489.   Shimura, S., et al., *Cyclosporin derivatives inhibit hepatitis B virus entry without interfering with NTCP transporter activity.* Journal of Hepatology, 2017. **66**(4): p. 685-692.

490.   Le Seyec, J., et al., *Infection Process of the Hepatitis B Virus Depends on the Presence of a Defined Sequence in the Pre-S1 Domain.* Journal of Virology, 1999. **73**(3): p. 2052.

491.   De Falco, S., et al., *Cloning and Expression of a Novel Hepatitis B Virus-binding Protein from HepG2 Cells*.* Journal of Biological Chemistry, 2001. **276**(39): p. 36613-36623.

492.   Budkowska, A., et al., *Hepatitis B virus (HBV) binding factor in human serum: candidate for a soluble form of hepatocyte HBV receptor.* Journal of virology, 1993. **67**(7): p. 4316-4322.

493.   Zhang, X., et al., *Asialoglycoprotein receptor interacts with the preS1 domain of hepatitis B virus in vivo and in vitro.* Archives of Virology, 2011. **156**(4): p. 637-645.

494.   Cooper, A. and Y. Shaul, *Clathrin-mediated Endocytosis and Lysosomal Cleavage of Hepatitis B Virus Capsid-like Core Particles*.* Journal of Biological Chemistry, 2006. **281**(24): p. 16563-16569.

495.   Chan, G., M.T. Nogalski, and A.D. Yurochko, *Activation of EGFR on monocytes is required for human cytomegalovirus entry and mediates cellular motility.* Proceedings of the National Academy of Sciences, 2009. **106**(52): p. 22369.

496.   Lupberger, J., et al., *EGFR and EphA2 are host factors for hepatitis C virus entry and possible targets for antiviral therapy.* Nature medicine, 2011. **17**(5): p. 589-595.

497.   French, A.R., et al., *Intracellular Trafficking of Epidermal Growth Factor Family Ligands Is Directly Influenced by the pH Sensitivity of the Receptor/Ligand Interaction (∗).* Journal of Biological Chemistry, 1995. **270**(9): p. 4334-4340.

498.   Roepstorff, K., et al., *Differential effects of EGFR ligands on endocytic sorting of the receptor.* Traffic (Copenhagen, Denmark), 2009. **10**(8): p. 1115-1127.

499.   Wang, X., et al., *The Na+-Taurocholate Cotransporting Polypeptide Traffics with the Epidermal Growth Factor Receptor.* Traffic, 2016. **17**(3): p. 230-244.

500.   Sigismund, S., et al., *Clathrin-Mediated Internalization Is Essential for Sustained EGFR Signaling but Dispensable for Degradation.* Developmental Cell, 2008. **15**(2): p. 209-219.

501. Sigismund, S., et al., *Clathrin-independent endocytosis of ubiquitinated cargos.* Proceedings of the National Academy of Sciences of the United States of America, 2005. **102**(8): p. 2760.

502. Zona, L., et al., *HRas signal transduction promotes hepatitis C virus cell entry by triggering assembly of the host tetraspanin receptor complex.* Cell Host Microbe, 2013. **13**(3): p. 302-13.

503. Maramotti, S., et al., *Soluble Epidermal Growth Factor Receptors (sEGFRs) in Cancer: Biological Aspects and Clinical Relevance.* International journal of molecular sciences, 2016. **17**(4): p. 593.

504. Guo, G., et al., *Ligand-Independent EGFR Signaling.* Cancer research, 2015. **75**(17): p. 3436-3441.

505. Endres, N.F., et al., *Conformational coupling across the plasma membrane in activation of the EGF receptor.* Cell, 2013. **152**(3): p. 543-556.

506. Chakraborty, S., et al., *Constitutive and ligand-induced EGFR signalling triggers distinct and mutually exclusive downstream signalling networks.* Nature communications, 2014. **5**: p. 5811-5811.

507. Gan, C.J., et al., *EGF receptor inhibitors comprehensively suppress hepatitis B virus by downregulation of STAT3 phosphorylation.* Biochemistry and Biophysics Reports, 2020. **22**: p. 100763.

508. Gerlich, W.H., *The Enigma of Concurrent Hepatitis B Surface Antigen (HBsAg) and Antibodies to HBsAg.* Clinical Infectious Diseases, 2007. **44**(9): p. 1170-1172.

509. Madalinski, K., et al., *Analysis of viral proteins in circulating immune complexes from chronic carriers of hepatitis B virus.* Clin Exp Immunol, 1991. **84**(3): p. 493-500.

510. Prange, R., *Host factors involved in hepatitis B virus maturation, assembly, and egress.* Medical Microbiology and Immunology, 2012. **201**(4): p. 449-461.

511. Bruns, M., et al., *Enhancement of hepatitis B virus infection by noninfectious subviral particles.* Journal of virology, 1998. **72**(2): p. 1462-1468.

512. Song, J.E. and D.Y. Kim, *Diagnosis of hepatitis B.* Annals of translational medicine, 2016. **4**(18): p. 338-338.

513. Krajden, M., G. McNabb, and M. Petric, *The laboratory diagnosis of hepatitis B virus.* The Canadian journal of infectious diseases & medical microbiology = Journal canadien des maladies infectieuses et de la microbiologie medicale, 2005. **16**(2): p. 65-72.

514. Coleman, P.F., *Detecting hepatitis B surface antigen mutants.* Emerging infectious diseases, 2006. **12**(2): p. 198-203.

515. Al-Rubaye, A., Z. Tariq, and L. Alrubaiy, *Prevalence of hepatitis B seromarkers and hepatitis C antibodies in blood donors in Basra, Iraq.* BMJ Open Gastroenterology, 2016. **3**(1): p. e000067.

516. Allain, J.P. and O. Opare-Sem, *Screening and diagnosis of HBV in low-income and middle-income countries.* Nat Rev Gastroenterol Hepatol, 2016. **13**(11): p. 643-653.

517. Gencay, M., et al., *Detection of in vivo hepatitis B virus surface antigen mutations-A comparison of four routine screening assays.* J Viral Hepat, 2018. **25**(10): p. 1132-1138.

518. Jain, R., P. Aggarwal, and G.N. Gupta, *Need for nucleic Acid testing in countries with high prevalence of transfusion-transmitted infections.* ISRN hematology, 2012. **2012**: p. 718671-718671.

519. Carman, W.F., et al., *Fulminant reactivation of hepatitis B due to envelope protein mutant that escaped detection by monoclonal HBsAg ELISA.* Lancet, 1995. **345**(8962): p. 1406-7.

520. Jammeh, S., H.C. Thomas, and P. Karayiannis, *Replicative competence of the T131I, K141E, and G145R surface variants of hepatitis B Virus.* J Infect Dis, 2007. **196**(7): p. 1010-3.

521. Yan, B., et al., *Temporal trend of hepatitis B surface mutations in the post-immunization period: 9 years of surveillance (2005–2013) in eastern China.* Scientific Reports, 2017. **7**(1): p. 6669.

522. Cooreman, M.P., G. Leroux-Roels, and W.P. Paulij, *Vaccine- and hepatitis B immune globulin-induced escape mutations of hepatitis B virus surface antigen.* J Biomed Sci, 2001. **8**(3): p. 237-47.

523. Komatsu, H., et al., *Evaluation of the G145R Mutant of the Hepatitis B Virus as a Minor Strain in Mother-to-Child Transmission.* PloS one, 2016. **11**(11): p. e0165674-e0165674.

524. Sayan, M., et al., *Monitoring of hepatitis B virus surface antigen escape mutations and concomitantly nucleos(t)ide analog resistance mutations in Turkish patients with chronic hepatitis B.* International Journal of Infectious Diseases, 2010. **14**: p. e136-e141.

525. Ochwoto, M., et al., *Hepatitis B infection is highly prevalent among patients presenting with jaundice in Kenya.* BMC Infectious Diseases, 2016. **16**(1): p. 101.

526. Konopleva, M.V., et al., *Detection of S-HBsAg Mutations in Patients with Hematologic Malignancies.* Diagnostics (Basel), 2021. **11**(6).

527. Kim, H.S., et al., *Frequency of hepatitis B surface antigen variants (HBsAg) in hepatitis B virus genotype B and C infected East- and Southeast Asian patients: Detection by the Elecsys® HBsAg II assay.* Journal of Clinical Virology, 2018. **103**: p. 48-56.

528. Baclig, M.O., et al., *Unique surface gene variants of hepatitis B virus isolated from patients in the Philippines.* Journal of Medical Virology, 2014. **86**(2): p. 209-216.

529. Ly, T.D., et al., *Sensitivities of four new commercial hepatitis B virus surface antigen (HBsAg) assays in detection of HBsAg mutant forms.* Journal of clinical microbiology, 2006. **44**(7): p. 2321-2326.

530. Shokatpour, N., et al., *Nucleotide Substitutions in Hepatitis B Viruses Derived from Chronic HBV Patients.* Mediterranean journal of hematology and infectious diseases, 2019. **11**(1): p. e2019046-e2019046.

531. Kwange, S.O., et al., *Hepatitis B virus subgenotype A1, occurrence of subgenotype D4, and S gene mutations among voluntary blood donors in Kenya.* Virus Genes, 2013. **47**(3): p. 448-455.

532. Chaudhuri, V., et al., *Occult hepatitis B virus infection in chronic liver disease: Full-length genome and analysis of mutant surface promoter.* Gastroenterology, 2004. **127**(5): p. 1356-1371.

533. Aydın, M., et al., *Molecular Characterization of Hepatitis B Virus Strains Isolated from Chronic Hepatitis B Patients in Southeastern Region of Turkey.* Viral Hepatitis Journal, 2019. **25**: p. 40-44.

534. Cerva, C., et al., *Hepatitis B reactivation characterized by HBsAg negativity and anti-HbsAg antibodies persistence in haematopoietic stem cell transplanted patient after lamivudine withdrawal.* BMC infectious diseases, 2017. **17**(1): p. 566-566.

535. Kırdar, S., et al., *[HBV pol/S gene mutations in chronic hepatitis B patients receiving nucleoside/nucleotide analogues treatment].* Mikrobiyol Bul, 2019. **53**(2): p. 144-155.

536. Kazim, S.N., et al., *Characterization of naturally occurring and Lamivudine-induced surface gene mutants of hepatitis B virus in patients with chronic hepatitis B in India.* Intervirology, 2006. **49**(3): p. 152-60.

537. Jing, Z.-T., et al., *Hepatitis B Virus Surface Antigen Enhances the Sensitivity of Hepatocytes to Fas-Mediated Apoptosis via Suppression of AKT Phosphorylation.* The Journal of Immunology, 2018. **201**(8): p. 2303.

538. Sterneck, M., et al., *Functional analysis of HBV genomes from patients with fulminant hepatitis.* Hepatology, 1998. **28**(5): p. 1390-7.

539. Bartholomeusz, A. and S. Locarnini, *Hepatitis B virus mutants and fulminant hepatitis B: Fitness plus phenotype.* Hepatology, 2001. **34**(2): p. 432-435.

540. Chaouch, H., et al., *Naturally Occurring Surface Antigen Variants of Hepatitis B Virus in Tunisian Patients.* Intervirology, 2016. **59**(1): p. 36-47.

541. La'ulu, S.L. and W.L. Roberts, *The analytic sensitivity and mutant detection capability of six hepatitis B surface antigen assays.* Am J Clin Pathol, 2006. **125**(5): p. 748-51.

542. Norouzi, M., et al., *Identification of Hepatitis B Virus Surface Antigen (HBsAg) Genotypes and Variations in Chronic Carriers from Isfahan Province, Iran.* Iranian journal of public health, 2012. **41**(3): p. 104-111.

543. Wilen, C.B., J.C. Tilton, and R.W. Doms, *HIV: cell binding and entry.* Cold Spring Harbor perspectives in medicine, 2012. **2**(8): p. a006866.

544. Hoffman, T.L., et al., *Stable exposure of the coreceptor-binding site in a CD4-independent HIV-1 envelope protein.* Proc Natl Acad Sci U S A, 1999. **96**(11): p. 6359-64.

545. Dumonceaux, J., et al., *Spontaneous mutations in the env gene of the human immunodeficiency virus type 1 NDK isolate are associated with a CD4-independent entry phenotype.* J Virol, 1998. **72**(1): p. 512-9.

546. Chenine, A.L., et al., *Adaptation of a CXCR4-using human immunodeficiency type 1 NDK virus in intestinal cells is associated with CD4-independent replication.* Virology, 2002. **304**(2): p. 403-14.

547. Yoshii, H., et al., *CD4-independent human immunodeficiency virus infection involves participation of endocytosis and cathepsin B.* PloS one, 2011. **6**(4): p. e19352-e19352.

548. Saha, K., et al., *Isolation of primary HIV-1 that target CD8+ T Lymphocytes using CD8 as a receptor.* Nature Medicine, 2001. **7**(1): p. 65-72.

549. Cullen, B.R., *A new entry route for HIV.* Nature Medicine, 2001. **7**(1): p. 20-21.

550. Bengali, Z., P.S. Satheshkumar, and B. Moss, *Orthopoxvirus species and strain differences in cell entry.* Virology, 2012. **433**(2): p. 506-512.

551. Bengali, Z., A.C. Townsley, and B. Moss, *Vaccinia virus strain differences in cell attachment and entry.* Virology, 2009. **389**(1): p. 132-140.

552. Mercer, J., et al., *Vaccinia virus strains use distinct forms of macropinocytosis for host-cell entry.* Proceedings of the National Academy of Sciences, 2010. **107**(20): p. 9346.

553. Klingmüller, U. and H. Schaller, *Hepadnavirus infection requires interaction between the viral pre-S domain and a specific hepatocellular receptor.* Journal of virology, 1993. **67**(12): p. 7414-7422.

554. Takahashi, S., et al., *Cloning and identification of annexin II as an autocrine/paracrine factor that increases osteoclast formation and bone resorption.* J Biol Chem, 1994. **269**(46): p. 28696-701.

555. Lai, C.-K., et al., *Association of Hepatitis C Virus Replication Complexes with Microtubules and Actin Filaments Is Dependent on the Interaction of NS3 and NS5A.* Journal of Virology, 2008. **82**(17): p. 8838-8848.

556. Backes, P., et al., *Role of Annexin A2 in the Production of Infectious Hepatitis C Virus Particles.* Journal of Virology, 2010. **84**(11): p. 5775-5789.

557.   Saxena, V., et al., *Annexin A2 Is Involved in the Formation of Hepatitis C Virus Replication Complex on the Lipid Raft.* Journal of Virology, 2012. **86**(8): p. 4139-4150.

558.   LeBouder, F., et al., *Annexin II Incorporated into Influenza Virus Particles Supports Virus Replication by Converting Plasminogen into Plasmin.* Journal of Virology, 2008. **82**(14): p. 6820-6828.

559.   Martin, D.N. and S.L. Uprichard, *Identification of transferrin receptor 1 as a hepatitis C virus entry factor.* Proceedings of the National Academy of Sciences, 2013. **110**(26): p. 10777.